Master Thesis in Geosciences

Reservoir quality of deeply buried, Upper Jurassic sandstones of the South Viking Graben

A sedimentological, petrophysical and modeling approach

Tom Erik Maast

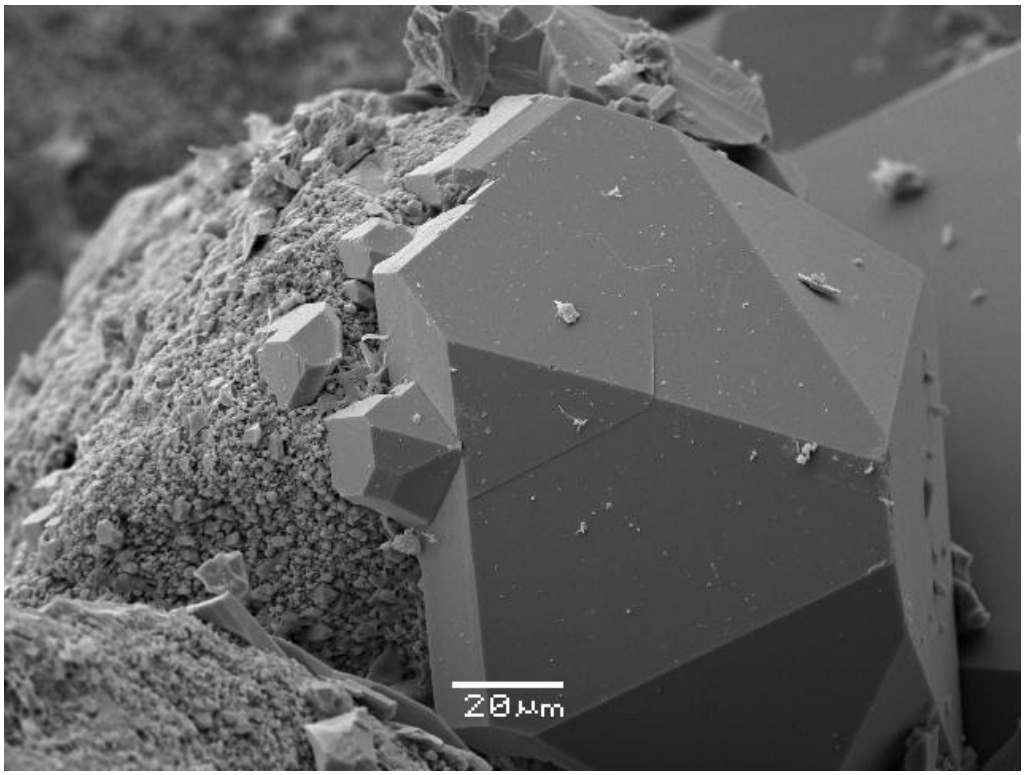

UNIVERSITY OF OSLO

FACULTY OF MATHEMATICS AND NATURAL SCIENCES

Reservoir quality of deeply buried, Upper Jurassic sandstones of the South Viking Graben

A sedimentological, petrophysical and modeling approach

Tom Erik Maast

Master Thesis in Geosciences

Discipline: PEGG

Department of Geosciences

Faculty of Mathematics and Natural Sciences

UNIVERSITY OF OSLO

01.06.2008

Tutor(s): Jens Jahren and Knut Bjørlykke
This work is published digitally through DUO – Digitale Utgivelser ved UiO
http://www.duo.uio.no
It is also catalogued in BIBSYS (http://www.bibsys.no/english)

ACKNOWLEDGEMENTS

I would like to thank my tutors, Jens Jahren and Knut Bjørlykke, for their guidance and insightful understanding of geology. Prof. Knut Bjørlykke officially retires from duty this semester. Bjørlykke has been an inspiration to a great many master- and PhD students during the entire (!) Norwegian petroleum history. His work as well as the work of several of his former students has been invaluable for this study and my own understanding of diagenesis and petroleum geology in general.

Further I would like to thank DNO (now merged with Pertra and called "Det Norske") for financial support and providing my data. Special thanks go to Peter Keller and Ståle Monstad who has been my contacts and supervisors in DNO.

Friends at the Geology department have been an important motivating factor and made the writing easier.

June 2008

Tom Erik Maast

ABSTRACT

Quartz cement, precipitated as syntaxial overgrowths on detrital quartz grains, is the dominant porosity-destroying process in deeply buried quartz-rich sandstones and has proven to be predominantly a pressure insensitive, precipitation rate controlled process in North-Sea reservoir sandstones. Grain-coats are the most important porosity-preserving mechanism in North-Sea sandstones buried to great depths (>4km), because they cover detrital quartz surfaces and thus block precipitation of syntaxial quartz overgrowths.

Petrophysical and petrographic data evaluated in this study indicate that grain-coats are common in Oxfordian to Tithonian sandstones located in the eastern parts of the South Viking Graben. Grain-coating micro-quartz is especially abundant, grain-coating illite occur in variable amounts. Grain-coating micro-quartz appears in deep marine as well as shallow marine sands and does not appear to be facies dependent. Grain-coating illite may depend on facies to a larger degree.

Grain-coating micro-quartz is common in the Upper Jurassic of the North Sea and is generated from transformation of siliceous sponge spicules from the ancient sponge Rhaxella Perforata. Though ubiquitous in Oxfordian to Tithonian sandstones of the eastern parts of the South Viking Graben, no micro-quartz was observed in the time-equivalent sandstones of the western South Viking Graben (Brae Formation), which implies that Rhaxella needed a relatively sediment starved environment to thrive.

Modeling calibrated to petrophysical and petrographic porosity-depth, mineralogical and textural data indicates that grain-coats may cause porosities 10-15% above the expected in deeply buried sandstones in the study area and preserve porosities above reservoir cut-off to burial depths of 5000-5500 meters (TVDRSF). These results however would be affected by overpressure variations. Current modeling algorithms (i.e. exemplar) does not account for mechanisms such as grain-crushing and very high silica super-saturations that will allow quartz cementation to continue despite optimally coating of detrital grains. Very high overpressures are present in the Upper Jurassic of the eastern South Viking Graben, where grain-coats are abundant. This will certainly prevent fracturing and most likely limit silica super-saturations, meaning that the conditions for porosity preservation are optimal in these sandstones and that the modeled depths of reservoir cut-off are realistic.

TABLE OF CONTENTS

CHAPTER 1: INTRODUCTION

1.1 INTRODUCTION

This master thesis is part of a collaboration project with DNO (Det Norske Oljeselskap) on reservoir quality in the Upper Jurassic of the South Viking Graben, related to licenses in blocks 15, 16, 24 and 25, in the South Viking Graben area, and the possible drilling of an exploration well in block 24. The research project consists of two post-doc studies on sand provenance and a master thesis on depositional environment from the area in addition to this contribution.

Quartz cementation and porosity-preserving mechanisms are very important factors when considering deeply buried compositionally mature sandstone prospects, because quartz cementation is the main porosity-destroying process below burial temperatures of approximately 80 ˚C in such sandstones, and will reduce reservoir properties (porosity and permeability) to cut-off level within approximately 3,5 - 4,5 km if it is able to continue unhindered during burial. Grain-coats are the most common factor inhibiting quartz cementation and thus preserving porosities to greater depths. The amount of quartz cement can be successfully modeled in sandstones with or without grain-coats. Development of grain-coats however, is hard to predict and the ability to say something about their distribution therefore depends on available core sections that can be investigated petrographically.

1.2 PURPOSE AND METHODS

The main purpose of this thesis is to provide valuable information on reservoir quality as a function of quartz cementation and porosity-preserving mechanisms in Upper Jurassic sandstones in the South Viking Graben buried to great depths (>4km). This will be accomplished by integration of methods on three levels of investigation:

i. Well correlation and petrophysical evaluation

ii. Core description and interpretation

iii. Petrographic analysis

Sandstone porosities obtained from the petrophysical evaluation have been applied to calibrate a model predicting porosities in deeply buried Upper Jurassic sandstones of the South Viking Graben, and thereby enabling prediction of the depth of reservoir cut-off in the area.

1.3 THE STUDY AREA

As mentioned the study area is within the South Viking Graben, more specifically the Vana and Vilje Sub-basins and the Gudrun and Heimdal Terraces, located in blocks 15/3, 24/12, 25/7 and 16/1 on the Norwegian continental shelf. When used the term "study area" will further refer to rocks of Late Jurassic age within this area.

Sediments deposited during the Upper Jurassic are characterized by large facies variability due to deposition parallel to the rifting event responsible for the majority of the hydrocarbon bearing structures in the North Sea. The Upper Jurassic sediments are also known for their high amount of organic material and make up the main source-rocks in the North Sea. Despite being most known for its organic rich shales, the Upper Jurassic contains several sandstone bodies that potentially will make good reservoir rocks unless they are too deeply buried. These sandstones are sourced pre-dominantly from erosion of middle Jurassic to Devonian rocks exposed on Utsira High and the East Shetland Platform due to footwall uplift, related to the Late Jurassic fault activity. The sandstones in the Vilje and Vana area are compositionally mature predominantly quartz- and sublithic arenites, deposited by sediment gravity-flow processes. The top of the Upper Jurassic rocks are at present buried to a depth of approximately 3500-4500m (depth of the base Cretaceous reflector) in this area, thickness variations are large and may be up to 3000m. Shallow marine deposition dominated on the basin flanks (Gudrun and Heimdal terraces). The basin flanks are important to consider as they are the source areas for the sediment gravity-flows deposited in the grabenal areas.

CHAPTER 2: GEOLOGICAL FRAMEWORK - THE SOUTH VIKING GRABEN

2.1 INTRODUCTION

The South Viking Graben is located in the central North Sea between approximately 59˚30´ - 58˚70´ north and 1˚30´-2˚30´ east. In this chapter the structural setting of the South Viking Graben will be described followed by a brief introduction to the stratigraphy of the study area. A great deal of literature has been published describing the structural evolution of the North Sea region and its stratigraphy (e.g. Brooks and Glennie, 1987; Deegan and Scull, 1977; Gabrielsen, 1986; Glennie, 1998; Nøttvedt et al., 1995; Vollset and Dorê, 1984). This chapter will focus its attention to the South Viking Graben area. For further reading the Millennium Atlas (Evans et al., 2003) and references therein gives a complete description of all aspects of the petroleum geology of the North Sea, along with the references already given.

2.2 STRUCTURAL SETTING

The South Viking Graben constitutes the northern arm of the triple junction between the Central-, Which Ground- and Viking Graben. The present day structural setting in the South Viking Graben (figure 2-1) is the result of two major extensional events, the first taking place at the transition between the Permian and Triassic (Ziegler, 1990) and the second during the Late Jurassic to Early Cretaceous (Rattey and Hayward, 1993). Both the extensional events were followed by thermal subsidence, thus producing the North Sea basin. However, episodes of tectonic inversion and uplift of the basin margins accompanied the thermal subsidence during the Cretaceous to Cenozoic (Zanella and Coward, 2003).

The Late Jurassic – Early Cretaceous rifting event caused the formation of rotational fault-block geometries in the Viking Graben. This fault activity has been the most important trap forming process in the Viking Graben, also for sediments of Upper Jurassic age (Fraser et al., 2003).

Figure 2-2 (next page) shows the structural elements and nomenclature of the study area.

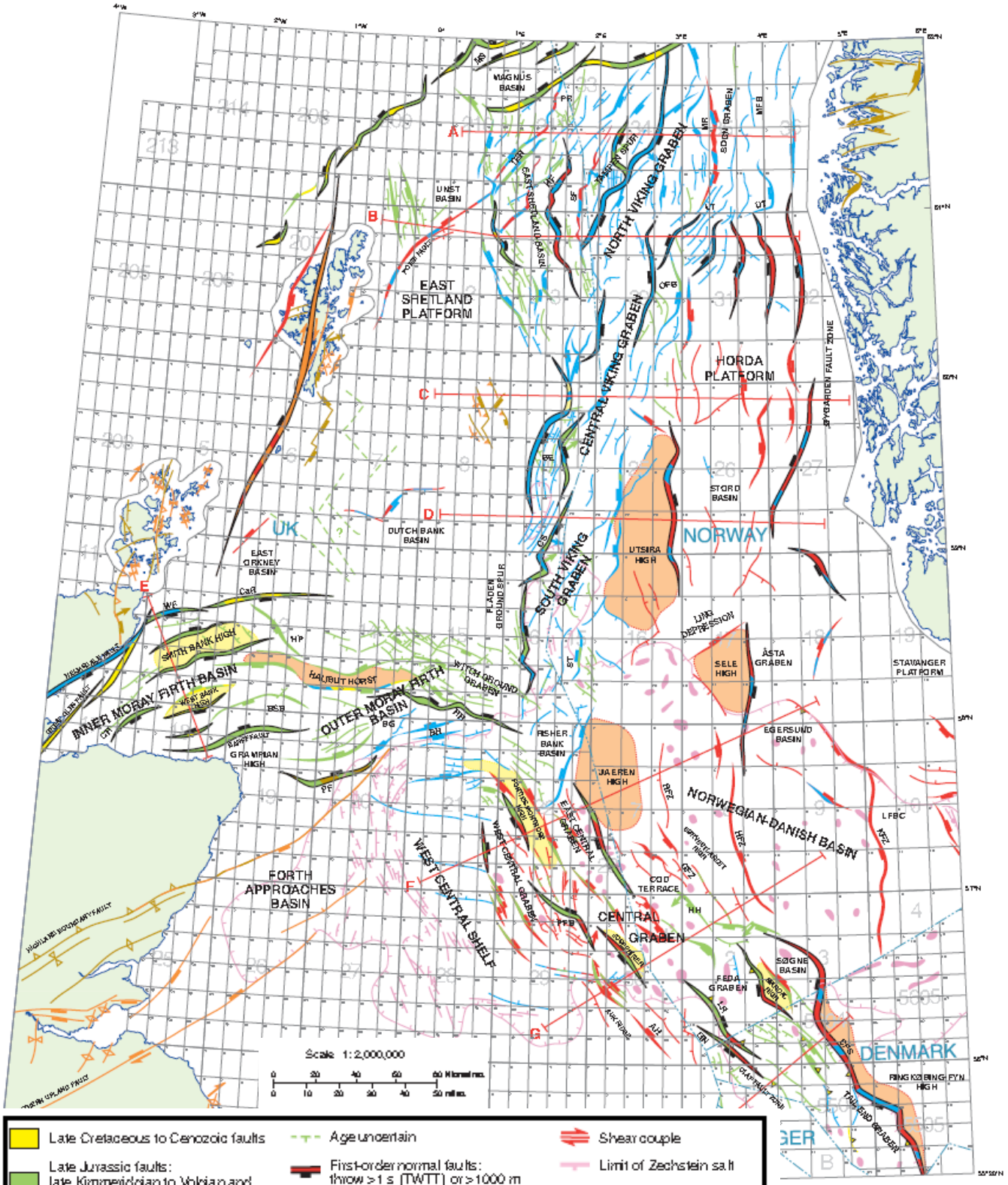

Figure 2-1. Regional structural framework. Modified after Zanella & Coward (2003)

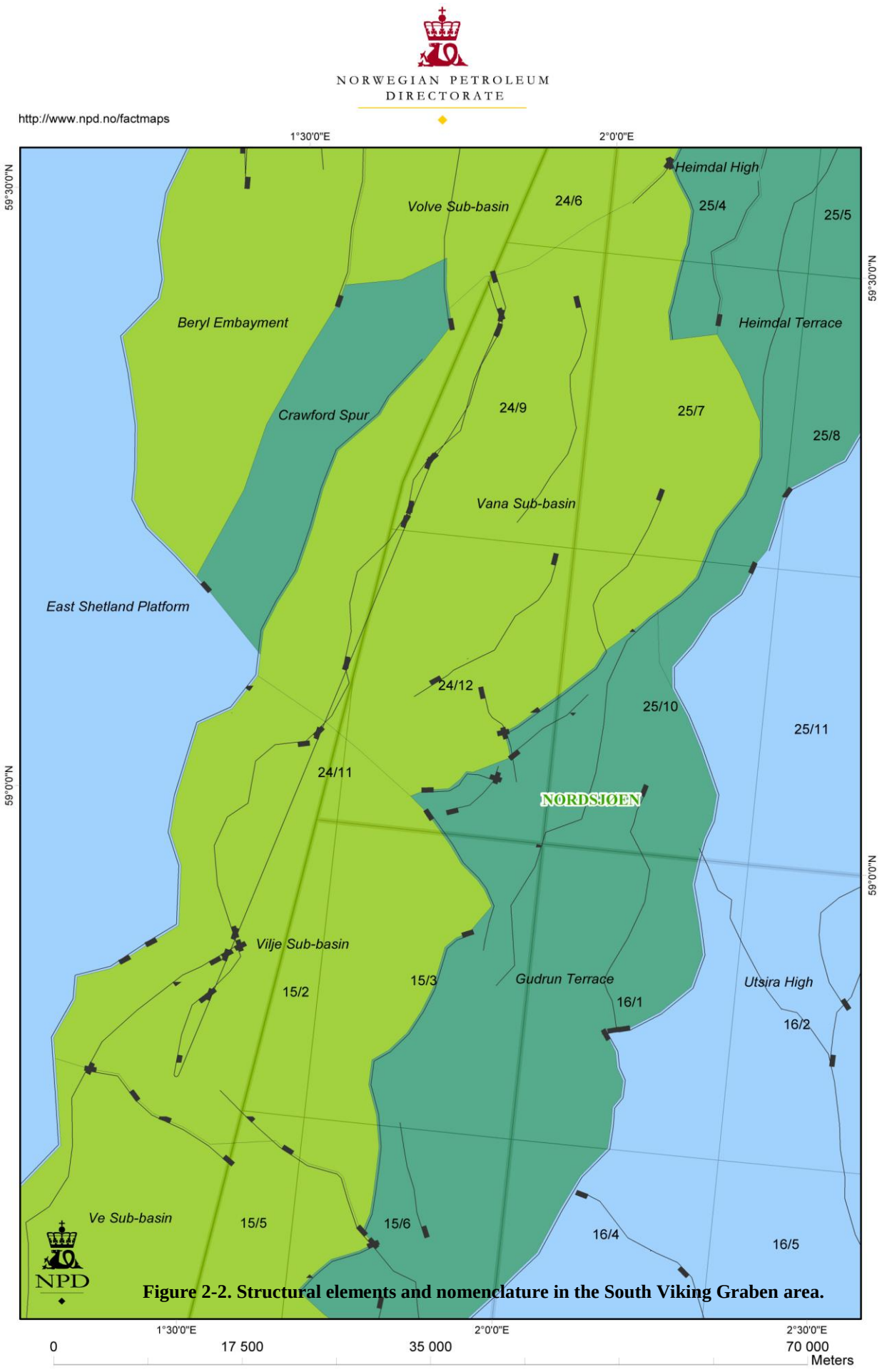

Figure 2-2. Structural elements and nomenclature in the South Viking Graben area.

2.3 STRATIGRAPHIC SETTING

In rift-basins the subsidence rates vary systematically through time, with a period of very rapid tectonic subsidence initially, followed by a period of gradual thermal subsidence. These systematic subsidence patterns strongly influence the geometry of the rift-basin fill, which makes it convenient to divide the stratigraphy into pre-, syn- and post-rift mega sequences (Hubbard, 1988). The Upper Jurassic Epoch extends from the Oxfordian to the Volgian spanning some 16Ma. In order to include the entire syn-rift mega-sequence however, it is common to include parts of the Callovian (latest mid-Jurassic) and Ryazanian (earliest Cretaceous) extending the Late Jurassic time interval to some 20Ma coinciding with the Late Jurassic – Early Cretaceous rifting event (Fraser et al., 2003).

In the North Sea basin most of the major reservoirs are found within the pre-rift mega-sequence (e.g. Brent Group, Statfjord and Dunlin Formations), trapped in rotational fault-block structures and capped primarily by the post-rift unit. The post-rift mega-sequence was deposited during thermal subsidence and consists mainly of clay and mudstones that provide efficient seals for the pre-rift and syn-rift reservoirs. However, the post-rift was also affected by basin margin uplift causing some subsequent sand deposition. Examples of such sands in the South Viking Graben include the Paleocene sediment gravity flow deposits making up the Balder and Jotun fields (Bergslien, 2002).

The Upper Jurassic, or syn-rift sediments, are preserved mainly in Grabenal areas where they can reach thicknesses of up to 3000m (Fraser et al., 2003). The top of the Upper Jurassic can easily be recognized on seismic by the regional Base-Cretaceous reflector. From mapping of Base-Cretaceous it is clear that the top of the Upper Jurassic is presently buried to about 3000-5000 m in the South Viking Graben and 2000-3000 m on the Graben flanks (Fraser et al., 2003). It is estimated that about 20% of the present hydrocarbon reserves in the North Sea is found in the Upper Jurassic. However, a majority of the yet-to-be-found reserves are expected to be found in the Upper Jurassic, which makes it one of the most important remaining exploration targets in the North Sea.

2.3.1 Lithostratigraphy

A standard lithostratigraphic nomenclature was established for the Norwegian North Sea by NPD during the 70's and 80's (Deegan and Scull, 1977; Vollset and Dorê, 1984). The Upper Jurassic rocks are engulfed by the Viking Group (UK equivalent: Humber Group) which consists of the Draupne (UK equivalent: Cimmeridge clay) and Heather Formations.

The fact that the Upper Jurassic succession was deposited during active rifting caused an irregular and fragmented bathymetry, even subaerial exposure of the crest of several rotated fault blocks which formed elongated islands at that time. This resulted in restricted oceanic circulation which, coupled with a rise in relative sea level and warm climate, caused anoxic conditions to develop in Graben areas during deposition, especially of the Draupne Formation. Because of this the Upper Jurassic succession is dominated by organic rich shale deposits. However pulses of sands, such as the Brae Formation, are quite common. This thesis is particularly interested in the reservoir properties of such sands that may be deposited within the Draupne Formation in the South Viking Graben as indicated in figure 2-3.

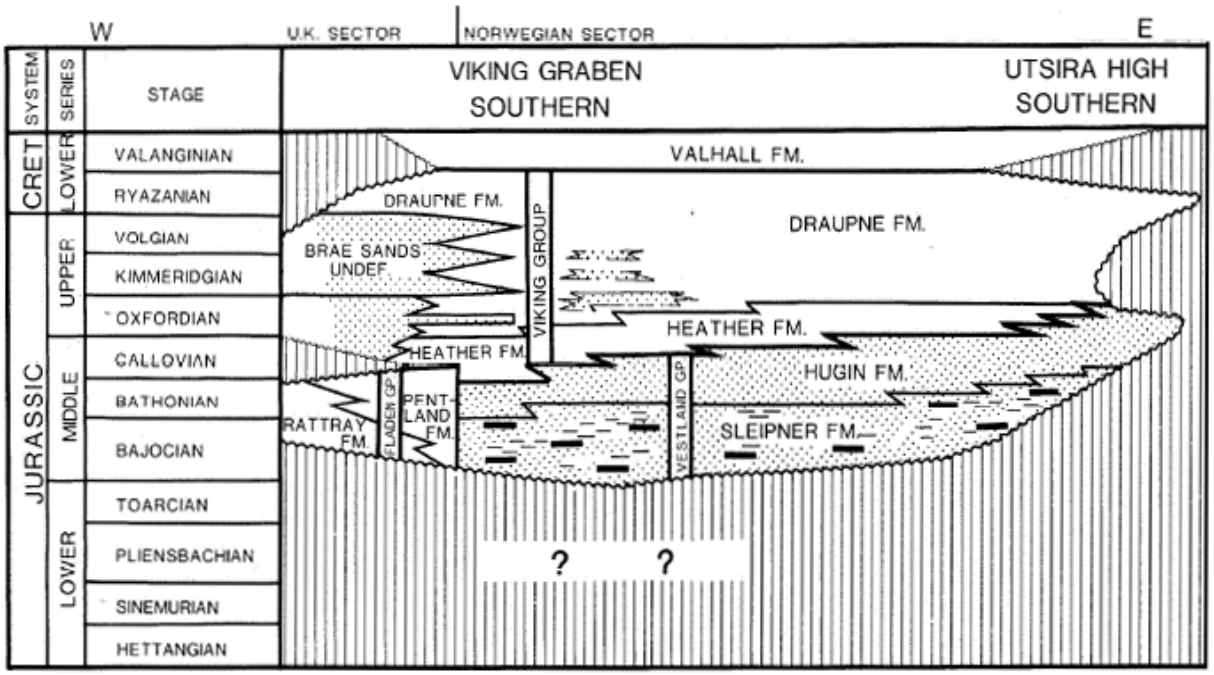

Figure 2-3. Jurassic lithostratigraphic nomenclature in the South Viking Graben. Modified after (Vollset and Dorê, 1984).

The deposition of such intra-Draupne sands are related to changes in relative sea-level, favoring sand deposition during lowstand (i.e. lowstand systems tract). Thus sequence stratigraphy is a powerful tool that enables correlation and prediction within the Upper Jurassic.

2.3.2 Sequence stratigraphic framework

Following Fraser et al. (2003) a total of eight genetic sequences (i.e. Galloway, 1989) are recognized on a sub-seismic level bounded by maximum flooding surfaces (figure 2-4 and 2-5). These sequences may be correlated with sequence stratigraphic boundaries and subdivided further (i.e. Partington et al., 1993; Rattey and Hayward, 1993).

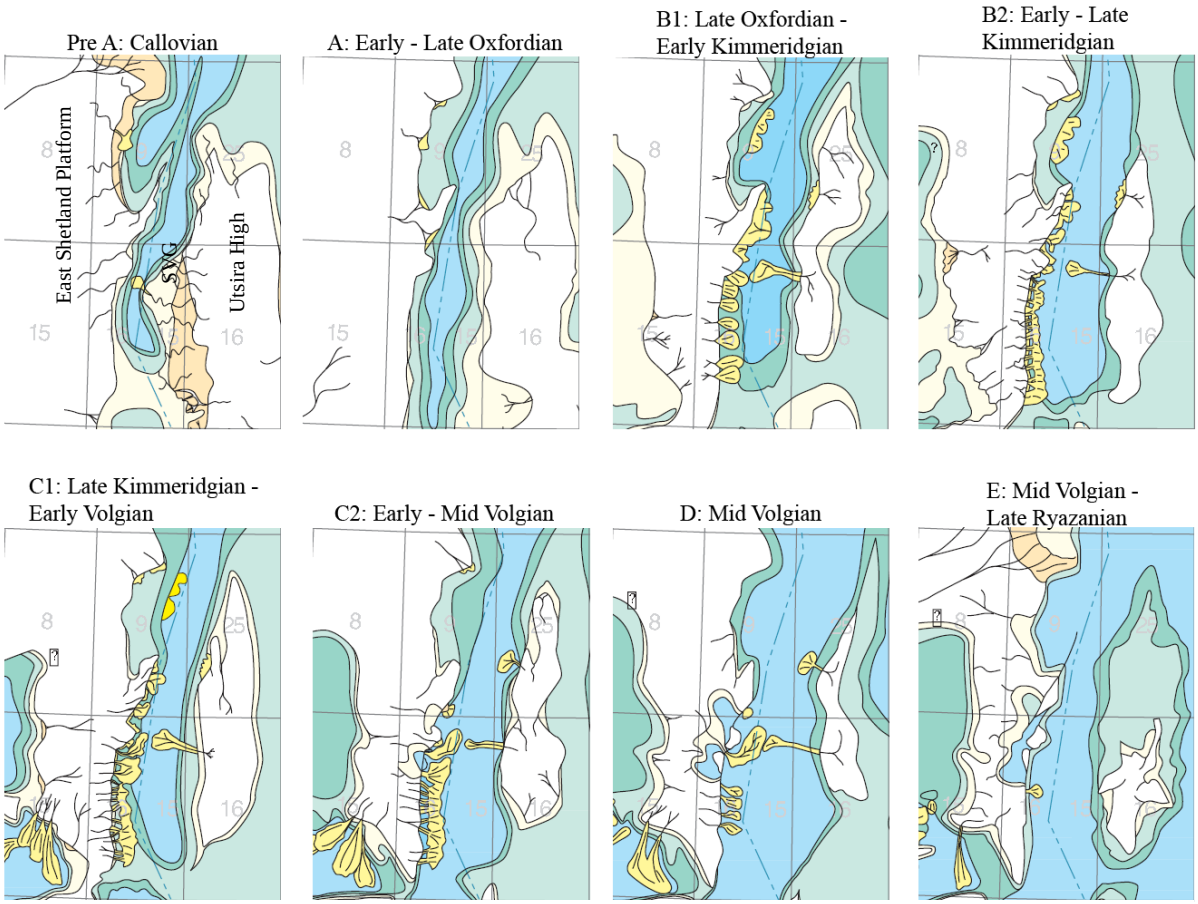

Figure 2-4. Genetic sequences and paleogeographic maps of the study area (modified after Fraser et al., 2003).

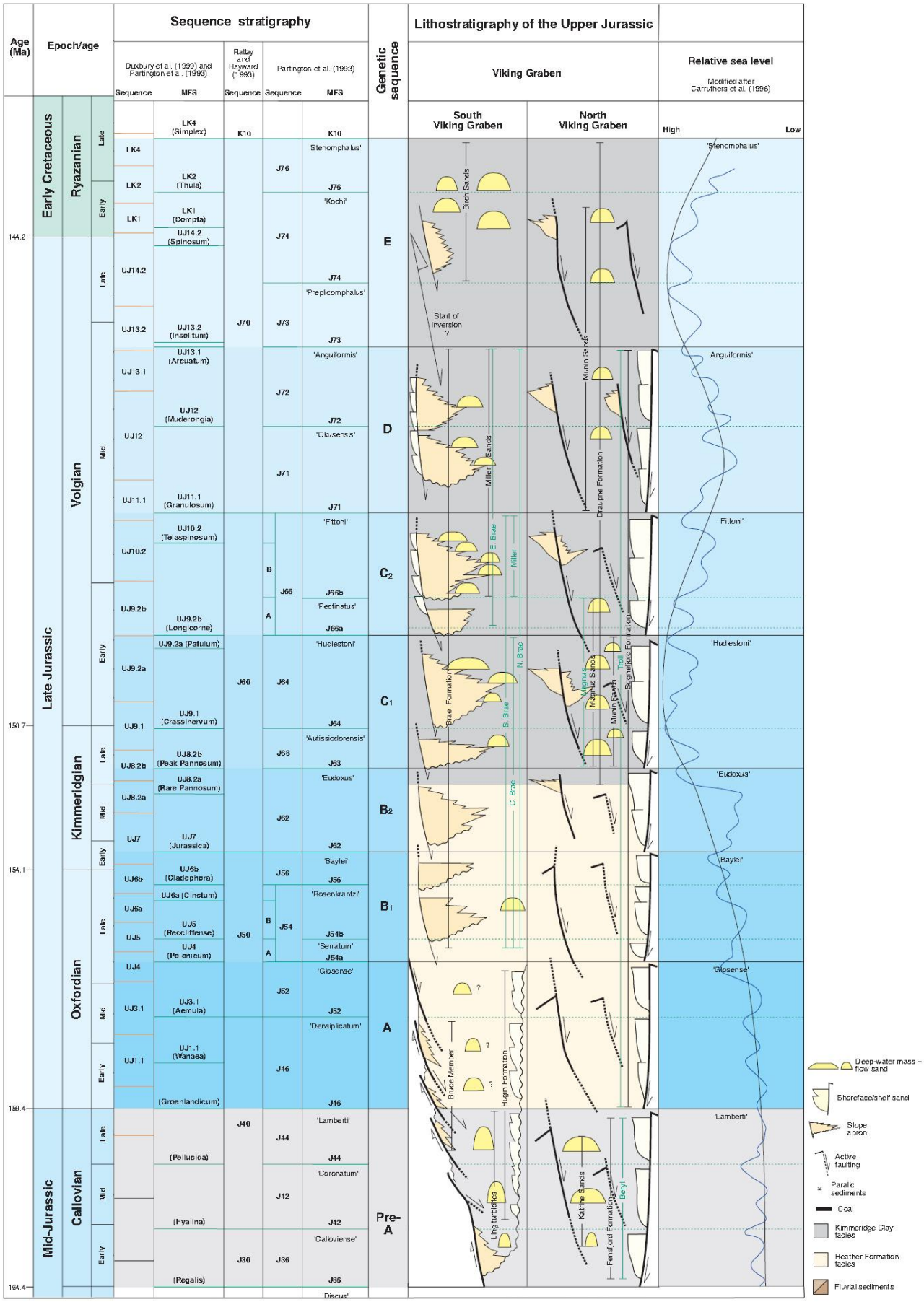

Figure 2-5. Sequence stratigraphic and lithostratigraphic framework of the study area. Modified after Fraser et al. (2003).

There are three major tectonically enhanced maximum flooding surfaces (TEMFS) that can be recognized as regional gamma-ray peaks on logs in entire North Sea basin (Partington et al., 1993). These are Eudoxus (J63), Fittoni (J71) and Anguiformis (J73) (see figure 2-5). It is important to realize that these TEMFS constrain most of the deep marine fan-systems in the study area (Partigton et al., 1993), and thus sequence stratigraphy is a very powerful exploration tool in the study area.

2.4 THE UPPER JURASSIC DEPOSITIONAL SYSTEM

Upper Jurassic sandstones are found in two main depositional settings in the South Viking Graben; submarine-fan systems and coastal-shelf/shallow marine systems (e.g. Fraser et al., 2003).

Most of the deeply buried, Upper Jurassic sandstones, which are the main target of investigation in the thesis, were deposited in a submarine-fan to deep-marine basin system (Harris and Fowler, 1987; Stow, 1985). These sediments correspond to the Brae Formation and its stratigraphic equivalents within the Draupne formation. These fans may be divided into two end member types, gravel-rich and sand rich fans, related to the Late Jurassic fault activity. The faulting led to initial conditions characterized by high hinterland relief, high stream gradients in a low efficiency system, causing fan deltas to build up gravel-rich submarine fan complexes. Later conditions are characterized by lower hinterland topography, lower stream gradients increasing the efficiency and causing sand-rich submarine-fan complexes (Fraser et al., 2003).

At the basin margins a coastal-shelf/shallow marine depositional system evolved during the Upper Jurassic (Hugin Formation). Despite the varying age of the shallow marine sediments, due to the complexity of the rifting, their physical characteristics are remarkably similar (Fraser et al., 2003).

It is not the purpose of this thesis to provide in-depth information about the depositional system. However, as for the sequence stratigraphic framework, the subdivision presented will enable the possibility of correlating the presence of porosity-preserving mechanisms, such as grain-coats to specific depositional environments or facies.

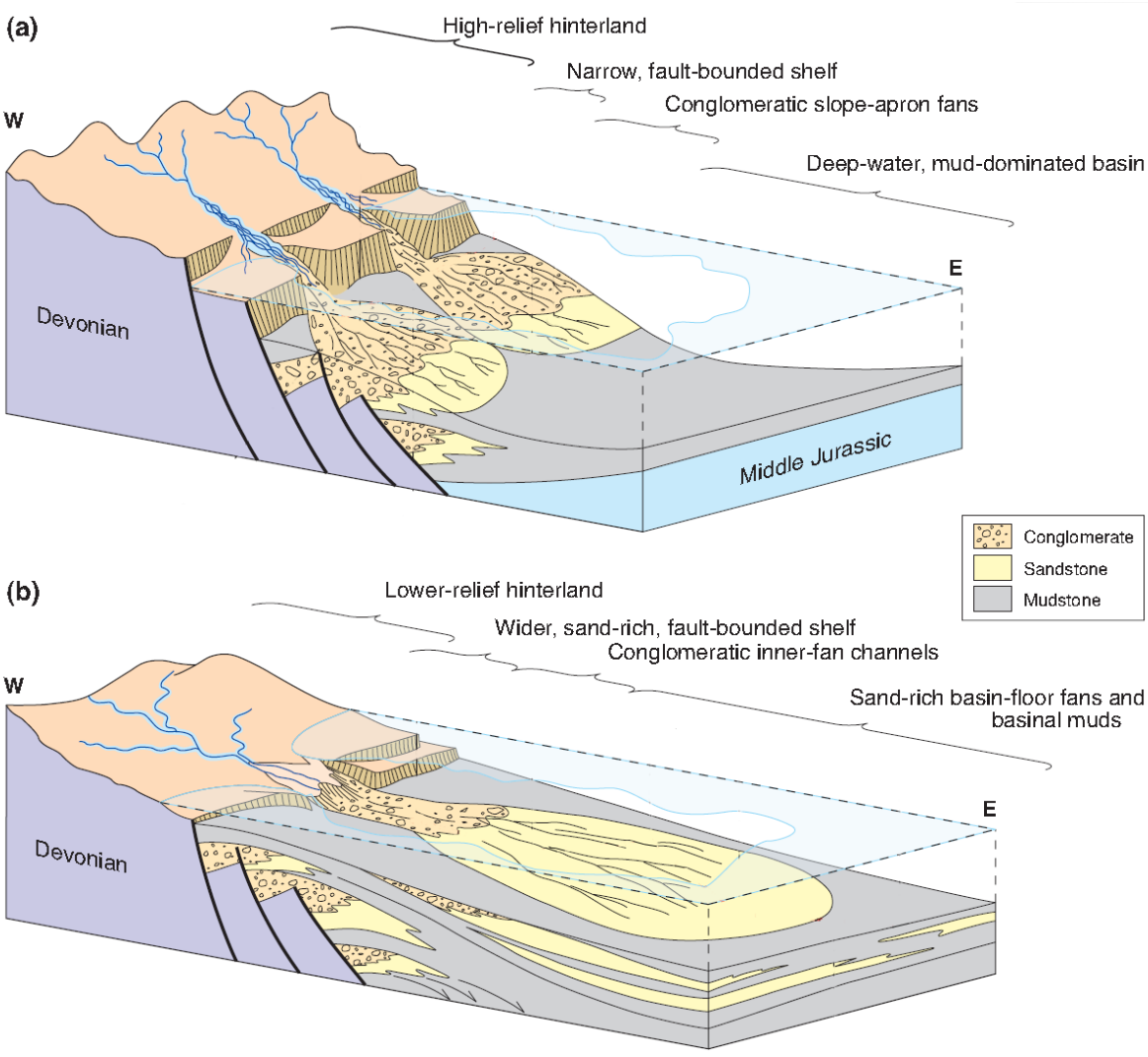

Figure 2-6. Schematic illustration of the two end member submarine fan models; gravel-rich (a) and sand-rich (b). The models are based on interpreted cores from the Brae Formation. Figure modified after Fraser et al. (2003).

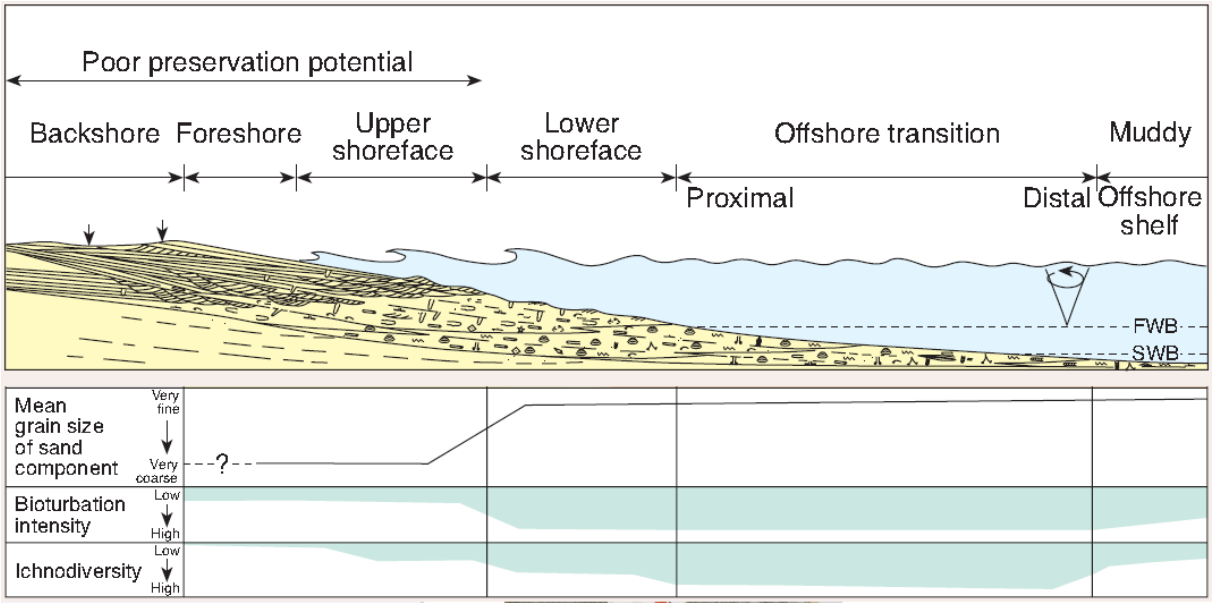

Figure 2–7. Idealized depositional model for shallow marine sandstones in the study area. Modified after Fraser et al. (2003).

CHAPTER 3: THEORETICAL BACKGROUND

3.1 DIAGENESIS IN RESERVOIR SANDSTONES

3.1.1 Introduction

During burial reservoir sandstones are subject to a large range of diagenetic processes that eventually destroy porosity, resulting in the sandstone becoming a tightly cemented quartzite. Mechanical compaction is responsible for most of the porosity loss during shallow burial, while chemical compaction becomes increasingly important at greater depth (Bjørlykke, 1999, 2003). Factors such as mineral- and textural composition and temperature-history of the sandstone are important controls on the chemical compaction of sandstones. Reservoir quality at depth is also very much linked to the initial reservoir properties immediately after deposition. These are primarily controlled by grain-size and sorting, while clay content and angularity of grains comprise important secondary controls on initial reservoir properties (e.g. Giles, 1997). Therefore depositional facies and environments are always important to consider as is provenance, which controls the sandstone composition.

This chapter will give further insight into the subjects of quartz cementation and porosity-preserving mechanisms, especially grain-coats, which provide important controls on reservoir properties in quartz-rich sandstones at intermediate and, especially, deep burial depths. First however, some of the main diagenetic processes acting on sandstones during burial will be briefly described. For these reasons it is useful to define shallow, intermediate and deep burial depths.

3.1.1.1 Defining shallow, intermediate and deep burial depths in sedimentary basins

This thesis will relate the various burial depths to important stages in sandstone diagenesis. Quartz cementation starts slowly at approximately 75-80˚C (Bjørlykke and Egeberg, 1993; Walderhaug, 1994b), which strengthens the rock and thereby marks an important transition in the sandstone diagenesis, namely the transition from mechanical compaction to chemical compaction being the main cause of depletion in reservoir properties with depth. A burial depth corresponding to 75-80˚C thus defines the boundary between shallow and intermediate burial.

The transition from intermediate to deep burial can be defined as the depth where porosities are expected to deplete below reservoir cut-off. Reservoir cut-off is generally when sandstone permeabilities deplete below 5 mD, corresponding to porosities of approximately 10-15%. In normal North-Sea sandstones this will be a function of quartz cementation, and modeling has shown to provide good approximations for this depth (Lander and Walderhaug, 1999; Walderhaug, 1996). Porosity-preserving mechanisms (i.e. grain-coats) are the exception rather than the rule and their presence may preserve porosities above reservoir cut-off well into the deep burial range.

In the North-Sea the transition from shallow to intermediate burial depths is normally at about 2-3 km, while the transition between intermediate and deep burial depths is typically around 3,5-4,5km.

3.1.2. Diagenetic processes in reservoir sandstones

Some of the main diagenetic processes acting on sandstones during burial will now be described. Quartz cementation, which is the main cause of porosity reduction during intermediate and deep burial in quartz-rich sandstones (e.g. Bjørlykke et al., 1989), will be handled more thoroughly in the following section (3.2).

3.1.2.1 Shallow burial

During shallow burial sand grains are rearranged and reorganized to form a more densely packed grid of framework grains. This process is usually referred to as mechanical compaction and may typically reduce porosity in sandstones from 40-42% initially to about 25-35% at stresses of 20-30 MPa (2-3 km) depending on grain-size and strength (Cuhan et al., 2002). Mechanical compaction is the main porosity-destroying agent during shallow burial, but chemical processes may also significantly affect reservoir properties. Two chemical processes of importance for reservoir properties during shallow burial are carbonate cementation and leaching of K-feldspar.

Carbonate cement will form at shallow depth mainly from biogenic carbonate within the rock. Biogenic carbonate becomes unstable below the redox boundary and will, due to the relatively high kinetic reaction rate of carbonate minerals, dissolve and re-precipitate as carbonate cement during shallow burial (Saigal and Bjørlykke, 1987). The fact that most carbonate cement is derived from biogenic precursors, makes the evolution of carbonate organisms important for the amount and depositional environments prone to developing carbonate cement. Pelagic planktonic calcareous organisms did not evolve until the Mesozoic (Bjørlykke, 2001), causing a "pelagic rain" of calcareous organisms. This drastically increased the amount of carbonate supplied to the sea floor, which before this time was limited to shallow water benthic organisms within the photic zone. Carbonate cement is common in Upper Jurassic sandstones and younger due to this "rain" of calcareous organisms. The biologic productivity is a major control on the amount of carbonate in the sediments, but the clastic sedimentation rate will be equally decisive. Therefore the distribution of carbonate cement is very much decided by the ratio of these two factors.

Leaching of K-feldspar and mica, and precipitation of pore filling kaolinite is a process known to significantly affect reservoir properties in important reservoirs such as the Brent Group (e.g. Bjørlykke et al., 1992). Kaolinite is thermodynamically unstable in the presence of K-feldspar, and will be transformed to illite during deep burial (120-140˚C). This illitization process will significantly affect the permeability of sandstones. The leaching of K-feldspar will cause secondary porosity enhancement as the K-feldspar grains are dissolved. However, kaolinite will precipitate in the pore space, causing only small changes in the overall porosity, but reducing the permeability. The leaching reactions can be written as:

$$\underset{\text{K-Feldspar}}{2K(Na)AlSi_3O_8} + 2H^+ + 9H_2O \rightarrow \underset{\text{Kaolinite}}{Al_2Si_2O_5(OH)_4} + \underset{\text{dissolved silica}}{4H_4SiO_4^{4+}} + 2K^+(2Na^+)$$

$$\underset{\text{Mica}}{2KAl_3Si_3O_{10}(OH)_2} + 2H^+ + 9H_2O \rightarrow \underset{\text{Kaolinite}}{Al_2Si_2O_5(OH)_4} + \underset{\text{dissolved silica}}{4H_4SiO_4^{4+}} + 2K^+(2Na^+)$$

After (Bjørlykke et al., 1992)

These reactions are not isochemical and is controlled by the K^+/H^+ ratio. Therefore the leaching reactions will stop unless there is a flow of (meteoric) water that is undersaturated with respect to the reaction products (K^+, Na^+), and thus can remove them (Bjørlykke, 1994). This is why leaching is generally strong in fluvial sediments such as the Brent Group.

3.1.2.2 Intermediate burial

Intermediate burial is marked by the onset of quartz cementation, which strengthens the rock and thereby stops further mechanical compaction. This means that from this depth on, chemical compaction is the main process acting on a reservoir sandstone.

Albitization of K-feldspar is an important diagenetic process that may significantly alter the composition of reservoir sandstones during intermediate burial. The reaction can be expressed as:

$$KAlSi_3O_8 + Na^+ \rightarrow NaAlSi_3O_8 + K^+$$

After Saigal et al. (1988)

Albitization starts at about 65 ˚C and is nearly complete at 105 ˚C (Saigal et al., 1988), corresponding to a burial depth range of about 2-3 km. As much as 30-50 % of the original K-feldspar may be albitized (Aagaard et al., 1990).

3.1.2.3 Deep burial

During deep burial the sandstone is gradually being cemented up, causing quartz cementation to start to decelerate. Quartz cementation will be described in section 3.3, but illitization is another important diagenetic process during deep burial.

The illitization of kaolinite, summarized by the reaction below, significantly reduces the permeability of reservoir sandstones.

$$\underset{\text{K-Feldspar}}{2K(Na)AlSi_3O_8} + \underset{\text{Kaolinite}}{Al_2Si_2O_5(OH)_4} \rightarrow \underset{\text{Illite}}{KAl_3Si_3O_{10}(OH)_2} + \underset{\text{quartz}}{SiO_2} + 2H_2O$$

After (Bjørlykke, 1980)

As was mentioned earlier, illitization takes place at burial depths corresponding to 120-140 C (3,7 – 4 km), given that kaolinite and K-feldspar are present (e.g. Cuhan et al., 2000). Kaolinite and K-feldspar are thermodynamically unstable if they are both present in the rock, but high activation energies are needed to drive the reaction, thus illitization takes place during deep burial. A marked decrease in permeability should be expected if the criteria for illitization are fulfilled, as is the case for example for the Brent Group. In the Brent Group permeabilities are reduced by 2 or 3 orders of magnitude at the depth where illitization is expected to kick in (Bjørlykke et al., 1992).

Besides quartz cementation, illitization is probably the most important process causing reduced reservoir properties during deep burial.

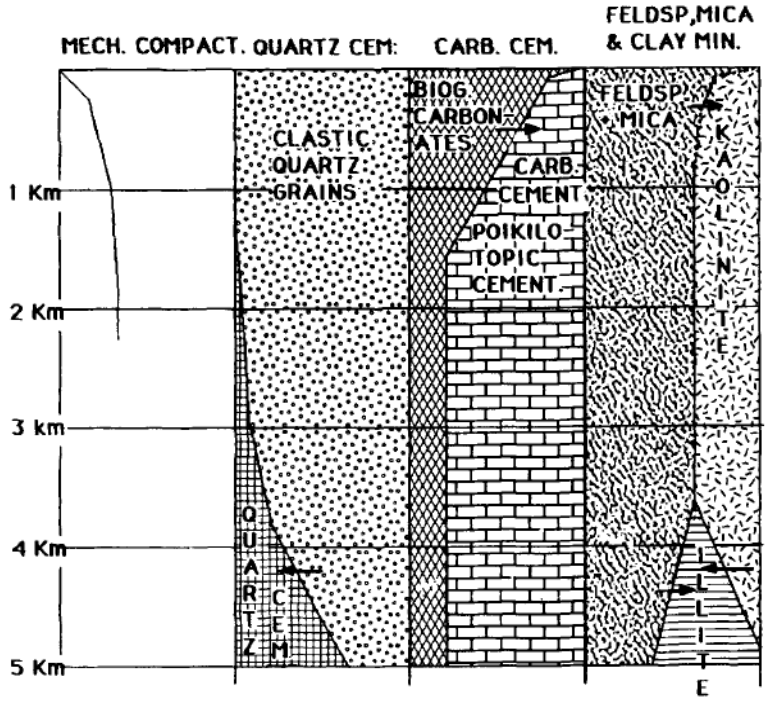

Figure 3-1. Overview of some of the main diagenetic processes affecting reservoir properties in sandstones. After Bjørlykke et al. (1992).

3.2 QUARTZ CEMENTATION IN RESERVOIR SANDSTONES

3.2.1 Introduction

Quartz cementation will become increasingly dominant as porosity-destroying agent during intermediate and deep burial as sandstone maturity increases, and has long been known as the most important process destroying porosity in deeply buried, quartz-rich sandstones (Bjørlykke et al., 1989; Blatt, 1979). However, the main source of silica and controlling factors on quartz cementation seem to have been unclear until the mid 90's with a large variety of explanations (e.g. McBride, 1989). These explanations include fluid flow processes transporting dissolved silica into sandstones from external sources and internal pressure solution processes from quartz-quartz contacts.

During the late 80's and 90's progress was made in understanding the process of quartz cementation. The models including fluid flow and pressure solution were criticized either because they require quantities of fluid flow unattainable in sedimentary basins (Bjørlykke, 1994; Bjørlykke and Egeberg, 1993; Bjørlykke et al., 1988), or because pressure solution at quartz-quartz contacts as source for silica was shown to be negligible (e.g. Bjørkum, 1996). Presently several authors have presented strong evidence that silica is sourced mainly by what Oelkers et al. (2000) referred to as illite-mica induced dissolution (I-MID) taking place at stylolites and clay rich or micaceous laminae (Bjørkum, 1996; Oelkers et al., 1992, 1996; Oelkers et al., 2000; Walderhaug, 1994a; Walderhaug, 1996). I-MID causes high enough silica supersaturations to precipitate quartz at depths as shallow as ~1km (Jahren and Ramm, 2000). However quartz cementation does not start before temperatures reach 75-80 C (2-3km) (e.g. Walderhaug, 1994b), which implies that it is the kinetics or rate of quartz precipitation, which is controlled by temperature, that exert the main control on quartz cementation (Oelkers et al., 1992, 1996).

3.3.2 Illite-Mica induced dissolution

According to the illite-mica induced dissolution model quartz cementation consists of a three step redistribution process of silica: (1) Quartz dissolution mainly taking place at stylolites and clay-rich or micaceous laminae, (2) short range diffusion of dissolved silica into the interstylolite pore space and (3) precipitation of quartz on quartz grain surfaces (see figure 3-2).

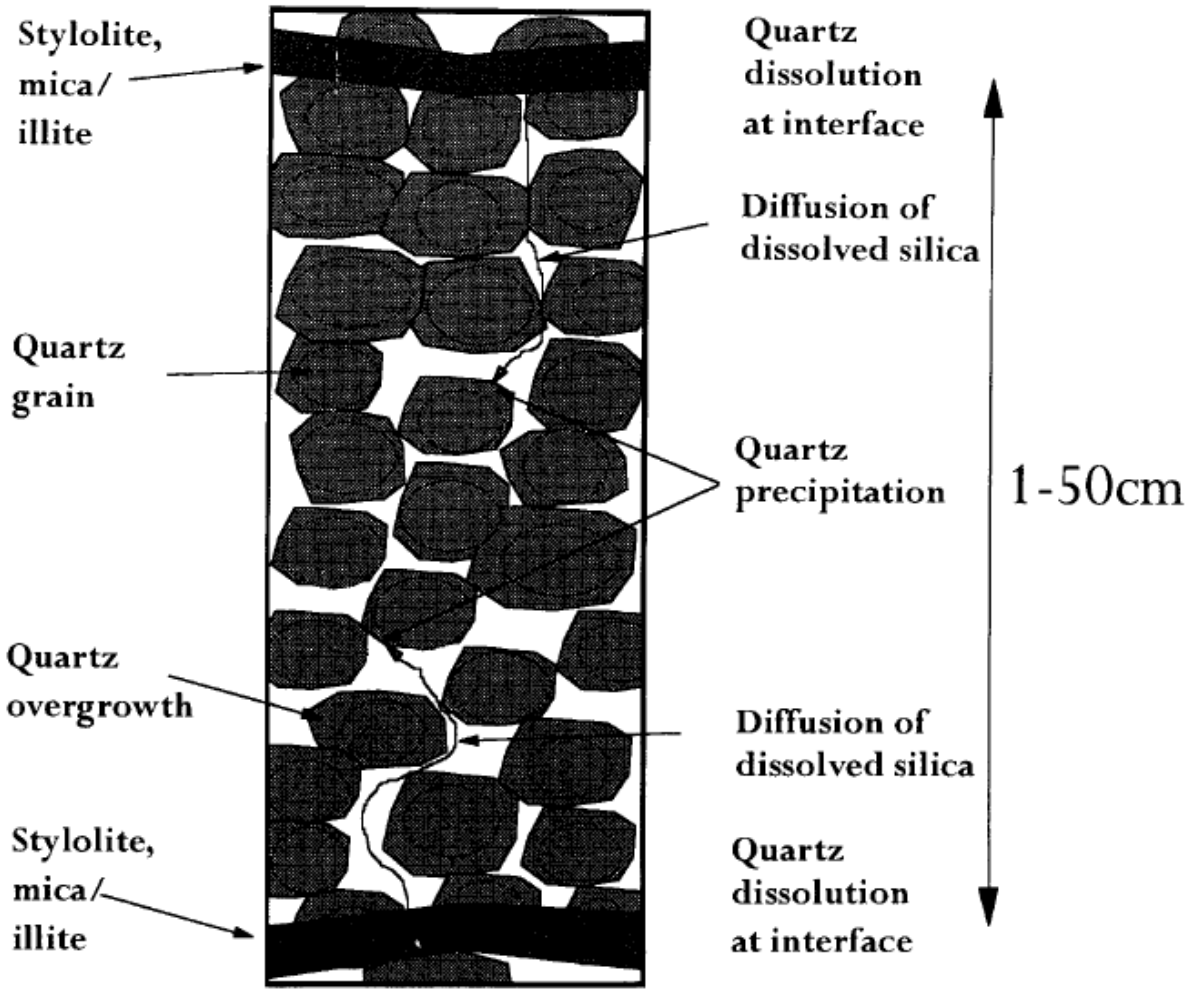

Figure 3-2. Schematic review of the I-MID model. After Oelkers et al. (2000)

The catalyzing effect of illite and mica on quartz dissolution is probably due to the charge on mica and illitic clay surfaces causing the solubility of quartz to increase slightly along these interfaces, which lead to higher silica concentrations compared to the surrounding formation

water at stylolites (Oelkers et al., 2000). This leads to a diffusion gradient of silica outwards from the stylolites where it may precipitate as quartz cement at the quartz grain surfaces.

The precipitation of quartz cement seem to be surface controlled in normal sandstones (stylolite spacing <50cm), meaning that the precipitation of quartz is the rate limiting step in this process (Oelkers et al., 1992, 1996). This makes it possible to model quartz cementation as a function of quartz surface area available for cementation and temperature-history (Walderhaug, 1994a; Walderhaug, 1996). However if the interstylolite spacing is unusually large (>50cm) gradients in the degree of quartz cementation may be observed away from the stylolites indicating that quartz cementation is transport controlled in such cases (Oelkers et al., 1992, 1996). The most mathematically advanced models take account of all three steps in the process and thus correctly predicts quartz cementation even if stylolite spacing is unusually high (Oelkers et al., 1996; Oelkers et al., 2000). However the simplified models (Lander and Walderhaug, 1999; Walderhaug, 1996) assume that quartz cementation is surface controlled and therefore model only the precipitation step thus over-predicting quartz cementation when the stylolite spacing is unusually large.

The I-MID model implies that porosity may be preserved in sandstones with large stylolite spacing (>50cm). Walderhaug and Bjørkum (2003) have reported porosities about 5-10% higher in sandstones with large stylolite spacing then expected in sandstones with normal stylolite spacing. Such sandstones are highly unusual on the Norwegian continental shelf, and the lack of stylolite precursors are probably only of local importance in preserving reservoir properties at depth (Walderhaug and Bjørkum, 2003).

Since quartz cementation is the most important porosity-destroying process in deeply buried sandstones, mechanisms that inhibit quartz overgrowths are important for preserving porosities at depth. The next chapter has been devoted to this topic.

3.3 POROSITY-PRESERVING MECHANISMS IN DEEPLY BURIED SANDSTONES

3.3.1 Introduction

All of the diagenetic process acting on reservoir sandstones described up to this point in chapter 3 affects reservoir quality. However, mechanical compaction and quartz cementation are the main process causing overall depletion in porosity during progressive burial in quartz rich (mature) sandstones. Therefore high porosities may be preserved to greater depths than anticipated in such sandstones if there are factors working against quartz cementation and mechanical compaction. If these factors are very significant, anomalously high porosities may occur in deeply buried sandstones.

Anomalously high porosity can be defined as being statistically higher then the maximum porosity in typical sandstone reservoirs of a given lithology, age and temperature/burial history (Bloch et al., 2002). The three main factors known for causing anomalously high porosity at depth are grain-coats, early emplacement of hydrocarbons and shallow development of fluid overpressure (e.g. Bloch et al., 2002).

Deeply buried sandstones, as defined in this thesis, will by definition normally have poor reservoir quality. However, the porosity-preserving mechanisms may cause enhanced reservoir quality in deeply buried sandstones and thus extend the economic basin such that some deeply buried prospects may be included.

3.3.2 Early hydrocarbon emplacement

A large amount of literature has been published on the relationship between hydrocarbon filling and porosity preservation. Until recently it seems that the conventional view was that early oil emplacement halts or significantly retards quartz cementation and thereby preserves porosity (e.g. Glasmann et al., 1989; Gluyas et al., 1993; Robinson and Gluyas, 1992). However, more recently it has been known that the effect of hydrocarbon emplacement on

porosity preservation has been over stated (Aase and Walderhaug, 2005; Barclay and Worden 2000b; Giles et al., 1992; Ramm and Bjorlykke, 1994; Walderhaug, 1994a).

The idea of early hydrocarbon emplacement halting quartz cementation is based on the simple fact that hydrocarbons filling the pores would halt inorganic chemical processes. However, even if a reservoir has reached maximum hydrocarbon saturation the pores will contain some water and the grain surfaces may still be in contact with water if the grains are preferably water-wet. The wettability, defined as "the tendency of one fluid to spread on or adhere to a solid surface in the presence of other immiscible fluids" (Craig, 1971), of the sandstone is therefore the most important factor to consider.

Worden et al. (1998) came up with three end-member models of how hydrocarbon emplacement would affect porosity, depending on three different quartz cementation scenarios; (1) open system, water wet, (2) closed system, water wet and (3)closed system, oil wet. The first scenario assumes silica to be supplied externally through advection. This is in conflict with the working model for quartz cementation and will be discarded. It was shown by Bjørlykke (1994) that silica for quartz cementation cannot be sourced from advection. However, the two scenarios assuming a closed system and varying wettability probably give a good picture of how hydrocarbon emplacement affects porosity preservation.

In the closed system, oil wet scenario quartz cementation is halted since no silica bearing water is in contact with the grain surface. In the water wet scenario quartz cementation may be retarded, due to reduced diffusion rates, but not halted. Carbonates are known to be predominantly oil-wet, while sandstones are predominantly water-wet (Barclay and Worden 2000a), but the composition of the oil and other factors such as grain-size and porosity may also affect the sandstone wettability (Barclay and Worden 2000a; Worden et al., 1998). However, work done on Jurassic sandstones on the Norwegian continental shelf suggests that quartz precipitation rates in these sandstones are not affected by the presence of hydrocarbons in the pore space (e.g. Walderhaug, 1994a). Instead, it is proposed that grain-coats may be the cause of anomalous porosity in several Upper Jurassic oil fields that have previously been

explained by early hydrocarbon emplacement (Aase et al., 1996; Aase and Walderhaug, 2005). W,1990

Porosity preservation due to early hydrocarbon emplacement in sandstones is controversial. The onset of hydrocarbon generation from Draupne in the study area was in the Paleocene peaking in middle Miocene (Justwan et al., 2006). The Upper Jurassic sandstones are often found within the Draupne Formation and may have been charged before significant quartz cementation took place, so the study area is potentially a good place to study early hydrocarbon emplacement in sandstones.

3.3.3 Fluid overpressure

Fluid overpressure is pore-fluid pressures significantly larger than hydrostatic pressure. Overpressure will significantly reduce the effective stress in sandstones, and thus reduce mechanical compaction significantly if it is introduced during shallow burial and persists through geologic time. Even if overpressure develops at shallow depths and persists through time it will have negliable effects on quartz cementation in typical North Sea reservoir sandstones (Bjørkum, 1996). Therefore, to which extent overpressure may be the cause of anomalous porosity in deeply buried, mature sandstones will be a function of quartz cementation as well as the timing of overpressure build up. In deeply buried, mature sandstones overpressure may be an important factor causing anomalous porosity if coupled with other factors slowing down quartz cementation, such as grain-coats. In immature sandstones containing a significant fraction of ductile grains and less quartz (meaning that quartz cementation is less effective in destroying porosity) overpressure will be more efficient as single porosity-preserving mechanism.

In the North Sea two mechanisms are responsible for the development of overpressures: (1) the rate of pore volume reduction is fast relative to the rate of fluid release or (2) the rate of pore fluid expansion is fast relative to the rate of fluid release (Bloch et al., 2002). The Lateral permeability distribution may typically be important for developing fluid overpressures. A continuous low permeability zone, even if it is thin, may cause the buildup of fluid

overpressures. Overpressures may build up to fracture pressure at which point it will leak-off. The fracture pressure is equal to the sum of the minimum stress (usually the horizontal stress) and the tensional strength of the rock.

Through the collaboration with DNO the IHF pressure-database for the Norwegian continental shelf has been accessible. The formation pressures and LOT indicating the fracture pressure from wells in the study area will be included when discussing the possible causes of anomalously high porosity in the study area (section 3.3.5).

3.3.4 Porosity-preserving grain-coats

Chlorite and several other grain-coating minerals with porosity-preserving effects have been recognized in sandstones (e.g. Heald and Larese, 1974). These coats may be formed on framework grains authigenically or allogenically (prior to burial). Grain-coats cover the grain surfaces and thus have similar effects on preventing quartz cementation and preserving porosity regardless of their genesis. Grain-coats may lead to porosity depth trends deviating by up to 15% from what should be expected for deeply buried sandstones based on regional trends (e.g. Aase et al., 1996; Ehrenberg, 1993). Authigenic grain-coats result from processes subsequent to burial, and thus cover the framework grain surfaces except at points of grain-to-grain contact. Allogenic grain-coats however, refer to rims on framework grains that form during transportation or at the place of deposition prior to burial, thus covering the entire grain (Wilson, 1992).

At present no satisfactory methods for predicting the occurrence and distribution of these high porosity, grain-coated sands have been developed in frontier basins. In mature basins such as the North Sea however, where cores and large datasets are available sedimentological models can be made to include the mechanisms leading to the formation of grain-coats. These mechanisms seem to be linked to depositional environment and provenance, though depositional environment is probably the most common control on the occurrence of grain-coats in the North Sea.

Authigenic grain-coating chlorite, illite and micro-quartz are reported to have porosity-preserving effects on the Norwegian continental shelf (e.g. Ehrenberg, 1993; Jahren and Ramm, 2000; Ramm, 1994; Storvoll et al., 2002). In order to better understand the genesis and distribution of these minerals in sandstones offshore Norway, it is important to compare with analogues world-wide. This section is the result of a literature study on authigenic as well as allogenic grain-coats, and aims to give an overview of some of the known occurrences of these minerals world-wide, and more importantly: the processes responsible for their generation.

It is considered important for this thesis with an extensive literature review of the subject of grain-coats for two reasons. First of all grain-coats are the most common cause of anomalous porosity in deeply buried sandstones in the study area (e.g. Ramm and Bang, 1991). Secondly, there are still many unanswered questions concerning this subject. This makes the subject of grain-coats extra appealing as new information may have significant economic consequences concerning overlooked deeply buried prospects.

3.3.4.1 Authigenic grain-coating clays

Authigenic grain-coating chlorite has long been known for its porosity-preserving effect (Heald, 1965; Heald and Larese, 1974; Pittmann and Lumsden, 1968; Wilson and Pittman, 1977) and is the most widely described grain-coating mineral in the literature, known from several sedimentary basins around the world (e.g. Hillier, 1994; Humphreys et al., 1994; Pittmann et al., 1992). Several compositional variations have been reported. Two broad compositional categories seem to exist, Fe-rich and Mg-rich chlorites (Hillier, 1994). Fe-rich Chlorites are by far the most common (Hillier, 1994; Pittmann et al., 1992).

Fe-rich chlorite coats have been reported to be formed by several processes, both depositional and provenance controlled. Ehrenberg (1993) proposes that Fe-rich grain-coating chlorite is a consequence of localized iron-rich river discharge into marine water in depositional environments analogue to modern Fe-clay facies (Verdine, ooilite ironstone and glaucony facies described by Odin (1988)). Depositional controlled Fe-rich chlorite and illitic grain-

coating has also been reported from turbidites. Houseknecht and Ross (1992) state that dispersed clays, associated with secondary sedimentary structures and dewatering of channelized turbidites may be precursors to authigenic chlorite. Depositional lobes and unconfined turbidite deposits contain less dispersed clay and are extensively quartz cemented in their area of study, the Arkoma basin, Oklahoma.

Provenance may also be an important factor providing a precursor for authigenic Fe-rich Chlorite coats. Partial dissolution of volcanic rock fragments in the Tuscaloosa sandstone, Louisiana, is likely to cause precipitation of chlorite coats in this Formation (Thompson, 1979). Similar mechanisms have been reported from the Santos basin, offshore eastern Brazil (Anjos et al., 2003). The amount of volcanic rock fragments however, is critical to maintain reservoir properties. The optimal volcanic rock fragment content in sandstones containing more than 65% detrital quartz are about 10%, if the volcanic rock fragment content is higher, ductile deformation will destroy reservoir properties (Pittmann et al., 1992). Volcanic ash that is mixed or interlayered within the sediments may also be diagenetically transformed, via smectite to porosity-preserving chlorite as reported from the north Sumatra back-arc basin (Humphreys et al., 1994). This model is similar to that of Storvoll et al. (2002) (will be discussed later).

Mg-rich chlorite coats are formed in sandstones associated with evaporite environments, from interaction with Mg-rich brines (Hillier, 1994; Kugler and McHugh, 1990). They are much less common than the Fe-rich chlorite coats but have been reported from Upper Jurassic sandstones from the Mexican Gulf coast (Kugler and McHugh, 1990; Thompson and Stancliffe, 1990) and the Permian Rotligend in northern Germany (Platt, 1993).

Although chlorite coats vary compositionally and are formed by different processes it is likely that they all are formed from a Fe/Mg-rich smectitic or berthierine precursor mineral (Aagard et al., 2000; Hillier, 1994).

Authigenic grain-coating illite is not as commonly described in the litterature as chlorite, but the porosity-preserving effect of illite coats has been known for several decades (e.g. Heald and Larese, 1974; Wilson and Pittman, 1977). Storvoll et al (2002) have reported about illite and illite/chlorite coats from the Norwegian continental shelf being equally effective as chlorite coats. They suggest that illite, illite/chlorite coats are formed from a smectite precursor that is precipitated directly on the grains as a consequence of dissolution of volcanoclastic material soon after deposition. As discussed earlier, the formation of chlorite coating in other parts of the world has also been explained using a similar model (Humphreys et al., 1994). It is likely that the amount of iron in the precursor controls whether illite or chlorite forms (Aagard et al., 2000).

On the Norwegian continental shelf anomalous porosity due to authigenic grain-coating chlorite and illite has been reported from several fields within lower-middle Jurassic reservoir sandstones of the Haltenbanken area and in the North Sea (Ehrenberg, 1993; Storvoll et al., 2002).

3.4.4.2 Allogenic grain-coating clays

Literature on allogenic grain-coating clays is sparse, but Wilson (1992) defined "inherited grain-rims" as clay coats that were present on the framework grains prior to their deposition. One of the most significant characteristics of these "inherited grain-rims" is their presence also at points of grain-to-grain contact. Bloch et al. (2002) used the term grain-rims to describe this kind of coats, since they also may be formed at the site of deposition, following transport (infiltrated clays). Grain-rims and inherited grain-rims, characterized by coats covering the entire grain surface are here termed allogenic grain-coats. According to Wilson (1992) allogenic clay-coats may be associated with shelf deposits and eolian deposits. Allogenic clay coats associated with shelf deposits will be briefly reviewed here.

In marine sandstones, allogenic clay coats are most common in shelf to offshore transition sandstones and are usually thought to be generated by the passage of sand through the guts of a variety of marine sediment-feeding organisms (Wilson, 1992). It has in fact been

demonstrated that clay coats form when sand is digested by the polychaete worm Arenicola marine (Needham et al., 2005), and by analogy clay coats should form from digestion by other sediment-feeding organisms that digest sand-size grains, such as gastropods. These allogenic grain-coats have further been proposed as precursors to authigenic chlorite (or illite) coats (Worden et al., 2006).

3.3.4.3 Micro-crystalline quartz coats

Micro-crystalline quartz coats (micro-quartz) are less frequently described in the literature compared to clay coats, and probably underreported because they may be hard to interpret from petrographical examinations (e.g. Bloch et al., 2002). However, Heald & Larese (1974) and Heald & Renton (1966) found "secondary chert" to prevent quartz growth. Most of the published literature on micro- quartz coats seem to be from the North Sea region where it has been reported in Upper Jurassic and Cretaceous sandstones of the Central Graben/Morray Firth (Aase et al., 1996; Hendry and Trewin, 1995; Ramm and Forsberg, 1991; Ramm et al., 1998) and South Viking Graben (Jahren and Ramm, 2000; Ramm and Bang, 1991).

The formation of micro-quartz is linked to diagenetic transformations of sponge spicules of the siliceous sponge Rhaxella Perforata (Hendry and Trewin, 1995; Ramm et al., 1998). Two, important constraints on the distribution of micro-quartz can be derived from this fact. Firstly Rhaxella is common in Late Jurassic to Early Cretaceous, which means that micro-quartz is limited to stratigraphic intervals of this age. Secondly the distribution of micro-quartz is limited to depositional environments prone to this kind of organism and their reworking paths into sand rich depositional systems (Aase et al., 1996). This implies a sedimentological control on micro-quartz distribution.

The actual diagenetic transformation of silica follows a dissolution-reprecipitation process of opal A to opal CT and opal CT to quartz, which is the stable SiO_2 polymorph in the shallow crust (Williams and Parks, 1985). Opal A and opal CT are thus metastable phases and exist only due to the slow kinetic reaction rate of the silica transformation process. The relationship between solubility and surface area of the various phases provide a good explanation to the

transformation of silica (figure 3-3) (Williams and Parks, 1985). The solubility of quartz as a function of surface area has been thought to be the explanation of the porosity-preserving properties of micro-quartz. According to Aase et al. (1996) micro-quartz coats preserve porosity by causing a slightly higher silica concentration in the adjacent pore-water compared to detrital quartz (because of the larger surface area of the micro-quartz coated surfaces). These concentrations are thought to act as concentration barriers hindering diffusive transportation of silica to the grain surfaces. Other authors (Ramm and Bang, 1991; Ramm et al., 1998) have suggested that the geometrical configuration (random) hinders growth of quartz overgrowths which are always in optical continuity with the detrital quartz. The latter is likely to be more important (J. Jahren, pers. comm.).

The transformation of silica probably takes place at burial depths corresponding to temperatures between and 35-71 C (Vagle et al., 1994). Similar observations have been reported by Hendry & Trewin (1995) from the Scapa Member in the North Sea region. They reported silica transformation taking place at a burial depth of about 1-2 km.

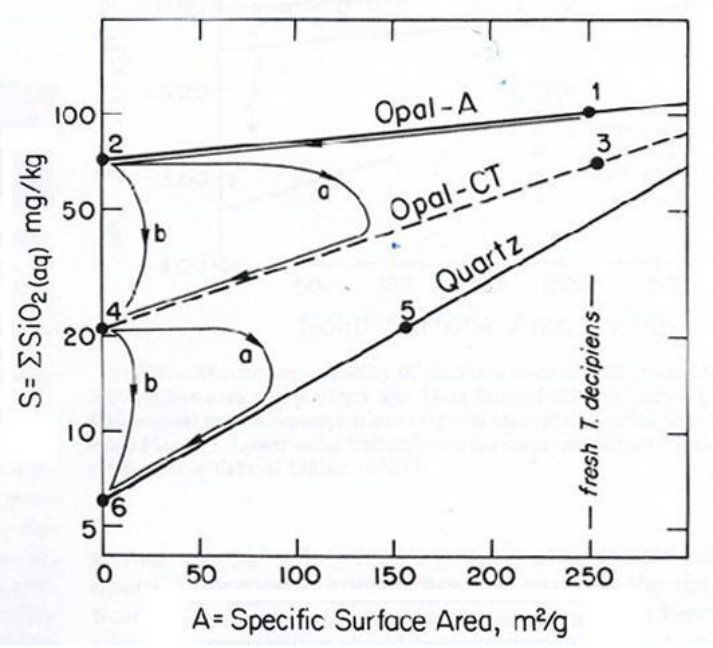

Figure 3-3. Transformation of silica after (Williams and Parks, 1985)

3.3.4.3 Controls on grain- coats

Through this section (3.3.4) it has been shown that grain-coats are controlled primarily by depositional environment and provenance. Table 3-1 lists the various types of grain-coats according to the factor most critical for their formation. Lithological factors such as grain-size exert a secondary control on grain-coats porosity-preserving effects at great depth in mature sandstones. Fine grained sands have a larger surface area than coarse grained sands, meaning that grain-coats are more likely to preserve porosity to a higher degree in coarse sands since the same coating-fraction will leave a larger surface area available for quartz overgrowths to precipitate in fine grained compared to coarse grained sands.

Table 3-1. Summary of the main controls on formation of the various grain-coats discussed in this section.

Grain coating mineral	Control: Depositional environment (DE) vs provenance (P)	References
Chlorite (Fe-rich)	DE: Shallow – marginal marine near Fe-rich, tropical river inputs	Ehrenberg (1993)
Chlorite (Fe-rich)	P: dissolution of volcanic rock fragments	Thompson (1979); Anjos et al. (2003)
Chlorite (Fe-rich), illite, illite/chlorite	P: Dissolution of volcanic ash	Strovoll et al. (2002); Humphreys et al. (1994)
Chlorite (Fe-rich)	DE: Confined turbidite channels	Houseknecht and Ross (1992)
Chlorite (Mg-rich)	DE: Aeolian or sabkha sands associated with evaporates	Kugler and McHugh (1990); Thompson and Stancliffe (1990); Platt (1993)
Clay	DE: Burrowed shelf to offshore-transition sands	Wilson (1992); Worden et al.(2006)
Micro-quartz	DE: Rhaxella Perforata	Aase et al. (1996); Hendry and Trewin (1995); Ramm et al. (1998)

3.3.5 Anomalously high porosity in the study area

Early hydrocarbon emplacement

Early hydrocarbon emplacement most likely have negliable effect on preserving porosity in sandstones in the study area (e.g. Aase and Walderhaug, 2005; Barclay and Worden 2000b; Walderhaug, 1994a). This is because they are water wet and therefore quartz grains are in contact with a continuous water film enabling silica diffusion. The effect of early hydrocarbon emplacement will not be investigated further here.

Fluid overpressure

Fluid-overpressures may be a significant factor in combination with grain-coats for preserving porosity to great depths in the study area. Figure 3-4 shows pressure data from the IHF database (Appendix F). It is clear that wells located on the Terraces are at hydrostatic pressures, while wells in the Vana and Vilje sub-basins are highly overpressured.

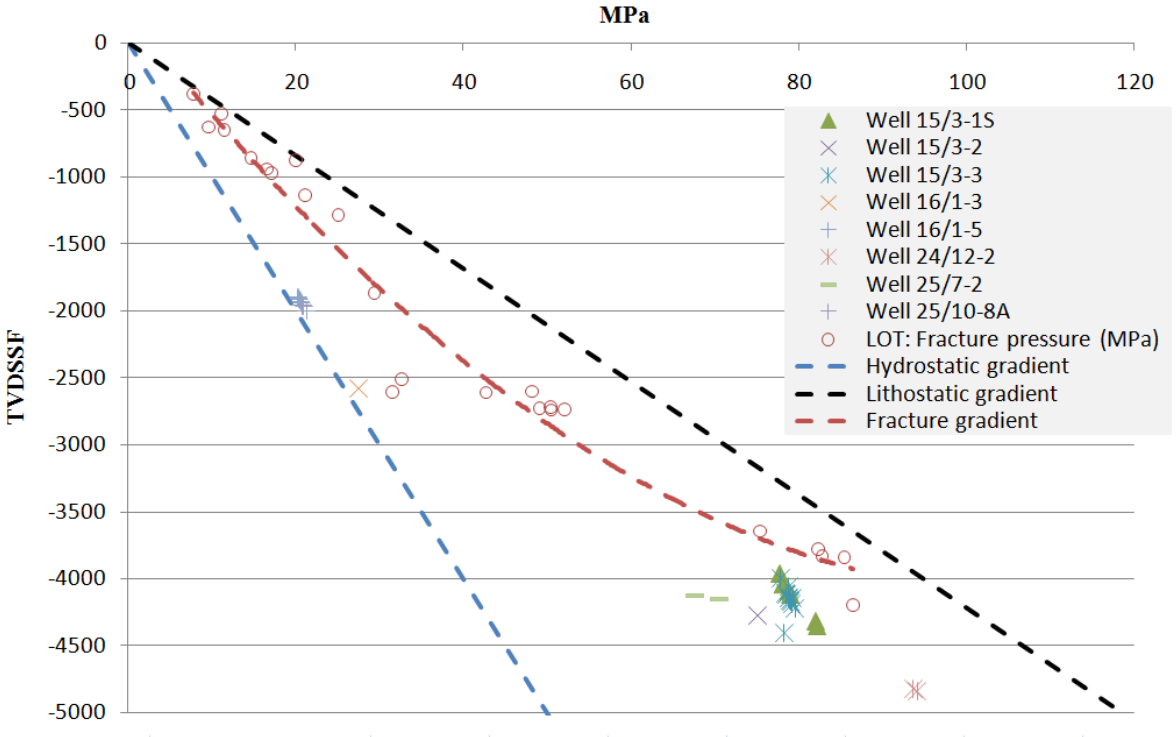

Figure 3-4. Formation pressure plot for the available Upper Jurassic data in the IHF pressure-database along with LOT plots and the hydrostatic and lithostatic gradients. Note the increase in the fracture gradient corresponding to the onset of quartz cementation.

It seems that the formation pressure distribution is related to the structural setting of the area. Graben areas, such as Vilje and Vana, have become pressure compartments sealed by shales vertically and faults (and/or shales) laterally, while pressure build-up on the Terraces has been able to bleed-off laterally. This implies that a disequilibrium compaction state may have been present since the Upper Jurassic in Vilje and Vana causing overpressures approaching the fracture gradient throughout this time. Alternatively overpressure may have developed at a later stage. Depending on early/late development of overpressure, two positive effects with respect to reservoir quality in deeply buried sandstones should be expected.

i. *Reduction in mechanical compaction*. This will cause the porosity at the onset of quartz cementation to be up to about 10% higher compared to hydrostatic conditions (Cuhan et al., 2002). The rate of quartz cementation should in such a case be higher due to the larger surface area available for quartz precipitation. It is necessary for overpressure to develop at an early stage to get this effect.

ii. *The depth to which coated sands preserve porosity*. Coated sandstones will have a lower compressibility compared to cemented sandstones. Thus coated sands will fracture at some point (effective stress equal to approximately 40MPa (Cuhan et al., 2002)), which will cause new nucleation surfaces for quartz cementation and rapid porosity loss. Consistent overpressure will delay this fracturing by reducing the effective stress. This effect should be of importance in the Vilje and Vana sandstones, since overpressure does not have to develop at shallow depths.

The effects of overpressure are for these reasons considered important and will be evaluated further in the chapter 7.

Grain-coats

Grain-coats are known to cause anomalous porosity in the study area and micro-quartz coats are commonly reported (Aase et al., 1996; Aase and Walderhaug, 2005; Hendry and Trewin, 1995; Jahren and Ramm, 2000; Ramm and Bang, 1991). Depositionally controlled chlorite and illite coats found in confined turbidite channels may be a yet-to-be-found cause of anomalous porosity in the study area, and channelized turbidite facies as described by

Houseknecht & Ross (1992) should therefore be interesting prospects. Clay-coats in general seem rare or absent in the study area judging by the literature search. This may however be because they are overlooked.

Summarizing remarks

The prospectivity of deeply buried sandstones in Vilje and Vana seems promising considering the high overpressures and frequent reporting of grain-coats in the area. In the following chapters this will be investigated further as results from the three levels of investigation, (i) well correlation and petrophysical evaluation, (ii) core description and (iii) petrographic analysis, will be presented. The results from these chapters will be evaluated further in a modeling study (chapter 8). Here porosity will be modeled as a function of mechanical compaction and quartz cementation.

CHAPTER 4: METHODS AND DATA

4.1. INTRODUCTION

This study has been subdivided into three levels of investigation that have different resolutions representative of the tool of investigation:

i. Well correlation and petrophysical evaluation is limited by the resolution of wire-line logs (~10^{-1}m).

ii. The core description is based on studies of the core in "hand-specimen" and is therefore limited to the resolution of the human eye (10^{-2} - 10^{-3} m).

iii. The resolution of the petrographic analysis is on a microscopical scale (10^{-3} - 10^{-6} m) depending on the microscopic tool.

Data from these levels of investigation are used to calibrate a porosity-predicting algorithm similar (simplified) to the exemplar algorithm (Lander and Walderhaug, 1999). These four "methods" will be described shortly.

It should be noted that a large amount of data has been available for this study through DNO. Well reports (e.g. Bastien et al., 1975; Bayliss, 1976; BP, 2001; Florvaag and Kristensen, 1982; Klungsøyr et al., 1999; Paoloni and Evensen, 1979) have been especially valuable, as has (unpublished) biostratigraphical reports (appendix E). In addition WDSS, maps and other information available at the Norwegian Petroleum Directorates webpage (www.npd.no) has been an invaluable source of information.

In order to be able to narrow down the discussion (chapter 9) to the subjects most critical to the purpose of this study some uncertainties related to the methods will be briefly discussed here. I want to point out that it is not the method of modeling or the various algorithms employed in the petrophysical evaluation that are the main purpose of this study. Therefore these algorithms may be improved, but are considered to provide acceptable results for this study.

4.2 WELL CORRELATION AND PETROPHYSICAL EVALUATION

4.2.1 Well correlation

Well correlation was carried out for both lithostratigraphic and sequence stratigraphic units.

The sequence stratigraphic subdivision (figure 2-5) is based on the recognition of maximum flooding surfaces, that represent sediment starved, condensed intervals. These surfaces usually appear as peaks on the gamma-ray log and may also be identified as sonic troughs and density peaks in shaly lithologies. Pulses of sand deposition complicated the interpretation in the deep marine environment, while hiatuses made correlation of wells in the shallow marine environment dependent upon biostratigraphical reports (e.g. appendix E).

Identification of lithostratigraphic units was easier in the study area. The Draupne Formation generally has a very high gamma-reading (often above 150 api), and a marked increase was observed compared to the Heather Formation. Hugin and Brae/intra Draupne Formations are sandy lithologies and can easily be distinguished from the Heather and Draupne. Coal beds in the Sleipner Formation were identified in several of the wells, and these were helpful marker beds in these wells.

The gamma-ray and density log will be used in well-correlation figures, but several other well logs that are good lithology indicators were also studied (these include the spontaneous potential log (SP), gamma-ray log (GR) and combinations of neutron (NPHI), sonic (DT) and density (RHO) logs).

The well correlation was carried out in Petrel.

4.2.2 Petrophysical evaluation

When the wells had been correlated and the sequences identified and subdivided, the logs and the well-tops were loaded into matlab. This gave the possibility to easily employ various algorithms to large amounts of data. The logs were sometimes loaded into excel where further calculations and plotting could be done. Petrel, Matlab and Excel was used interactively. The results presented from the petrophysical evaluation are mainly an evaluation of sandstone porosity from the density log (water saturations and porosity from other logs were also evaluated, but will not be presented here), since density-porosity gave the best correlation when compared to Helium-porosity measurements. The resulting excel sheets with well-log and density-porosity data for Upper Jurassic sandstones are given in appendix C.

The petrophysical evaluation may for simplicity be divided into two steps that will be explained in more detail.

Step 1 is a matlab algorithm that applies filters enabling the removal of shales and carbonate/carbonate cemented lithologies and sorts the well-data into the genetic sequences described. Turning filters on or off enables a large amount of different evaluations. For example porosity data from clean sandstones can be obtained and compared to modeled porosity-depth trends, or the sandstone porosity distribution in each genetic sequence may be investigated, etc.

Step 2 describes the method used to calculate the porosity in these sandstones. In addition a brief discussion on the error sources related to the density-porosity is included.

Step 1: Filtering

The Viking Group intervals of the available logs were loaded into matlab as matrixes. The column vectors of the matrixes corresponded to the various wire-line logs, while the row vectors gave the log readings at a certain depth in a specific well. By organizing the log data in this manner filters could be employed in order to eliminate row vectors corresponding to non-sand dominated intervals (figure 4-2). For evaluation of sands the filter was set to eliminate row vectors with GR readings below 60 (shale filter). In addition to this the density and sonic logs proved quite efficient in order to identify and eliminate calcite cemented sandstones and lithologies containing significant amounts of dolomite and calcite. These intervals were removed by eliminating row vectors with a bulk density reading above 2,65 and a sonic reading below 56 (carbonate filter). The matlab code for the filtering process is given in appendix B.

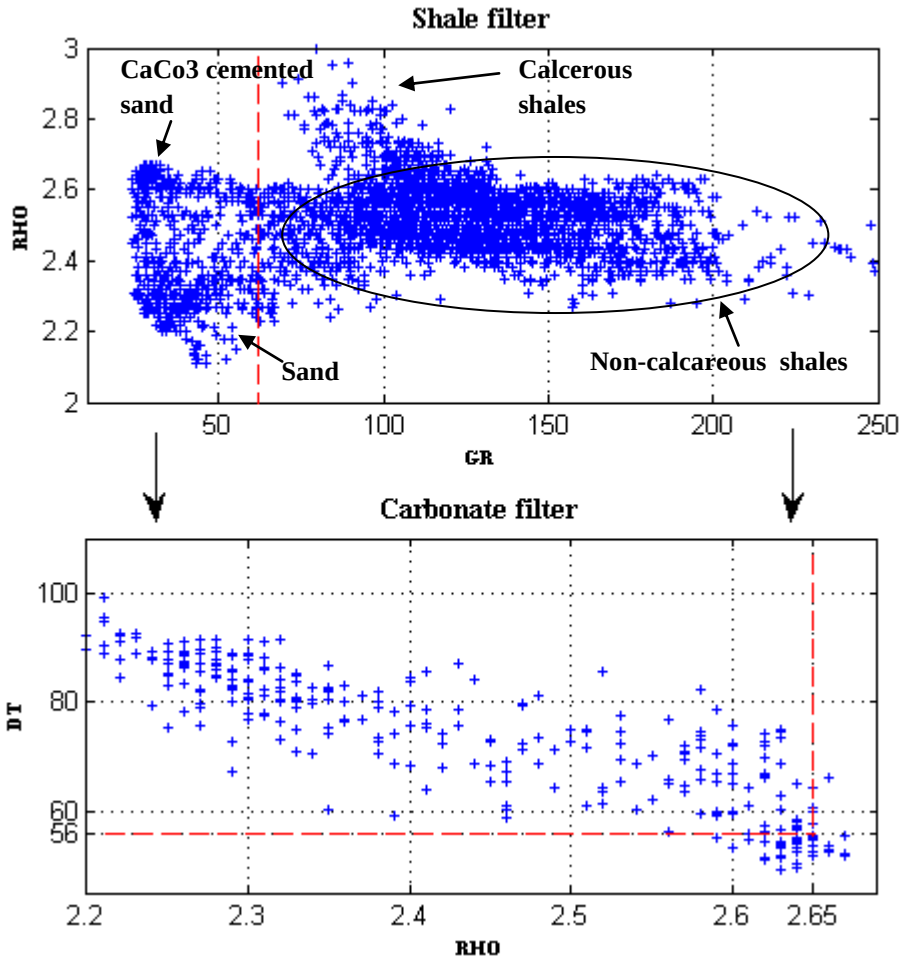

Figure 4-2. Graphical illustration of the filtering process (step 1). The shale filter removes shales (GR>60). Thereafter the carbonate filter removes extensively carbonate cemented sands and carbonate lithologies. The data in the figure is taken from well 15/3-7.

Step 2: Calculating porosity

In pure quartz-arenites the bulk density, ρ_b, can be expressed as an arithmetic average:

$$\rho_b = \Phi \times \rho_f + (1 - \Phi)\rho_{qz} \qquad \text{(equation 4-1)}$$

The bulk density of quartz-rich sandstones containing a certain fraction of shale, V_{sh}, may be expressed:

$$\rho_b = \Phi \times \rho_f + V_{sh}\rho_{sh} + (1 - \Phi - V_{sh})\rho_{qz} \qquad \text{(equation 4-2)}$$

These expressions were employed to calculate sandstone porosities from the density log. The porosity equations become:

$$\Phi = (V_{sh}(\rho_{sh} - \rho_{qz}) + \rho_{qz} - \rho_b) / (\rho_{qz} - \rho_f) \qquad \text{(equation 4-3)}$$

Or, if ρ_{sh} is assumed to be equal to ρqz:

$$\Phi = (\rho_{qz} - \rho_b) / (\rho_{qz} - \rho_f) \qquad \text{(equation 4-4)}$$

The density log has the capacity of penetrating only approximately 30 cm into the formation (e.g. Schlumberger, 1998). This means that the density tool measures in the flushed zone in permeable formations. Therefore, the fluid-density may be assumed to be equal to the mudfiltrate density for permeable intervals. The drilling-mud densities varies from approximately 1,3 – 2 g/cm^3 in the Upper Jurassic intervals of the wells in the study area (www.npd.no and well reports). However the mudfiltrate density should be somewhat lower then the drilling-mud density assuming that the less dense particles will tend to invade the formation more readily. In the calculations the fluid-density is assumed to be equal to the mudfiltrate-density which is set to be 1,1 g/cm^3.

The volume of shale will also be of importance for the porosity equations if $\rho_{sh} \neq \rho_{qz}$. The volume of shale will be expressed as follows for consolidated rocks (intermediate and deep burial):

$$V_{sh} = 0{,}33\ (2^{(2\text{-}IGR)}\text{-}1) \qquad \text{(equation 4-5, Desbrandes, 1985)}$$

And for unconsolidated rocks (shallow burial):

$$V_{sh} = 0{,}083\ (2^{(3{,}7\text{-}IGR)}\text{-}1) \qquad \text{(equation 4-6, Desbrandes, 1985)}$$

Where

$$I_{GR} = (GR_{log} - GR_{clean}) / (GR_{shale} - GR_{clean}) \quad \text{(equation 4-7)}$$

Whether $\rho_{sh} \neq \rho_{qz}$ will be investigated in section 4.3.2.1. Values for GR_{shale} and GR_{clean} will also be obtained in this section. Since the Upper Jurassic (Draupne Formation especially) has such high gamma readings the mean GR value for shales (GR>60) will be used as GR_{shale}. GR_{clean} will be set equal to the minimum gamma-ray value. Each well will be assigned unique values derived from Upper Jurassic intervals only.

Error sources related to density-porosity

There are several pitfalls in the calculated density-porosity. The most obvious errors are related to (i) residual gas in the flushed zone and (ii) collapse of the bore-hole, both cases causing erroneous high density-porosity. The caliper log was used to evaluate bore-hole collapse, and in general they were rarely encountered. Helium-porosity measurements from core-plugs are a more accurate way of measuring porosity, especially in hydrocarbon-bearing zones. Helium-porosity from hydrocarbon bearing Upper Jurassic intervals from well 15/3-1S were available (Bastien et al., 1975; Delclaud, 1975) and comparison with this data showed acceptable deviations between density- and helium-porosity in these hydrocarbon bearing zones. However, figure 4-3 indicates that residual gas may cause an apparent density-porosity that is about 5% (< 5%) above the actual porosity. The purpose of this study however, is not to obtain accurate porosity-depth trends, but rather to locate zones of anomalously high porosity. For this purpose the density-porosity is considered satisfactory.

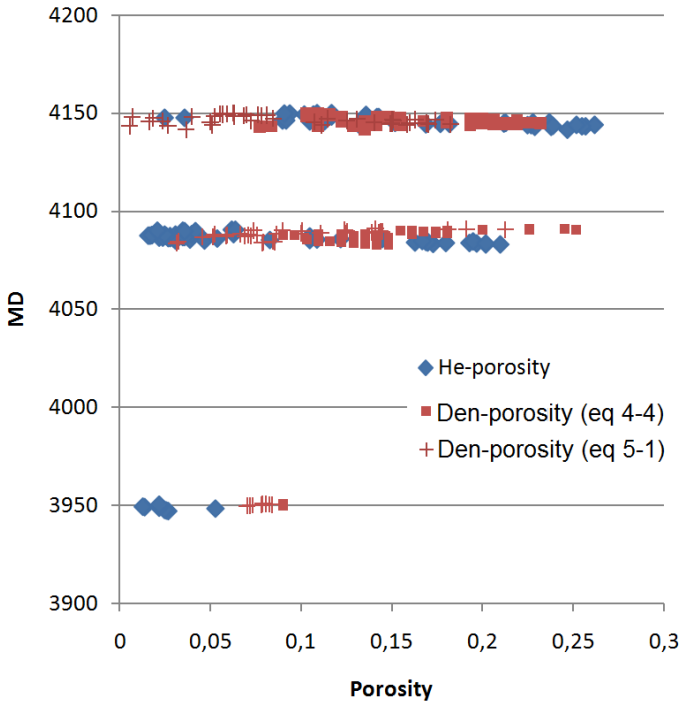

Figure 4-3. Comparison of density-porosity and He-porosity in hydrocarbon bearing intervals (15/3-1S).

4.3 CORE DESCRIPTION

The core description will give a brief interpretation of the facies and depositional environment of the cores studied. The facies (/ facies groups) identified are quite broad and related to sedimentary processes.

Helium-porosity and permeability measurements from core-plugs (Delclaud, 1975; Statoil, ?-a, b) taken from well 15/3-1S and 15/3-7 has been evaluated to establish an estimate of reservoir cut-off.

4.4 PETROGRAPHIC ANALYSIS

Samples were taken from some of the cores and these were studied in SEM and optical microscope.

SEM analysis was performed using a JEOL JSM-6460LV Scanning Electron Microscope (SEM) with a LINK INCA Energy 300 Energy Dispersive X-ray (EDX) system. Both freshly fractured stub-mounted samples coated with gold and carbon coated thin sections were studied in the SEM.

Thin sections were also investigated in an optical microscope where point counting (400 points per sample) was carried out to get an estimate of the composition and porosity of the samples. The grain-size distribution is not investigated statistically, but an estimate of the average grain-size of each sample is provided based on the overall impression of the interpreter.

4.5 POROSITY MODELING ALGORITHM

Porosity was modeled by simulating mechanical compaction and quartz cementation. The modeling algorithm was thus divided into two parts, porosity loss during shallow burial and porosity loss during intermediate and deep burial. Shallow burial is simulated by assuming that mechanical compaction follow simple exponential functions of the form (e.g. Athy, 1930):

$$\Phi\ (\text{TVDRSF}) = \Phi_{dep} \times \exp\ (-x \times \text{TVDRSF}) \qquad \text{(equation 7-1)}$$

Where the porosity with depth, Φ (TVDRSF), is a function of the initial or depositional porosity, Φ_{dep} and a constant, x, that will vary depending on lithological factors and pressure regime.

During intermediate and deep burial porosity is assumed to be a function of quartz cementation and porosity loss is modeled based on various publications of Walderhaug (Walderhaug, 1994a; Walderhaug, 1996). Following Walderhaug (1996) the total volume of quartz (V_{qz}) precipitated at time (t) after onset of quartz cementation can be expressed as follows:

$$V_{qz} = \Phi_0 - \Phi_0 \exp\left(\frac{-MaA_0}{\rho\Phi_0 bc\ln 10}\ (10^{bt} - 1)\right) = \Phi_0 - \Phi_0 \exp(u) \qquad \text{(eq. 7-2)}$$

Where Φ_0 is the porosity at onset of quartz cementation, M and ρ is the molar mass (60,09 g/mole) and density (2,65g/cm^3) of quartz. The constants a and b are empirically determined quartz precipitation rate constants. The values of the rate constants are taken from Walderhaug (1994a) from Jurassic sandstones on the Norwegian continental shelf. The heating rate, c, will vary according to burial/temperature-history.

The surface area available for quartz precipitation at onset of quartz cementation (A_0) is besides the heating rate the most important input variable. A_0 may be expressed as:

$$A_0 = 6f\ (1 - \Phi_0)\ (1-g)/D \qquad \text{(equation 7-3)}$$

Where f is the fraction of quartz, (1- Φ_0) is the fraction framework grains and D is the grain diameter. The term (1-g) copes with the effects of grain-coats, where g is the fraction of the quartz surface area covered by grain-coats. These variables depend upon conditions related to depositional environment and provenance and are therefore termed lithological variables (table 8-1).

The mathematical approach of calculating A_0 does not take into account the reduction in surface area available for quartz precipitation due to contact points between grains. Textural parameters such as sphericity and rounding are also not included in the calculations of the surface area of the grains. In reality grains are not perfect spheres and will therefore tend to have a larger surface area than calculated, however the exclusion of the contact points will cancel this effect and the errors from these two simplifications are therefore assumed to cancel out (e.g. Walderhaug, 1996).

As cementation commences the surface area available for quartz precipitation will be reduced. This can be adjusted for by:

$$A=A_0\times\Phi_t/\Phi_0 \qquad \text{(equation 7-4)}$$

Where Φ_t is the porosity at time, t, which can be expressed as:

$$\Phi_t = (\Phi_0 - V_{qz}) \qquad \text{(equation 7-5)}$$

The burial depth (TVDRSF) and temperature (T) at a given time are further assumed to be linear functions of time (t) such that:

$$TVDRSF(t) = c \times t / (dT/dz) \quad \text{and} \quad T(TVDRSF) = dT/dz \times TVDRSF$$

This implies the assumption of a constant geothermal gradient (dT/dz = 30 C/km) in space and over time and a constant (average) heating rate, c. The range of expected heating rates can be found from burial depth and thickness data of the Upper Jurassic in the South Viking Graben, derived from seismic (Fraser et al., 2003). This gives constant, linearly approximated

heating rates of about 0,8-1,2˚C/Ma in the Vana and Vilje Sub-basins and 0,7-0,85 on the Heimdal and Gudrun Terrace. In reality the heating rate will not be a linear curve. In order to get a more accurate estimate basin modeling should be applied and the heating rates could then be based on thermal history plots, as has been demonstrated by Walderhaug (e.g. Walderhaug, 2000), this is however beyond the scope of this assignment.

There are several uncertainties related to the model input parameters, mainly associated with the parameters listed below. Values (with arguments) for modeling porosity-depth trends are also given:

i. *Surface area available for quartz precipitation*. The variables f (fraction quartz) and D (grain-size) was evaluated in section 7.2.3 which agrees with the general impression from studying the cores in ”hand-specimen”. Thus f was set as a constant equal to 0,8. D was set equal to 0.02 cm for minimum porosity trends and 0,05 cm for maximum porosity trends. D equal to 0,035 cm was used for modeling average porosity trends.

ii. *Heating rate*. The heating rate was adjusted to optimize the model in order to get a best-fit against calculated porosity values from well logs (e.g. figure 5-7, 8-1 and 8-2).

iii. *Porosity at onset of quartz cementation(Φ_0).* For well-sorted sands Φ_0 can be assumed to be equal to the porosity of cubic closest packing (CCP) of spheres (~25%). Φ_0 equal to 25% has been used when calculated average porosity trends. Shallow development of overpressure will increase Φ_0, therefore Φ_0 equal to 30% will be used for maximum porosity trends. If sandstones are not well sorted Φ_0 will tend to be less than 25%, therefore Φ_0 equal to 20% will be used for minimum porosity trends.

The variable values given here are mostly derived from the results of chapters 5-7 and are summarized in the introduction to the modeling chapter (table 8.1). It has also been useful to subdivide the variables according to table 8.1.

The modeling was carried out in matlab R2007. For more details about the algorithm the reader is referenced to Appendix B, which shows the matlab program generating figure 8-1 and 8-2.

CHAPTER 5: WELL CORRELATION AND PETROPHYSICAL EVALUATION

5.1 INTRODUCTION

There are several wells in the area of interest, but only a few of which penetrate all the way down to Upper Jurassic sediments and wire-line logs were not run in all of them. Figure 5-1 gives an overview of all wells penetrating into the Upper Jurassic. The database for the petrophysical evaluation has been the wells in table 5-1.

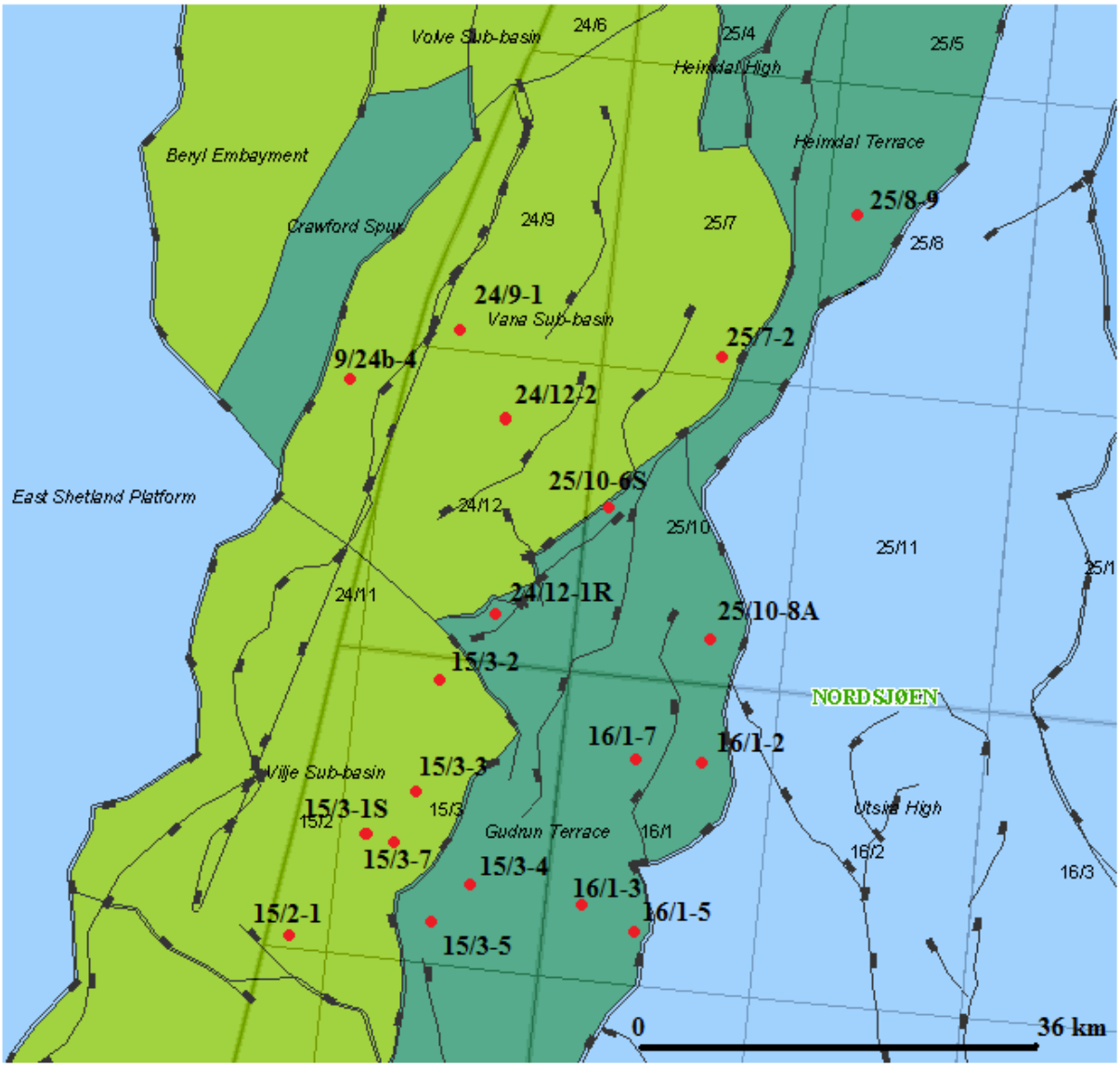

Figure 5-1. Overview of wells on norwegian sector penetrating the Upper Jurassic. UK well 9/24b-4 is also shown. The map is taken from NPD (www.npd.no).

Table 5-1. The database for the petrophysical evaluation.

Well	Location	Viking Gr (MD)* Min	Max	TD (RKB)*	TVD (RKB)*	Water depth*	KB*	TVDRSF Min	Max
15/2-1	2	3878	4356	4600		109	25	3744	4222
15/3-1S	2	3947	4985	5129		109	25	3813	4851
15/3-2	2	4235	4400	4762		116	24	4095	4260
15/3-3	2	4017	4520	5116		109	24	3884	4387
15/3-7	2	4049	4607	4818	4817	109	18	3921	4481
24/9-1	1	4330	4907	4907		118	25	4187	4764
24/12-2	1	4261	5100	5100	5091	119	30	4104	4960
25/7-2	1	4056	4407	4850	4857	100	25	3928	4285
15/3-4	3	3675	3786	4259	4259	107	25	3543	3654
15/3-5	3	3808	3935	4130	4130	103	25	3680	3807
16/1-3	3	2707	2730	3498	3496	108	25	2572	2599
16/1-5	3	2020	2175	2460	2458	105	25	1888	2044
24/12-1R	3	4055	4350	4825	4825	125	25	3917	4212
25/10-8A	3	3090	3460	3460	2537	115	25	1758	1985

*From WDSS (www.npd.no) and well reports

Location: 1: Vana sub-basin, 2: Vilje sub-basin, 3: Gudrun Terrace, 4: Heimdal Terrace

Depth Viking Gr (TVDRSF):	Location 1/2 :	Location 3/4:
	3744 - 4960	1758 - 4628

The main purpose with the well correlation has been to (i) identify lithostratigraphic and sequence stratigraphic units and (ii) to identify sandstone intervals within these sequences. The main purpose with the petrophysical evaluation has been to calculate sandstone porosities from logs. This was done in order to (i) calibrate a model capable of predicting porosities in the study area as a function quartz cementation (chapter 8) and (ii) to define intervals of anomalously high porosities. Whether grain-coats are the cause of such high porosities in these intervals could then be investigated further in chapter 7.

5.2 RESULTS

The well correlations are important because they provide a sequence stratigraphic and lithostratigraphic framework for the cores and samples that have been studied. Therefore well-correlations for selected wells will be presented in the following section (5.2.1). Large amounts of information can be derived from the petrophysical logs. However, the focus here has been on calculating porosities and correlating anomalously high porosity zones to sequence stratigraphic units. These results will be presented in section (5.2.2)

5.2.1 Well correlations

Figure 5-2 shows the sequence stratigraphic interpretation applied in this study for selected Vilje- and Vana Sub-basin wells. Figure 2-5 provides a good overview of lithostratigraphic units relative to the maximum flooding surfaces interpreted (i.e. Heather-Draupne boundary correlates closely to the Eudoxus TEMFS (J63)) and therefore only the sequence stratigraphic interpretation is presented here.

Well correlations on the Gudrun Terrace had to be carried out based on biostratigraphical reports (appendix E). Hiatuses are present here complicating the interpretation; in addition well 25/10-8A is dipping considerably.

Note that the cored sections that have been studied (chapter 6 & 7) are marked on the well correlations and thus the sequence stratigraphic framework of the cores and samples are given.

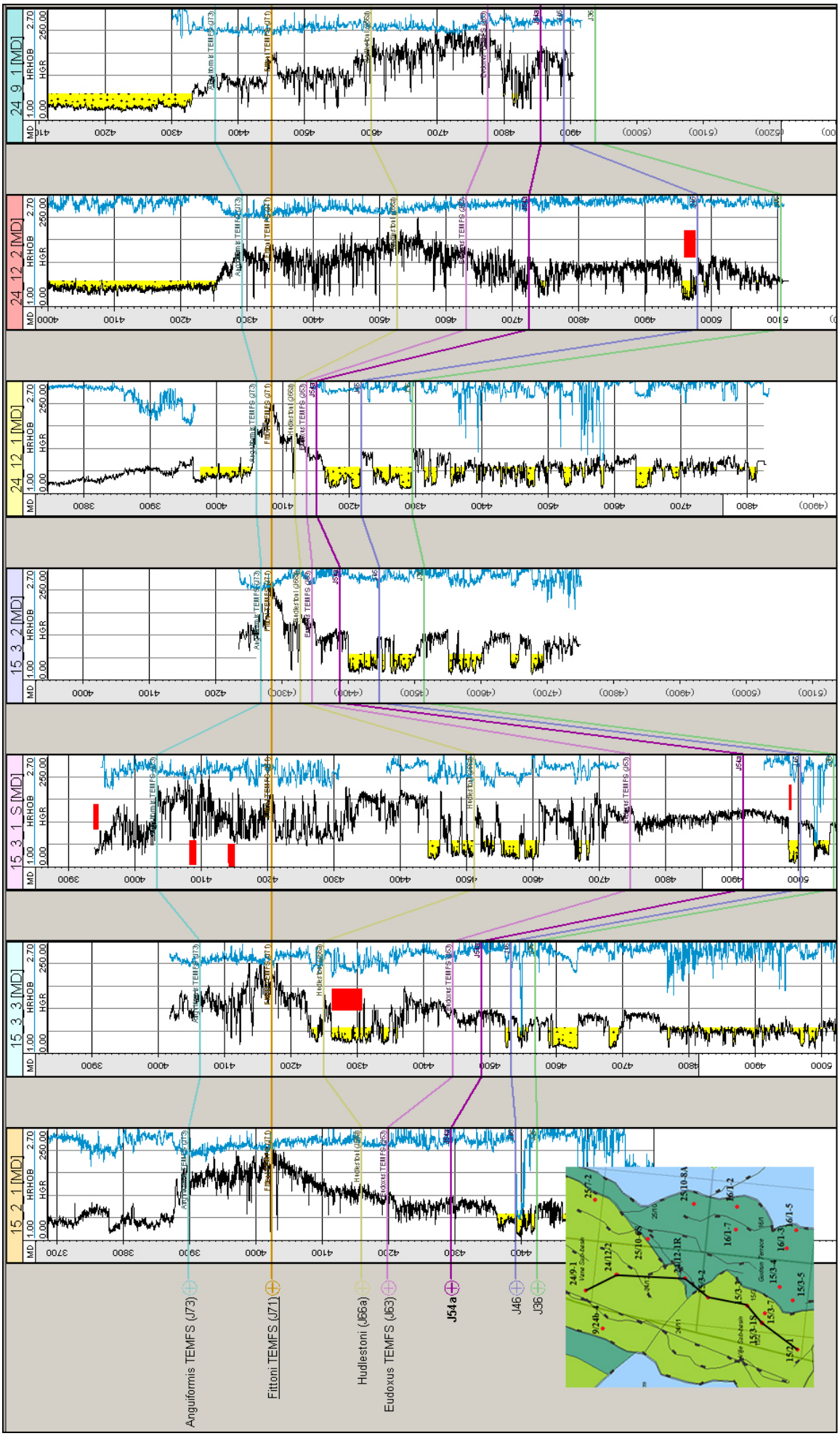

Figure 5-2. Well correlation and studied cores (red) in selected Vilje and Vana wells.

5.2.2 Petrophysical evaluation

In order to calculate porosities some input variables are needed. These will be presented in section 5.2.2.1. Thereby porosity-depth plots and porosity distributions for most of the wells in the study area will be presented, followed by a sequence stratigraphic evaluation of the porosity distribution.

5.2.2.1 Input variables: porosity calculations

The density of quartz is 2,65 g/cm^3. As can be seen in figure 5-3 most shales in the study area have a density of about 2,3-2,6 g/cm^3. Shales were defined as GR > 60. The resulting distribution of the density and gamma-ray measurements for all shales in the study area is given in figure 5-4 and 5-5. Shales proved to have a mean density of 2,48 g/cm^3 and a mean gamma-ray reading of 102,7. This density difference gives a porosity correction of approximately 0-3 % depending on the Vsh, which was considered enough to correct porosities calculated from the density log for the effect of shale.

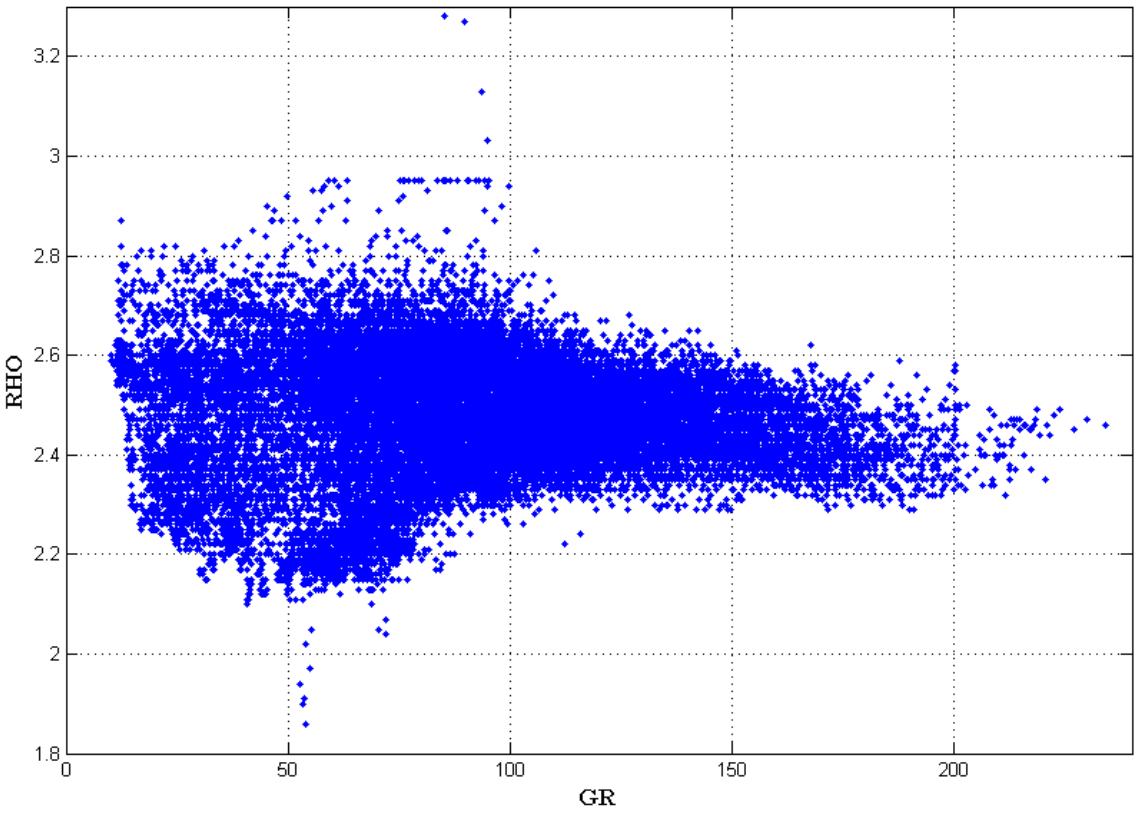

Figure 5-3. Cross-plot of gamma-ray vs density for Upper Jurassic intervals of all wells (table 4-1). Defining shales as having a gamma-ray reading above 60 gave a mean shale density of 2,48.

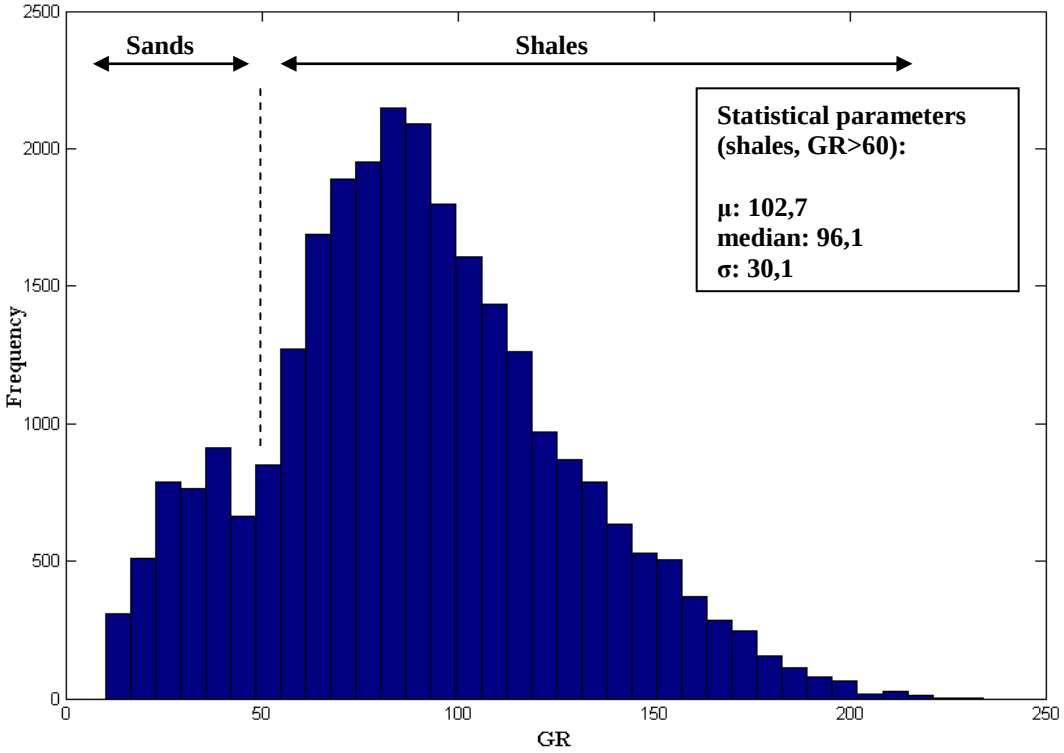

Figure 5-4. Gamma-ray distribution for the Upper Jurassic sections of all wells (table 5-1). Note the bimodal trend corresponding to sand and shale lithologies respectively. The shales are strongly skewed.

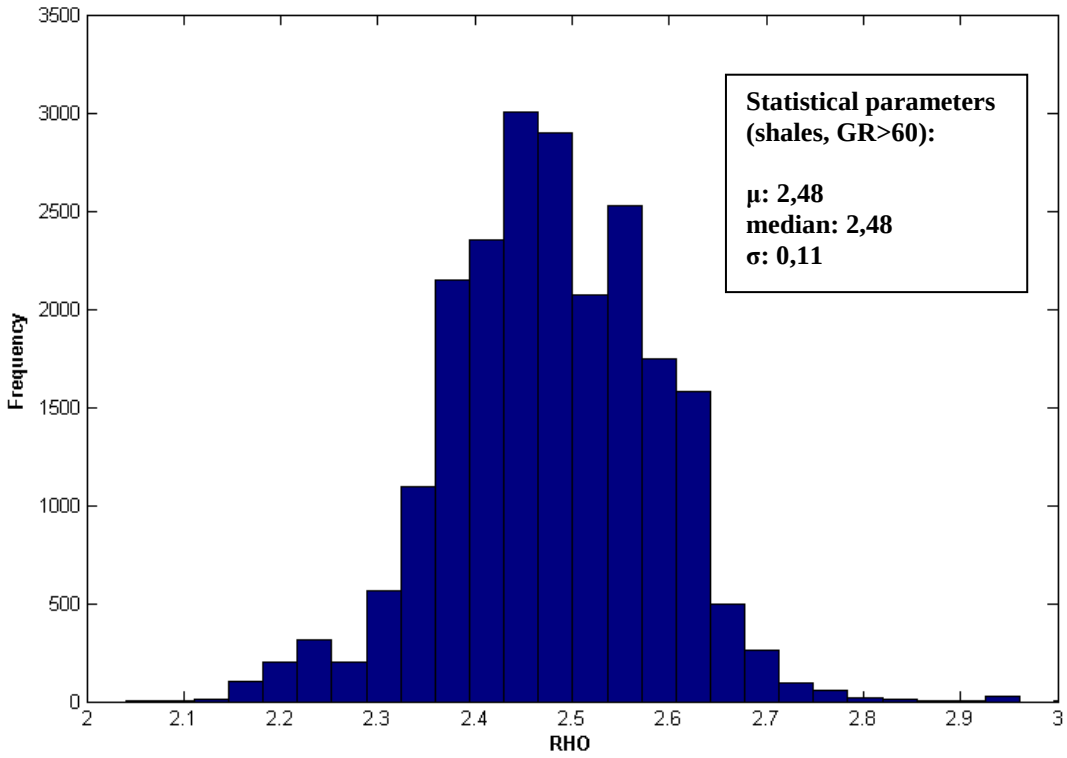

Figure 5-5. Density distribution of Upper Jurassic shales (GR>60) from all wells (table 5-1).

Ones it had been established that the effect of shale should be corrected for the mean density and gamma-ray reading of shales in each well were found (table 5-2). These values were used to calculate the gamma-ray index (equation 4-7) and porosity. The final porosity equation becomes:

$$\Phi = (V_{sh} (\Delta\rho_{well}) + 2{,}65 - RHO) / (2{,}65 - 1{,}1) \qquad \text{(equation 5-1)}$$

The porosity equation resulted in some values becoming negative (see Appendix C). Under the assumption that V_{sh} and ρ_{shale} estimates are correct, these negative porosity values were interpreted as carbonate cemented intervals that the filtering did not remove.

Table 5-2. Input variables (equation 4-5, 4-6 and 4-8).

Well	Grclean	Grshale	ρshale	Δρ
15/2-1	19,05	114,24	2,46	-0,19
15/3-1	13,09	112,14	2,47	-0,18
15/3-2	46,81	118,96	2,54	-0,11
15/3-3	20,41	107,56	2,48	-0,17
15/3-4	39,66	80,29	2,48	-0,17
15/3-5	41,74	83,9	2,51	-0,14
15/3-7	23,91	126,51	2,53	-0,12
16/1-3	35,52	81,02	2,38	-0,27
16/1-5	49,69	76,73	2,30	-0,35
24/9-1	25,7	122,25	2,42	-0,23
25/7-2	13,28	85,18	2,56	-0,09
25/8-9	54,27	79,85	2,34	-0,31
24/12-1	10,12	108,93	2,66	0,01
24/12-2	16,0	99,6	2,53	-0,12
25/10-8A	33,62	89,86	2,40	-0,25

5.2.2.3 Porosity plots

Based on equation 5-1 porosity-depth plots for all wells containing Upper Jurassic sandstones are given in figure 5-6. Note that carbonate cemented sandstones are attempted filtered away. This is because the porosity-depth plot will be used to optimize the model in chapter 8.

The Porosity distribution of selected wells containing deeply buried intra Draupne sandstones are given in figure 5-7 (the carbonate filter has not been applied in this figure). The porosity distribution tended to be bimodal for several of the wells in the Vilje sub-basin. In deeply buried, mature sandstones of similar lithology this is a good indication that grain-coats are present (e.g. Bloch et al., 2002). The wells in the Vana-west however do not display a bimodal trend, but approaches a normal distribution (slightly skewed). This indicates that grain-coats may be absent or ineffective in these sandstones. Well 25/7-2 located in Vana-east has a slightly bimodal and almost uniform distribution. This may indicate poorly sorted sands/conglomerates and/or variable degree of coating.

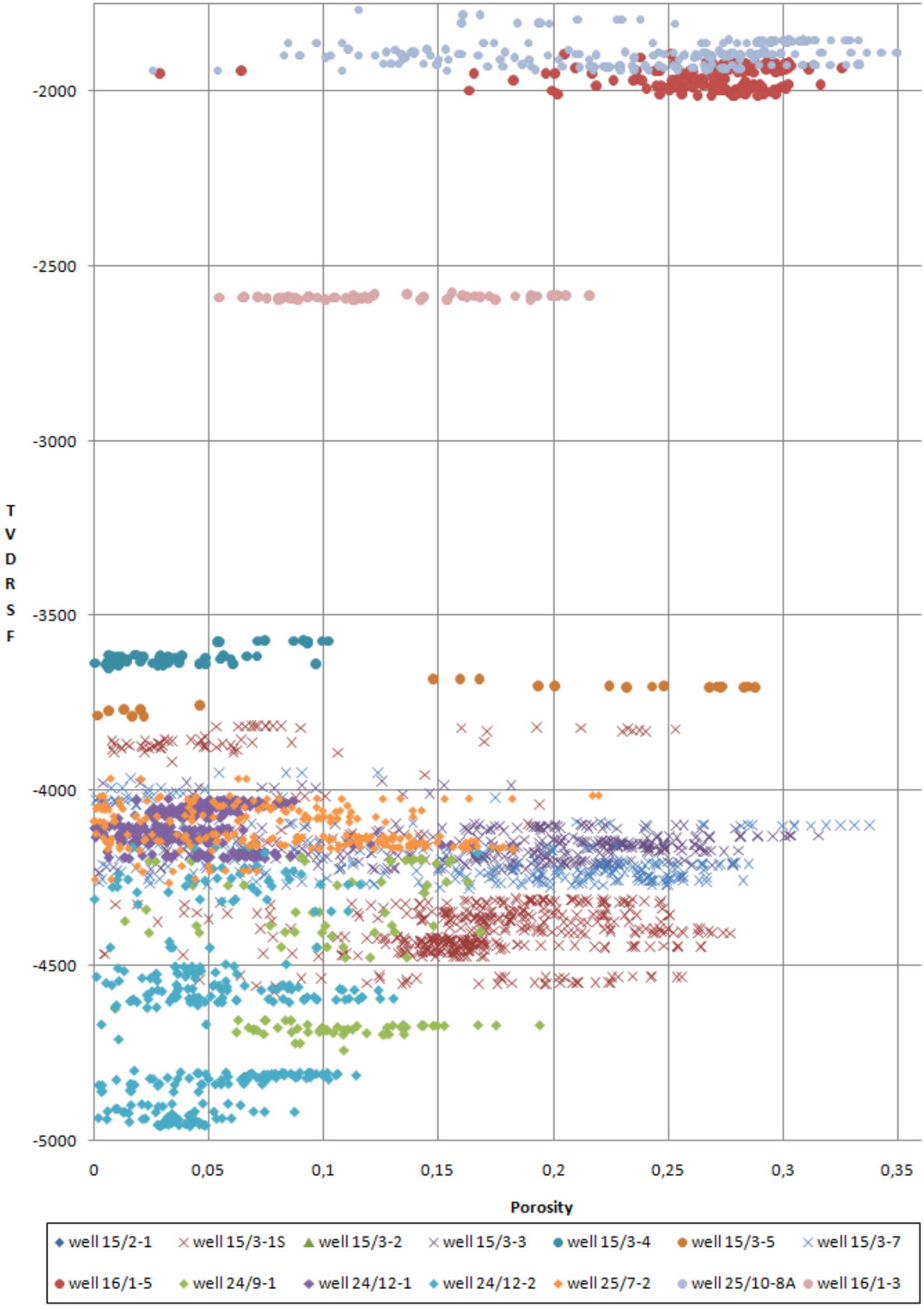

Figure 5-6. Density-porosity vs depth plot for most of the Upper Jurassic wells in the study area. Apparent density-porosity values in the Gudrun wells above ~30% may be affected by the presence of gas. He-porosity values of maximum 28% are measured in these wells.

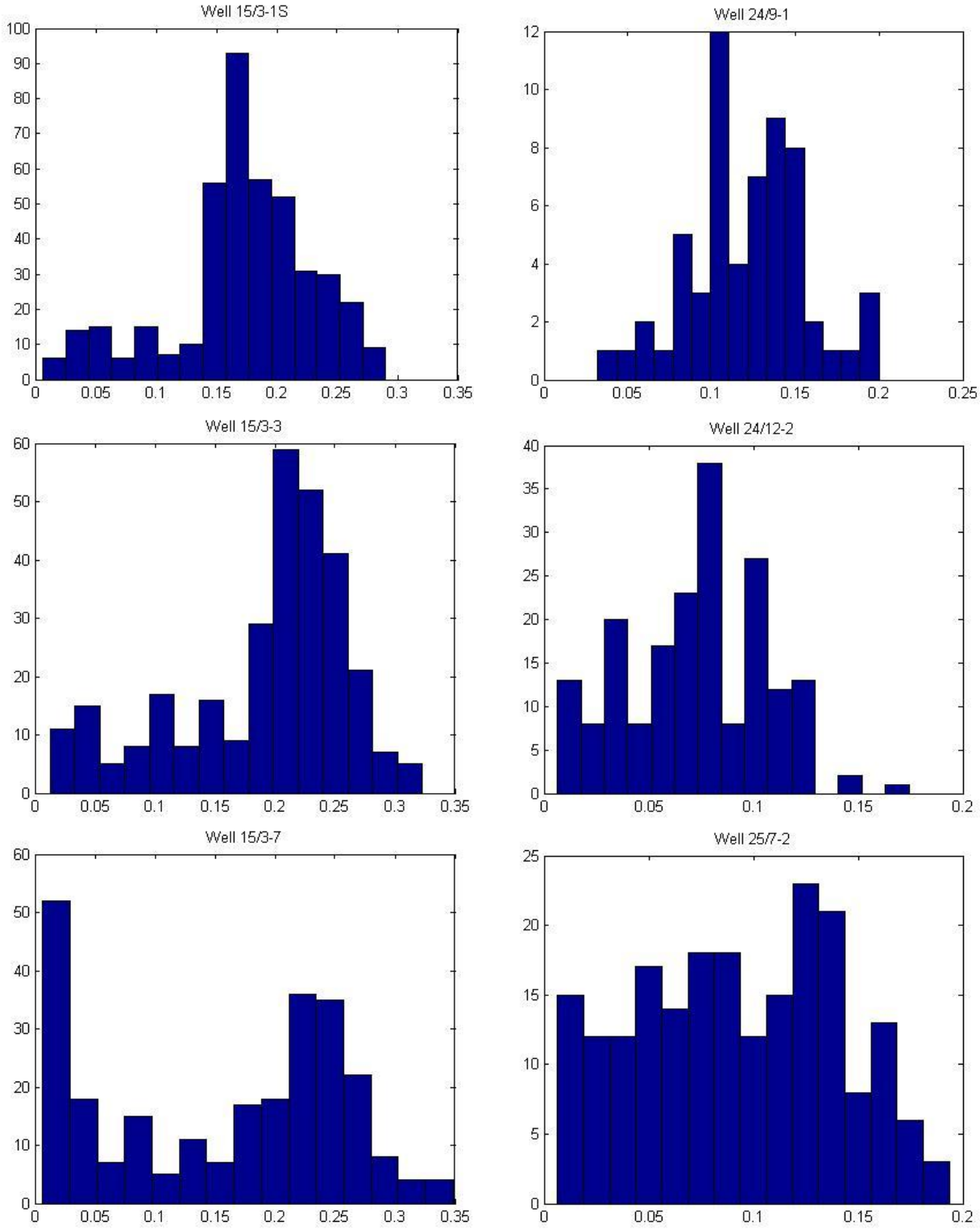

Figure 5-7. Showing the porosity distribution in deeply buried intra Draupne sandstone units in selected wells in the study area. Note the bimodal distribution of the Vilje sub-basin wells (15/3-1S, 15/3-3, 15/3-7) indicating the presence of extensively grain-coated intervals. The wells in Vana-west display a distribution approaching a normal distribution indicating that grain-coats are absent or ineffective in these wells. Well 25/7-2 located in Vana-east has a slightly bimodal and almost uniform distribution. This may indicate facies variability such as poorly sorted sands and/or variable degree of coating.

5.2.2.4 Porosity distribution in a sequence stratigraphic framework

The porosity distribution in each of the genetic sequences described by Fraser et al. (2003) (see figure 2-5) was calculated and is given in figure 5-8 below. Note the increasing amount of porosities above reservoir cut-off for sequence C (C1 and C2) and to a certain extent also sequence D and E.

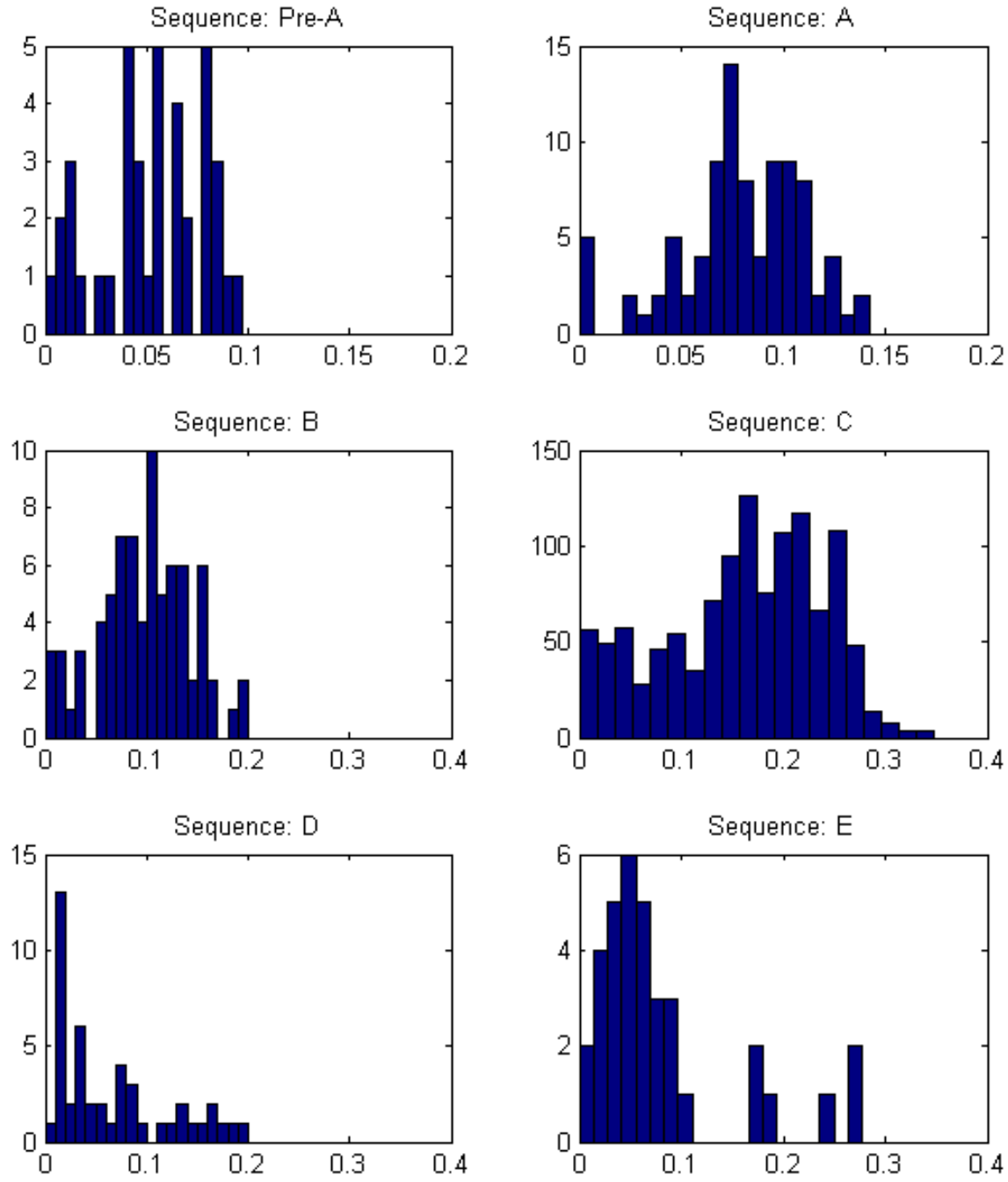

Figure 5-8. Porosity distribution of deeply buried sandstones in the genetic sequences.

Grain-coats are suspected to be the main cause of anomalous porosity in the study area, and it will be shown in chapter 7 that micro-quartz is locally abundant in the samples studied. It was mentioned in chapter 3 that micro-quartz form from transformation of sponge spicules from Rhaxella Perforata. Thus time intervals (sequences) with favourable conditions for this sponge may be sequences with anomalously high porosity. Figure 5-9 demonstrates that deeply buried sequences post-dating Eudoxus seem to have significant amounts of sandstones with anomalously high porosity. If micro-quartz is restricted to this time interval will be investigated further in chapter 7.

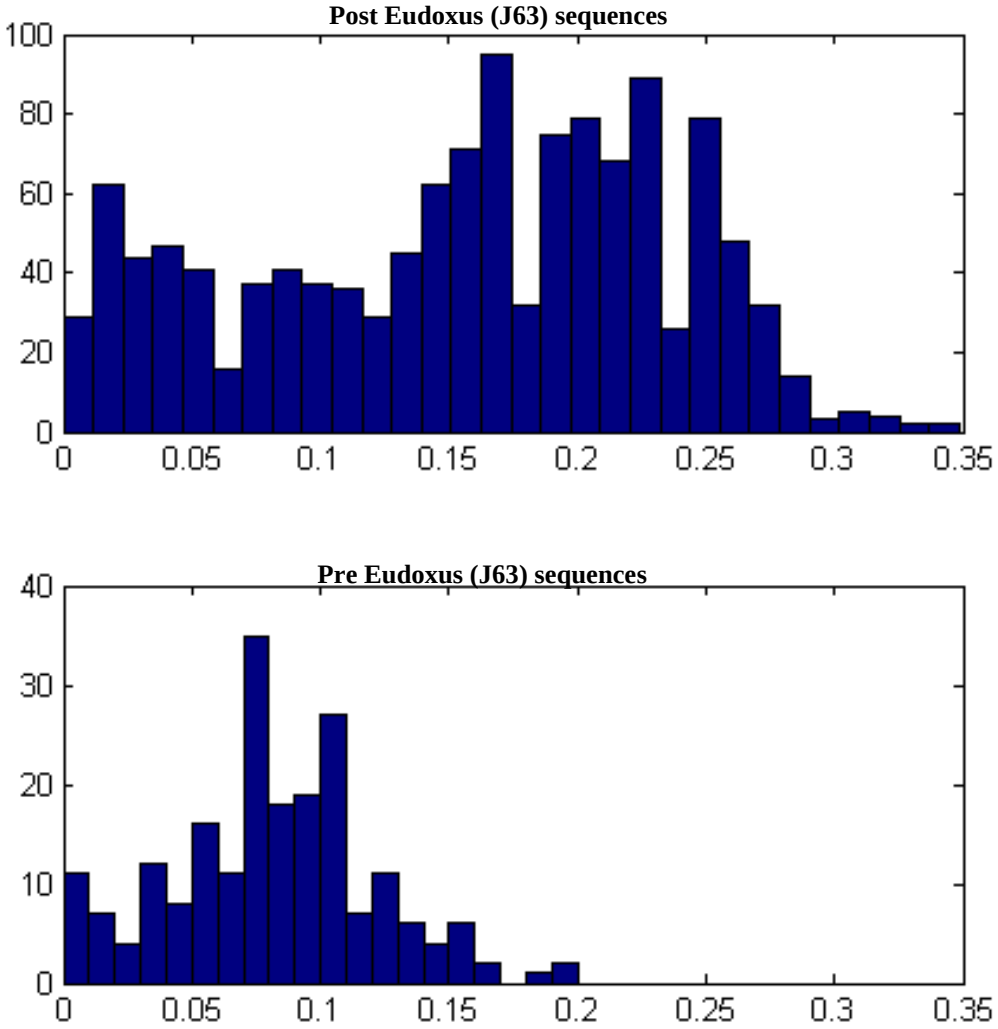

Figure 5-9. Sandstone porosity distribution in post and pre Eudoxus (J63) sequences.

CHAPTER 6: CORE DESCRIPTION

6.1 INTRODUCTION

In chapter 5 the stratigraphic framework of the cores studied was given. It was also shown that anomalously high porosities are common in the studied wells and that these high porosity values seem to be linked to certain sequences. The cores that have been sampled and studied (see table 6-1) will now be briefly described and interpreted (chapter 6.2) based on sedimentological core-logs (see appendix D). This will sort the samples further into facies, which reflect the depositional processes and enables interpretation of the depositional environment. The defined facies (table 6-2) are quite broad, and could be subdivided further. However, an in depth interpretation of the depositional environment is not emphasized in this thesis (see Islam, in press) therefore a broad interpretation is applied.

In addition to core-logs, helium-porosity and permeability measurements performed on core-plugs in the laboratory have been evaluated in order to establish an estimate of reservoir cut-off (chapter 6.3).

6.2 CORE-LOGS

The cores studied represent deep marine sedimentation, with the exception of the cores from well 16/1-5, 16/1-5A and 25/10-8A. These three wells, located on the Gudrun Terrace close Utsira High have been studied because they may represent the source sands that are deposited as sediment gravity flows in the Vana- and Vilje sub-basins.

Well	Depth interval (mRT)	Facies	Sequence
16/1-5	2023-2066	B2 – B3	A-B1
16/1-5A	2123-2150	B1 – B2	A-B1
15/3-1S			C1-C2
Core #1	3947 – 3951	A2	
Core #2	4083 – 4091	A2	
Core #3	4141 – 4150	A2	
Core #4	4991 – 4994	B2	
15/3-3	4262 – 4308	A1-A3	C1-C2
9/24b-4			B1-B2
Core #1	4793 – 4794	A2	
Core #2	4806 – 4807,5	A2	
Core #3	4895 – 4904	A2	
Core #4	4972 – 4979	A2	
24/12-2	4960 – 4978	A1- A3	B1
25/10-8A	3110 - 3202		B2

Table 6-1. List of wells and depths of the cores studied along with a summary of the interpreted facies.

6.2.1 Facies

Three different facies are distinguished in the deep marine cores, while four have been identified in the shallow marine cores. These are summarized in table 6-2. Figure 6-1, 6-2, 6-3 and 6-4 shows typical examples of how the facies appeared in the cores.

Table 6-2. General description and interpretation of the facies observed.

Depositional environment	Facies	Description	Interpretation
A: Deep marine			
	A1	Massive, coarse to medium grained sandstone. Normal grading common. Structure-less. Rip-up clasts common.	High density turbidity currents and sandy debris flows.
	A2	Interbeded mudstone and thin-bedded, fine-grained sandstone. Ripple cross-lamination common.	Low density turbidity currents and hemipelagic settling
	A3	Laminated mudstone	Dilute turbidity currents and hemipelagic settling
B: Shallow marine			
	B1	Medium to coarse grained, graded and cross-bedded sandstone.	Foreshore to upper shoreface
	B2	Medium grained, well sorted, extremely massive sandstone. Locally pebbly and cross-stratified	Lower shoreface
	B3	Fine grained, highly bioturbated sandstones.	Offshore transition zone
	B4	Laminated, calcareous mudstone. Textbook examples of laminar flow. Thin fine to medium sand beds appear.	Shelf mud-flows and grain-flows

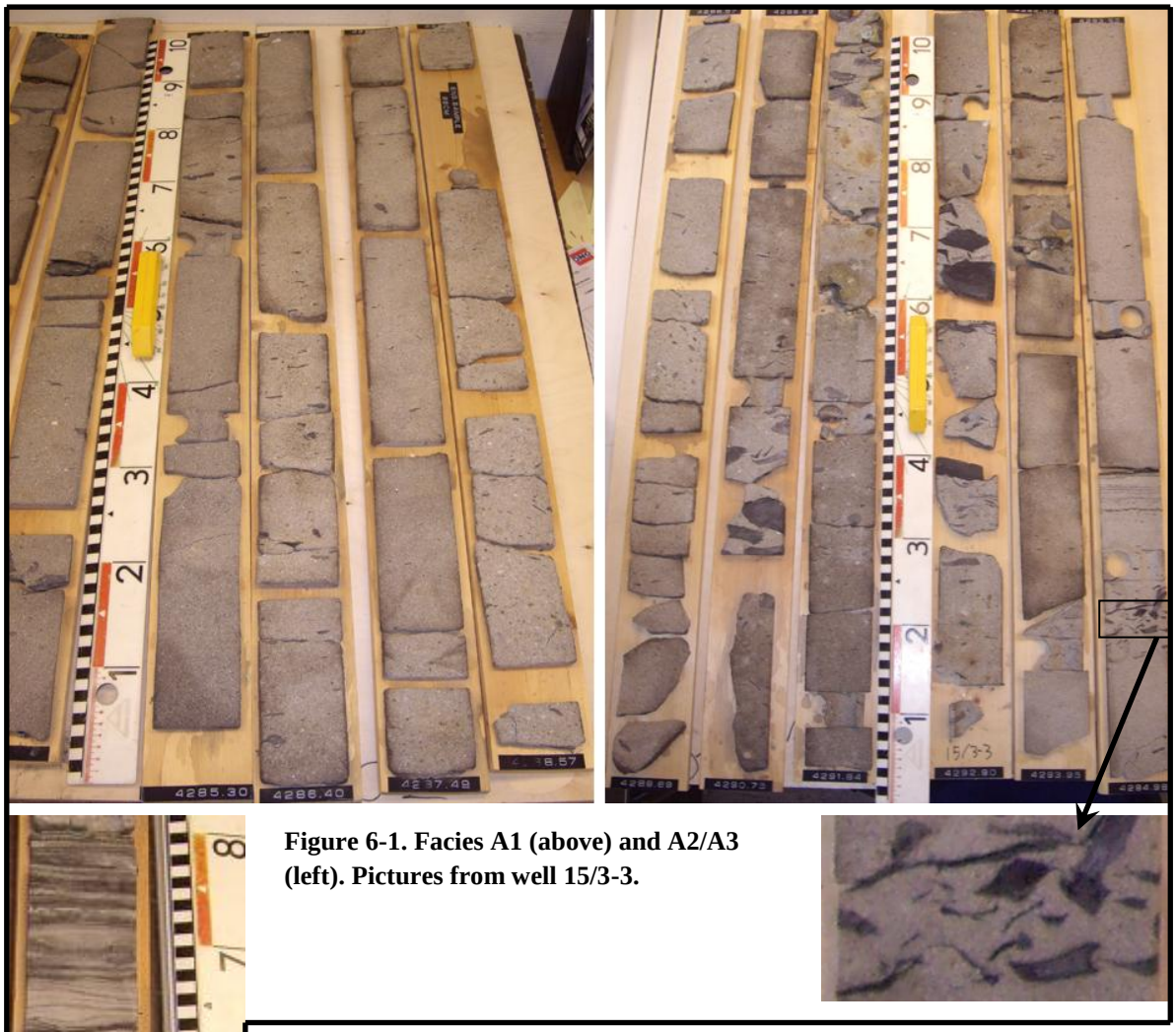

Figure 6-1. Facies A1 (above) and A2/A3 (left). Pictures from well 15/3-3.

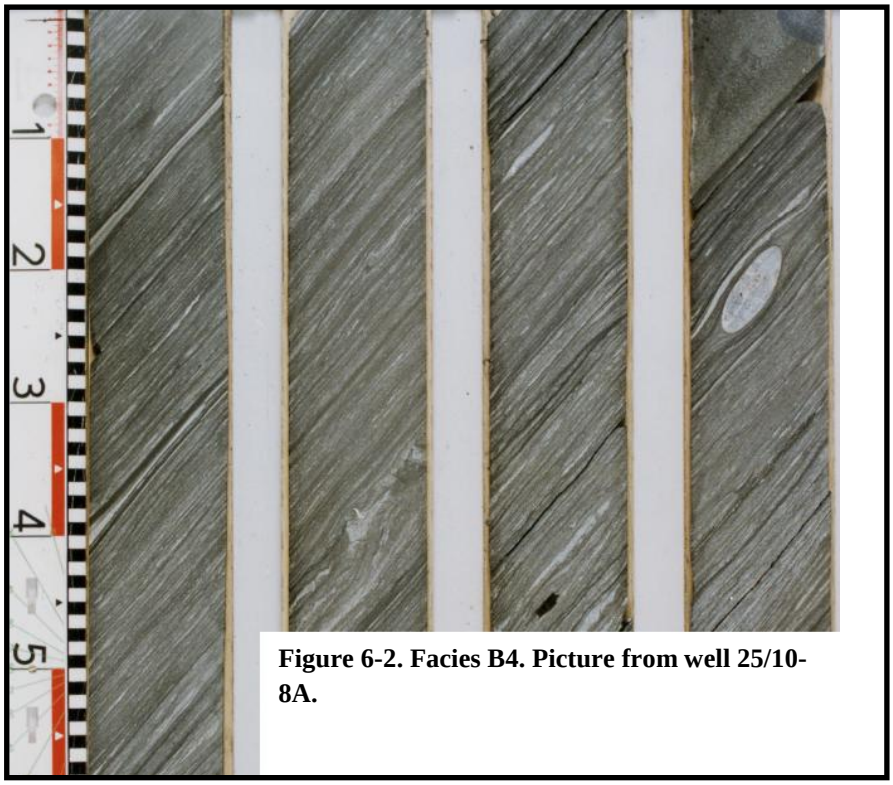

Figure 6-2. Facies B4. Picture from well 25/10-8A.

Figure 6-3. Facies B2. Massive, structure-less sandstone. The pictures are from well 16/1-5A.

Figure 6-4. Facies B1 (above). Note the normal grading and cross-bedding. Picture from well 16/1-5A.

Facies B3 (left). Note the extensive bioturbation. Picture from well 16/1-5.

6.2.2 Depositional environment

Two end member submarine fan systems were mentioned in chapter 2.3, the gravel-rich versus the sand-rich systems. In addition an eastern or western provenance is considered a potentially important distinction, thus four generalized end member submarine fan systems are recognized.

i. Sand-rich submarine fan, western provenance.
ii. Sand-rich submarine fan, eastern provenance.
iii. Gravel-rich submarine fan, western provenance.
iv. Gravel-rich submarine fan, eastern provenance.

Well 15/3-3 and well15/3-1S are interpreted as part of the same sand-rich submarine fan complex sourced from Utsira High. Amalgamated, massive beds of high density turbidity current deposits dominate the logged sections in well 15/3-3 although some debris flow deposits are interpreted (both making up facies A1). These deposits are interpreted as channelized upper to middle fan sandstones. Thin low density turbidity current deposits and laminated mudstones (facies A2 and A3) were more common in well 15/3-1S and the deepest core contained shallow marine sands (Hugin Formation). Four cores at different depths making up about 25 meters of an approximately 1000 meter thick transgressive sequence were studied. Massive shallow marine sands (facies B2) were recorded in the deepest core (core #4). Core #3 contained graded high density turbidites (A1) and low density turbidites interbedded with mudstone (A2), while core #2 also contained organic rich laminated mudstones (facies A3) in addition to facies A2. Core #1 contained mainly organic rich laminated mudstones (A3), sometimes interbedded with lenses of fine sand (A2). Based on this the sequence was interpreted as a transgressive marine mega-sequence evolving from a shallow marine environment to submarine fan sequence representing middle- and lower fan lobes and lobe channels, with basin plain deposits increasingly dominant at the top.

The Brae Formation was studied in well 9/24b-4 and it is believed that very distal turbidites from this fan system was encountered in well 24/12-2 (see chapter 7.2.2). The Brae Formation represents a gravel-rich to sand-rich submarine fan, sourced from the East Shetland Platform.

The cores studied in well 9/24b-4 contained facies identical to those studied in well 15/3-3 and well 15/3-1S (core 1-3).

Well 16/1-5, 16/1-5A and 25/10-8A represent shallow marine sediments associated with a shelf environment around Utsira High. Well 25/10-8A contains about hundred meters of facies B4, with a few sand intervals in-between. The deposits are textbook examples of laminar flow and are interpreted as shelf mudflows, probably triggered by tectonic activity. The deposits are highly calcareous implying a sediment starved environment. Well 16/1-5 and its sidetrack (16/1-5A) represent “typical” (as described by Fraser et al. (2003) and others) Upper Jurassic shoreface and offshore-transition sandstones. Some of the main characteristics of these deposits are extensive bioturbation (facies B3) and large intervals of massive sandstones (facies B2).

6.3 RESERVOIR CUT-OFF ESTIMATES

The reservoir cut-off estimates are based core-analysis reports (Delclaud, 1975; Statoil, ?-a, b) from well 15/3-1S and 15/3-7. These two wells were the only ones with such reports available. The reports were studied in order to establish porosity-permeability relationships that can be used to estimate reservoir cut-off. The core analysis reports contained both vertical and horizontal permeability measurements along with porosity measurements from core-plugs. Figure 6-5 illustrates that the vertical permeability tended to be somewhat lower then the horizontal permeability, although more measurements are desired to really establish this trend. Therefore porosity-permeability relationships were established assuming an isotropic medium (figure 6-6).

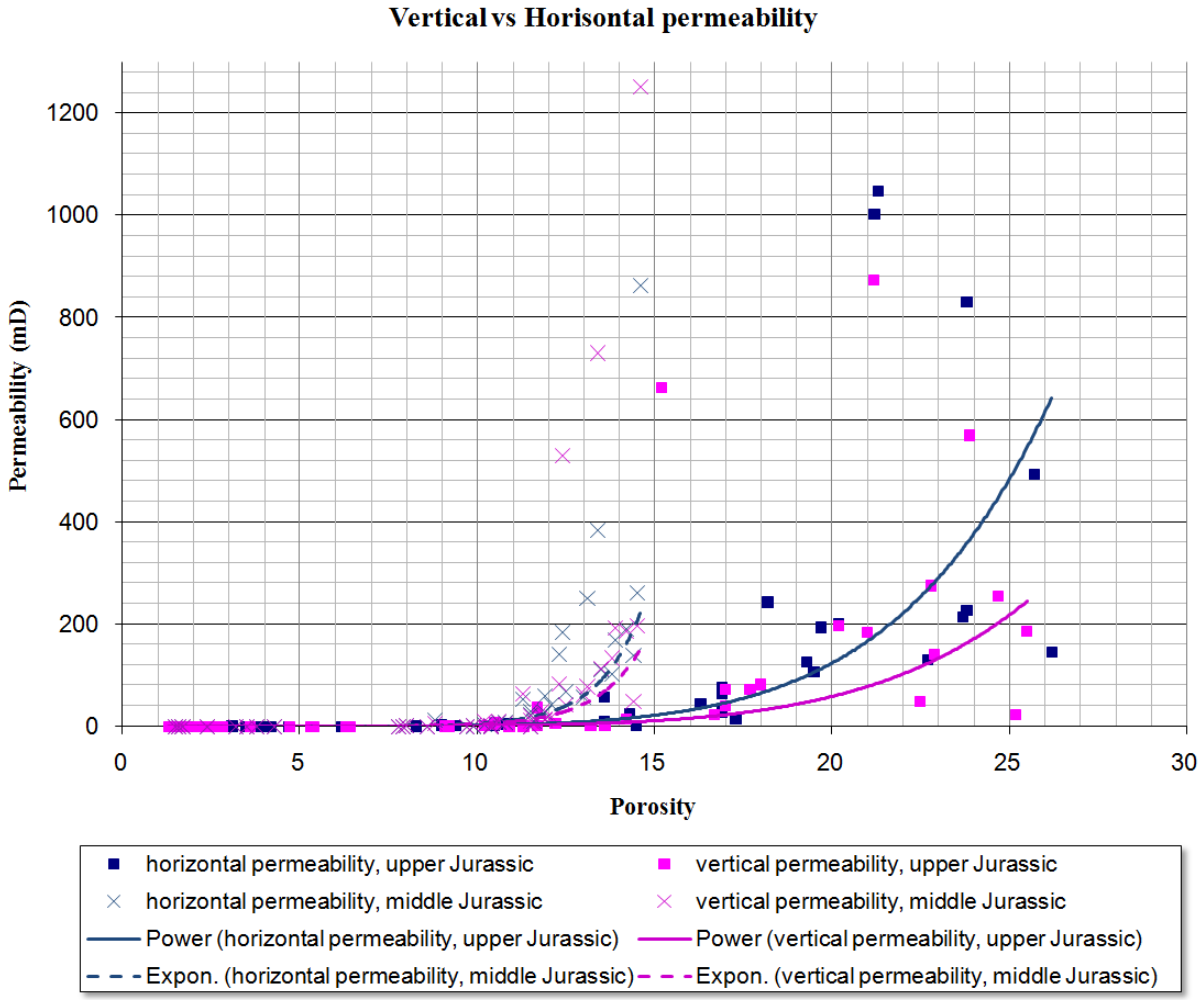

Figure 6-5. Comparison of vertical and horizontal permeabilities in upper- and middle Jurassic samples.

It was found that permeability could be best expressed as an exponential function of porosity for the middle Jurassic measurements. For the Upper Jurassic measurements porosity raised to a power gave a higher correlation than an exponential function. Note that permeabilities are lower in Upper Jurassic samples.

Reservoir cut-off is typically 5mD. According to the empirical porosity-permeability relationship established this corresponds to a porosity of 12,9% for Upper Jurassic sandstones in these wells. By comparison cut-off is set at a porosity of 6% in the Devenick field (Brae Formation, well 9/24b-4) (BP, 2001). As the petrographic analysis will show, this is probably related both to the lack of extensive grain-coats, but also to an overall coarser-grained lithology.

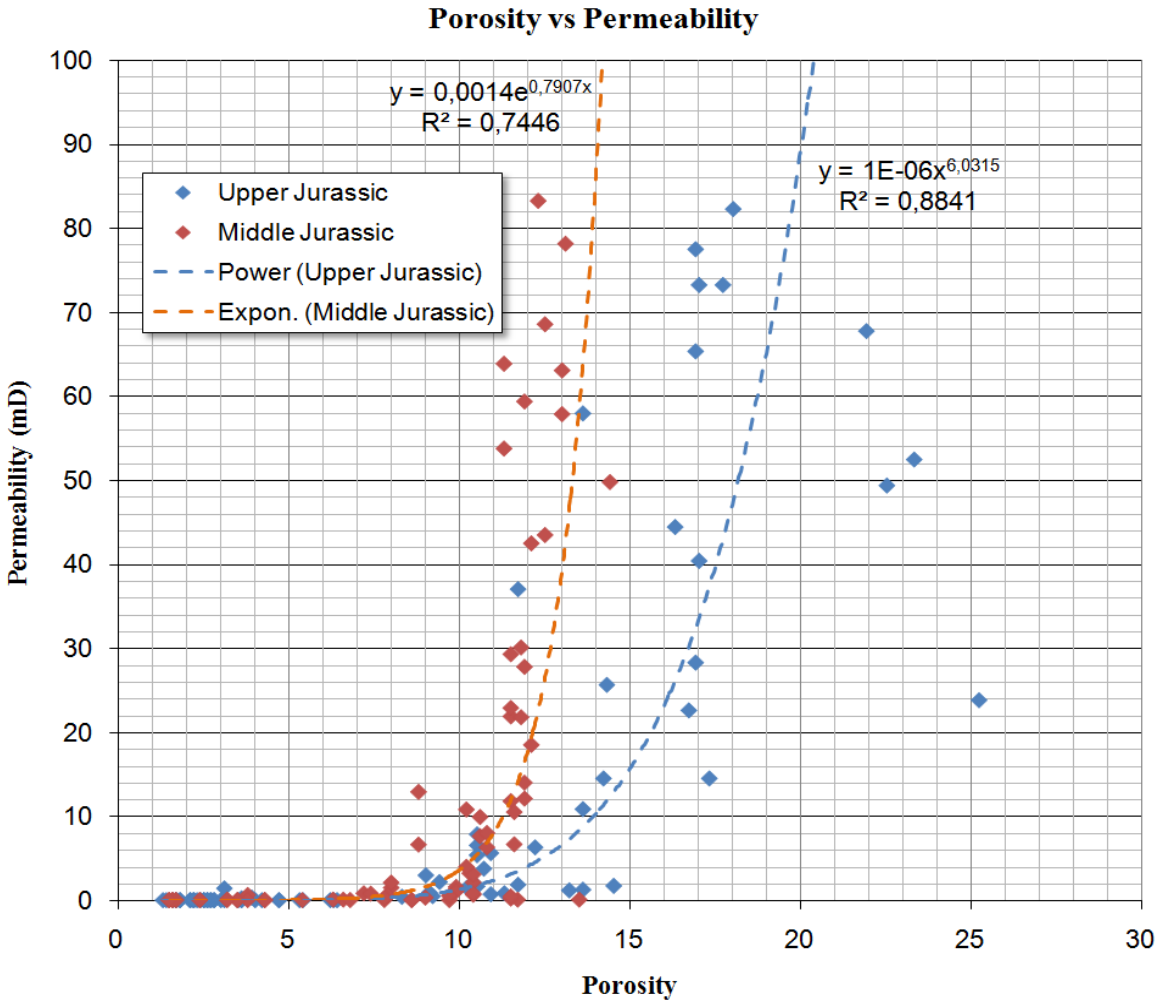

Figure 6-6. Porosity-permeability relationships in upper- and middle Jurassic samples. Note the lower permeabilities in Upper Jurassic samples. This may be related to grain-coats reducing the size of pore-throats.

CHAPTER 7: PETROGRAPHY

7.1 INTRODUCTION

Up to this point it is evident that porosities above the estimated reservoir cut-off of 12,9% are quite common in the deeply buried Upper Jurassic sandstones, and seem to be restricted to the C1, C2, D and E sequences above the Eudoxus maximum flooding surface. The samples taken from the wells described in the previous chapter were examined petrographically in order to determine if grain-coats were present, what types of grain-coats were present, and to which degree the grains were covered. It was also desired to investigate if grain-coats were restricted to certain facies or depositional environments; however the limited amount of samples restricted how far facies could be correlated to grain-coats. Further it was desired to investigate if the pre-Eudoxus sequences are a representative time window for expected anomalously high porosity sandstones.

Characteristic features of quartz cementation have also been studied with special emphasis on the mechanisms controlling the critical moment when quartz cementation commences despite optimally coated sands.

The results obtained here are important input parameters when modeling porosity-depth trends in the area (chapter 8). It is also interesting to see if it is possible to establish any links to the various grain-coating models presented in chapter 3.

7.2 RESULTS

Most of the samples studied in the SEM contained some degree of grain-coating. Two figures will now be presented as an introduction to the petrographic results. Figure 7-1 gives typical examples of clay and micro-quartz coats in the deep marine samples. Figure 7-2 is meant to illustrate how much pore-space the grain-coats actually are capable of preserving. Note also that the main results of the petrographic analysis are found in table 7-2 (at the end of chapter 7).

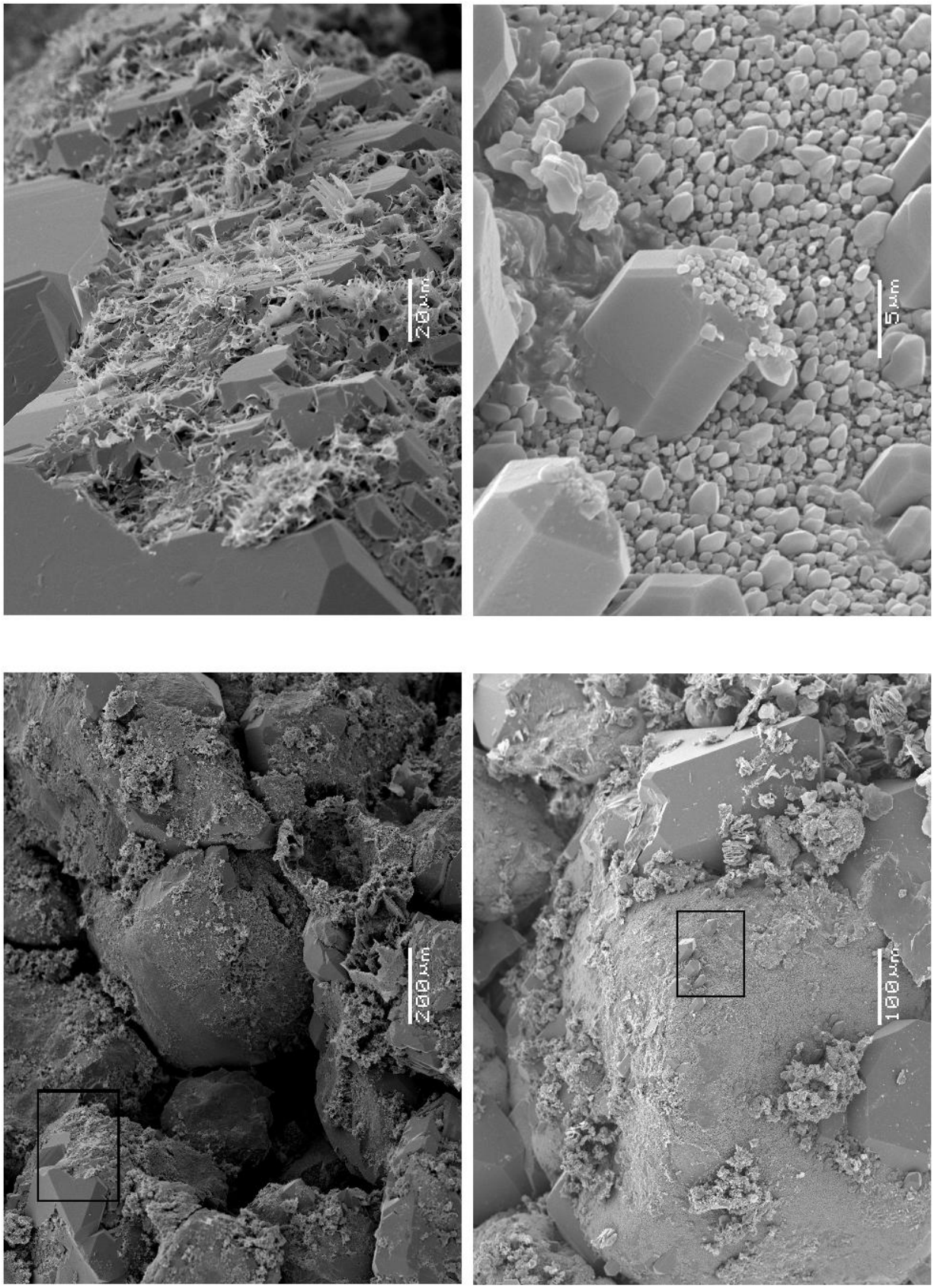

Figure 7-1. Typical examples of grain-coating clay (illite) and micro-quartz inhibiting quartz cementation.

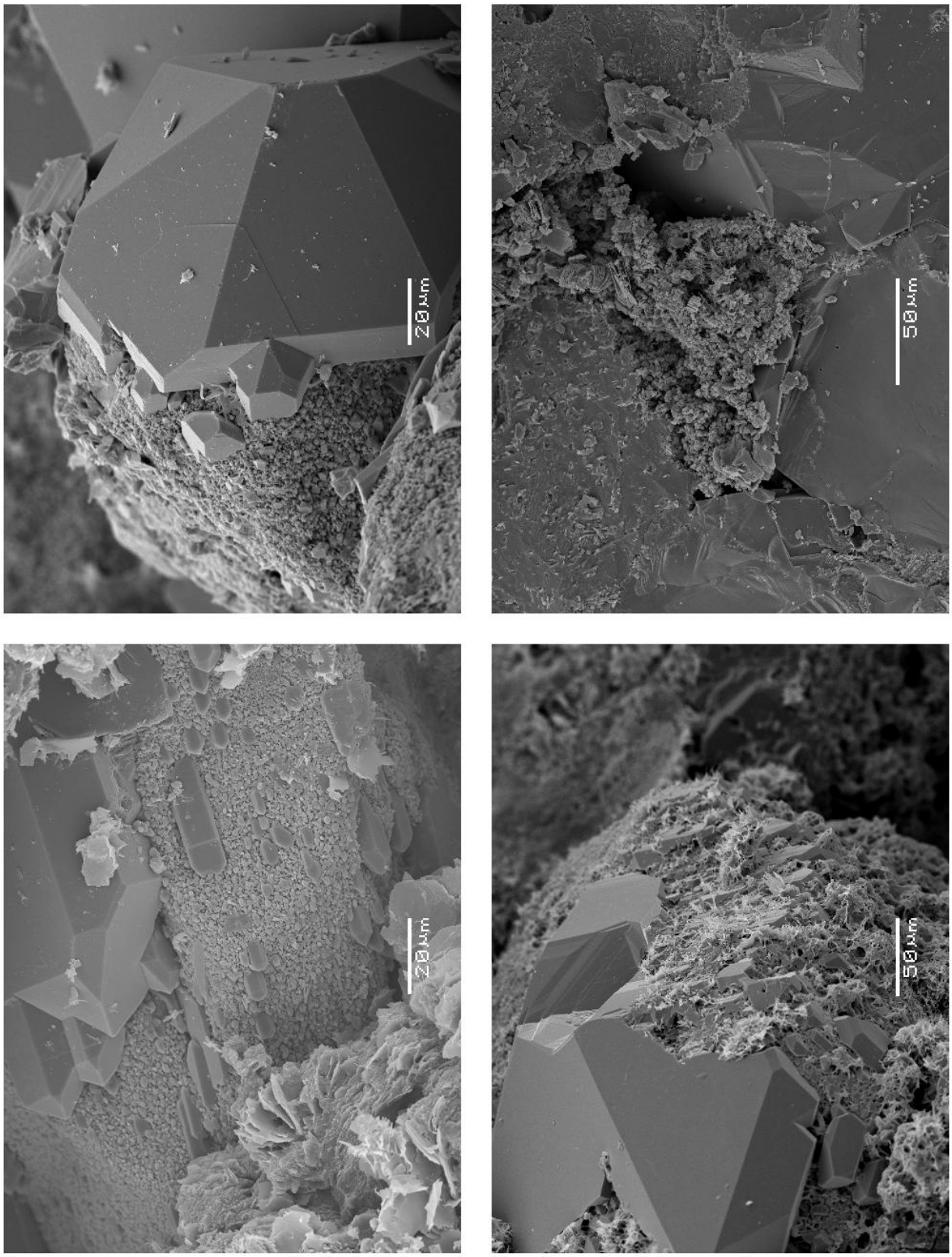

Figure 7-2. Three coated samples with plenty of void in contrast to a cemented sample with pore-filling kaolinite / illite (partly transformed) destroying what might be left of reservoir properties.

7.2.1 Grain-coats

Grain-coating micro-quartz crystals typically ranged in size from a diameter of around 5 μm down to 0,5 μm or even less (figure 7-3). The grain surface coverage was typically extensive, especially in the samples taken from shallow marine sandstones. A simple classification of grain-coats was developed (table 7-1) related to the effect on reservoir properties at depth.

The shallow marine samples studied were all extensively covered by micro-quartz (3-4), and micro-quartz crystals were occasionally seen building out into the pore space (e.g. figure 7-3). Despite their shallow burial (about 1850-1950 mTVDRSF, corresponding to temperatures of about 65-75 ˚C) no evidence of Rhaxella spicules were observed, meaning that the silica transformation process was complete. As expected no quartz overgrowths were observed at this depth and there were no signs of clay-coats. It should be noted that the main emphasis of the thesis is on the deep marine samples, since they are the ones buried to greater depths. Therefore only a few shallow marine samples were chosen. Ideally several samples covering the entire shallow marine range should have been studied to learn more about the distribution pattern in shallow marine sandstones. However extensive micro-quartz coverage was observed in all shallow marine samples representing facies B2, B3 and B4.

The deep marine samples were also often extensively covered by micro-quartz, but seemed to contain a somewhat less extensive grain surface coverage (< 4). Minor quartz overgrowths were observed together with grain-coating micro-quartz, thus indicating that the sandstones had entered intermediate burial depths and that some sites of nucleation were present. Grain-coating clays also occurred in the deep marine samples. Illite was the most frequently observed grain-coating clay, but grain-coating chlorite was also rarely encountered. Clay coats were often observed in combination with grain-coating micro-quartz (figure 7-5), but were also observed where no micro-quartz was present (figure 7-6). Although clay coats were observed in the samples micro-quartz seem to be much more abundant and is therefore belived to be the primary cause of anomalously high porosity.

Table 7-1. Classification of grain-coats based on effects on reservoir properties at depth.

Coating class	Description	Effects on porosity and permeability at depth	Porosity/ permeability preserving potential
4	Thick coats of large micro-quartz crystals (>1-2µm) or thick clay coats completely covering all grains (> 95%). Micro-quartz are commonly building out into the pores.	Will halt quartz cementation effectively and thereby preserve porosity, but some porosity will be lost due to the thick coats often building out into the pores. The permeability will be significantly reduced as pore-throats will become smaller.	Good
3	Complete coverage of all grains (>95%). The coats are not as thick and not building out into the pore-space.	Will effectively halt quartz cementation, but only have minor negative affects on permeability. This is optimal for preserving reservoir properties at depth.	Very good
2	Good to moderate coverage of the grains (50-95%), some nucleation sites are present.	Will inhibit, but not halt quartz cementation. Preserves some porosity and only minor negative effects on permeability.	Good - moderate
1	Poor grain coverage (10-50%). The coats are thin and discontinuous.	Minor-moderate porosity-preserving effect will not affect permeability	Moderate - poor
0	Coats are absent or locally present only in minor amounts (0-10%)	Will not affect porosity or permeability	No effect

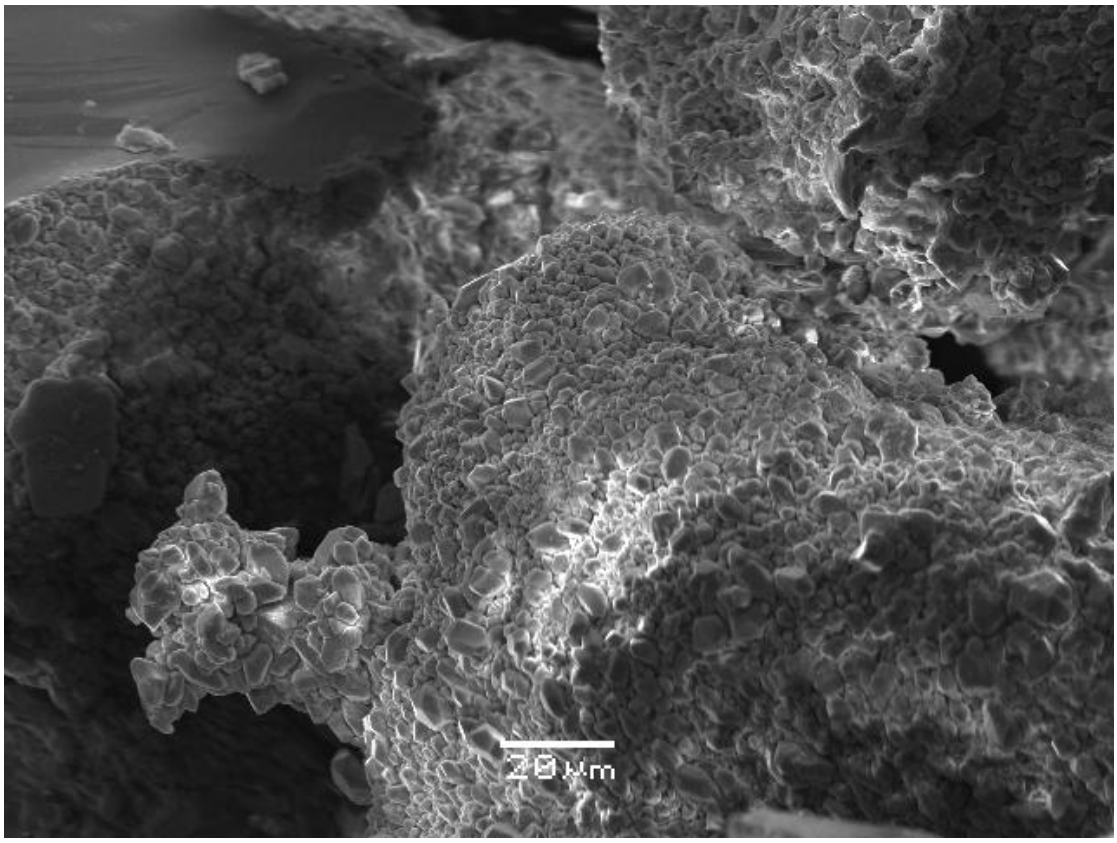

Figure 7-3. Extensive micro-quartz coverage (typical class 4) building out into the pore space. Picture taken from sample F1 (well 25/10-8A, shallow marine).

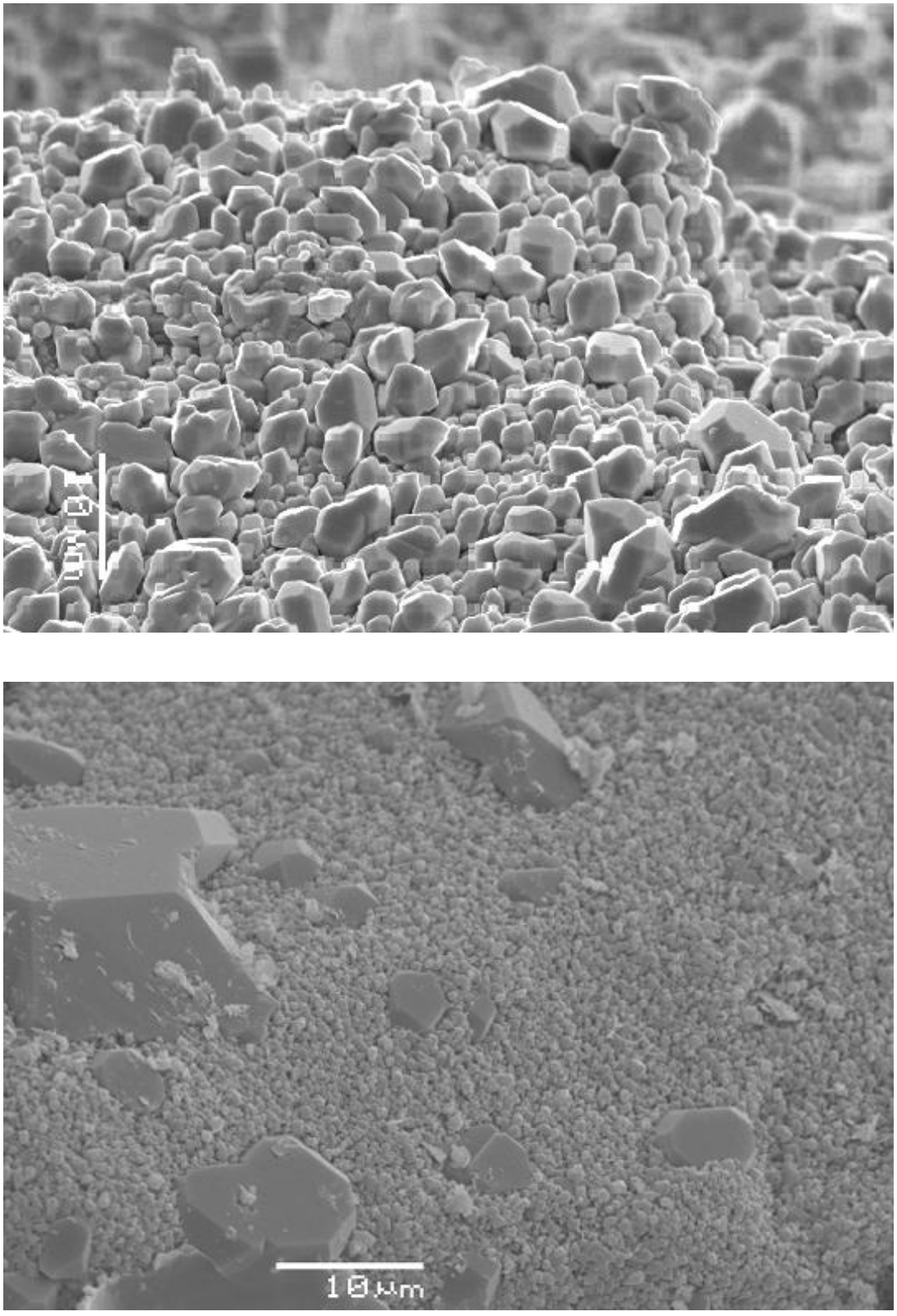

Figure 7-4. Size variation in micro-quartz crystals. Picture I (above) is taken from sample F1. Picture II (below) is taken from sample D2. The diameter of the micro-quartz crystals ranged from 5 µm to less then 0,5 µm.

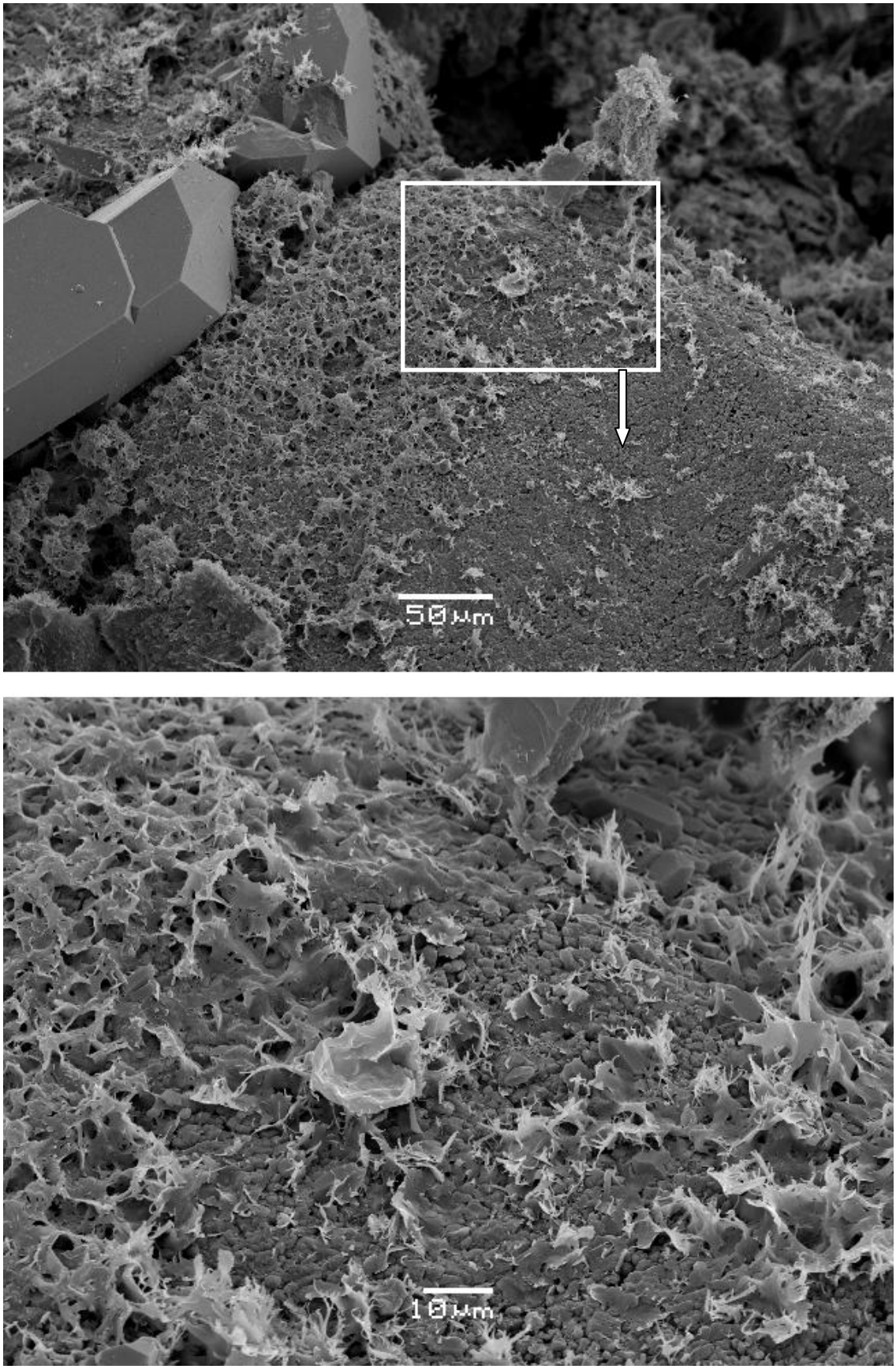

Figure 7-5. Grain-coating micro-quartz and grain-coating illite/smectite. Note that the clay coat is authigenic and post dates the micro-quartz coating. Pictures from sample B4 (well 15/3-3).

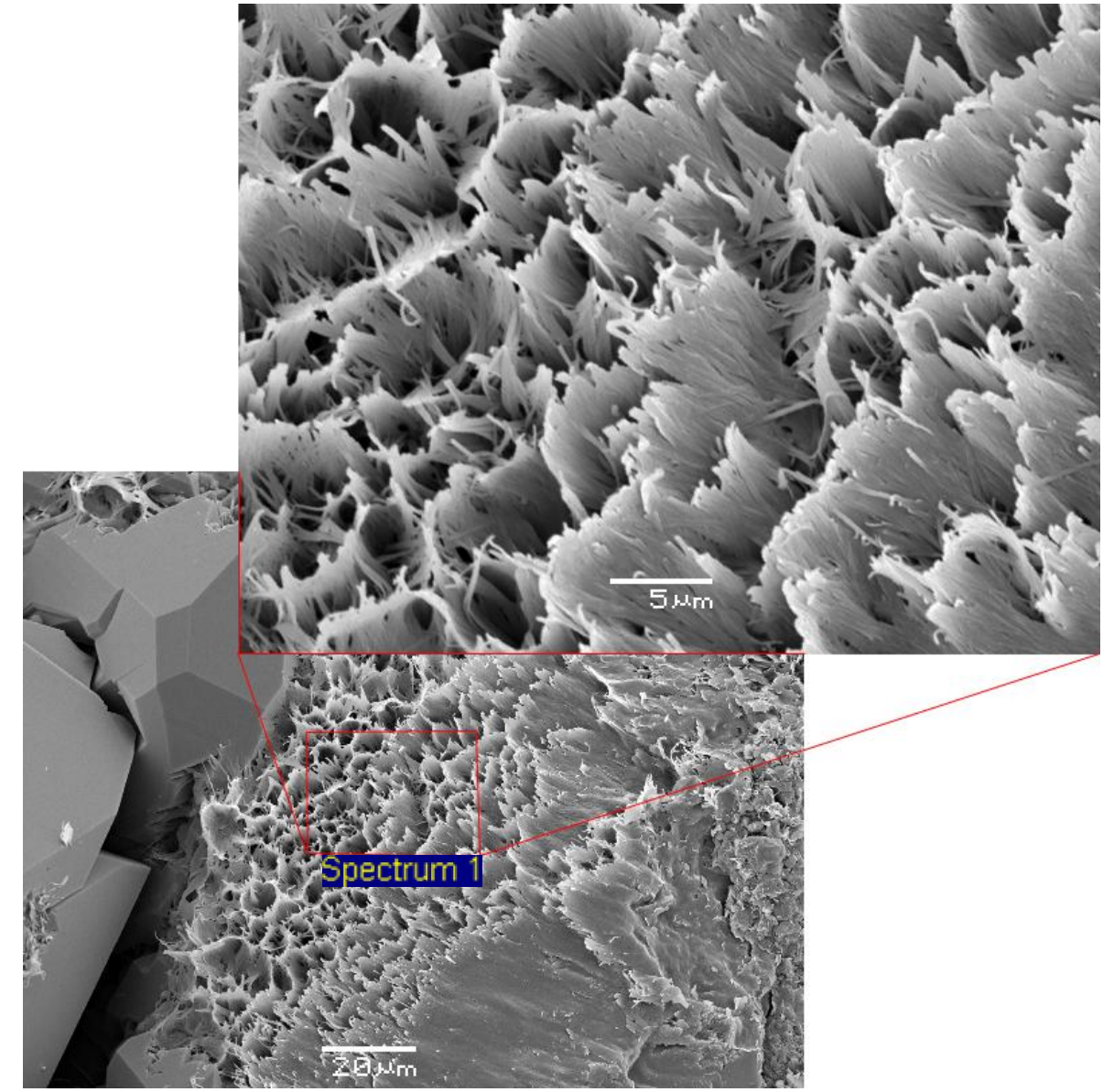

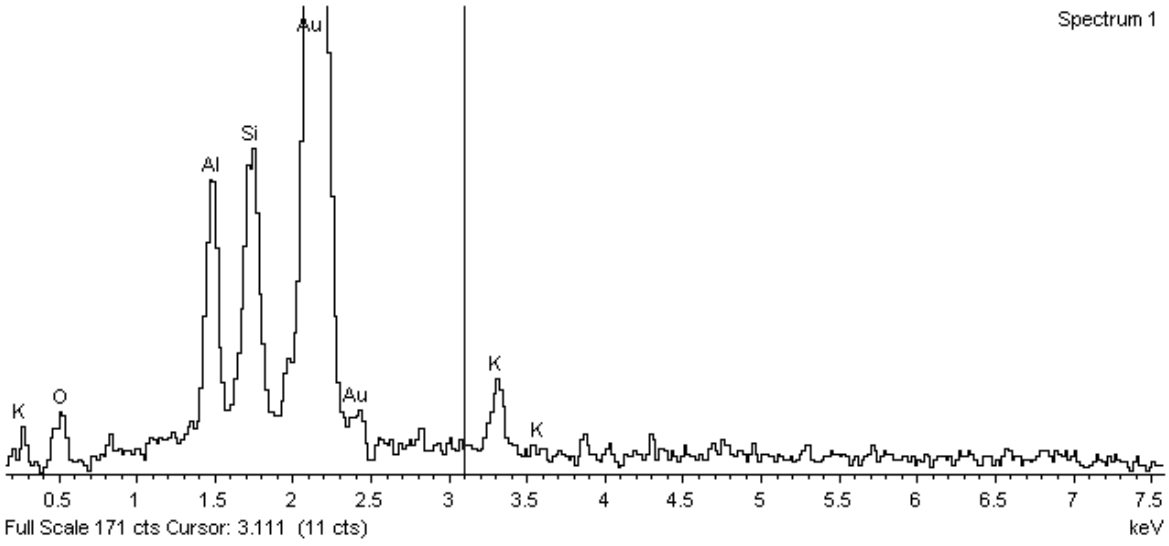

Figure 7-6. Grain-coating illite and quartz overgrowth. Pictures and EDX spectrum from sample B4 (well 15/3-3)

7.2.2 Quartz overgrowth mechanisms

In the absence of grain-coats quartz overgrowths will grow primarily through spiral-growth, resulting in "normal" quartz overgrowths as seen in figure 7-7. This kind of quartz overgrowth requires low silica super-saturations (< 5% (Jahren and Ramm, 2000)). Grain-coats however will halt or impede spiral-growth on detrital quartz, and thus quartz cementation will be inhibited until silica supersaturations build up to a certain higher level. At this stage growth of macro-quartz crystals may commence and grain-coats will gradually be overgrown by quartz overgrowths (figure 7-8 & 7-9).

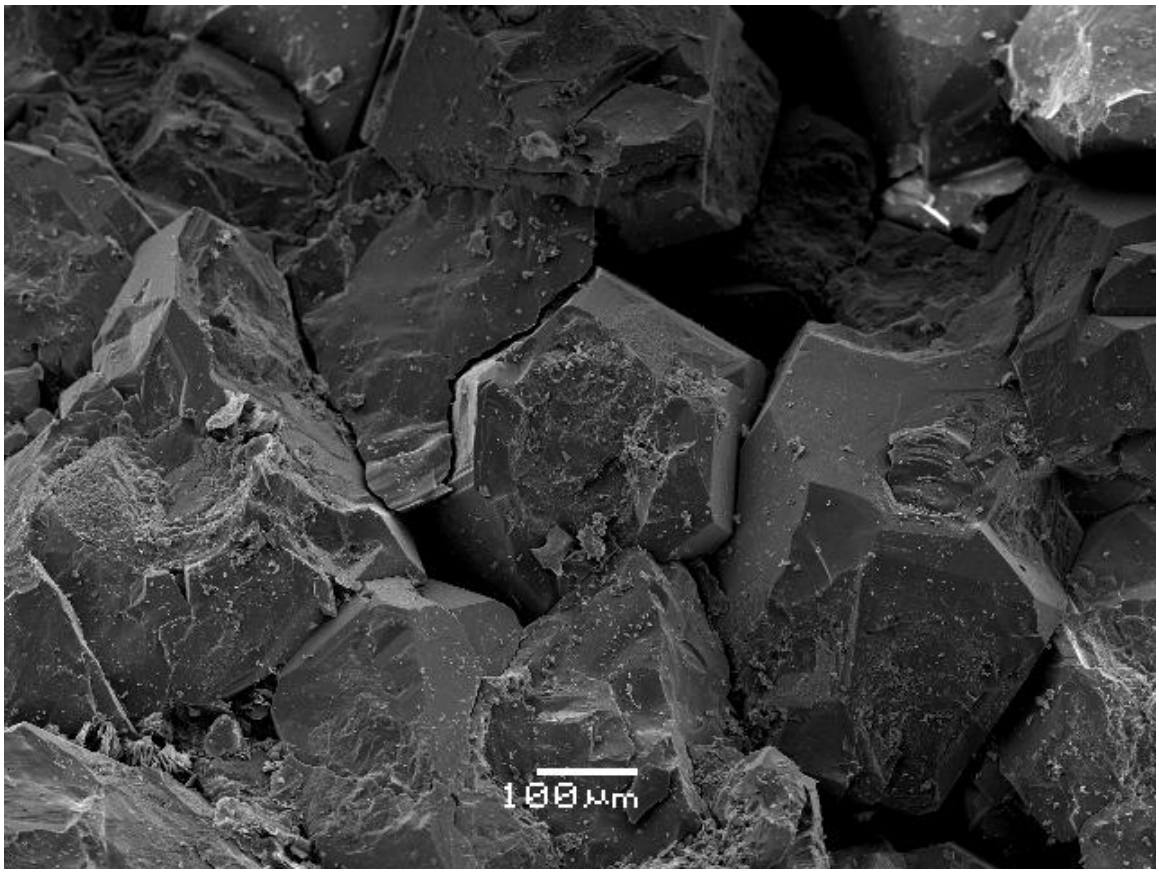

Figure 7-7. Quartz cementation in absence of grain-coats takes place primarily through spiral growth (picture from sample A21).

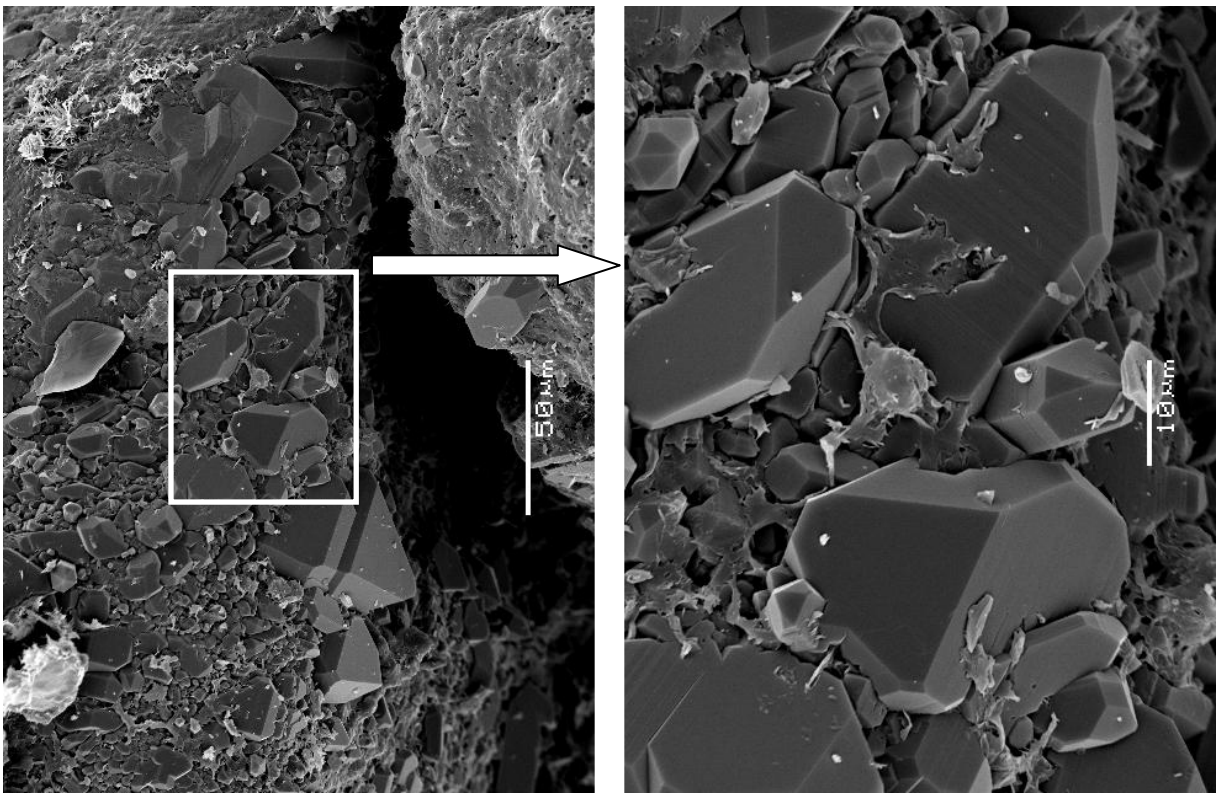

Figure 7-8. Quartz overgrowths have nucleated and started to overgrow the coating (pictures from sample B3).

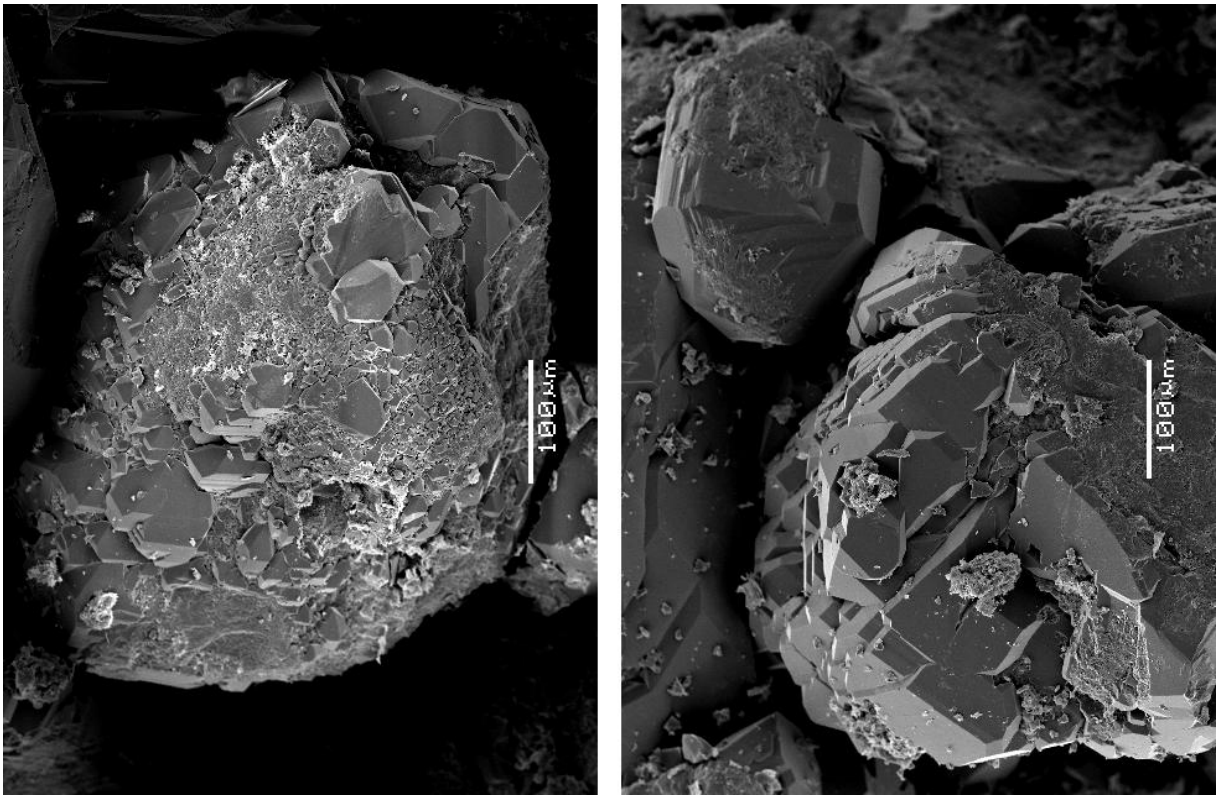

Figure 7-9. Quartz cementation of micro-quartz coated detrital quartz grains. The pictures above are interpreted to represent progressively more advanced stages of quartz cement overgrowing coated sands (pictures from sample B3).

7.2.3 Composition and texture

The sampled sandstones are sourced predominantly from erosion of pre-rift sedimentary rocks that was uplifted along Utsira High and the East Shetland Platform during the Late Jurassic – Early Cretaceous rifting. It was therefore expected that the samples should be compositionally mature (high quartz content). Point-counting indicates that the samples may be classified as quartz- to sublithic arenites (figure 7-9) and thereby confirms the compositional maturity that was expected. Although weathering of basement rocks seem have had an influence on the composition of the sandstones that are sourced from Utsira High.

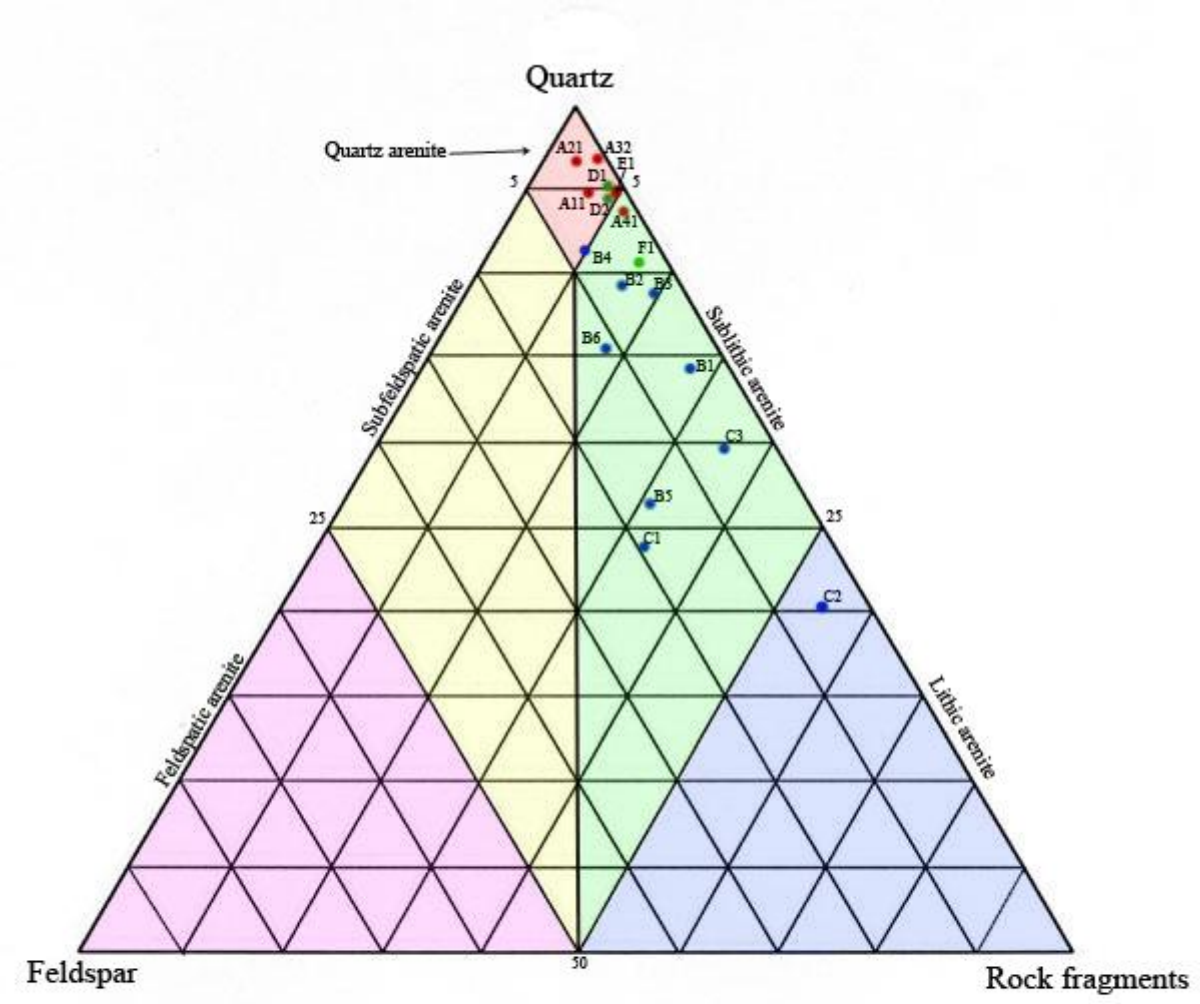

Figure 7-10. Clasification of the samples following Pettijohn (1987). The green dots are shallow marine samples with an eastern provenance. The red dots are deep marine samples with a western provenance, while the blue dots are deep marine samples with an eastern provenance. The composition is also given in table 7-2.

It is interesting to note compositional and textural differences related to the provenance and facies of the sandstones. The deep marine samples contain a higher fraction of rock fragments when sourced from the Utsira High area compared to those sourced from the East Shetland Platform. These samples were also significantly better rounded and more well-sorted. Thus it seems that the Upper Jurassic sands with a western provenance are both texturally and compositionally more mature. This information may be useful if there is any doubt as to an eastern or western provenance. For example it seems that the deep marine sands in well 24/12-2 are sourced from the west since it plots as a quartz arenite in figure 7-9.

Table 7-2. Main results of the petrographic analysis.

Well	Sample	Depth (mRT)	Average grain-size	Frame work composition			Matrix	Porosity / calcite cement	Grain-coating			Sequence	Facies
				Quartz	Fld	LRF			Illite	Chlorite	Micro-quartz		
9/24b-4	A11	4793	0,4	95,0	1,8	3,2	0,8	10,7	0	0	0	B2	A2
9/24b-4	A21	4806	0,375	97,2	0,6	2,2	0,8	9,3	0	0	0	B2	A1
9/24b-4	A32	4390	0,375	97,2	0,0	2,8	1,8	8,5	0	0	0	B1	A1
9/24b-4	A41	4442	0,4	93,5	0,5	6,0	1,3	5,2 / 2,0	0	0	0	B1	A1
15/3-3	B1	4267	0,375	84,9	1,8	13,3	4,9	22,0 / 5,6	0	0	3	C1	A1
15/3-3	B2	4277	0,3	89,7	3,0	7,3	3,4	14,9	1	1	0	C1	A1
15/3-3	B3	4282	0,375	89,1	1,7	9,2	4,7	19,7	2	0	2	C1	A1
15/3-3	B4	4286	0,35	91,7	3,8	4,5	7,9	17,8 / 0,8	2	1	3	C1	A1
15/3-3	B5	4293	0,45	76,4	8,2	15,4	6,8	12,4 / 0,3	2	1	0	C1	A1
15/3-3	B6	4303	0,4	85,8	5,7	8,5	7,4	21,0 / 0,7	0	0	3	C1	A1
15/3-1S	C1	4086	0,55	74,2	9,6	16,3	1,4	8,4 / 3,6	0	0	0	D	A2
15/3-1S	C2	4143	0,25	70,3	2,3	27,4	5,0	16,3 / 5,6	0	0	2	D	A1
15/3-1S	C3	4145	0,5	79,8	2,9	17,3	6,0	17,5 / 3,2	1	0	2	D	A1
16/1-5	D1	2027	0,175	95,0	0,8	4,2	6,4	25,9	0	0	3	B1	B1
16/1-5	D2	2055	0,125	94,4	1,5	4,1	10,3	22,1	0	0	3	A	B2
24/12-2	E1	4961	0,125	94,7	0,8	4,5	0,0	0,0 / 40,7	-	-	-	Pre A	A1
25/10-8A	F1	3166	0,2	90,7	1,6	7,7	1,7	33,5	0	0	4	C1	B4

CHAPTER 8: MODELING

8.1 INTRODUCTION

It has been argued that porosity loss in quartz-rich sandstones during intermediate and deep burial is primarily a function of quartz cementation (chapter 3), while mechanical compaction is the dominant factor during shallow burial. The modeling algorithm described in chapter 4 was employed to simulate mechanical compaction and quartz-cementation, and predict porosities at depth. This chapter is devoted to modeling porosity-depth trends in the study area aiming to (*i*) optimize the model parameters based on the results from earlier chapters, and (*ii*) investigate and simulate the effects of grain-coats, as well as lithological effects, on porosity in deeply buried sandstones in the study area.

It is useful to provide some terminological definitions applied in this chapter. Average porosity trends are the modeled porosity-depth trends that result from using statistical mean variable (grain-size, fraction quartz, etc.) values. Maximum and minimum porosity trends are the modeled porosity depth trends that result from using variable values within the expected statistical range that favor high or low porosities respectively.

Table 8-1. Overview and subdivision of the most important input variables used in the porosity algorithm.

Lithological variables				
	Depositional porosity (Φ_{dep})	Grain-size (D)	Fraction-qz (f)	Coating fraction (g)
Values:	0,4	0,0125 – 0,2 cm	0,7 – 1	0 – 1
Critical factors:	Depositional environment, provenance			
Variables related to basin dynamics				
	Heating rate (c)	Porosity at onset of quartz cementation (Φ_0)		
Values:	0,7 – 1,2 ˚C/Ma	0,2-0,3		
Critical factors:	Pressure regime, Thermal history (subsidence rates, heat flow)			
Physical and chemical constants				
	Kinetic constants, quartz (a and b)	Molar mass, quartz (M)	Density, quartz (ρ)	
Values:	Walderhaug, 1994a	60,09 g/mole	2,65 g/cm^3	

8.2 RESULTS

8.2.1 Modeling porosity-depth trends

It turned out that a heating rate equal to 0.75 gave a satisfactory fit for most of the wells and may therefore be used as a general value for the study area. Figure 8-1 shows modeled minimum, average and maximum porosity depth-trends for deep marine sandstones (grain-coats not accounted for), compared to calculated porosities for all wells.

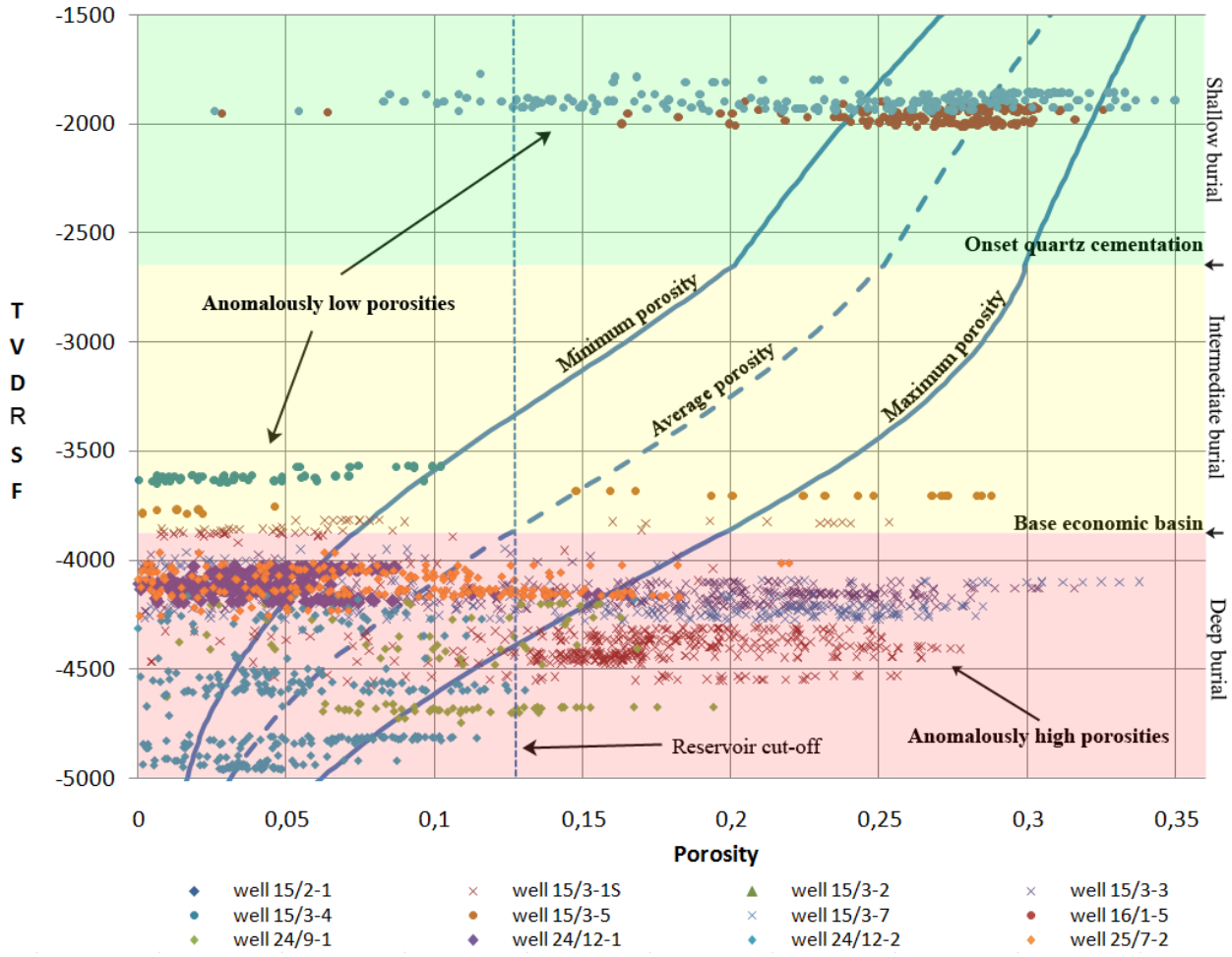

Figure 8-1. Calculated sandstone porosities compared to modeled porosity-depth trends for average lithological variables values in deep marine sandstones. Note the anomalously low porosities in well 24/12-1, 25/10-8A and 15/3-4. These are interpreted as shallow marine sandstones (Facies B1-B3) and the petrographic investigation indicates that they are finer grained and contain a higher fraction of quartz compared to the deep marine sandstones (this leads to a more rapid porosity decay at depth).

Some of the calculated porosity values fall outside the modeled minimum porosity trend. In the case of well 24/12-1, which is the most obvious outlier, this is most likely because the sands are not deep marine, but shallow marine sands, and thus will be finer grained and compact more rapidly during intermediate and deep burial. In general anomalously low porosity may be explained by; (i) the temperature-history or lithological parameters deviates from assumptions made or (ii) calcite cement has destroyed porosity. The calculated porosity values falling outside the maximum porosity trend are most likely all coated sands. Note however that residual gas in the flushed zone probably have amplified the anomalously high porosities by about 5% in gas-sands of the Gudrun Field (e.g. 15/3-3, 15/3-1S and 15/3-7). Note also the subdivision of shallow, intermediate and deep burial (as defined in section 3.1.1.1) based on the modeled average porosity-depth trend. It is clear from figure 8-1 that the expected depth of reservoir cut-off is at ~3800m (TVDRSF) in deep marine sandstones.

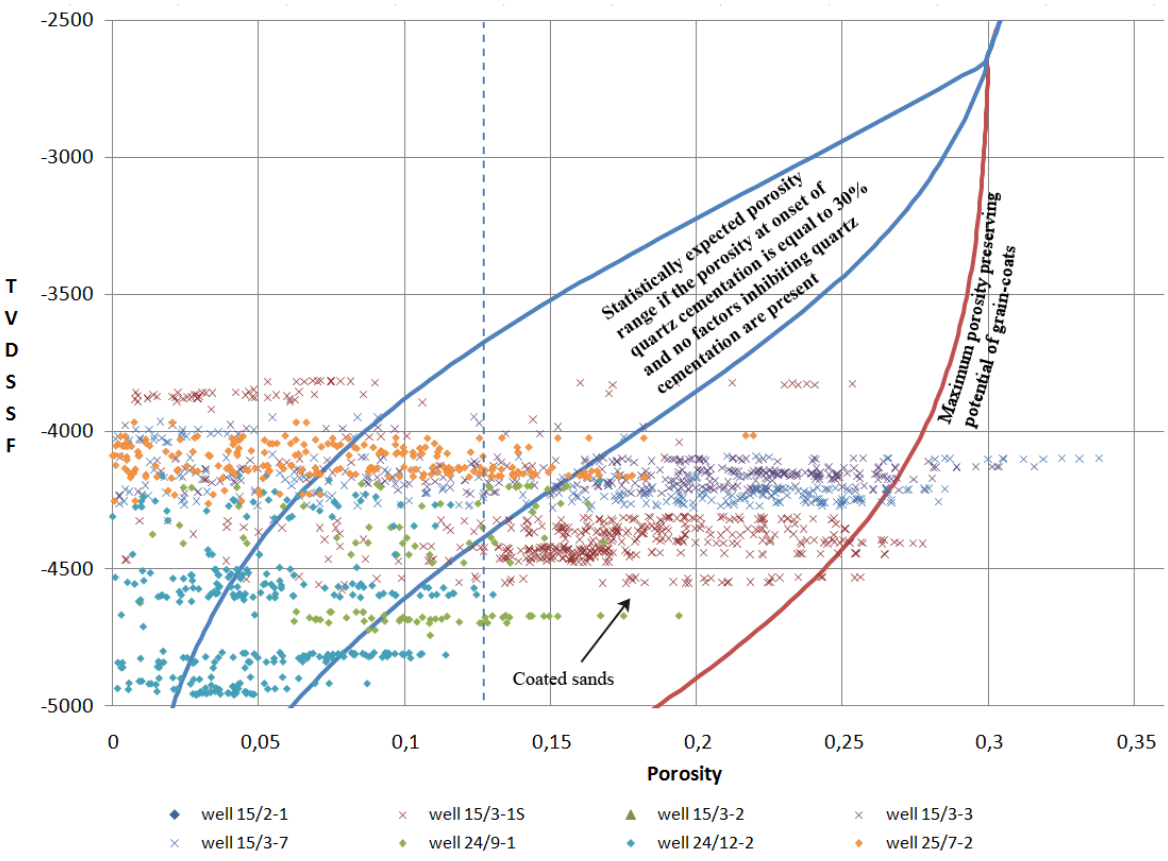

Figure 8-2. Calculated porosities in deep marine sandstones compared against modeled maximum porosity-preserving potential of grain-coats. Note that the depth of reservoir cut-off most likely may be extended to burial depths of approximately 5000-5500 m (TVDRSF) under optimal conditions, due to grain-coats and overpressure.

The maximum porosity-preserving potential of grain-coats is modeled in figure 8-2. This assumes overpressures to be present throughout the burial history of the rock, causing a reduction in mechanical compaction of 5% on average and delaying the fracturing of quartz grains to somewhere below 5000m. Note that the modeled porosity-depth trends in figure 8-2 are compared only to deep marine sandstones.

Most of the calculated sandstone porosities are within the modeled range of porosity variations that occur due to coating fraction and other lithological variables. The modeled maximum preservation potential of grain-coats gives a good fit to the calculated porosities. Note also that grain-coats, according to the model, may preserve porosities above reservoir cut-off to burial depths below 5000 m.

8.2.2 Observed effects of grain-coats on porosity

As has just been showed the modeling algorithm is quite capable of predicting sandstone porosities in the study area, also for coated sands. Table 8-2 and figure 8-3 shows an analysis of the porosity-preserving effect of grain-coats in the samples evaluated in chapter 7.

The compositional and textural results achieved in chapter 7 were used as input variables in the modeling algorithm along with heating rate estimates (derived from TVDRSF and age of the samples), in order to establish an expected porosity in the samples if grain-coats were absent (see table 7-1). This made it possible to estimate quantitatively the porosity-preserving effect of grain-coats in each sample (Δ porosity). As can be seen there is a good correlation between the observed amount of grain-coats and high values of Δ porosity. There are several potential errors in the estimated Δ porosity; however porosity values that are 10% or even more above the expected seem to be quite common in the Upper Jurassic sandstones sourced from the Utsira High area, while the sands sourced from the East Shetland seem to lack the presence of effective grain-coats.

Table 8-2. Petrographic and modeled data from deeply buried, deep marine samples.

Sample	Model input			Output	Petrographic observations		Δ porosity
	Depth (TVDRSF)	Average grain-size	Quartz fraction	Modeled porosity (no coating)	Observed porosity (point counting)	Coating fraction	
A11	4317	0,4	95	9,3	10,7	0	1,4
A21	4326	0,375	97,2	8,9	9,3	0	0,4
A32	4390	0,375	97,2	6,4	8,5	0	2,1
A41	4442	0,4	93,5	5,0	5,2	0	0,2
B1	4234	0,375	84,9	8,3	22,0	3MQ/1Cl	13,7
B2	4144	0,3	89,7	7,2	14,9	1Cl	7,7
B3	4149	0,375	89,1	10,5	19,7	3MQ?	9,2
B4	4153	0,35	93	8,3	17,8	3MQ/2Cl	9,5
B5	4160	0,45	76,4	6,4	12,4	2Cl	6
B6	4170	0,4	85,8	6	21,0	3MQ	15
C1	3952	0,55	74,2	5,3	8,4	0	3,1
C2	4009	0,25	70,3	7,6	16,3	2MQ	8,7
C3	4011	0,5	79,8	8,9	17,5	2MQ/1Cl	8,6

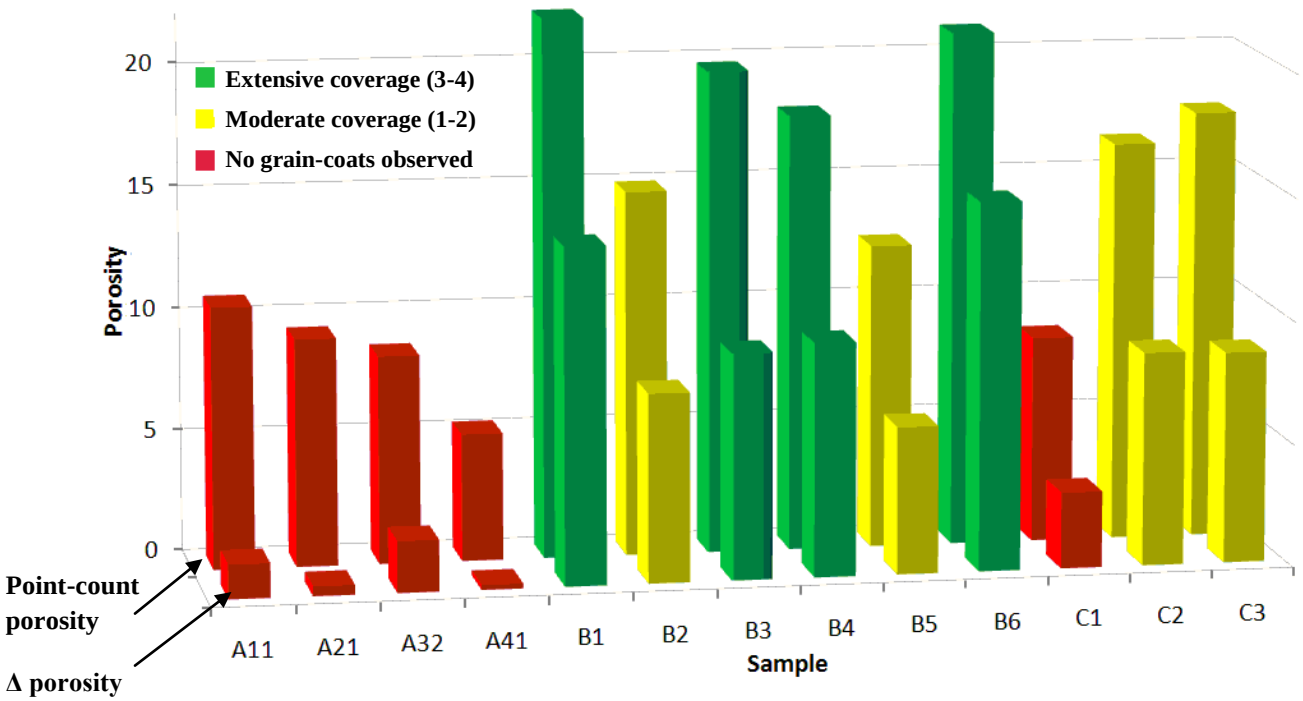

Figure 8-3. Illustration of the porosity-preserving effect of grain-coats (MQ: micro-quartz, Cl: clay) from the samples. Note the good correlation between the observed extent of coating and the estimated porosity-preserving effect of the grain-coats (Δ porosity).

8.2.3 Modeling effects of grain-coats and overpressure on porosity

The previous section gave a brief analysis of the porosity-preserving effect of grain-coats in the samples evaluated in chapter 7. Now the general effects of grain-coats on sandstone porosity in the study area will be highlighted further through modeling examples. Lithological parameters (except coating fraction) will in this section be set according to values observed for deep marine sandstones sourced from Utsira High. Note however that lithological parameters will significantly influence the surface area available for quartz precipitation (illustrated in figure 8-4 and 8-5) and thus will have profound effect on modeled porosity.

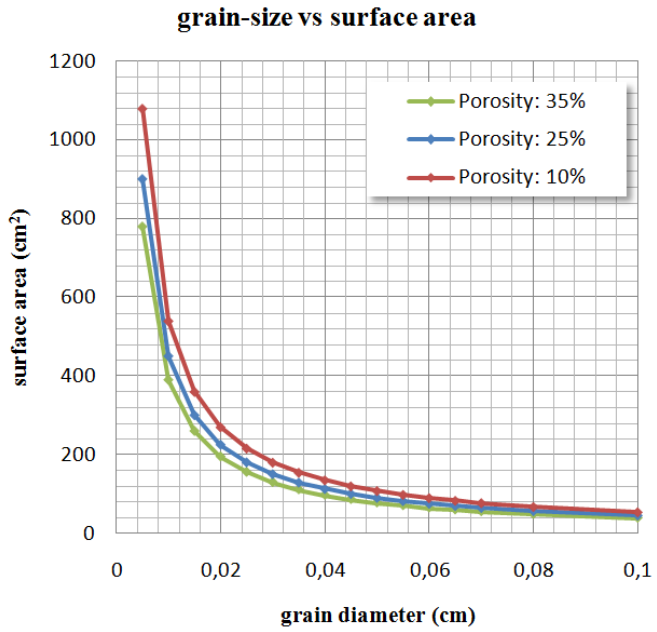

Figure 8-4 (left). Showing grain surface area as a function of grain-size. Note that fine grained sands will tend to have a surface area that is approximately one order of magnitude larger than coarse grained sands.

Figure 8-5 (below). Showing porosity-depth modeling examples illustrating the effects of grain-size and fraction-quartz on porosity. These parameters have impact on the surface area available for quartz precipitation. Note especially the large impact grain-size has on the modeling results.

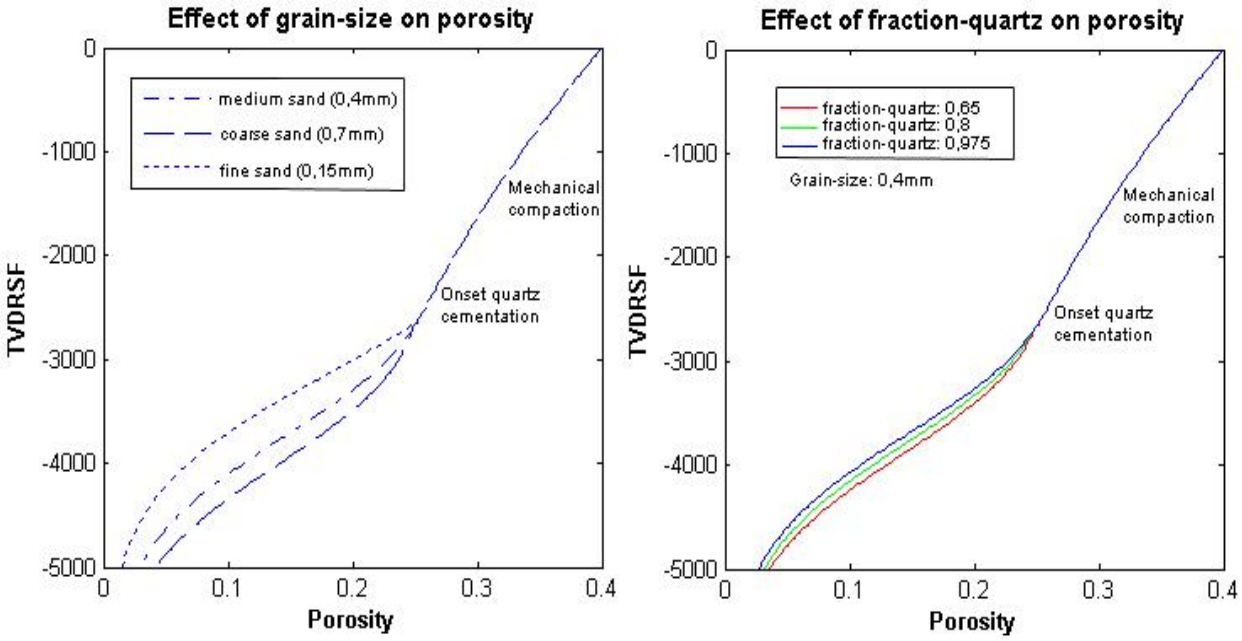

It was shown in figure 8-2 and 8-3 that grain-coats are capable of preserving porosities of atleast 10%. Modeling indicates that the maximum porosity-preserving potential of grain-coats are about 15% in the study area (figure 8-6). In such cases it is critical that overpressure is present, at least during deep burial, because this will delay fracturing of coated quartz grains and probably also limit the levels of silica super-saturation preventing quartz starting to overgrow the coating (Jahren and Ramm, 2000).

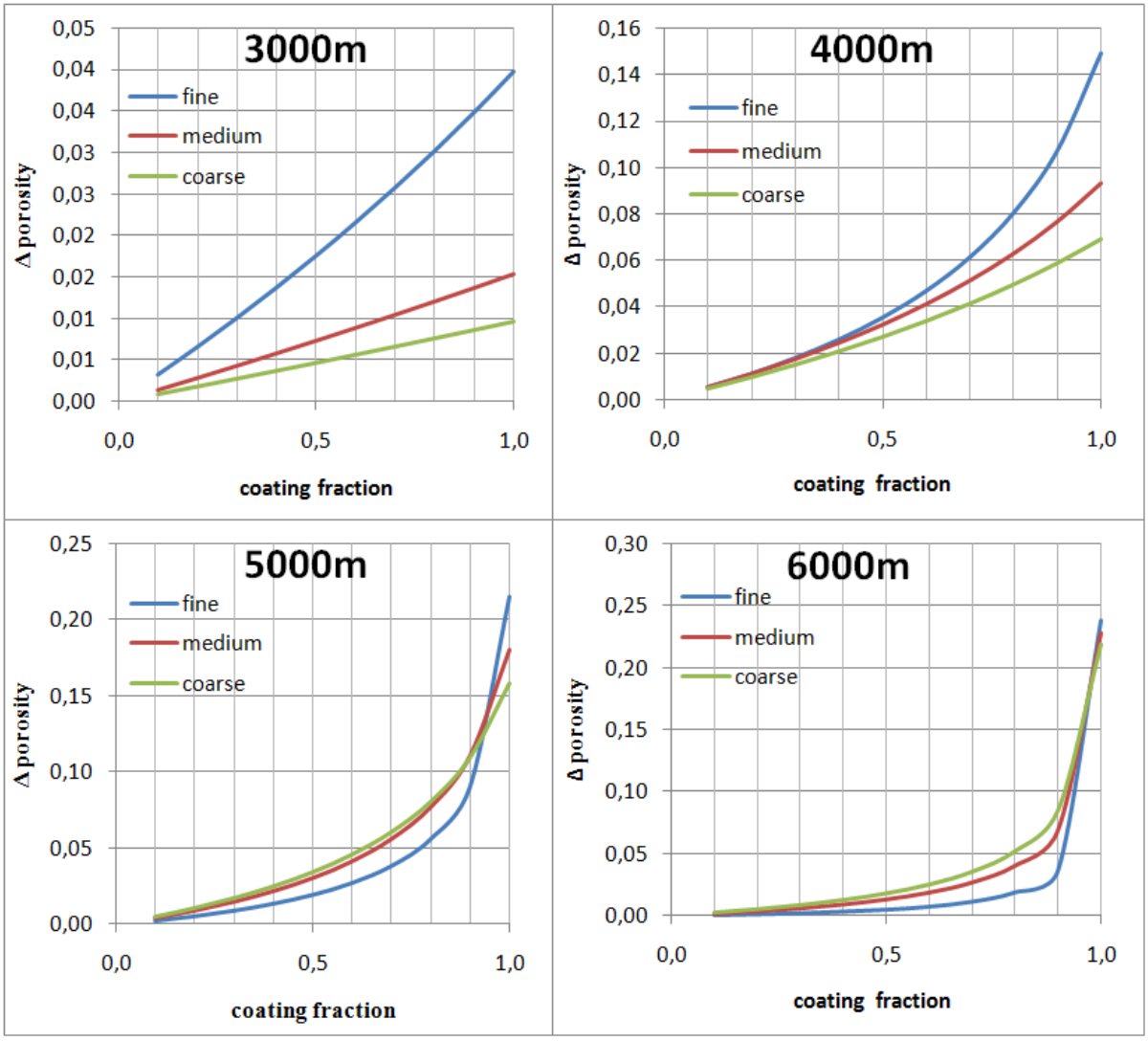

Figure 8-6. Modeled porosity-preserving effects of grain-coats (Δ porosity) at various depths in the study area. The porosity at onset of quartz cementation is assumed to be equal to CCP and grains are assumed not to fracture.

These two variables seem to be overlooked in the exemplar algorithm, and therefore two additional variables should be incorporated in the algorithm:

i. A variable dealing with fracturing of coated grains when a critical effective stress value is reached (~40 MPa (Chuhan et al., 2002) but this will depend on the grain-size).

ii. A variable dealing with the super-saturation level permitting macro-quartz to overgrow grain-coats. This critical silica super-saturation level is likely controlled by the effective stress and temperature in coated sands and would be difficult to quantify.

Figure 8-7 gives hypothetical examples of how porosity-depth curves in coated sandstones may deviate from the modeling predictions (green lines).

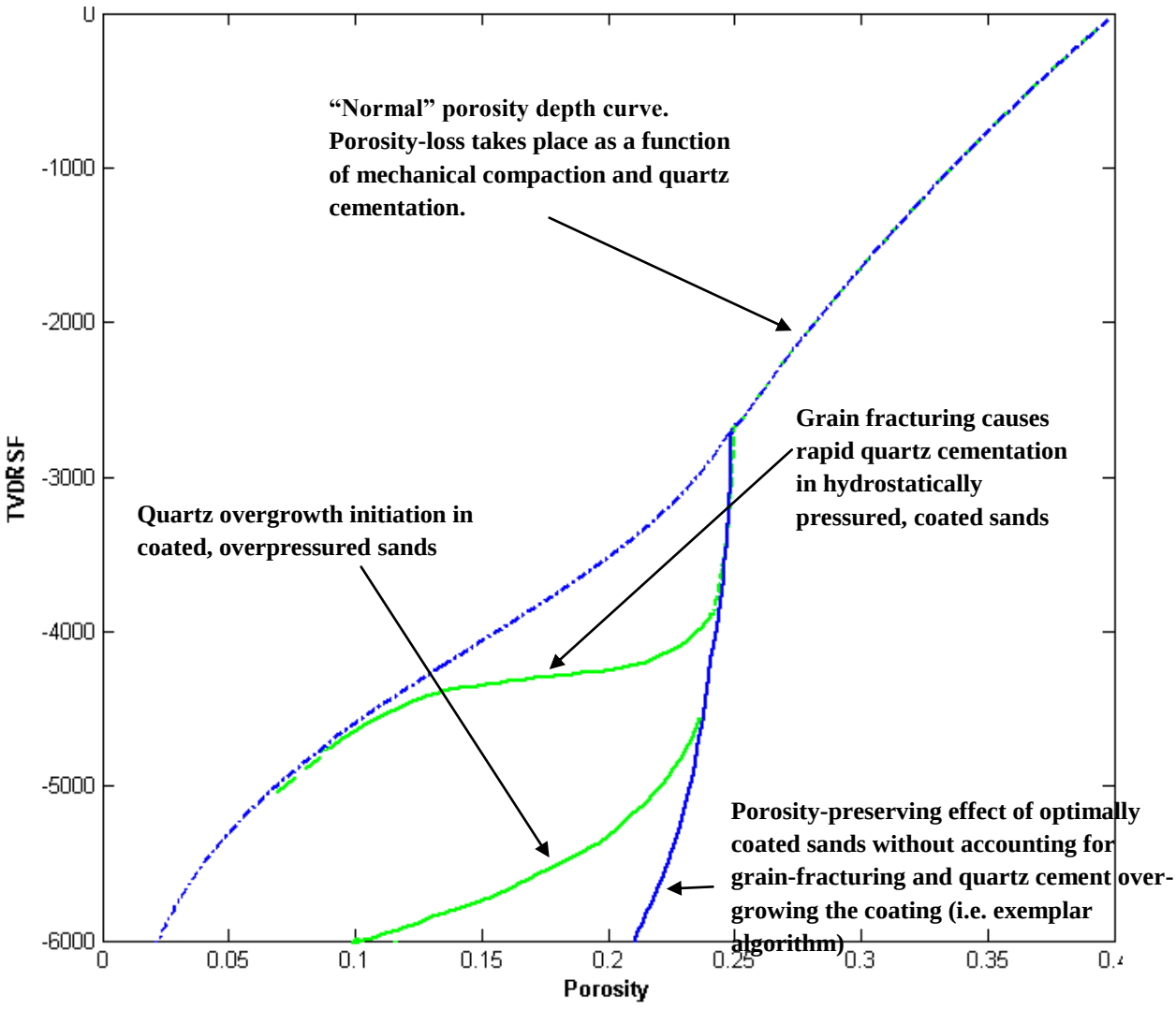

Figure 8-7. Porosity depth curves for uncoated and optimally coated sands as predicted by the modeling algorithm (blue lines). The green lines are schematic illustrations of the effect of (i) grain-fracturing in coated, hydrostatically pressured sandstones and (ii) quartz cementation despite optimal coating in overpressured sandstones.

CHAPTER 9: DISCUSSION

9.1 INTRODUCTION

Through the last four chapters it has been shown that grain-coats may preserve porosities of 10-15% above expected in optimal cases and seem to be of primary importance for preserving reservoir properties in deeply buried sandstones in the study area.

High overpressure is present in the Vilje and Vana sub-basins and is most likely an important secondary factor to consider, probably more important then current modeling algorithms (exemplar) account for. In addition the depositional environment and provenance are factors that may affect diagenesis and destruction of reservoir properties further.

These factors and their significance to reservoir quality in the area will now be considered.

9.2 POROSITY-PRESERVING MECHANISMS

9.2.1 Significance of porosity-preserving mechanisms on reservoir quality in the study area

It became clear during the petrophysical evaluation that the percentage of coated-sands in sandstones in the study area could be very significant (i.e. the Gudrun Field). The petrographic analysis and modeling indicate that grain-coats actually are the primary cause of porosities above reservoir cut-off in the high porosity zones found in the petrophysical evaluation. Based on the petrophysical data the intra sandstone Net-Gross for the Gudrun wells (15/3-3, 15/3-1S, 15/3-7) was approximately 68%, where about 8% of the gross are carbonate cemented intervals (as defined by the carbonate filter). Converted to meters (sample interval: 30 cm) these three wells contain 490 meters of coated sands and only 245 meters of tightly carbonate or quartz cemented sandstones. Thus potential analogues to the depositional system making up the Gudrun reservoir may maintain significant pay volumes to burial depths greater than anticipated.

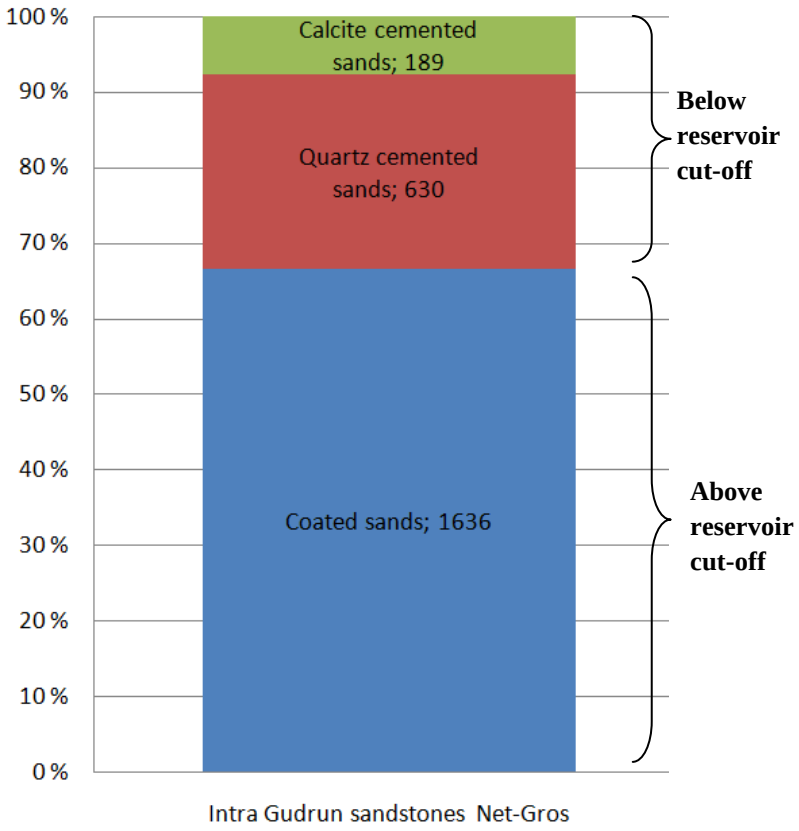

Figure 9-1. Intra sandstone Net-Gross estimates in deeply buried Upper Jurassic Gudrun sandstones (well 15/3-1S, 15/3-3 and 15/3-7). The figure is based on petrophysical interpretation.

Petrographical analysis indicates that grain-coating micro-quartz is the primary cause of high porosities in the Gudrun wells. The origin of micro-quartz coats in the study area is, as has

been mentioned, linked to transformation of spicules from the siliceous sponge Rhaxella Perforata. It is desired, however to integrate the effects of micro-quartz in reservoir models, and some useful indicators has been found in this study.

9.2.1 Grain-coating micro-quartz: Reservoir model implications

Micro-quartz coats in the North Sea are caused by transformation of spicules of the ancient siliceous sponge Rhaxella Perforata (Aase et al., 1996; Hendry and Trewin, 1995), thus depositional environment and sediment age are important controls on the occurrence of micro-quartz (chapter 3).

Spicules and specimen of Rhaxella Perforata was first reported from the Lower Calcareous Grit Formation (Lower Oxfordian) in Yorkshire (Hinde, 1890) and is common in the Upper Jurassic to Lower Cretaceous of the North Sea as well as onshore England (Table 9-1). Rhaxella spicules is abundant in several shallow marine deposits in the North Sea region (e.g. Alness Spiculite Member, the Fulmar Formation), but are also common in deep marine turbiditic reservoirs (e.g. Scapa, Ten foot turbidites). Thus, as was pointed out by Aase et al. (1996) the reworking paths of sands from shallow marine environments where Rhaxella Perforata lived are possible depositional environments with enhanced porosity.

By analogy sedimentary reworking of sponge spicules should be of importance as distributive mechanism in shallow marine sandstones and Rhaxella Spicules are in fact known to be ubiquitous in shallow marine (Oxfordian) rocks onshore southern England (e.g. Wilson, 1968). Vagle et al. (1994) argued that Rhaxella Perforata was subject to a rapid post-mortem decomposition, which enabled sedimentary reworking of the spicules prior to deposition. Thus it seems, from the large range of environments in which Rhaxella spicules and micro-quartz is found, that the spicules may be transported by sediment-gravity, tidal-, and wave-processes and deposited in these different depositional settings. The necessary conditions for a Rhaxella Perforata habitat may therefore be hard to interpret, it may seem however that their presence is linked to a warm, tropical, shallow marine environment with low or moderate sedimentation rates (table 9-1).

Table 9-1. Some known locations where Rhaxella Spicules are common.

Location	Formation / Member	Age	Depositional environment	Reference
southern England	Corallian beds	Oxfordian	Sediment starved lagoon	(Talbot, 1973; Wilson, 1968)
Moray Firth	Alness Spiculite Member	Mid Oxfordian	Large subtidal shoal	(Andrews and Brown, 1987)
Scapa Field (Moray Firth)	Scapa Member	Valanginian – late Hauterivian	Turbidites	(Hendry and Trewin, 1995)
Brora (Inner Moray Firth)	Brora Arenaceous, Brora Argillaceous	Oxfordian – callovian	Coastal sand bar: Tidal sand waves	(Vagle et al.,1994)
Moray Firth (Claymore Field)	Cimmeridge Clay Formation Formation (Ten Foot turbidites)	Kimmeridgian – early Tithonian	Turbidites	(Spark and Trewin, 1986)
Central Viking Graben (Fulmar Field)	Fulmar Formation	Kimmeridgian – Oxfordian	Highly bioturbated, shelf - lower shoreface	(Gowland, 1996; van der Helm et al., 1990)
Central Viking Graben (Ula Field)	Ula Formation	Early Tithonian	Shoreface, offshore bar, tidal sand waves	(Ramm and Forsberg, 1991; Vollset and Dorê, 1984)

It is hard to interpret any clear correlations between micro-quartz and facies from the limited amount of samples studied. However lobe- and slope-channel facies (A1, most of the samples studied) are commonly optimally coated and display good reservoir quality despite burial depths greater than 4000 mTVDRSF. Evidence of micro-quartz absence related to high energy exposure was however observed in pebbly channel lag deposits (sample C1). Since micro-quartz is so abundant in other samples from this and the neighboring well (15/3-3, 15/3-1S) it is likely that the higher energy levels present at the base of a high density turbidite is an unfavorable site of deposition for Rhaxella spicules. Rhaxella spicules have been reported as absent also in coarse grained shallow marine sandstones (Vagle et al., 1994), so there are implications that Rhaxella spicules are more abundant in the finer grained portions of sandstone sequences. The shallow marine samples in this study however all contained large amounts of micro-quartz even though the most proximal sample is interpreted as distal upper shoreface (Appendix D).

It seems as micro-quartz coats are common in depositional systems that locally met the conditions necessary for Rhaxella Perforata to thrive. Thus sequence stratigraphy is probably just as important as depositional environment in predicting the presence of micro-quartz. The results presented in this study indicate that micro-quartz is abundant in Late Oxfordian-Mid Tithonian deep marine sandstones (i.e. genetic sequence B1-E) sourced from Utsira High (e.g. Gudrun Field), while they seem absent in the Brae Formation (seq. B1-B2). Shallow marine sandstones, from Utsira High/Gudrun Terrace, representing sequences A, B1 and B2 was also found to contain abundant micro-quartz coats. Thus the presence of micro-quartz can not be linked to a few sequences only, but seem to be common in sandstones associated with the Late Jurassic shallow marine environment around Utsira High. This implies that deeply buried sandstones of both shallow marine and deep marine environments sourced from the Late Jurassic Utsira High area are promising plays for future exploration.

9.2.2 Grain-coating illite: Origin and effects on reservoir quality

Illite is the dominant clay mineral in the study area (Bjørlykke and Aagaard, 1992), but minor amounts of grain-coating chlorite and pore-filling kaolinite was also observed. Illite may generally form from two diagenetic processes, illitization of kaolinite and K-feldspar or from a smectite pre-cursor (Bjørlykke and Aagaard, 1992). The latter is probably the case for the grain-coating illite observed in this study (i.e. figure 7-5). Storvoll et al. (2002) interpreted illite-coats in middle Jurassic Haltenbanken sandstones to form from dissolution of volcanic ash (rich in smectite) mixed in the sediments. However, it seems just as likely that the grain-coating illite are genetically related to the chlorite/illite-coats described by Houseknecht (1992) (chapter 3), since they are typically observed in channelized turbidite deposits (lobe- and slope channels, facies A1). If the illite-coats are genetically related to those described by Houseknecht (1992) this would enhance the play further in lobe- and slope-channel sandstones, which make up a large portion of the deep marine, Upper Jurassic cores studied.

The effect of illite-coats on porosity has been hard to quantify/estimate in this study, because micro-quartz is more abundant and usually present in the samples containing illite-coats. The illite-coats are often quite thin and may therefore not be as effective as micro-quartz even if they were as abundant. This is why illite (and occasionally chlorite) is considered as a

secondary contributor to inhibiting quartz cementation in the study area. It is possible that illite-coats could be of greater importance locally. In a more mud-rich system for example, more infiltrated clays would be present in the turbidites after dewatering.

9.2.3 Overpressure

The effects of overpressure have only been very generally treated in this study, with assumptions on the effect of overpressure on mechanical compaction and fracturing of coated quartz grains during deep burial. These assumptions may only be considered as hypothetical examples.

It has however become clear that overpressure may be more critical when modeling porosity as a function of quartz-cementation in deeply buried, quartz-rich sandstones than currently accounted for in algorithms such as exemplar. Fracturing of coated quartz grains and very high silica super-saturations, probably sourced partially from grain to grain contacts (Jahren and Ramm, 2000) as well as stylolites, will enable quartz-cementation to continue in deeply buried sandstones but at a much lower rate due to less efficient supply of silica. Models simulating these two effects should be incorporated in porosity modeling of coated sands because they may be critical in predicting the depth of reservoir cut-off.

9.3 SIGNIFICANCE OF OTHER DIAGENETIC MINERALS ON RESERVOIR QUALITY

9.3.1 Pore-filling kaolinite and pore-filling illite

Only minor amounts of pore-filling illite and kaolinite were observed in this study. This indicates that meteoric water flushing has been minor-moderate in the study area. It is well known that the Upper Jurassic was a time of warm and wet climate this normally is accompanied by large fluxes of meteoric water (Bjørlykke, 1994). It is therefore likely that the topography (i.e. potentiometric head) was insufficient to cause significant fluxes of meteoric water into the Late Jurassic basin. There may however have been differences in the meteoric water flow in sandstones associated with the East Shetland platform compared to the

Utsira High. The Utsira High area generally had lower topographic relief and wider shelf areas (Fraser et al., 2003). This would lead to lower fluxes of meteoric water adjacent to Utsira High, the significance of this has not been investigated here however.

It also seems that there are compositional variations related to the provenance of the sands. The sands of the Brae Formation seem to be predominantly quartz arenites, while sands sourced from Utsira High contained a larger fraction of unstable rock fragments and feldspars. The petrographic analysis revealed that the unstable grains were often completely-partly dissolved. This may be a source of clay minerals in these sandstones. However the generally low contents of feldspar in the study area is probably a factor limiting kaolinitization and illitization further.

The effects of pore-filling kaolinite and pore-filling illite (chapter 3) are for these reasons consider as less important in the study area than in other typical North Sea reservoir sandstones (i.e. Brent Group) and are probably minor compared to the effects of quartz cementation and grain-coats on reservoir quality.

9.3.2 Carbonate cement

Carbonate cements are locally quite common, but seem to be associated with short range diffusion around biogenic precursors. This observation agrees with other studies in the area (e.g. Ramm and Forsberg, 1991). The carbonate filter suggests that about 8% of the Gudrun sandstones are carbonate cemented (figure 9-1). This filter will only react to extensively cemented zones however, meaning that a larger number is more realistic. This implies that carbonate cements may be important locally in reducing the net pay reservoir volume and act as fluid barriers in reservoirs in zones rich in biogenic carbonate material.

CHAPTER 10: CONCLUSION

- Grain-coating micro-quartz is common in the study area. Grain-coating illite is present in deeply buried deep marine samples to varying degree. Micro-quartz seems to be the primary cause of anomalously high porosity.

- Petrophysical and petrographic analysis indicate that grain-coats and anomalous porosity are restricted to sands associated with the Late Jurassic shallow marine environment in the Utsira High area. This includes deep marine sands sourced from the Utsira High area.

- No clear correlation was observed between micro-quartz and facies. It is likely that micro-quartz coats are common in both deep marine and shallow marine sandstones due to a rapid post mortem decomposition and sedimentary reworking of Rhaxella spicules. Thus conditions favorable for Rhaxella Perforata locally within the depositional system are sufficient for effective micro-quartz coatings to develop in both deep marine and shallow marine sands.

- Micro-quartz seems to be present in all the Upper Jurassic sequences (i.e. figure 2-5) except the Callovian (Middle Jurassic) sequence Pre A.

- Modeling indicates that grain-coats, in the study area, may preserve porosities of 10 – 15% higher than expected in sandstones where quartz cementation may continue unhindered. The depth of reservoir cut-off may in such optimal cases be extended to 5000-5500 meters (TVDRSF).

- Thus, in the study area, future exploration should be focused to sequences A-F, to plays associated with Utsira High. In Vana- and Vilje sub-basin such plays are likely to maintain reservoir properties above cut-off to depths of 5000-5500 meters (TVDRSF).

- Reservoir quality algorithms (i.e. exemplar algorithm) should incorporate variables dealing with effective stress during deep burial in order to model the depth where quartz-cementation commences despite optimal grain-coating coverage of detrital quartz grains. This would enable a more precise prediction of the depth of reservoir cut-off in coated, deeply buried reservoir-sandstones.

REFERENCES

Aagaard, P., P. K. Egeberg, G. C. Saigal, S. Morad, and K. Bjørlykke, 1990, Diagenetic albitization of detrital K-feldspars in Jurassic, lower Cretaceous and Tertiary clastic reservoirs from offshore Norway, II. Formation water chemistry and kinetic considerations: Journal of Sedimentary Petrology, v. 60, p. 575-581.

Aagard, P., J. S. Jahren, A. O. Harstad, O. Nilsen, and M. Ramm, 2000, Formation of grain-coating chlorite in sandstones. Laboratory vs. natural occurrences: Clay Minerals, v. 35, p. 261-269.

Aase, N. E., P. A. Bjørkum, and P. H. Nadeau, 1996, The effect of grain-coating microquartz on preservation of reservoir porosity.: AAPG Bulletin, v. 80, p. 1654-1673.

Aase, N. E., and A. Walderhaug, 2005, The effect of hydrocarbons on quartz cementation: diagenesis in the Upper Jurassic sandstones of the Miller Field, North Sea, revisited: Petroleum Geoscience, v. 11, p. 215-223.

Andrews, I. J., and S. Brown, 1987, Stratigraphic evolution of the Jurassic, Moray Firth, *in* J. Brooks, and K. W. Glennie, eds., Petroleum Geology of North West Europe, v. 2: London, Graham & Trotman, p. 785-795.

Anjos, S. M. C., L. F. De Ros, and C. M. A. Silva, 2003, Chlorite authigenesis and porosity preservation in the Upper Cretaceous marine sandstones of the Santos Basin, offshore eastern Brazil, *in* S. Morad, and R. H. Worden, eds., Clay mineral cements in sandstones, v. 34: Malden, Mass., Blackwell Publishing, p. 291-316.

Athy, L. F., 1930, Density, porosity, and compaction of sedimentary rocks: AAPG Bulletin, v. 14, p. 1-22.

Barclay, S. A., and R. H. Worden 2000a, Effects of reservoir wettability on quartz cementation in oil fields, *in* R. H. Worden , and S. Morad, eds., Quartz Cementation in Sandstones, v. Spec. Publs int. Ass. Sediment. 29: Oxford, Blackwell Science, p. 103-117.

Barclay, S. A., and R. H. Worden 2000b, Petrophysical and petrographical analysis of quartz cement across oil-water contacts in the Magnus Field, northern North Sea, *in* R. H. Worden , and S. Morad, eds., Quartz Cementation in Sandstones, v. Spec. Publs int. Ass. Sediment. 29: Oxford, Blackwell Science, p. 147-161.

Bastien, C., J. C. Portalis, and M. Vossougui, 1975, Final report well 15/3-1S, Elf Aquitaine Norge A/S, p. 7.

Bayliss, D. D., 1976, Stratigraphical/Paleontological Final Report, well 24/9-1, Conoco Norway inc., p. 14.

Bergslien, D., 2002, Balder and Jotun - two sides of the same coin? A comparison of two Tertiary oil fields in the Norwegian North Sea: Petroleum Geoscience, v. 8, p. 349-363.

Bjørkum, P. A., 1996, How important is pressure in causing dissolution of quartz in sandstones?: Journal of Sedimentary Research, v. 66, p. 147-154.

Bjørlykke, K., 1980, Clastic diagenesis and basin evolution: Revisto del Instituto de Investigaciones Geologicas, v. 34, p. 21-44.

Bjørlykke, K., 1994, Fluid-flow processes and diagenesis in sedimentary basins, *in* J. Parnell, ed., Geofluids: Origin, Migration and Evolution of Fluids in Sedimentary Basins, v. Special Publications of the Geological Society of London 78, p. 127-140.

Bjørlykke, K., 1999, An overview of factors controlling rates of compaction, fluid generation and flow in sedimentary basins, *in* B. Jamtveit, and P. Meakin, eds., Growth, Dissolution and Pattern Formation in Geosystemss, Kluwer Academic Publishers, p. 381-404.

Bjørlykke, K., 2001, Sedimentologi og petroleumsgeologi: Oslo, Gyldendal yrkesopplæring, 334 s. p.

Bjørlykke, K., 2003, Compaction (consolidation) of sediments, *in* G. V. Middleton, ed., Encyclopedia of Sediments and Sedimentary Rocks, Kluwer Academic Publishers, p. 161-168.

Bjørlykke, K., and P. Aagaard, 1992, Clay minerals in North Sea sandstones, *in* D. W. Houseknecht, and E. D. Pittman, eds., Origin, diagenesis, and petrophysics of clay minerals in sandstones, v. Special Publication No. 47, SEPM (Society for Sedimentary Geology).

Bjørlykke, K., and P. K. Egeberg, 1993, Quartz cementation in sedimentary basins: AAPG Bulletin, v. 77, p. 1538-1548.

Bjørlykke, K., A. Mo, and K. Palm, 1988, Modeling of thermal convection in sedimentary basins and its relevance to diagenetic reactions: Marine and Petroleum Geology, v. 5, p. 338-351.

Bjørlykke, K., T. Nedkvikne, M. Ramm, and G. C. Saigal, 1992, Diagenetic processes in the Brent Group (middle Jurassic) reservoirs of the North Sea; an overviw, *in* A. C. Morton, R. S. Haszeldine, M. R. Giles, and S. Brown, eds., Geology of the Brent Group: Geological Society Special Publication, v. 61, Geological Society of London, p. 263-289.

Bjørlykke, K., M. Ramm, and G. C. Saigal, 1989, Sandstone diagenesis and porosity modification during basin evolution: Geologische Rundschau, v. 78, p. 243-268.

Blatt, H., 1979, Diagenetic processes in sandstones, *in* P. A. Scholle, and P. R. Schluger, eds., Aspects of Diagenesis: SEPM, Special Publications, v. 26, p. 141-157.

Bloch, S., R. H. Lander, and L. Bonnell, 2002, Anomalously high porosity and permeability in deeply buried sandstone reservoirs: Origin and predictability: AAPG Bulletin, v. 82, p. 301-328.

BP, 2001, Viking Graben 9/24b-4: United Kingdom Discovery Digest, v. vol. 13, p. 152-160.

Brooks, J., and K. W. Glennie, 1987, Petroleum Geology of North West Europe: London, Graham & Trotman, 1209 p.

Craig, F. F., 1971, The Reservoir Engeneering aspects of Waterflooding: Monograph Series, SPE, v. 3.

Cuhan, F. A., K. Bjørlykke, and C. Lowrey, 2000, The role of provenance in illitization of deeply buried reservoir sandstones from Haltenbanken and north Viking Graben, offshore Norway: Marine and Petroleum Geology, v. 17, p. 673-689.

Cuhan, F. A., A. Kjeldstad, K. Bjørlykke, and K. Høeg, 2002, Porosity loss in sand by grain crushing -experimental evidence and relevance to reservoir quality: Marine and Petroleum Geology, v. 19, p. 39-53.

Deegan, C. E., and J. Scull, 1977, A proposed standard lithostratigraphic nomenclature for the central and Northern North-Sea: Bull. NPD, v. No. 1.

Delclaud, J., 1975, Routine core analysis well 15/3-1S, p. 11.

Desbrandes, R., 1985, Encyclopedia of well logging: London, Graham & Trotman limited, 584 p.

Ehrenberg, S. N., 1993, Preservation of Anomalously High Porosity in Deeply Buried Sandstones by Grain-Coating Chlorite: Examples from the Norwegian Continental shelf.: AAPG Bulletin, v. 77, p. 1260-1286.

Evans, D., C. Graham, A. Armour, and P. Bathurst, eds., 2003, Millennium atlas; petroluem geology of the central and northern North Sea, Geological Society of London.

Florvaag, M., and J. Kristensen, 1982, Completeion report 24/12-2, Statoil, Texaco, Norsk Hydro, Saga, p. 121.

Fraser, S. I., A. M. Robinson, H. D. Johnson, J. R. Underhill, D. G. A. Kadolsky, R. Connell, P. Johannessen, and R. Ravnås, 2003, Upper Jurassic, *in* D. Evans, A. Armour, and P. Bathurst, eds., Millennium Atlas: petroleum geology of the central and northern North Sea: London, The Geological Society of London.

Gabrielsen, R. H., 1986, Structural elements in graben systems and their influence on hydrocarbon trap types, *in* S. A.M., ed., Habitat of Hydrocarbons on the Norwegian Continental Shelf: London, Graham and Trotman, Norwegian Petroleum Society, p. 55-60.

Galloway, W. E., 1989, Genetic statigraphic sequences in basin analysis: architecture and genesis of flooding surface bounded depositional units: AAPG Bulletin, v. 73.

Giles, M. R., 1997, Diagenesis: A Quantitative Perspective: Dordrecht, Kluwer Academic Publishers.

Giles, M. R., S. Stevenson, S. V. Martin, S. J. C. Cannon, P. J. Hamilton, J. D. Marshall, and G. M. Samways, 1992, The reservoir properties and diagenesis of the Brent Group; a regional perspective: Morton A C, v. 61, p. 289-327.

Glasmann, J. R., R. A. Clark, S. R. Larter, N. A. Briedis, and P. D. Lundegard, 1989, Diagenesis and Hydrocarbon Accumulation, Brent Sandstone(Jurassic), Bergen High Area, North Sea: AAPG Bulletin, v. 73, p. 1341-1360.

Glennie, K. W., 1998, Petroleum Geology of the North Sea. Basic concepts and recent advances, Blackwell Science, 613 p.

Gluyas, J., A. G. Robinson, D. Emery, S. M. Grant, and N. H. Oxtoby, 1993, The link between petroleum emplacement and sandstone cementation, *in* J. R. Parker, ed., Petroleum Geology of Northwest Europe: Proceedings of the 4th Conference: London, Geological Society of London, p. 1395-1402.

Gowland, S., 1996, Facies characteristics and depositional models of highly bioturbated shallow marine siliciclastic strata: an example from the Fulmar Formation (Late Jurassic), UK Central Graben, *in* A. Hurst, H. D. Johnson, S. D. Burley, A. C. Canham, and D. S. Mackertich, eds., Geology of the Humber Group, v. Special Publication No. 114, Geological Society of London, p. 185-214.

Harris, J. P., and R. M. Fowler, 1987, Enhanced prospectivity of the Mid-Late Jurassic sediments of the South Viking Graben, northern North Sea, *in* J. Brooks, and K. W. Glennie, eds., Petroleum Geology of North West Europe, v. 2: London, Graham & Trotman, p. 879-898.

Heald, M. T., 1965, Lithification of of sandstones in West Virginia: Virginia Geological and Economical Survey Bulletin, v. 30.

Heald, M. T., and R. E. Larese, 1974, Influence of coatings on quartz cementation: Journal of Sedimentary Research, v. 44, p. 1269-1274.

Heald, M. T., and J. J. Renton, 1966, Experimental study of sandstone cementation: Journal of Sedimentary Petrology, v. 36, p. 977-991.

Hendry, J. P., and N. H. Trewin, 1995, Authigenic quartz microfabrics in Cretaceous turbidites: evidence for silica transformation processes in sandstones: Journal of Sedimentary research, v. A65, p. 380-392.

Hillier, S., 1994, Pore-lining chlorites in siliciclastic reservoir sandstones: electron microprobe, SEM and XRD data, and implications for their origin: Clay Minerals, v. 29, p. 665-679.

Hinde, G. J., 1890, On a new Genus of Siliceous Sponges from the Lower Calcerous Grit of Yorkshire: Quarterly Journal of the Geological Society, v. 46, p. 54-61.

Houseknecht, D. W., and L. M. Ross, 1992, Clay minerals in Atokan deep-water sandstone facies, Arkoma basin: origins and influence on diagenesis and reservoir quality, *in* D. W. Houseknecht, and E. D. Pittman, eds., Origin, diagenesis and petrophysics of clay minerals in sandstones: Tulsa, Okla., Society for Sedimentary Geology, p. 227-241.

Hubbard, R. J., 1988, Age and significants of sequence boundaries on Jurassic and Early Cretaceous rifted continental margins: AAPG Bulletin, v. 72, p. 49-72.

Humphreys, B., S. J. Kemp, G. K. Lott, Bermanto, D. A. Dharmayanti, and I. Samsori, 1994, Origin of grain-coating Chlorite by Smectite transformation: an example from miocene sandstones, north Sumatra back-arc basin, Indonesia.: Clay Minerals, v. 29, p. 681-692.

Islam, T., in press, Reservoir Quality of Deeply Buried Upper Jurassic Sandstones of the Southern Viking Graben: Provenance & Depositional Environment, UiO, Oslo.

Jahren, J., and M. Ramm, 2000, The porosity-preserving effects of microcrystalline quartz coatings in arenitic sandstones: examples from the Norwegian continental shelf, *in* R. H. Worden , and S. Morad, eds., Quartz Cementation in Sandstones, v. Spec. Publs int. Ass. Sediment. 29: Oxford, Blackwell Science, p. 271-280.

Justwan, H., I. Meisingset, B. Dahl, and G. H. Isaksen, 2006, Geothermal history and petroleum generation in the Norwegian South Viking Graben revealed by pseudo-3D basin modelling: Marine and Petroleum Geology, v. 23, p. 791-819.

Klungsøyr, T., P. Furmyr, J. E. KHaugen, D. Frafjord, A. B. Sommervoll, and H. Hveding, 1999, Final well report well 16/1-5 &16/1-5A, Statoil, p. 154.

Kugler, R. L., and A. McHugh, 1990, Regional diagenetic variation in Norphlet Sandstone: implications for reservoir quality and the origin of porosity: Transactions of the Gulf Coast Association of Geological Societies, v. 40, p. 411-423.

Lander, R. H., and A. Walderhaug, 1999, Reservoir quality prediction through simulation of sandstone compaction and quartz cementation: AAPG Bulletin, v. 83, p. 433-449.

McBride, E. F., 1989, Quartz cement in sandstones: a review: Earth Science Reviews, v. 26, p. 69-112.

Needham, S. J., R. H. Worden , and D. McIlroy, 2005, Experimental production of clay rims by macrobiotic sediment ingestion and excretion processes: Journal of Sedimentary Research, v. 75, p. 1028-1037.

Nøttvedt, A., R. H. Gabrielsen, and R. J. Steel, 1995, Tectonostratigrphy and sedimentary arcitecture of rift basins, with reference to the northern North Sea: Marine and Petroleum Geology, v. 12, p. 881-901.

Odin, G. S., 1988, Green marine clays: oolitic ironstone facies, verdine facies, glaucony faciesand celadonite-bearing facies : a comparative study: Amsterdam, Elsevier, XXIV, 445 s. p.

Oelkers, E. H., P. A. Bjørkum, and W. M. Murphy, 1992, The mechanism of porosity reduction, stylolite development and quartz cementation in North Sea sandstones., *in* Y. K. Kharaka, and A. S. Maest, eds., Water Rock Interaction: Rotterdam, p. 1183-1186.

Oelkers, E. H., P. A. Bjørkum, and W. M. Murphy, 1996, A petrographic and computational investigation of quartz cement and porosity reduction in North Sea sandstones: American Journal of Science, v. 296, p. 420-452.

Oelkers, E. H., P. A. Bjørkum, O. Walderhaug, P. H. Nadeau, and W. M. Murphy, 2000, Making diagenesis obey thermodynamics and kinetics: The case of quartz cementation in sandstones from offshore mid-norway.: Applied Geochemistry, v. 15, p. 295-309.

Paoloni, A., and C. R. Evensen, 1979, Geological completeion report, well 15/3-3, Stavanger, Elf Aquitane Norge A/S, p. 38.

Partington, M. A., P. Copestake, B. C. Mitchener, and J. R. Underhill, 1993, Biostratigraphic calibration of genetic stratigraphic sequences in the Jurassic-lowermost Cretaceous (Hettangian to Ryazanian) of the North Sea and adjacent areas., *in* J. R. Parker, ed., Petroleum Geology of Northwest Europe: Proceedings of the 4th Conference.: London, The Geological Society of London, p. 371-386.

Pettijohn, J., P. E. Potter, and R. Siever, 1987, Sand and sandstone: New York, Springer Verlag.

Pittmann, E. D., R. E. Larese, and M. T. Heald, 1992, Clay coats: occurence and relevance to preservation of porosity in sandstones, *in* D. W. Houseknecht, and E. D. Pittmann, eds., Diagenesis and Petrophysics of Clay Minerals in sandstones: SEPM special publication No. 47, p. 241-255.

Pittmann, E. D., and D. N. Lumsden, 1968, Relationship between chlorite coatings on quartz grains and porosity, Spiro Sand, Oklahoma: Journal of Sedimentary research, v. 38, p. 668-670

Platt, J. D., 1993, Controls on clay mineral distribution and chemistry in the early Permian Rotliegend of Germany: Clay Minerals, v. 28, p. 393-416.

Ramm, M., 1994, Porosity/ depth trends in Upper Jurassic reservoirs, Norwegian Central Graben; an example of porosity preservation at deep burial by grain-coating micro-quartz: Anonymous In: AAPG annual convention. [Abstract, Serial, Conference Document] Annual Meeting Abstracts American Association of Petroleum Geologists and Society of Economic Paleontologists and Mineralogists, v. 241, p. U-American.

Ramm, M., and N. A. Bang, 1991, Porosity distribution in Middle Jurassic sandstones of the southern Viking Graben, North Sea, UiO, Oslo.

Ramm, M., and K. Bjorlykke, 1994, Porosity/depth trends in reservoir sandstones; assessing the quantitative effects of varying pore-pressure, temperature history and mineralogy, Norwegian Shelf data: Clay Minerals, v. 29, p. 475-490.

Ramm, M., and A. W. Forsberg, 1991, Porosity versus depth trends in Upper Jurassic sansdtones from the Cod - Terrace area, central North Sea: Dr. Scient thesis, University of Oslo, Oslo.

Ramm, M., A. W. Forsberg, and J. Jahren, 1998, Porosity-depth trends in deeply buried Upper Jurassic reservoirs in the Norwegian Central Graben: an example of porosity preservation beneath normal economic basement by grain-coating micro-quartz, *in* J. A. Kupecz, J. Gluyas, and S. Bloch, eds., Reservoir quality prediction in sandstones and carbonates: AAPG Memoir, v. 69, p. 177-199.

Rattey, R. P., and A. P. Hayward, 1993, Petroleum geology of Northwest Europe: proceedings of the 4th conference, held at the Barbican Centre, London 29 March-1 April 1992, p. 215-249.

Robinson, A. M., and J. Gluyas, 1992, Duration of quartz cementation in sandstones, North Sea and Haltenbanken Basins: Marine and Petroleum Geology, v. 9, p. 324-327.

Saigal, G. C., and K. Bjørlykke, 1987, Carbonate cement in clastic reservoir rocks from offshore Norway -relationship between isotopic composition, textural development and burial depth, *in* J. D. Marshall, ed., The diagenesis of Sedimentary Sequences: Spec. Publ., v. 36, Geol. Soc. London.

Saigal, G. C., S. Morad, K. Bjørlykke, P. K. Egeberg, and P. Aagaard, 1988, Diagenetic albitization of detrital K-feldspars in Jurassic, lower Cretaceous and Tertiary clastic reservoirs from offshore Norway, I. Textures and origin: Journal of Sedimentary Petrology, v. 58, p. 1003-1013.

Schlumberger, 1998, Log interpretatio Principles/Applications, Sclumberger wireline & testing.

Spark, I. S. C., and N. H. Trewin, 1986, Facies related diagenesis in the main Claymore oilfield sandstones: Clay Minerals, v. 21, p. 479-496.

Statoil, ?-a, Routine core analysis 15/3-7 (doc. nr.: 9407), p. 4.

Statoil, ?-b, Sidewallcore results 15/3-7 (doc. nr.:9408), p. 1.

Storvoll, V., K. Bjørlykke, D. Karlsen, and G. Saigal, 2002, Porosity preservation in reservoir sandstones due to grain-coating illite: a study of the Jurassic Garn Formation from the Kristin and Lavrans fields, offshore Mid-Norway.: Marine and Petroleum Geology, v. 19, p. 767-781.

Stow, D. A. V., 1985, Brae Oilfield Turbidite System, North Sea, *in* A. H. Bouma, W. R. Normark, and N. E. Barnes, eds., Submarine fans and related turbidite systems, Springer-Verlag, p. 231-237.

Talbot, M. R., 1973, Major sedimentary cycles in the Corallian Beds (Oxfordian) of southern England: Palaeogeography, Palaeoclimatology, Palaeoecology, v. 14, p. 293-317.

Thompson, A., 1979, Preservation of porosity in the deep Woodbine/Tuscaloosa trend: Transactions of the Gulf Coast Association of Geological Societies, v. 30, p. 396-403.

Thompson, A., and R. J. Stancliffe, 1990, Diagenetic controls on reservoir quality, eolian Norphlet Formation, south State Line field, Mississippi, *in* J. H. Barwis, J. G. McPherson, and R. J. Studlick, eds., Sandstone petroleum reservoirs: New York, Spreinger-Verlag, p. 205-224.

Vagle, G. B., A. Hurst, and H. Dypvik, 1994, Origin of quartz cements in some sandstones from the Jurassic of the Inner Moray Firth (UK): Sedimentology, v. 41, p. 363-377.

van der Helm, A. A., D. I. Gray, M. A. Cook, and A. M. Schulte, 1990, Fulmar: The development of a large North Sea Field, *in* A. T. Buller, E. Berg, O. Hjelmeland, J. Kleppe, O. Torsæter, and J. O. Aasen, eds., North Sea Oil & Gas reservoirs -II, Graham & Trotman, p. 25-47.

Vollset, J., and A. G. Dorê, 1984, A revised triassic and Jurassic lithostratigraphic nomenclature for the Norwegian North-Sea: Bull. NPD, v. No. 3.

Walderhaug, O., 1994a, Precipitation rates for quartz cement in sandstones determined by fluid-inclusion microthermometry and temperature-history modeling: Journal of Sedimentary research, v. A64, p. 324-333.

Walderhaug, O., 1994b, Temperatures of quartz cementation in Jurassic sandstones from the norwegian continental shelf -evidence from fluid inclusions: Journal of Sedimentary research, v. A64, p. 311-323.

Walderhaug, O., 1996, Kinetic modelling of quartz cementation and porosity loss in deeply buried sandstone reservoirs.: AAPG Bulletin, v. 80, p. 731-745.

Walderhaug, O., and P. A. Bjørkum, 2003, The effect of stylolite spacing on quartz cementation in the lower Jurassic Stø Formation, southern Barents Sea: Journal of Sedimentary Research, v. 73, p. 146-156.

Williams, L. A., and G. A. Parks, 1985, Silica diagenesis, I. Solubility controls: Journal of Sedimentary Petrology, v. 55, p. 301-311.

Wilson, M. D., 1992, Inherited grain-rimming clays in sandstones from eolian and shelf environments: their origin and control on reservoir properties, *in* D. W. Houseknecht,

and E. D. Pittman, eds., Origin, diagenesis and petrophysics of clay minerals in sandstones, p. 209-227s.

Wilson, M. D., and E. D. Pittman, 1977, Authigenic clays in sandstones: recognition and influence on reservoir properties and paleoenvironmental analysis: Journal of Sedimentary Petrology, v. 47, p. 3-31.

Wilson, R. C. L., 1968, Carbonate facies variation within the Osmington oolite series in southern England: Palaeogeography, Palaeoclimatology, Palaeoecology, v. 4, p. 89-123.

Worden , R. H., S. J. Needham, and J. Cuadros, 2006, The worm gut; a natural clay mineral factory and a possible cause of diagenetic grain coats in sandstones: Journal of Geochemical Exploration, v. 89, p. 428-431.

Worden, R. H., N. H. Oxtoby, and C. P. Smalley, 1998, Can oil emplacement prevent quartz cementation in sandstones?: Petroleum Geoscience, v. 4, p. 129-137.

Zanella, E., and M. P. Coward, 2003, Structural framework, *in* D. Evans, C. Graham, A. Armour, and P. Bathurst, eds., Millennium Atlas: London, The Geological Society of London, p. 45-59.

Ziegler, P. A., 1990, Tectonic and paleogeographic development of the North Sea rift system, *in* D. J. Blundell, and A. D. Gibbs, eds., Tectonic evolution of the North Sea rifts: New York, Oxford University Press, p. 1-36.

APPENDIX

APPENDIX A: ABBREVATIONS AND SYMBOLS

CALI: Caliper log

F: Formation factor

GR: Gamma ray log

I-MID: Illite-mica induced dissolution

M: Molar mass

MD: Measured depth

Por_den: Porosity calculated from the density log

R_0: Resistivity of brine saturated rock

RD: Deep resistivity log

RHO: Density log

RKB: Relative to Kelly bushing

RM: Medium resistivity log

RS: Shallow resistivity log

RT: Relative to rotary table

R_t: True resistivity

R_w: Formation water resistivity

SP: Spontaneous potential log

SS: Sub Sea

RSF: Relative to sea-floor

S_w: Water saturation

TD: Total depth

TDS: Total dissolved solids (g/cm^3)

TVD: Total vertical depth

WDSS: Well data summary sheet

ρ_{brine} : Density brine

ρ_{hc} : Density hydrocarbons

ρ_{qz} : Density quartz

Φ: Porosity

Φ_{dep}: Depositional porosity

APPENDIX B: MATLAB PROGRAMS

B.1 Filtering algorithm

```
uiimport('petrophys_alldata.xls')  %importing well data

welldata=[horzcat(WELL),horzcat(TVDRSF),horzcat(MD),horzcat(GR),horzcat(RHO
),horzcat(RD),horzcat(DT)];
X=welldata;
m=size(X(:,1));

X(1:2:m(1),:)=[];

m=size(X(:,1));
n=(1:7);
for k=1:1:m
if X(k,4)<60 && X(k,5)<2.65 && X(k,7)>56 % Carbonate and shale filter
n=[n;vertcat(X(k,:))];
end
end

n(1,:)=[];
X=n;
m=size(X(:,1));


xlswrite('petrophys_sand.xls',X) % writing filtered well data to excel file
```

B.2 Sequence stratigraphic algorithm

```
sequence=xlsread('well_tops.xls') %table
welldata=xlsread(' petrophys.xls') %petrophys.xls corresponds to appendix B
m=size(sequence);
n=size(welldata);
nrwells=0;
nrseq=8;
porE=0;porD=0;porC=0;porB=0;porA=0;porPreA=0;

for i=1:1:m(1)
      if i==1
      nrwells=1;
      elseif sequence(i,1) ~= sequence(i-1,1)
      nrwells=nrwells+1;
      end

end

for i=1:1:m(1)
      if sequence(i,2)==73
```

```
            for k=1:1:n
            if sequence(i,1)==welldata(k,1) && welldata(k,2)>=sequence(i-
1,3) && welldata(k,2)<=sequence(i,3)
                  porE=[porE;welldata(k,8)];
            end
            end
      elseif sequence(i,2)==71
            for k=1:1:n
            if sequence(i,1)==welldata(k,1) && welldata(k,2)>=sequence(i-
1,3) && welldata(k,2)<=sequence(i,3)
                  porD=[porD;welldata(k,8)];
            end
            end
      elseif sequence(i,2)==63
            for k=1:1:n
            if sequence(i,1)==welldata(k,1) && welldata(k,2)>=sequence(i-
2,3) && welldata(k,2)<=sequence(i,3)
                  porC=[porC;welldata(k,8)];
            end
            end
      elseif sequence(i,2)==54
            for k=1:1:n
            if sequence(i,1)==welldata(k,1) && welldata(k,2)>=sequence(i-
1,3) && welldata(k,2)<=sequence(i,3)
                  porB=[porB;welldata(k,8)];
            end
            end
      elseif sequence(i,2)==46
            for k=1:1:n
            if sequence(i,1)==welldata(k,1) && welldata(k,2)>=sequence(i-
1,3) && welldata(k,2)<=sequence(i,3)
                  porA=[porA;welldata(k,8)];
            end
            end
      elseif sequence(i,2)==36
            for k=1:1:n
            if sequence(i,1)==welldata(k,1) && welldata(k,2)>=sequence(i-
1,3) && welldata(k,2)<=sequence(i,3)
                  porPreA=[porPreA;welldata(k,8)];
            end
            end
      end
end

subplot(3,2,1)
hist(porPreA,20)
title('Sequence: Pre-A');
subplot(3,2,2)
hist(porA,20)
title('Sequence: A');
subplot(3,2,3)
hist(porB,20)
```

```
title('Sequence: B');
subplot(3,2,4)
hist(porC,20)
title('Sequence: C');
subplot(3,2,5)
hist(porD,20)
title('Sequence: D');
subplot(3,2,6)
hist(porE,20)
title('Sequence: E');
```

B.3 Modeling porosity-depth trends algorithm

```
           %reading and plotting porosity values from appendix B
por_xls=xlsread('por_xlsread.xls')
m=size(por_xls(:,1));
  for i=1:1:m
 if por_xls(i,1)==1521 || por_xls(i,1)==1531 || por_xls(i,1)==1532 ||
por_xls(i,1)==1533 || por_xls(i,1)==1534 || por_xls(i,1)==1535 ||
por_xls(i,1)==1537 || por_xls(i,1)==1615
subplot(2,1,1)
plot(por_xls(i,4), por_xls(i,2),'bx');hold on;grid on;
subplot(2,1,2)
plot(por_xls(i,4), por_xls(i,2),'bx');hold on;grid on;
 else
subplot(2,1,1)
plot(por_xls(i,4), por_xls(i,2),'bx');hold on;grid on;
subplot(2,1,2)
plot(por_xls(i,4), por_xls(i,2),'bx');hold on;grid on;
 end
  end
grid on; axis([0 0.36 -5000 -1500]);
porosity_depth=0;


                      %VARIABLES

n=0.25;     %porosity at onset of quartz cementation (Assumed to be ~CCP)
a=2*10^-22; %kinetic constant
b=0.025;    %kinetic constant
scale=0.75; %heating rate (C/Ma). Linearized
c=scale/(10^6*365*24*60*60);     %heating rate (C/sec)
M=60.09;    %molar mass, quartz (g/mole)
d=2.65;           %density quartz(g/cm3)
gradT=0.03; %geothermal gradient (C/m), assumed constant through time
D=0.03;           %Grain size diameter (fine medium coarse)(cm)
f=0.95;           %fraction quartz
g=0.5;            %fraction of surface area covered by grain-coats

  for run=1:1:4   %scenario 1 2 3 4
  for var=1:1:2   %variables
```

```
 if run==1  %Max,min,mean OP
   if var==1
      D=0.01;n=0.3;g=0.0;
   elseif var==2
      D=0.05;n=0.3;g=0.0;
   end
 elseif run==2    %optimal porosity pres
   if var==1
      D=0.05;n=0.3;g=0.95;
   elseif var==2
      %D=0.02;n=0.3;g=0.7;
   end
 elseif run==3    %Max and min porosity
   if var==1
      D=0.01;n=0.2;g=0.0;
   elseif var==2
      D=0.05;n=0.3;g=0.0;
   end
 elseif run==4    %average porosity and g crit
   if var==1
      D=0.03;n=0.25;g=0.0;
   elseif var==2
      D=0.03;n=0.25;g=0.7;
   end
end

for time=1:1:200        % Linearly approximated burial depths of %rocks 1-
                        200Ma %old
      if time==1
      burial(time)=round(scale/gradT);
      else
      burial(time)=burial(time-1)+round(scale/gradT);
      end
end


temp(1:1:200)=gradT.*burial;  %Linearly approximated %temperature as a
                              %function of time(1-%200 Ma ago)

for depth=1:1:burial(200)     %Mechanical compaction model, %hydrostatic
                              conditions. Only valid %until onset of quartz
                              %cementation
      if n== 0.25
      por_mec(depth)=0.4*exp(depth*-0.000175);
      elseif n== 0.3
      por_mec(depth)=0.4*exp(depth*-0.00011);
      elseif n== 0.35
      por_mec(depth)=0.4*exp(depth*-0.00005);
      elseif n== 0.2
      por_mec(depth)=0.4*exp(depth*-0.00026);
      elseif n== 0.15
      por_mec(depth)=0.4*exp(depth*-0.000375);
```

```
      end
end

                  %START POROSITY-DEPTH MODELING

A0=6*f*(1-n)*(1-g)/D;   %Initial surface area(cm2) available for quartz
                        %precipitation pr qubic cm sandstone
A=6*f*(1-n)*(1-g)/D;
x=1;        %time(Ma) after onset of quartz cementation
i=0;

for time=1:1:200  %Modeling porosity 1-200Ma after deposition

  if temp(time)>80      %Modeling quartz cementation

        u(time)=((-M*a*A)/(d*n*b*c*log(10)))*(10^(b*x)-1); %exponent
        Vq(time)=n - n*exp(u(time));      %Vq:Volume of quartz
        por(time)=n-Vq(time);       %porosity as a function of time
      if por(time)<0.02
        i=1; end  %correction
      if i==1;
        por(time)=por(time-1)*exp(time*-0.00018);
      end
        x=x+1;
        A=A0*por(time)/n;     %calculating surface area available for
                              %quartz cementation on next time step

  else            %Modeling mechanical compaction
      por(time)=por_mec(burial(time));
  end
end

%porosity_depth: Column 1:depth, column 2-x: porosityrow1: grainsize,
%row2:quartz fraction, row3: coating fraction, %row4: heating-rate(C/Ma)

 if length(porosity_depth(1,:))==1
porosity_depth=[vertcat(D,f,g,scale,burial(1:1:200)'),
vertcat(D,f,g,scale,por')]  % first run
 else
porosity_depth=[porosity_depth, vertcat(D,f,g,scale,por')]  %later runs
 end

  end %variables
  end %run


                  %PLOTTING (equivalent to figure 7-x and 7-x)
m=size(porosity_depth);

for fig=1:1:2
if fig == 2
  subplot(2,1,1)
```

```
  plot(porosity_depth(5:m(1),6:9),-porosity_depth(5:m(1),1))
  axis([0 0.36 -5000 -1500]);
  hold on;
  elseif fig == 1
  subplot(2,1,2)
  plot(porosity_depth(5:m(1),2:5),-porosity_depth(5:m(1),1))
  axis([0 0.36 -5000 -1500]);
  hold on;
  end

end   %fig
```

APPENDIX C: FILTERED WELL DATA AND CALCULATED POROSITIES

Well	TVDRSF	MD	GR	RHO	RD	DT	I_{GR} (4-7)	V_{sh} (4-5/6)	Porosity (eq 5-1)	Porosity (eq 4-4)
1521	-3888.65	4022.65	25.14	2.64	43.75	56.59	0.064	0.03	0.003	0.006
1521	-3888.95	4022.95	19.05	2.62	52.25	57.78	0.000	0.00	0.019	0.019
1521	-3889.26	4023.26	26.63	2.59	46.47	61.59	0.080	0.04	0.034	0.039
1521	-3898.4	4032.40	46.47	2.48	10.11	65.38	0.288	0.16	0.090	0.110
1521	-3898.71	4032.71	32.66	2.53	20.05	66.19	0.143	0.07	0.069	0.077
1521	-3899.01	4033.01	26.06	2.49	28.08	67.75	0.074	0.04	0.099	0.103
1521	-3899.32	4033.32	27.64	2.53	17.45	63.19	0.090	0.04	0.072	0.077
1521	-4057.35	4191.35	56.47	2.54	4.2	80	0.393	0.24	0.042	0.071
1521	-4077.78	4211.78	59.41	2.55	2.21	82.38	0.424	0.26	0.032	0.065
1521	-4082.04	4216.04	41.38	2.63	3.1	61.59	0.235	0.13	-0.003	0.013
1521	-4082.35	4216.35	58.25	2.5	2.98	67	0.412	0.25	0.066	0.097
1521	-4083.41	4217.41	58.53	2.5	1.55	80.38	0.415	0.26	0.065	0.097
1521	-4090.12	4224.12	58.91	2.64	2.23	79.19	0.419	0.26	-0.025	0.006
1521	-4098.04	4232.04	53.63	2.64	1.47	85	0.363	0.22	-0.020	0.006
1521	-4098.35	4232.35	43.75	2.54	1.77	66	0.259	0.14	0.053	0.071
1521	-4099.87	4233.87	58.88	2.62	1.43	73	0.418	0.26	-0.012	0.019
1521	-4102.46	4236.46	49.84	2.55	1.46	73.75	0.323	0.19	0.042	0.065
1521	-4102.77	4236.77	57.81	2.52	1.55	71.19	0.407	0.25	0.053	0.084
1521	-4109.17	4243.17	55.75	2.53	1.29	80.19	0.386	0.23	0.049	0.077
1521	-4109.93	4243.93	56.63	2.51	1.37	75.56	0.395	0.24	0.061	0.090
1521	-4113.13	4247.13	43.84	2.64	2.29	63.38	0.260	0.14	-0.011	0.006
1521	-4122.89	4256.89	57.06	2.59	1.45	72.38	0.399	0.24	0.009	0.039
1521	-4123.19	4257.19	44.5	2.39	2.01	60.59	0.267	0.15	0.150	0.168
1521	-4123.5	4257.50	58.28	2.39	2.27	59.19	0.412	0.25	0.137	0.168
1521	-4124.56	4258.56	56.84	2.38	1.91	73.75	0.397	0.24	0.145	0.174
1521	-4125.17	4259.17	59.63	2.4	2.17	63.19	0.426	0.27	0.129	0.161
1521	-4131.73	4265.73	55.34	2.51	1.36	77.38	0.381	0.23	0.062	0.090
1521	-4136.91	4270.91	54.53	2.48	3.13	62.78	0.373	0.22	0.082	0.110
1521	-4137.21	4271.21	34.81	2.43	3.06	57.59	0.166	0.09	0.131	0.142
1521	-4137.52	4271.52	50.72	2.43	2.55	75.38	0.333	0.19	0.118	0.142
1521	-4158.7	4292.70	58.16	2.61	2.45	73.75	0.411	0.25	-0.005	0.026
1521	-4166.62	4300.62	52.84	2.63	3.56	67.56	0.355	0.21	-0.013	0.013
1521	-4166.93	4300.93	53.5	2.64	3.73	69.56	0.362	0.22	-0.020	0.006
1521	-4167.23	4301.23	48.66	2.51	3.28	58	0.311	0.18	0.069	0.090
1521	-4167.54	4301.54	51.84	2.53	2.67	62.38	0.344	0.20	0.053	0.077
1521	-4181.1	4315.10	59.28	2.58	2.49	76.75	0.423	0.26	0.013	0.045
1521	-4203.51	4337.51	58.25	2.46	2.13	86	0.412	0.25	0.091	0.123
1521	-4206.1	4340.10	56.09	2.52	2.53	71.19	0.389	0.24	0.055	0.084
1531	-3815.8	3949.80	46.71	2.51	8.03	85.6	0.339	0.20	0.069	0.090
1531	-3816.1	3950.10	43.21	2.51	7.45	83.12	0.304	0.17	0.071	0.090
1531	-3816.41	3950.41	28.69	2.51	6.49	84.88	0.157	0.08	0.081	0.090
1531	-3816.71	3950.71	34.01	2.51	8.34	85.01	0.211	0.11	0.078	0.090
1531	-3817.02	3951.02	38.44	2.51	8.95	94.79	0.256	0.14	0.075	0.090
1531	-3817.32	3951.32	38.86	2.51	9.21	100.03	0.260	0.14	0.075	0.090
1531	-3817.63	3951.63	44.63	2.51	7.48	101.01	0.318	0.18	0.070	0.090
1531	-3817.93	3951.93	53.46	2.51	6.55	100.36	0.408	0.25	0.063	0.090
1531	-3818.24	3952.24	50.2	2.51	6.23	99.47	0.375	0.22	0.066	0.090
1531	-3818.54	3952.54	49.74	2.53	5.86	104.8	0.370	0.22	0.053	0.077
1531	-3820.37	3954.37	59.2	2.3	6.7	87.55	0.466	0.30	0.193	0.226
1531	-3822.05	3956.05	52.33	2.28	9.07	79.79	0.396	0.24	0.212	0.239
1531	-3822.35	3956.35	36.67	2.38	10.94	73.47	0.238	0.13	0.160	0.174
1531	-3822.66	3956.66	59.08	2.46	9.12	89.04	0.464	0.30	0.090	0.123
1531	-3825.25	3959.25	58.11	2.24	7.4	97.75	0.455	0.29	0.233	0.265
1531	-3826.77	3960.77	49.48	2.22	9.33	91.92	0.367	0.22	0.253	0.277
1531	-3827.08	3961.08	59.68	2.23	9.58	98.43	0.470	0.30	0.238	0.271
1531	-3830.58	3964.58	55.85	2.24	11.84	82.43	0.432	0.27	0.235	0.265

Well	TVDRSF	MD	GR	RHO	RD	DT	I_{GR} (4-7)	V_{sh} (4-5/6)	Porosity (eq 5-1)	Porosity (eq 4-4)
1531	-3830.89	3964.89	49.52	2.24	16.18	77.61	0.368	0.22	0.240	0.265
1531	-3831.19	3965.19	37.95	2.27	20.39	79.34	0.251	0.14	0.230	0.245
1531	-3831.5	3965.50	54.83	2.34	16.09	89.81	0.421	0.26	0.171	0.200
1531	-3848.41	3982.41	47.72	2.54	14.85	72.94	0.350	0.21	0.048	0.071
1531	-3855.88	3989.88	52.3	2.51	15.78	76.56	0.396	0.24	0.064	0.090
1531	-3856.19	3990.19	41.66	2.55	18.45	72.16	0.288	0.16	0.047	0.065
1531	-3856.49	3990.49	39.2	2.56	21.99	72.56	0.264	0.15	0.042	0.058
1531	-3856.8	3990.80	45.64	2.57	21.38	73.13	0.329	0.19	0.031	0.052
1531	-3857.1	3991.10	41.94	2.61	17.78	68.77	0.291	0.16	0.008	0.026
1531	-3857.41	3991.41	48.09	2.58	16.43	77.84	0.353	0.21	0.022	0.045
1531	-3859.84	3993.84	44.05	2.57	15.06	70.63	0.313	0.18	0.032	0.052
1531	-3860.15	3994.15	49.36	2.56	13.7	80.1	0.366	0.22	0.034	0.058
1531	-3861.37	3995.37	48.95	2.35	15.24	75.37	0.362	0.22	0.170	0.194
1531	-3864.42	3998.42	56.42	2.47	15.03	81.19	0.437	0.28	0.086	0.116
1531	-3864.72	3998.72	46.13	2.51	15.1	73.47	0.334	0.19	0.069	0.090
1531	-3865.03	3999.03	49.13	2.57	16.32	71.6	0.364	0.22	0.028	0.052
1531	-3865.33	3999.33	59.11	2.64	16.15	72	0.465	0.30	-0.026	0.006
1531	-3865.63	3999.63	55.51	2.56	15.09	73.67	0.428	0.27	0.029	0.058
1531	-3867.16	4001.16	53.91	2.52	21.48	73.1	0.412	0.25	0.056	0.084
1531	-3867.46	4001.46	43.42	2.55	24.83	72.14	0.306	0.17	0.045	0.065
1531	-3867.77	4001.77	42.31	2.6	25.01	65.05	0.295	0.17	0.014	0.032
1531	-3868.07	4002.07	44.48	2.62	25.01	68.11	0.317	0.18	-0.001	0.019
1531	-3868.38	4002.38	56.41	2.59	23.11	70.7	0.437	0.28	0.009	0.039
1531	-3871.43	4005.43	41.64	2.53	24.42	66.36	0.288	0.16	0.060	0.077
1531	-3871.73	4005.73	55.45	2.53	20.54	69.78	0.428	0.27	0.048	0.077
1531	-3873.25	4007.25	42.32	2.59	19.27	64.14	0.295	0.17	0.020	0.039
1531	-3873.56	4007.56	54.29	2.56	21.8	67.11	0.416	0.26	0.030	0.058
1531	-3873.86	4007.86	48.83	2.59	18.21	69.53	0.361	0.21	0.015	0.039
1531	-3874.78	4008.78	57.53	2.56	15.54	75.4	0.449	0.28	0.027	0.058
1531	-3875.08	4009.08	58.83	2.56	15.76	78.1	0.462	0.30	0.026	0.058
1531	-3875.39	4009.39	55.78	2.53	14.56	76.14	0.431	0.27	0.048	0.077
1531	-3877.06	4011.06	41.85	2.54	22.16	69.37	0.290	0.16	0.053	0.071
1531	-3877.37	4011.37	29.48	2.56	26.64	60.02	0.165	0.09	0.049	0.058
1531	-3877.67	4011.67	31.9	2.6	29.92	62.65	0.190	0.10	0.021	0.032
1531	-3877.98	4011.98	48.04	2.57	27.28	71.4	0.353	0.21	0.029	0.052
1531	-3878.28	4012.28	52.58	2.59	21.55	70.95	0.399	0.24	0.012	0.039
1531	-3878.59	4012.59	54.92	2.56	19.24	77.87	0.422	0.26	0.029	0.058
1531	-3881.03	4015.03	37.3	2.59	15.31	67.67	0.244	0.13	0.024	0.039
1531	-3881.33	4015.33	36.24	2.61	21.2	62.91	0.234	0.13	0.012	0.026
1531	-3881.64	4015.64	51.24	2.62	21.43	71.59	0.385	0.23	-0.006	0.019
1531	-3881.94	4015.94	54.36	2.61	17.46	64.09	0.417	0.26	-0.002	0.026
1531	-3882.25	4016.25	42.14	2.61	18.41	66.41	0.293	0.17	0.008	0.026
1531	-3883.16	4017.16	55.84	2.51	14.35	74.66	0.432	0.27	0.061	0.090
1531	-3885.14	4019.14	54.05	2.51	13.7	71.96	0.414	0.26	0.062	0.090
1531	-3890.32	4024.32	55.81	2.57	17.44	68.25	0.431	0.27	0.022	0.052
1531	-3890.63	4024.63	56.3	2.59	18.31	66.42	0.436	0.27	0.009	0.039
1531	-3893.22	4027.22	48.35	2.52	23.79	79.07	0.356	0.21	0.061	0.084
1531	-3893.52	4027.52	55.58	2.44	17.46	84.22	0.429	0.27	0.106	0.135
1531	-3919.89	4053.89	57.04	2.55	28.95	71.51	0.444	0.28	0.034	0.065
1531	-3955.4	4089.40	56.45	2.38	22.53	83.48	0.438	0.28	0.144	0.174
1531	-4016.97	4150.97	54.29	2.45	43.08	64.07	0.416	0.26	0.101	0.129
1531	-4017.27	4151.27	56.94	2.46	23.45	65.06	0.443	0.28	0.092	0.123
1531	-4020.02	4154.02	56.01	2.48	14.81	86.45	0.433	0.27	0.080	0.110
1531	-4020.32	4154.32	54.32	2.47	14.03	84.48	0.416	0.26	0.088	0.116
1531	-4039.37	4173.37	58.11	2.3	10.84	95.57	0.455	0.29	0.194	0.226
1531	-4049.12	4183.12	59.85	2.59	27.23	61.11	0.472	0.30	0.005	0.039
1531	-4094.39	4228.39	49.31	2.32	0.92	89.28	0.366	0.22	0.189	0.213
1531	-4098.81	4232.81	56.45	2.57	2.28	59.22	0.438	0.28	0.021	0.052
1531	-4099.11	4233.11	52.16	2.51	1.77	59.31	0.394	0.24	0.064	0.090
1531	-4110.69	4244.69	59.69	2.51	2.19	56.98	0.470	0.30	0.057	0.090
1531	-4112.68	4246.68	54	2.48	3.53	57.68	0.413	0.26	0.082	0.110
1531	-4112.98	4246.98	57.02	2.51	2.8	69.93	0.444	0.28	0.060	0.090
1531	-4124.11	4258.11	55.63	2.43	3.52	57.06	0.429	0.27	0.112	0.142

Well	TVDRSF	MD	GR	RHO	RD	DT	I_{GR} (4-7)	V_{sh} (4-5/6)	Porosity (eq 5-1)	Porosity (eq 4-4)
1531	-4124.41	4258.41	49.25	2.44	3.14	57.13	0.365	0.22	0.112	0.135
1531	-4124.71	4258.71	59.22	2.38	2.61	69.3	0.466	0.30	0.141	0.174
1531	-4125.02	4259.02	57.14	2.4	1.97	66.59	0.445	0.28	0.130	0.161
1531	-4125.32	4259.32	49.39	2.39	1.41	63.88	0.366	0.22	0.144	0.168
1531	-4125.63	4259.63	52.11	2.4	1.16	69.09	0.394	0.24	0.135	0.161
1531	-4143.31	4277.31	54.87	2.58	1.11	67.99	0.422	0.26	0.016	0.045
1531	-4143.61	4277.61	57.03	2.45	0.69	85.29	0.444	0.28	0.098	0.129
1531	-4148.49	4282.49	53.9	2.49	0.97	57.72	0.412	0.25	0.075	0.103
1531	-4173.33	4307.33	59.47	2.55	4.96	59.09	0.468	0.30	0.031	0.065
1531	-4174.09	4308.09	56.7	2.5	11.35	61.39	0.440	0.28	0.066	0.097
1531	-4174.4	4308.40	59.03	2.55	9.27	62.94	0.464	0.30	0.032	0.065
1531	-4308.81	4442.81	30.36	2.35	6.3	84.56	0.174	0.09	0.184	0.194
1531	-4309.12	4443.12	21.19	2.28	9.74	82.48	0.082	0.04	0.234	0.239
1531	-4309.42	4443.42	20.31	2.3	11.29	80.43	0.073	0.04	0.222	0.226
1531	-4309.73	4443.73	20.12	2.32	10.91	77.74	0.071	0.03	0.209	0.213
1531	-4310.03	4444.03	19.13	2.35	11.19	77.36	0.061	0.03	0.190	0.194
1531	-4310.34	4444.34	18.72	2.35	11.77	77.52	0.057	0.03	0.191	0.194
1531	-4310.64	4444.64	20.76	2.34	11.34	77.02	0.077	0.04	0.196	0.200
1531	-4310.95	4444.95	21.69	2.34	11.18	77.62	0.087	0.04	0.195	0.200
1531	-4311.25	4445.25	21.88	2.32	11.49	78.37	0.089	0.04	0.208	0.213
1531	-4311.56	4445.56	22.06	2.31	11.97	78.55	0.091	0.04	0.215	0.219
1531	-4311.86	4445.86	21.72	2.32	12.69	78.15	0.087	0.04	0.208	0.213
1531	-4312.17	4446.17	20.34	2.34	14.13	77.64	0.073	0.04	0.196	0.200
1531	-4312.47	4446.47	20.8	2.35	15.41	77.18	0.078	0.04	0.189	0.194
1531	-4312.78	4446.78	18.77	2.36	15.21	74.65	0.057	0.03	0.184	0.187
1531	-4313.08	4447.08	19.98	2.37	14.61	74.82	0.070	0.03	0.177	0.181
1531	-4313.39	4447.39	22	2.39	13.92	76.75	0.090	0.04	0.163	0.168
1531	-4313.69	4447.69	24.83	2.39	12.73	77.4	0.119	0.06	0.161	0.168
1531	-4314	4448.00	23.77	2.37	12.32	78.92	0.108	0.05	0.175	0.181
1531	-4314.3	4448.30	22.89	2.33	12.19	79.88	0.099	0.05	0.201	0.206
1531	-4314.61	4448.61	27.23	2.33	12.62	81.58	0.143	0.07	0.199	0.206
1531	-4314.91	4448.91	29.7	2.34	11.19	80.75	0.168	0.09	0.191	0.200
1531	-4315.21	4449.21	25.26	2.34	9.85	77.68	0.123	0.06	0.193	0.200
1531	-4315.52	4449.52	29.26	2.29	9.92	78.91	0.163	0.08	0.223	0.232
1531	-4315.82	4449.82	26.4	2.28	9.06	80.96	0.134	0.07	0.231	0.239
1531	-4316.13	4450.13	21.8	2.26	8.45	81.76	0.088	0.04	0.247	0.252
1531	-4316.43	4450.43	22.64	2.27	9.31	81.18	0.096	0.05	0.240	0.245
1531	-4316.74	4450.74	24.77	2.31	9.93	82.71	0.118	0.06	0.213	0.219
1531	-4317.04	4451.04	19.71	2.3	11.22	82.32	0.067	0.03	0.222	0.226
1531	-4317.35	4451.35	15.48	2.29	15.51	82.1	0.024	0.01	0.231	0.232
1531	-4317.65	4451.65	14.67	2.34	19.64	74.5	0.016	0.01	0.199	0.200
1531	-4317.96	4451.96	15.08	2.39	17.63	74.26	0.020	0.01	0.167	0.168
1531	-4318.26	4452.26	16.46	2.37	16.16	81.19	0.034	0.02	0.179	0.181
1531	-4318.57	4452.57	19.2	2.29	17.71	83.91	0.062	0.03	0.229	0.232
1531	-4318.87	4452.87	19.8	2.3	18.77	78.34	0.068	0.03	0.222	0.226
1531	-4319.18	4453.18	17.79	2.37	17.45	71.46	0.047	0.02	0.178	0.181
1531	-4319.48	4453.48	18.19	2.42	19.41	72.4	0.051	0.02	0.146	0.148
1531	-4319.79	4453.79	19.33	2.38	23.24	83.79	0.063	0.03	0.171	0.174
1531	-4320.09	4454.09	21.79	2.3	13.87	82.01	0.088	0.04	0.221	0.226
1531	-4320.4	4454.40	27.49	2.31	9.64	81.17	0.145	0.07	0.211	0.219
1531	-4320.7	4454.70	31.54	2.3	10.39	91.48	0.186	0.10	0.215	0.226
1531	-4321.01	4455.01	22.82	2.26	10.55	93.91	0.098	0.05	0.246	0.252
1531	-4321.31	4455.31	23.02	2.28	8.42	76.06	0.100	0.05	0.233	0.239
1531	-4321.62	4455.62	26.4	2.38	8.89	73.04	0.134	0.07	0.167	0.174
1531	-4321.92	4455.92	26.79	2.4	11.3	83.1	0.138	0.07	0.154	0.161
1531	-4322.23	4456.23	23.9	2.35	12.67	79.85	0.109	0.05	0.188	0.194
1531	-4322.53	4456.53	23.88	2.35	11.69	72.26	0.109	0.05	0.188	0.194
1531	-4322.83	4456.83	24.49	2.42	15.25	68.93	0.115	0.06	0.142	0.148
1531	-4323.14	4457.14	24.52	2.43	16.88	63.06	0.115	0.06	0.136	0.142
1531	-4323.44	4457.44	30.82	2.46	12.19	72.39	0.179	0.09	0.112	0.123
1531	-4323.75	4457.75	40.42	2.42	10.89	83.62	0.276	0.15	0.132	0.148
1531	-4324.05	4458.05	39.07	2.36	8.96	79.54	0.262	0.14	0.171	0.187
1531	-4324.36	4458.36	43.97	2.4	7.24	82.25	0.312	0.18	0.142	0.161

Well	TVDRSF	MD	GR	RHO	RD	DT	I_{GR} (4-7)	V_{sh} (4-5/6)	Porosity (eq 5-1)	Porosity (eq 4-4)
1531	-4324.66	4458.66	34.49	2.42	9.17	79.94	0.216	0.12	0.136	0.148
1531	-4324.97	4458.97	25.63	2.52	12.49	61.69	0.127	0.06	0.077	0.084
1531	-4325.27	4459.27	30.7	2.62	16.51	59.93	0.178	0.09	0.009	0.019
1531	-4325.58	4459.58	35.64	2.6	30.54	66.32	0.228	0.12	0.019	0.032
1531	-4325.88	4459.88	42.86	2.56	24.29	79.66	0.301	0.17	0.039	0.058
1531	-4326.19	4460.19	53.95	2.42	15.03	82.15	0.413	0.25	0.120	0.148
1531	-4326.49	4460.49	57.96	2.34	11.21	84.2	0.453	0.29	0.168	0.200
1531	-4334.42	4468.42	54.93	2.41	6.29	74.42	0.422	0.26	0.126	0.155
1531	-4337.16	4471.16	48.74	2.31	2.75	86.8	0.360	0.21	0.196	0.219
1531	-4337.47	4471.47	30.98	2.25	2.77	85.34	0.181	0.09	0.248	0.258
1531	-4337.77	4471.77	32.89	2.27	2.83	84.45	0.200	0.11	0.234	0.245
1531	-4338.07	4472.07	38.53	2.28	2.88	84.03	0.257	0.14	0.223	0.239
1531	-4338.38	4472.38	49.51	2.3	3.09	84.48	0.368	0.22	0.202	0.226
1531	-4342.95	4476.95	42.46	2.37	4.08	79.69	0.297	0.17	0.162	0.181
1531	-4343.26	4477.26	28.84	2.35	4.07	77.74	0.159	0.08	0.185	0.194
1531	-4343.56	4477.56	31.11	2.35	4.01	76.61	0.182	0.09	0.183	0.194
1531	-4343.87	4477.87	34.2	2.34	3.97	76.36	0.213	0.11	0.188	0.200
1531	-4344.17	4478.17	35.74	2.34	3.8	77.29	0.229	0.12	0.186	0.200
1531	-4344.48	4478.48	43.24	2.36	3.75	76.98	0.304	0.17	0.168	0.187
1531	-4344.78	4478.78	47.56	2.38	3.94	79.82	0.348	0.20	0.152	0.174
1531	-4345.09	4479.09	45.39	2.39	4.3	78.67	0.326	0.19	0.147	0.168
1531	-4345.39	4479.39	23.29	2.36	4.78	72.7	0.103	0.05	0.182	0.187
1531	-4345.69	4479.69	24.27	2.36	5.27	72.51	0.113	0.06	0.181	0.187
1531	-4346	4480.00	26.24	2.37	5.24	71.88	0.133	0.07	0.173	0.181
1531	-4346.3	4480.30	27.98	2.37	4.8	71.66	0.150	0.08	0.172	0.181
1531	-4346.61	4480.61	31.41	2.38	4.18	74.1	0.185	0.10	0.164	0.174
1531	-4346.91	4480.91	36.26	2.39	3.55	76.75	0.234	0.13	0.154	0.168
1531	-4347.22	4481.22	45.17	2.38	3.25	77.23	0.324	0.19	0.154	0.174
1531	-4347.52	4481.52	37.65	2.39	3.14	78.08	0.248	0.14	0.153	0.168
1531	-4347.83	4481.83	34.81	2.39	3.06	74.95	0.219	0.12	0.155	0.168
1531	-4348.13	4482.13	32.9	2.39	3.2	74.85	0.200	0.11	0.156	0.168
1531	-4348.44	4482.44	28	2.4	3.6	74.4	0.151	0.08	0.153	0.161
1531	-4348.74	4482.74	27.58	2.46	4.54	69.55	0.146	0.07	0.114	0.123
1531	-4349.05	4483.05	25.3	2.57	6.2	57.72	0.123	0.06	0.045	0.052
1531	-4349.35	4483.35	24.33	2.58	9.16	56.25	0.113	0.06	0.039	0.045
1531	-4349.66	4483.66	24.89	2.53	11.36	58.22	0.119	0.06	0.071	0.077
1531	-4349.96	4483.96	24.93	2.55	9.23	58.13	0.120	0.06	0.058	0.065
1531	-4350.27	4484.27	26.66	2.52	6.68	65.72	0.137	0.07	0.076	0.084
1531	-4350.57	4484.57	33.51	2.42	5.32	73.92	0.206	0.11	0.136	0.148
1531	-4350.88	4484.88	34.32	2.41	4.14	74.03	0.214	0.11	0.142	0.155
1531	-4351.18	4485.18	36.18	2.41	3.22	75.44	0.233	0.13	0.141	0.155
1531	-4351.49	4485.49	35.86	2.39	2.75	79.07	0.230	0.12	0.154	0.168
1531	-4351.79	4485.79	26.91	2.35	2.48	80.38	0.140	0.07	0.186	0.194
1531	-4352.1	4486.10	25.62	2.33	2.27	80.62	0.127	0.06	0.200	0.206
1531	-4352.4	4486.40	30.34	2.33	2.17	80.71	0.174	0.09	0.197	0.206
1531	-4352.71	4486.71	31.07	2.34	2.08	83.08	0.182	0.09	0.190	0.200
1531	-4353.01	4487.01	33.28	2.32	1.98	84.35	0.204	0.11	0.201	0.213
1531	-4353.31	4487.31	27.94	2.3	2.01	84.34	0.150	0.08	0.217	0.226
1531	-4353.62	4487.62	28.28	2.27	2.16	85.24	0.153	0.08	0.237	0.245
1531	-4353.92	4487.92	26.42	2.25	2.19	87.51	0.135	0.07	0.251	0.258
1531	-4354.23	4488.23	25.81	2.25	2.17	87.64	0.128	0.06	0.251	0.258
1531	-4354.53	4488.53	26.72	2.28	1.97	84.73	0.138	0.07	0.231	0.239
1531	-4354.84	4488.84	29.92	2.29	1.7	84.09	0.170	0.09	0.223	0.232
1531	-4355.14	4489.14	33.39	2.29	1.53	83.72	0.205	0.11	0.220	0.232
1531	-4355.45	4489.45	40.5	2.28	1.44	82.45	0.277	0.15	0.222	0.239
1531	-4355.75	4489.75	46.77	2.29	1.36	83.93	0.340	0.20	0.210	0.232
1531	-4356.06	4490.06	54.17	2.29	1.27	83.74	0.415	0.26	0.204	0.232
1531	-4359.56	4493.56	52.11	2.43	1.61	79.96	0.394	0.24	0.116	0.142
1531	-4359.87	4493.87	50.7	2.36	1.66	80.67	0.380	0.23	0.162	0.187
1531	-4360.17	4494.17	36.7	2.36	1.77	78.14	0.238	0.13	0.173	0.187
1531	-4360.48	4494.48	29.86	2.34	1.96	75.82	0.169	0.09	0.190	0.200
1531	-4360.78	4494.78	32.76	2.35	2.14	76.6	0.199	0.10	0.182	0.194
1531	-4361.09	4495.09	37.32	2.37	2.16	79.19	0.245	0.13	0.166	0.181

Well	TVDRSF	MD	GR	RHO	RD	DT	I_{GR} (4-7)	V_{sh} (4-5/6)	Porosity (eq 5-1)	Porosity (eq 4-4)
1531	-4361.39	4495.39	29.49	2.37	2.1	77.85	0.166	0.09	0.171	0.181
1531	-4361.7	4495.70	26.3	2.36	1.97	77.13	0.133	0.07	0.180	0.187
1531	-4362	4496.00	31.43	2.36	1.84	75.77	0.185	0.10	0.177	0.187
1531	-4362.31	4496.31	37.11	2.36	1.69	74.42	0.243	0.13	0.173	0.187
1531	-4362.61	4496.61	37.58	2.36	1.52	77.73	0.247	0.13	0.172	0.187
1531	-4362.92	4496.92	39.05	2.38	1.42	79.08	0.262	0.14	0.158	0.174
1531	-4363.22	4497.22	28.41	2.4	1.39	75.31	0.155	0.08	0.153	0.161
1531	-4363.53	4497.53	24.48	2.38	1.36	74.21	0.115	0.06	0.168	0.174
1531	-4363.83	4497.83	23.3	2.35	1.39	71.41	0.103	0.05	0.188	0.194
1531	-4364.14	4498.14	25.76	2.35	1.48	74.09	0.128	0.06	0.187	0.194
1531	-4364.44	4498.44	23.44	2.39	1.78	74.05	0.104	0.05	0.162	0.168
1531	-4364.74	4498.74	22.75	2.45	2.4	62.42	0.098	0.05	0.124	0.129
1531	-4365.66	4499.66	25.95	2.64	3.47	58.7	0.130	0.07	-0.001	0.006
1531	-4365.96	4499.96	27.51	2.56	2.19	68.65	0.146	0.07	0.050	0.058
1531	-4366.27	4500.27	31.3	2.41	1.55	76.09	0.184	0.10	0.144	0.155
1531	-4366.57	4500.57	34.01	2.37	1.2	76.11	0.211	0.11	0.168	0.181
1531	-4366.88	4500.88	36.11	2.38	1.04	76	0.232	0.13	0.160	0.174
1531	-4367.18	4501.18	37.83	2.37	0.96	78.25	0.250	0.14	0.166	0.181
1531	-4367.49	4501.49	45.18	2.35	0.92	80.89	0.324	0.19	0.173	0.194
1531	-4368.4	4502.40	57.76	2.38	0.96	87.94	0.451	0.29	0.143	0.174
1531	-4368.71	4502.71	34.55	2.39	0.97	77.97	0.217	0.12	0.155	0.168
1531	-4369.01	4503.01	32.4	2.36	0.95	76.35	0.195	0.10	0.176	0.187
1531	-4369.32	4503.32	40.95	2.36	0.95	77.55	0.281	0.16	0.170	0.187
1531	-4369.62	4503.62	33.6	2.35	0.94	78.15	0.207	0.11	0.182	0.194
1531	-4369.93	4503.93	24.21	2.36	0.93	75.18	0.112	0.06	0.181	0.187
1531	-4370.23	4504.23	22.83	2.36	0.93	75.53	0.098	0.05	0.182	0.187
1531	-4370.54	4504.54	27.58	2.37	0.92	75.34	0.146	0.07	0.173	0.181
1531	-4370.84	4504.84	33.6	2.37	0.94	77.21	0.207	0.11	0.169	0.181
1531	-4371.15	4505.15	40.22	2.36	0.96	77.37	0.274	0.15	0.170	0.187
1531	-4371.45	4505.45	42.79	2.38	1.03	80.25	0.300	0.17	0.156	0.174
1531	-4371.76	4505.76	33.94	2.41	1.27	75.05	0.210	0.11	0.143	0.155
1531	-4372.06	4506.06	24.5	2.52	1.75	60.92	0.115	0.06	0.078	0.084
1531	-4373.28	4507.28	32.28	2.59	2.04	74.1	0.194	0.10	0.028	0.039
1531	-4373.58	4507.58	35.62	2.39	1.25	84.08	0.227	0.12	0.154	0.168
1531	-4373.89	4507.89	27.98	2.29	0.86	84.99	0.150	0.08	0.224	0.232
1531	-4374.19	4508.19	23.21	2.28	0.71	83.73	0.102	0.05	0.233	0.239
1531	-4374.5	4508.50	21.71	2.26	0.67	81.41	0.087	0.04	0.247	0.252
1531	-4374.8	4508.80	23.09	2.29	0.66	80.39	0.101	0.05	0.227	0.232
1531	-4375.11	4509.11	24.64	2.3	0.67	78	0.117	0.06	0.219	0.226
1531	-4375.41	4509.41	27.66	2.32	0.69	77.04	0.147	0.07	0.205	0.213
1531	-4375.72	4509.72	31.57	2.33	0.7	78.65	0.187	0.10	0.196	0.206
1531	-4376.02	4510.02	30.9	2.33	0.72	80.04	0.180	0.09	0.196	0.206
1531	-4376.33	4510.33	25.96	2.31	0.7	80.98	0.130	0.07	0.212	0.219
1531	-4376.63	4510.63	31.85	2.3	0.64	82.38	0.189	0.10	0.215	0.226
1531	-4376.94	4510.94	41.46	2.3	0.61	83.06	0.286	0.16	0.208	0.226
1531	-4388.37	4522.37	47.8	2.32	1.13	84.72	0.350	0.21	0.190	0.213
1531	-4388.67	4522.67	33.21	2.34	0.84	80.78	0.203	0.11	0.188	0.200
1531	-4388.98	4522.98	38.78	2.36	0.72	79.31	0.259	0.14	0.171	0.187
1531	-4389.28	4523.28	51.44	2.37	0.81	79.97	0.387	0.23	0.155	0.181
1531	-4391.57	4525.57	36.24	2.34	1.07	81.5	0.234	0.13	0.186	0.200
1531	-4391.87	4525.87	45.2	2.34	0.82	81.41	0.324	0.19	0.179	0.200
1531	-4392.18	4526.18	41.69	2.32	0.73	82.42	0.289	0.16	0.195	0.213
1531	-4392.48	4526.48	45.46	2.37	0.75	84.02	0.327	0.19	0.160	0.181
1531	-4392.79	4526.79	56.58	2.47	0.85	77.67	0.439	0.28	0.086	0.116
1531	-4393.09	4527.09	41.68	2.51	0.94	63.48	0.289	0.16	0.073	0.090
1531	-4393.4	4527.40	32.34	2.37	0.89	69.44	0.194	0.10	0.169	0.181
1531	-4393.7	4527.70	36.21	2.25	0.75	86.28	0.233	0.13	0.244	0.258
1531	-4394.01	4528.01	41.9	2.24	0.54	86.75	0.291	0.16	0.247	0.265
1531	-4394.31	4528.31	41.56	2.25	0.37	89.9	0.287	0.16	0.240	0.258
1531	-4394.62	4528.62	35.37	2.22	0.31	92.75	0.225	0.12	0.264	0.277
1531	-4394.92	4528.92	36.89	2.22	0.29	93.62	0.240	0.13	0.263	0.277
1531	-4395.22	4529.22	37.16	2.24	0.3	90.99	0.243	0.13	0.250	0.265
1531	-4395.53	4529.53	44.56	2.27	0.31	86.27	0.318	0.18	0.225	0.245

Well	TVDRSF	MD	GR	RHO	RD	DT	I_{GR} (4-7)	V_{sh} (4-5/6)	Porosity (eq 5-1)	Porosity (eq 4-4)
1531	-4395.83	4529.83	44.99	2.25	0.32	90.69	0.322	0.19	0.238	0.258
1531	-4396.14	4530.14	47.78	2.27	0.39	89.3	0.350	0.21	0.223	0.245
1531	-4397.36	4531.36	55.26	2.35	0.96	84.49	0.426	0.27	0.164	0.194
1531	-4397.66	4531.66	44.65	2.32	0.9	83.31	0.319	0.18	0.193	0.213
1531	-4397.97	4531.97	55.21	2.34	0.84	83.63	0.425	0.27	0.171	0.200
1531	-4398.58	4532.58	42.28	2.36	0.86	82.72	0.295	0.17	0.169	0.187
1531	-4398.88	4532.88	25.63	2.34	0.92	78.19	0.127	0.06	0.193	0.200
1531	-4399.19	4533.19	24.13	2.34	0.92	77.39	0.111	0.06	0.194	0.200
1531	-4399.49	4533.49	23.89	2.35	0.97	77.57	0.109	0.05	0.188	0.194
1531	-4399.8	4533.80	27.59	2.36	1.03	77.08	0.146	0.07	0.179	0.187
1531	-4400.1	4534.10	34.51	2.36	0.99	75.47	0.216	0.12	0.174	0.187
1531	-4400.41	4534.41	44.81	2.36	0.82	78.62	0.320	0.18	0.167	0.187
1531	-4400.71	4534.71	43.61	2.32	0.64	86.29	0.308	0.18	0.194	0.213
1531	-4401.02	4535.02	32.01	2.25	0.5	90.04	0.191	0.10	0.247	0.258
1531	-4401.32	4535.32	29.93	2.22	0.4	90.76	0.170	0.09	0.268	0.277
1531	-4401.63	4535.63	37.54	2.23	0.34	92.08	0.247	0.13	0.256	0.271
1531	-4401.93	4535.93	47.69	2.25	0.34	93.6	0.349	0.21	0.236	0.258
1531	-4402.24	4536.24	52.35	2.26	0.37	88.9	0.396	0.24	0.225	0.252
1531	-4402.54	4536.54	41.2	2.32	0.41	82.64	0.284	0.16	0.195	0.213
1531	-4402.84	4536.84	47.1	2.3	0.45	86.83	0.343	0.20	0.204	0.226
1531	-4403.76	4537.76	48.62	2.36	0.49	93.3	0.359	0.21	0.164	0.187
1531	-4404.06	4538.06	25.47	2.33	0.48	88.62	0.125	0.06	0.200	0.206
1531	-4404.37	4538.37	29	2.25	0.45	89.84	0.161	0.08	0.249	0.258
1531	-4404.67	4538.67	33.61	2.24	0.44	89.56	0.207	0.11	0.252	0.265
1531	-4404.98	4538.98	37.33	2.25	0.43	89.17	0.245	0.13	0.243	0.258
1531	-4405.28	4539.28	26.89	2.24	0.4	90.89	0.139	0.07	0.257	0.265
1531	-4405.59	4539.59	27.19	2.22	0.39	92.7	0.142	0.07	0.270	0.277
1531	-4405.89	4539.89	30.24	2.21	0.39	91.12	0.173	0.09	0.274	0.284
1531	-4406.2	4540.20	33.73	2.24	0.42	86.55	0.208	0.11	0.252	0.265
1531	-4406.5	4540.50	35.8	2.3	0.49	83.42	0.229	0.12	0.212	0.226
1531	-4406.81	4540.81	34.39	2.31	0.52	81.58	0.215	0.11	0.207	0.219
1531	-4407.11	4541.11	40.11	2.3	0.46	87.15	0.273	0.15	0.209	0.226
1531	-4407.42	4541.42	35.47	2.25	0.38	93.15	0.226	0.12	0.245	0.258
1531	-4407.72	4541.72	35.01	2.2	0.33	93.12	0.221	0.12	0.277	0.290
1531	-4408.03	4542.03	36.38	2.22	0.32	86.26	0.235	0.13	0.263	0.277
1531	-4408.33	4542.33	38.83	2.26	0.38	85.18	0.260	0.14	0.236	0.252
1531	-4408.64	4542.64	50.48	2.28	0.51	83.41	0.377	0.23	0.214	0.239
1531	-4417.78	4551.78	58.12	2.48	2.45	78.07	0.455	0.29	0.078	0.110
1531	-4418.08	4552.08	59.13	2.43	2.48	76.26	0.465	0.30	0.109	0.142
1531	-4418.39	4552.39	55.28	2.44	2.3	75.65	0.426	0.27	0.106	0.135
1531	-4418.69	4552.69	47.86	2.41	2.1	74.28	0.351	0.21	0.132	0.155
1531	-4419	4553.00	41.96	2.39	1.97	75.55	0.291	0.16	0.150	0.168
1531	-4419.3	4553.30	30	2.4	1.84	72.14	0.171	0.09	0.152	0.161
1531	-4419.61	4553.61	25.13	2.4	1.76	70.8	0.122	0.06	0.155	0.161
1531	-4419.91	4553.91	25.64	2.4	1.74	71.88	0.127	0.06	0.154	0.161
1531	-4420.22	4554.22	23.93	2.41	1.69	72.19	0.109	0.05	0.149	0.155
1531	-4420.52	4554.52	25.91	2.41	1.66	71.83	0.129	0.06	0.148	0.155
1531	-4420.83	4554.83	27.91	2.41	1.69	71.6	0.150	0.08	0.146	0.155
1531	-4421.13	4555.13	25.73	2.43	1.76	71.59	0.128	0.06	0.135	0.142
1531	-4421.44	4555.44	30.03	2.43	1.82	70.64	0.171	0.09	0.132	0.142
1531	-4421.74	4555.74	39.03	2.43	1.81	72.85	0.262	0.14	0.126	0.142
1531	-4422.05	4556.05	53.47	2.41	1.81	78.4	0.408	0.25	0.127	0.155
1531	-4422.35	4556.35	57.81	2.41	1.8	79.74	0.451	0.29	0.123	0.155
1531	-4422.66	4556.66	48.15	2.43	1.82	75.33	0.354	0.21	0.119	0.142
1531	-4422.96	4556.96	27.09	2.41	1.78	72.18	0.141	0.07	0.147	0.155
1531	-4423.27	4557.27	26.86	2.38	1.69	72.9	0.139	0.07	0.167	0.174
1531	-4423.57	4557.57	24.6	2.38	1.62	74.06	0.116	0.06	0.168	0.174
1531	-4423.88	4557.88	22.71	2.39	1.56	71.99	0.097	0.05	0.163	0.168
1531	-4424.18	4558.18	21.53	2.38	1.5	70.74	0.085	0.04	0.170	0.174
1531	-4424.49	4558.49	21.37	2.38	1.49	70.76	0.084	0.04	0.170	0.174
1531	-4424.79	4558.79	24.93	2.38	1.51	71.35	0.120	0.06	0.168	0.174
1531	-4425.1	4559.10	27.27	2.38	1.53	71.52	0.143	0.07	0.166	0.174
1531	-4425.4	4559.40	29.99	2.38	1.51	71.89	0.171	0.09	0.165	0.174

Well	TVDRSF	MD	GR	RHO	RD	DT	I_{GR} (4-7)	V_{sh} (4-5/6)	Porosity (eq 5-1)	Porosity (eq 4-4)
1531	-4425.7	4559.70	33.23	2.39	1.54	72.88	0.203	0.11	0.156	0.168
1531	-4426.01	4560.01	37.14	2.38	1.6	76.55	0.243	0.13	0.160	0.174
1531	-4426.31	4560.31	29.77	2.4	1.68	73.61	0.168	0.09	0.152	0.161
1531	-4426.62	4560.62	24.92	2.39	1.8	68.38	0.119	0.06	0.161	0.168
1531	-4426.92	4560.92	23.51	2.41	1.91	68.7	0.105	0.05	0.149	0.155
1531	-4427.23	4561.23	23.96	2.42	2.04	68.9	0.110	0.05	0.142	0.148
1531	-4427.53	4561.53	23.6	2.42	2.15	69.48	0.106	0.05	0.143	0.148
1531	-4427.84	4561.84	24.69	2.43	2.21	69.27	0.117	0.06	0.136	0.142
1531	-4428.14	4562.14	25.03	2.43	2.21	68.9	0.121	0.06	0.135	0.142
1531	-4428.45	4562.45	23.71	2.42	2.14	69.31	0.107	0.05	0.143	0.148
1531	-4428.75	4562.75	23.98	2.4	2.01	70.7	0.110	0.05	0.155	0.161
1531	-4429.06	4563.06	25.43	2.39	1.89	72.19	0.125	0.06	0.161	0.168
1531	-4429.36	4563.36	25.5	2.39	1.77	72.29	0.125	0.06	0.161	0.168
1531	-4429.67	4563.67	24.99	2.4	1.7	71.98	0.120	0.06	0.155	0.161
1531	-4429.97	4563.97	23.6	2.4	1.66	71.51	0.106	0.05	0.156	0.161
1531	-4430.28	4564.28	25.22	2.41	1.66	70.95	0.122	0.06	0.148	0.155
1531	-4430.58	4564.58	28.73	2.41	1.69	71.6	0.158	0.08	0.146	0.155
1531	-4430.89	4564.89	35.38	2.39	1.71	74.98	0.225	0.12	0.154	0.168
1531	-4431.19	4565.19	35.64	2.4	1.73	75.19	0.228	0.12	0.148	0.161
1531	-4431.5	4565.50	23.03	2.38	1.73	71.29	0.100	0.05	0.169	0.174
1531	-4431.8	4565.80	22.37	2.37	1.71	70.11	0.094	0.05	0.176	0.181
1531	-4432.11	4566.11	22.96	2.4	1.72	70.1	0.100	0.05	0.156	0.161
1531	-4432.41	4566.41	23.41	2.42	1.74	70.55	0.104	0.05	0.143	0.148
1531	-4432.72	4566.72	24.68	2.42	1.77	71.26	0.117	0.06	0.142	0.148
1531	-4433.02	4567.02	26.38	2.43	1.77	70.55	0.134	0.07	0.135	0.142
1531	-4433.32	4567.32	28.29	2.42	1.74	70.93	0.153	0.08	0.140	0.148
1531	-4433.63	4567.63	30.11	2.4	1.66	72.21	0.172	0.09	0.152	0.161
1531	-4433.93	4567.93	30.13	2.4	1.58	73.46	0.172	0.09	0.152	0.161
1531	-4434.24	4568.24	29.99	2.4	1.53	74.62	0.171	0.09	0.152	0.161
1531	-4434.54	4568.54	26.79	2.39	1.49	73.74	0.138	0.07	0.160	0.168
1531	-4434.85	4568.85	22.18	2.38	1.45	71.84	0.092	0.04	0.169	0.174
1531	-4435.15	4569.15	27.34	2.4	1.45	72.41	0.144	0.07	0.153	0.161
1531	-4435.46	4569.46	31.23	2.41	1.5	72.85	0.183	0.10	0.144	0.155
1531	-4435.76	4569.76	24.34	2.39	1.54	71.07	0.114	0.06	0.162	0.168
1531	-4436.07	4570.07	31.14	2.41	1.56	71.07	0.182	0.09	0.144	0.155
1531	-4436.37	4570.37	37.86	2.43	1.53	73.78	0.250	0.14	0.127	0.142
1531	-4436.68	4570.68	23.59	2.43	1.45	73.98	0.106	0.05	0.136	0.142
1531	-4436.98	4570.98	18.49	2.39	1.38	72.63	0.055	0.03	0.165	0.168
1531	-4437.29	4571.29	21.08	2.39	1.31	72.21	0.081	0.04	0.163	0.168
1531	-4437.59	4571.59	24.13	2.38	1.27	72.77	0.111	0.06	0.168	0.174
1531	-4437.9	4571.90	29.18	2.38	1.28	75.53	0.162	0.08	0.165	0.174
1531	-4438.2	4572.20	30.92	2.39	1.3	77.67	0.180	0.09	0.157	0.168
1531	-4438.51	4572.51	25.57	2.39	1.28	76.35	0.126	0.06	0.161	0.168
1531	-4438.81	4572.81	28.75	2.38	1.25	76.24	0.158	0.08	0.165	0.174
1531	-4439.12	4573.12	26.59	2.38	1.22	75.55	0.136	0.07	0.167	0.174
1531	-4439.42	4573.42	17.53	2.36	1.17	74.38	0.045	0.02	0.185	0.187
1531	-4439.73	4573.73	17.79	2.36	1.13	74.46	0.047	0.02	0.185	0.187
1531	-4440.03	4574.03	18.42	2.38	1.14	73.1	0.054	0.03	0.171	0.174
1531	-4440.34	4574.34	17.46	2.4	1.15	71.91	0.044	0.02	0.159	0.161
1531	-4440.64	4574.64	19.12	2.39	1.11	72.49	0.061	0.03	0.165	0.168
1531	-4440.94	4574.94	20.66	2.38	1.03	73.9	0.076	0.04	0.170	0.174
1531	-4441.25	4575.25	21.55	2.37	0.94	76.22	0.085	0.04	0.176	0.181
1531	-4441.55	4575.55	24.13	2.35	0.85	77.49	0.111	0.06	0.188	0.194
1531	-4441.86	4575.86	23.14	2.34	0.77	77.2	0.101	0.05	0.195	0.200
1531	-4442.16	4576.16	20.7	2.33	0.67	76.54	0.077	0.04	0.202	0.206
1531	-4442.47	4576.47	19.5	2.32	0.57	78.39	0.065	0.03	0.210	0.213
1531	-4442.77	4576.77	19.4	2.28	0.49	82.67	0.064	0.03	0.235	0.239
1531	-4443.08	4577.08	20.08	2.25	0.45	82.96	0.071	0.03	0.254	0.258
1531	-4443.38	4577.38	19.68	2.25	0.44	82.73	0.067	0.03	0.255	0.258
1531	-4443.69	4577.69	19.41	2.26	0.44	81.7	0.064	0.03	0.248	0.252
1531	-4443.99	4577.99	21.14	2.28	0.44	81.31	0.081	0.04	0.234	0.239
1531	-4444.3	4578.30	19.46	2.3	0.43	82.46	0.064	0.03	0.222	0.226
1531	-4444.6	4578.60	18.19	2.28	0.39	84.27	0.051	0.02	0.236	0.239

Well	TVDRSF	MD	GR	RHO	RD	DT	I_{GR} (4-7)	V_{sh} (4-5/6)	Porosity (eq 5-1)	Porosity (eq 4-4)
1531	-4444.91	4578.91	18.28	2.27	0.36	83.56	0.052	0.02	0.242	0.245
1531	-4445.21	4579.21	19.76	2.25	0.32	82.77	0.067	0.03	0.255	0.258
1531	-4445.52	4579.52	19.57	2.25	0.29	84.96	0.065	0.03	0.255	0.258
1531	-4445.82	4579.82	25.33	2.23	0.28	87.5	0.124	0.06	0.264	0.271
1531	-4446.13	4580.13	34.89	2.22	0.29	88.64	0.220	0.12	0.265	0.277
1531	-4446.43	4580.43	52.79	2.27	0.34	87.83	0.401	0.25	0.218	0.245
1531	-4447.96	4581.96	53.12	2.33	1.32	85.55	0.404	0.25	0.179	0.206
1531	-4449.17	4583.17	55.06	2.33	0.61	91.72	0.424	0.26	0.178	0.206
1531	-4449.48	4583.48	47.54	2.27	0.53	86.3	0.348	0.20	0.223	0.245
1531	-4450.7	4584.70	50.87	2.36	1.01	80.05	0.381	0.23	0.162	0.187
1531	-4451	4585.00	53.17	2.36	0.94	81.08	0.405	0.25	0.160	0.187
1531	-4451.31	4585.31	55.92	2.36	0.93	82.79	0.432	0.27	0.157	0.187
1531	-4451.61	4585.61	56	2.35	1.02	80.2	0.433	0.27	0.164	0.194
1531	-4453.75	4587.75	49.03	2.38	1.39	76.53	0.363	0.22	0.151	0.174
1531	-4454.05	4588.05	40.51	2.39	1.34	73.78	0.277	0.15	0.151	0.168
1531	-4454.36	4588.36	23.97	2.41	1.36	71.99	0.110	0.05	0.149	0.155
1531	-4454.66	4588.66	20.06	2.37	1.44	71.1	0.070	0.03	0.177	0.181
1531	-4454.97	4588.97	21.17	2.38	1.51	70.72	0.082	0.04	0.170	0.174
1531	-4455.27	4589.27	18.02	2.39	1.58	70.75	0.050	0.02	0.165	0.168
1531	-4455.58	4589.58	17.79	2.4	1.61	70.06	0.047	0.02	0.159	0.161
1531	-4455.88	4589.88	18.59	2.42	1.64	69.28	0.056	0.03	0.145	0.148
1531	-4456.18	4590.18	20.3	2.42	1.7	69.55	0.073	0.04	0.145	0.148
1531	-4456.49	4590.49	24.7	2.41	1.73	69.88	0.117	0.06	0.148	0.155
1531	-4456.79	4590.79	32.93	2.42	1.72	71.31	0.200	0.11	0.137	0.148
1531	-4457.1	4591.10	36.12	2.42	1.69	74.92	0.233	0.13	0.135	0.148
1531	-4457.4	4591.40	22.06	2.39	1.66	74.58	0.091	0.04	0.163	0.168
1531	-4457.71	4591.71	21.25	2.39	1.61	73.15	0.082	0.04	0.163	0.168
1531	-4458.01	4592.01	20.66	2.39	1.56	72.14	0.076	0.04	0.164	0.168
1531	-4458.32	4592.32	20.49	2.4	1.56	71.59	0.075	0.04	0.157	0.161
1531	-4458.62	4592.62	20.8	2.4	1.6	70.89	0.078	0.04	0.157	0.161
1531	-4458.93	4592.93	21.36	2.39	1.63	70.53	0.083	0.04	0.163	0.168
1531	-4459.23	4593.23	26.56	2.41	1.67	70.84	0.136	0.07	0.147	0.155
1531	-4459.54	4593.54	32.94	2.41	1.71	71.42	0.200	0.11	0.143	0.155
1531	-4459.84	4593.84	35.01	2.42	1.78	72.68	0.221	0.12	0.135	0.148
1531	-4460.15	4594.15	27.68	2.43	1.9	72.67	0.147	0.07	0.134	0.142
1531	-4460.45	4594.45	25.18	2.42	2	70.45	0.122	0.06	0.142	0.148
1531	-4460.76	4594.76	25.69	2.4	2.1	70.11	0.127	0.06	0.154	0.161
1531	-4461.06	4595.06	30.31	2.4	2.22	70.4	0.174	0.09	0.151	0.161
1531	-4461.37	4595.37	26.18	2.4	2.23	69.31	0.132	0.07	0.154	0.161
1531	-4461.67	4595.67	20.53	2.4	2.14	69.29	0.075	0.04	0.157	0.161
1531	-4461.98	4595.98	27.86	2.41	2.14	70.5	0.149	0.08	0.147	0.155
1531	-4462.28	4596.28	32.95	2.41	2.14	71.64	0.201	0.11	0.143	0.155
1531	-4462.59	4596.59	39.17	2.42	2.13	72.5	0.263	0.15	0.132	0.148
1531	-4462.89	4596.89	32.1	2.4	2.08	71.2	0.192	0.10	0.150	0.161
1531	-4463.2	4597.20	22.4	2.4	2.04	70.68	0.094	0.05	0.156	0.161
1531	-4463.5	4597.50	21.93	2.4	2.01	69.32	0.089	0.04	0.157	0.161
1531	-4463.8	4597.80	26.19	2.43	2.06	68.15	0.132	0.07	0.135	0.142
1531	-4464.11	4598.11	34.43	2.46	2.2	71.1	0.215	0.11	0.110	0.123
1531	-4464.41	4598.41	40.28	2.49	2.39	72.12	0.275	0.15	0.086	0.103
1531	-4464.72	4598.72	30.54	2.52	2.71	63.54	0.176	0.09	0.074	0.084
1531	-4466.55	4600.55	16.36	2.64	8.17	57.27	0.033	0.02	0.005	0.006
1531	-4466.85	4600.85	17.15	2.64	7.88	57.25	0.041	0.02	0.004	0.006
1531	-4469.6	4603.60	24.6	2.58	4.17	63.1	0.116	0.06	0.039	0.045
1531	-4469.9	4603.90	27.31	2.47	3.55	66.52	0.144	0.07	0.108	0.116
1531	-4470.21	4604.21	35.9	2.46	2.98	68.31	0.230	0.12	0.109	0.123
1531	-4470.51	4604.51	45.75	2.45	2.64	69.71	0.330	0.19	0.108	0.129
1531	-4470.82	4604.82	52.94	2.43	2.56	72.63	0.402	0.25	0.115	0.142
1531	-4472.19	4606.19	42.32	2.47	2.27	76.9	0.295	0.17	0.098	0.116
1531	-4472.49	4606.49	29.69	2.42	1.9	71.92	0.168	0.09	0.139	0.148
1531	-4472.8	4606.80	24.45	2.41	1.66	71.04	0.115	0.06	0.149	0.155
1531	-4473.1	4607.10	21.17	2.4	1.5	69.6	0.082	0.04	0.157	0.161
1531	-4473.41	4607.41	21.13	2.38	1.42	70.87	0.081	0.04	0.170	0.174
1531	-4473.71	4607.71	22.72	2.39	1.34	71.04	0.097	0.05	0.163	0.168

Well	TVDRSF	MD	GR	RHO	RD	DT	I_{GR} (4-7)	V_{sh} (4-5/6)	Porosity (eq 5-1)	Porosity (eq 4-4)
1531	-4474.02	4608.02	25.08	2.39	1.27	71.13	0.121	0.06	0.161	0.168
1531	-4474.32	4608.32	27.62	2.39	1.2	71.03	0.147	0.07	0.160	0.168
1531	-4474.63	4608.63	33.19	2.37	1.15	72.98	0.203	0.11	0.169	0.181
1531	-4474.93	4608.93	39.73	2.38	1.13	72.53	0.269	0.15	0.158	0.174
1531	-4475.23	4609.23	57.63	2.38	1.21	74.58	0.450	0.29	0.143	0.174
1531	-4528.42	4662.42	59.42	2.5	1.29	79.73	0.468	0.30	0.064	0.097
1531	-4528.73	4662.73	49.72	2.42	1.06	75.41	0.370	0.22	0.124	0.148
1531	-4529.64	4663.64	40.29	2.35	0.5	82.26	0.275	0.15	0.177	0.194
1531	-4529.95	4663.95	20.47	2.28	0.44	81.23	0.075	0.04	0.235	0.239
1531	-4530.25	4664.25	16.81	2.27	0.43	84.57	0.038	0.02	0.243	0.245
1531	-4530.56	4664.56	16.92	2.25	0.47	86.66	0.039	0.02	0.256	0.258
1531	-4530.86	4664.86	18.04	2.27	0.56	86.04	0.050	0.02	0.243	0.245
1531	-4531.17	4665.17	20.5	2.25	0.68	84.12	0.075	0.04	0.254	0.258
1531	-4531.47	4665.47	25.03	2.29	0.82	81.6	0.121	0.06	0.226	0.232
1531	-4531.78	4665.78	40.2	2.27	0.93	79.61	0.274	0.15	0.228	0.245
1531	-4532.54	4666.54	45.57	2.34	0.92	90.32	0.328	0.19	0.179	0.200
1531	-4532.84	4666.84	18.97	2.34	0.93	75.78	0.059	0.03	0.197	0.200
1531	-4533.15	4667.15	20.33	2.33	1.04	77.09	0.073	0.04	0.203	0.206
1531	-4533.45	4667.45	27.39	2.32	1.23	75.66	0.144	0.07	0.205	0.213
1531	-4533.76	4667.76	47.72	2.34	1.43	78.42	0.350	0.21	0.177	0.200
1531	-4534.82	4668.82	40.8	2.47	2.32	76.31	0.280	0.16	0.099	0.116
1531	-4535.13	4669.13	26.98	2.42	3.27	75	0.140	0.07	0.141	0.148
1531	-4535.43	4669.43	21.27	2.45	5.7	69.1	0.083	0.04	0.125	0.129
1531	-4535.74	4669.74	13.09	2.51	13.97	59.46	0.000	0.00	0.090	0.090
1531	-4538.48	4672.48	23.67	2.57	1.41	70.48	0.107	0.05	0.046	0.052
1531	-4538.79	4672.79	33.6	2.42	1.43	77.84	0.207	0.11	0.136	0.148
1531	-4539.09	4673.09	46.95	2.34	1.66	80.6	0.342	0.20	0.178	0.200
1531	-4546.71	4680.71	58.07	2.39	0.85	87	0.454	0.29	0.136	0.168
1531	-4547.02	4681.02	27.39	2.34	0.72	81.09	0.144	0.07	0.192	0.200
1531	-4547.32	4681.32	16.81	2.32	0.66	77.34	0.038	0.02	0.211	0.213
1531	-4547.62	4681.62	14.83	2.31	0.63	78.93	0.018	0.01	0.218	0.219
1531	-4547.93	4681.93	14.53	2.3	0.61	80.04	0.015	0.01	0.225	0.226
1531	-4548.23	4682.23	15.89	2.3	0.61	80.07	0.028	0.01	0.224	0.226
1531	-4548.54	4682.54	17.71	2.32	0.66	79.13	0.047	0.02	0.210	0.213
1531	-4548.84	4682.84	19.37	2.33	0.8	77.69	0.063	0.03	0.203	0.206
1531	-4549.15	4683.15	20.89	2.32	1.08	77.47	0.079	0.04	0.209	0.213
1531	-4549.45	4683.45	22.28	2.36	1.47	79.77	0.093	0.05	0.182	0.187
1531	-4549.76	4683.76	20.33	2.46	1.73	73.16	0.073	0.04	0.119	0.123
1531	-4550.67	4684.67	26.95	2.43	0.93	66.53	0.140	0.07	0.134	0.142
1531	-4550.98	4684.98	32.54	2.36	0.89	78.55	0.196	0.10	0.176	0.187
1531	-4551.28	4685.28	30.98	2.33	0.96	81.14	0.181	0.09	0.196	0.206
1531	-4551.59	4685.59	38.81	2.32	1.13	79.93	0.260	0.14	0.197	0.213
1531	-4551.89	4685.89	58.55	2.34	1.44	81.96	0.459	0.29	0.168	0.200
1531	-4557.07	4691.07	59.01	2.49	6.39	78.48	0.464	0.30	0.071	0.103
1531	-4557.38	4691.38	49.34	2.49	5.97	68.35	0.366	0.22	0.079	0.103
1531	-4575.51	4709.51	57.35	2.48	6.36	74.22	0.447	0.28	0.079	0.110
1532	-4173.73	4313.73	59.38	2.61	25.77	72.21	0.442	0.28	-0.005	0.026
1532	-4175.56	4315.56	58.21	2.63	10.99	62.19	0.427	0.27	-0.016	0.013
1533	-3970.88	4103.88	51.19	2.42	11.63	64.73	0.353	0.21	0.126	0.148
1533	-3976.67	4109.67	45.29	2.56	16.63	64.42	0.285	0.16	0.040	0.058
1533	-3976.97	4109.97	33.85	2.63	22.6	57.59	0.154	0.08	0.004	0.013
1533	-3977.28	4110.28	46	2.59	20.63	64.34	0.294	0.17	0.021	0.039
1533	-3984.14	4117.14	46.09	2.34	18.59	77.36	0.295	0.17	0.182	0.200
1533	-3984.44	4117.44	42.53	2.39	20.65	68.16	0.254	0.14	0.152	0.168
1533	-3984.74	4117.74	53.67	2.47	20.25	75.07	0.382	0.23	0.091	0.116
1533	-3989.93	4122.93	27.45	2.53	18.62	56.75	0.081	0.04	0.073	0.077
1533	-3990.23	4123.23	19.1	2.58	28.17	63.86	-0.015	-0.01	0.046	0.045
1533	-3990.54	4123.54	28.54	2.52	27.17	80.44	0.093	0.05	0.079	0.084
1533	-3990.84	4123.84	47.51	2.47	16.45	87.41	0.311	0.18	0.097	0.116
1533	-4008.37	4141.37	49.63	2.39	13.13	79.47	0.335	0.20	0.146	0.168
1533	-4008.67	4141.67	40.6	2.42	12.02	79.54	0.232	0.12	0.135	0.148
1533	-4008.98	4141.98	56.29	2.54	10.24	86.8	0.412	0.25	0.043	0.071

Well	TVDRSF	MD	GR	RHO	RD	DT	I_{GR} (4-7)	V_{sh} (4-5/6)	Porosity (eq 5-1)	Porosity (eq 4-4)
1533	-4092.34	4225.34	50.19	2.62	5.08	63.99	0.342	0.20	-0.003	0.019
1533	-4092.64	4225.64	51.67	2.61	4.52	71.25	0.359	0.21	0.002	0.026
1533	-4094.63	4227.63	51.45	2.41	3.09	74.02	0.356	0.21	0.132	0.155
1533	-4094.93	4227.93	37.71	2.5	2.97	69.98	0.199	0.10	0.085	0.097
1533	-4095.23	4228.23	36.95	2.47	2.8	76.75	0.190	0.10	0.105	0.116
1533	-4095.54	4228.54	49.58	2.36	2.63	79.04	0.335	0.19	0.166	0.187
1533	-4097.22	4230.22	47.02	2.36	1.09	87.69	0.305	0.17	0.168	0.187
1533	-4097.52	4230.52	40.38	2.3	0.79	87	0.229	0.12	0.212	0.226
1533	-4097.83	4230.83	47.56	2.29	0.65	89.68	0.312	0.18	0.213	0.232
1533	-4098.13	4231.13	46.21	2.31	0.69	86.9	0.296	0.17	0.201	0.219
1533	-4098.44	4231.44	37.45	2.26	0.8	69.46	0.196	0.10	0.240	0.252
1533	-4098.74	4231.74	36.71	2.24	0.9	63.19	0.187	0.10	0.254	0.265
1533	-4099.04	4232.04	40.88	2.23	0.97	73.21	0.235	0.13	0.257	0.271
1533	-4099.35	4232.35	45.32	2.29	0.95	82.48	0.286	0.16	0.215	0.232
1533	-4099.65	4232.65	42.48	2.29	0.87	87.83	0.253	0.14	0.217	0.232
1533	-4099.96	4232.96	43.16	2.28	0.82	88.96	0.261	0.14	0.223	0.239
1533	-4100.26	4233.26	49.14	2.31	0.82	88.77	0.330	0.19	0.198	0.219
1533	-4100.57	4233.57	53.87	2.34	0.88	87.73	0.384	0.23	0.175	0.200
1533	-4100.87	4233.87	51.82	2.34	0.93	86.31	0.360	0.21	0.177	0.200
1533	-4101.18	4234.18	43.6	2.33	0.95	83.73	0.266	0.15	0.190	0.206
1533	-4101.48	4234.48	36.6	2.32	0.97	83.73	0.186	0.10	0.202	0.213
1533	-4101.79	4234.79	42.66	2.32	0.95	86.2	0.255	0.14	0.198	0.213
1533	-4102.09	4235.09	40.8	2.33	0.91	85.14	0.234	0.13	0.193	0.206
1533	-4102.4	4235.40	38.54	2.32	0.85	86.38	0.208	0.11	0.201	0.213
1533	-4102.7	4235.70	40.66	2.33	0.82	86.13	0.232	0.13	0.193	0.206
1533	-4103.01	4236.01	33.26	2.34	0.86	82.89	0.147	0.07	0.192	0.200
1533	-4103.31	4236.31	29.37	2.33	0.94	78.89	0.103	0.05	0.201	0.206
1533	-4103.62	4236.62	29.58	2.34	1.15	78.69	0.105	0.05	0.194	0.200
1533	-4103.92	4236.92	29.26	2.34	1.57	80.12	0.102	0.05	0.195	0.200
1533	-4104.23	4237.23	30.25	2.39	2.12	71.17	0.113	0.06	0.162	0.168
1533	-4104.53	4237.53	28.45	2.5	2.95	60.04	0.092	0.05	0.092	0.097
1533	-4105.45	4238.45	27.31	2.62	6.34	57.09	0.079	0.04	0.015	0.019
1533	-4105.75	4238.75	27.68	2.57	3.99	62.82	0.083	0.04	0.047	0.052
1533	-4106.06	4239.06	26.95	2.53	2.77	76.73	0.075	0.04	0.073	0.077
1533	-4106.36	4239.36	25.48	2.41	1.98	84.86	0.058	0.03	0.152	0.155
1533	-4106.66	4239.66	26.73	2.31	1.53	83.98	0.073	0.03	0.216	0.219
1533	-4106.97	4239.97	27.46	2.3	1.35	83.88	0.081	0.04	0.222	0.226
1533	-4107.27	4240.27	35.36	2.32	1.25	82.93	0.172	0.09	0.203	0.213
1533	-4107.58	4240.58	50.03	2.33	1	87.29	0.340	0.20	0.185	0.206
1533	-4108.19	4241.19	55.62	2.34	0.52	96.32	0.404	0.25	0.173	0.200
1533	-4108.49	4241.49	38.1	2.26	0.4	97.72	0.203	0.11	0.240	0.252
1533	-4108.8	4241.80	36.78	2.2	0.34	97.05	0.188	0.10	0.280	0.290
1533	-4109.1	4242.10	40.12	2.22	0.39	92.55	0.226	0.12	0.264	0.277
1533	-4109.41	4242.41	45.04	2.27	0.49	87.64	0.283	0.16	0.228	0.245
1533	-4109.71	4242.71	51.68	2.31	0.65	82.37	0.359	0.21	0.196	0.219
1533	-4110.02	4243.02	48.5	2.36	0.92	79.69	0.322	0.19	0.167	0.187
1533	-4110.32	4243.32	53.45	2.36	1.18	79.14	0.379	0.23	0.162	0.187
1533	-4111.39	4244.39	48.98	2.35	0.98	89.02	0.328	0.19	0.173	0.194
1533	-4111.69	4244.69	53.3	2.31	1.08	82.4	0.377	0.23	0.194	0.219
1533	-4112	4245.00	57.18	2.34	1.32	71.61	0.422	0.26	0.171	0.200
1533	-4112.3	4245.30	59.13	2.41	1.91	75.77	0.444	0.28	0.124	0.155
1533	-4113.22	4246.22	42.52	2.42	3.05	76.03	0.254	0.14	0.133	0.148
1533	-4113.52	4246.52	42.06	2.35	3.18	82.63	0.248	0.14	0.179	0.194
1533	-4113.83	4246.83	58.39	2.35	3.31	83.65	0.436	0.27	0.164	0.194
1533	-4116.88	4249.88	44.94	2.43	6.95	75.47	0.281	0.16	0.125	0.142
1533	-4117.18	4250.18	53.97	2.42	6.77	85.43	0.385	0.23	0.123	0.148
1533	-4128.15	4261.15	39.11	2.25	8.44	97.16	0.215	0.11	0.246	0.258
1533	-4128.46	4261.46	32.53	2.19	16.86	104.32	0.139	0.07	0.289	0.297
1533	-4128.76	4261.76	31.4	2.15	24.57	105.05	0.126	0.06	0.316	0.323
1533	-4129.07	4262.07	29.98	2.17	24.87	107.27	0.110	0.05	0.304	0.310
1533	-4129.37	4262.37	31.15	2.17	26.02	107.28	0.123	0.06	0.303	0.310
1533	-4129.68	4262.68	32.39	2.18	26.61	106.45	0.137	0.07	0.296	0.303
1533	-4129.98	4262.98	33.45	2.17	26.35	106.22	0.150	0.08	0.301	0.310

Well	TVDRSF	MD	GR	RHO	RD	DT	I_{GR} (4-7)	V_{sh} (4-5/6)	Porosity (eq 5-1)	Porosity (eq 4-4)
1533	-4130.29	4263.29	33.31	2.2	25.62	104.09	0.148	0.08	0.282	0.290
1533	-4130.59	4263.59	33.57	2.23	24.45	99.51	0.151	0.08	0.263	0.271
1533	-4130.9	4263.90	34.83	2.22	22.15	98.17	0.165	0.09	0.268	0.277
1533	-4131.2	4264.20	34.67	2.2	18.63	100.11	0.164	0.08	0.281	0.290
1533	-4131.51	4264.51	32.56	2.19	17.73	92.94	0.139	0.07	0.289	0.297
1533	-4131.81	4264.81	32.41	2.25	19.32	67.88	0.138	0.07	0.250	0.258
1533	-4132.12	4265.12	31.74	2.41	22.17	56.91	0.130	0.07	0.148	0.155
1533	-4132.42	4265.42	28.68	2.6	21.32	58.57	0.095	0.05	0.027	0.032
1533	-4132.73	4265.73	31.67	2.57	14.78	72.73	0.129	0.06	0.045	0.052
1533	-4133.03	4266.03	37.89	2.46	11.12	89.88	0.201	0.11	0.111	0.123
1533	-4133.33	4266.33	44.63	2.3	9.96	99.26	0.278	0.16	0.209	0.226
1533	-4133.64	4266.64	39.6	2.25	9.37	103.82	0.220	0.12	0.245	0.258
1533	-4133.94	4266.94	34.13	2.23	9.54	106.99	0.157	0.08	0.262	0.271
1533	-4134.25	4267.25	34.65	2.22	9.87	106.47	0.163	0.08	0.268	0.277
1533	-4134.55	4267.55	36.47	2.24	9.55	97.35	0.184	0.10	0.254	0.265
1533	-4134.86	4267.86	36.57	2.26	9.45	89.08	0.185	0.10	0.241	0.252
1533	-4135.16	4268.16	33.05	2.32	10.36	73.72	0.145	0.07	0.205	0.213
1533	-4135.47	4268.47	28.34	2.45	11.42	65.43	0.091	0.04	0.124	0.129
1533	-4135.77	4268.77	28.9	2.53	14.35	72.22	0.097	0.05	0.072	0.077
1533	-4136.08	4269.08	30.85	2.5	18.24	68.96	0.120	0.06	0.090	0.097
1533	-4136.38	4269.38	29.27	2.57	18.22	58.07	0.102	0.05	0.046	0.052
1533	-4136.69	4269.69	31.07	2.59	17.74	57.76	0.122	0.06	0.032	0.039
1533	-4136.99	4269.99	33.6	2.56	18.62	59.57	0.151	0.08	0.050	0.058
1533	-4137.3	4270.30	31.31	2.59	15.7	58.98	0.125	0.06	0.032	0.039
1533	-4137.6	4270.60	32.23	2.6	11.64	63.19	0.136	0.07	0.025	0.032
1533	-4137.91	4270.91	32.84	2.57	7.73	63.74	0.143	0.07	0.044	0.052
1533	-4138.21	4271.21	41.57	2.56	4.7	65.86	0.243	0.13	0.044	0.058
1533	-4138.52	4271.52	55.58	2.51	3.17	80.26	0.404	0.25	0.063	0.090
1533	-4139.13	4272.13	39.6	2.37	1.67	82.57	0.220	0.12	0.168	0.181
1533	-4139.43	4272.43	30.59	2.42	1.35	68.3	0.117	0.06	0.142	0.148
1533	-4139.74	4272.74	29.12	2.48	1.14	72.78	0.100	0.05	0.104	0.110
1533	-4140.04	4273.04	32.95	2.46	0.99	85.57	0.144	0.07	0.115	0.123
1533	-4140.35	4273.35	33.39	2.31	0.87	86.05	0.149	0.08	0.211	0.219
1533	-4140.65	4273.65	29.96	2.33	0.76	84.33	0.110	0.05	0.201	0.206
1533	-4140.95	4273.95	29.96	2.35	0.7	84.78	0.110	0.05	0.188	0.194
1533	-4141.26	4274.26	30.38	2.33	0.66	86.77	0.114	0.06	0.200	0.206
1533	-4141.56	4274.56	28.2	2.34	0.64	88.49	0.089	0.04	0.195	0.200
1533	-4141.87	4274.87	27.89	2.3	0.62	89.28	0.086	0.04	0.221	0.226
1533	-4142.17	4275.17	29.23	2.29	0.62	88.38	0.101	0.05	0.227	0.232
1533	-4142.48	4275.48	28.29	2.3	0.63	87.07	0.090	0.04	0.221	0.226
1533	-4142.78	4275.78	31.52	2.29	0.63	86.16	0.127	0.06	0.225	0.232
1533	-4143.09	4276.09	34.65	2.32	0.65	85.71	0.163	0.08	0.204	0.213
1533	-4143.39	4276.39	37.5	2.32	0.68	88.32	0.196	0.10	0.202	0.213
1533	-4143.7	4276.70	43.3	2.31	0.7	88.34	0.263	0.14	0.203	0.219
1533	-4144	4277.00	45.03	2.34	0.68	86.27	0.283	0.16	0.183	0.200
1533	-4144.31	4277.31	41.07	2.36	0.66	86.34	0.237	0.13	0.173	0.187
1533	-4144.61	4277.61	32	2.31	0.63	84.93	0.133	0.07	0.212	0.219
1533	-4144.92	4277.92	27.67	2.3	0.59	84.6	0.083	0.04	0.221	0.226
1533	-4145.22	4278.22	25.31	2.3	0.56	85.35	0.056	0.03	0.223	0.226
1533	-4145.53	4278.53	25.72	2.3	0.57	85.85	0.061	0.03	0.223	0.226
1533	-4145.83	4278.83	28.34	2.31	0.61	86.11	0.091	0.04	0.214	0.219
1533	-4146.14	4279.14	30.22	2.3	0.71	86.88	0.113	0.06	0.220	0.226
1533	-4146.44	4279.44	30.01	2.31	0.89	80.42	0.110	0.05	0.213	0.219
1533	-4146.75	4279.75	30.48	2.47	0.91	66.75	0.116	0.06	0.110	0.116
1533	-4147.05	4280.05	27.35	2.52	0.84	73.95	0.080	0.04	0.080	0.084
1533	-4147.36	4280.36	23.83	2.4	0.72	84.65	0.039	0.02	0.159	0.161
1533	-4147.66	4280.66	23.76	2.29	0.61	85.37	0.038	0.02	0.230	0.232
1533	-4147.97	4280.97	25.89	2.29	0.56	85.28	0.063	0.03	0.229	0.232
1533	-4148.27	4281.27	30.12	2.29	0.58	84.87	0.111	0.06	0.226	0.232
1533	-4148.57	4281.57	29.7	2.28	0.61	83.97	0.107	0.05	0.233	0.239
1533	-4148.88	4281.88	28.73	2.3	0.64	83.29	0.095	0.05	0.221	0.226
1533	-4149.18	4282.18	31.12	2.31	0.69	78.97	0.123	0.06	0.213	0.219
1533	-4149.49	4282.49	30.15	2.34	0.77	79.22	0.112	0.06	0.194	0.200

Well	TVDRSF	MD	GR	RHO	RD	DT	I_{GR} (4-7)	V_{sh} (4-5/6)	Porosity (eq 5-1)	Porosity (eq 4-4)
1533	-4149.79	4282.79	26.16	2.33	0.84	80.44	0.066	0.03	0.203	0.206
1533	-4150.1	4283.10	24.03	2.3	0.87	78.13	0.042	0.02	0.224	0.226
1533	-4150.4	4283.40	24.72	2.27	0.84	78.81	0.049	0.02	0.243	0.245
1533	-4150.71	4283.71	24.99	2.27	0.8	82.04	0.053	0.02	0.242	0.245
1533	-4151.01	4284.01	23.01	2.28	0.73	85.15	0.030	0.01	0.237	0.239
1533	-4151.32	4284.32	26.03	2.26	0.68	87.29	0.064	0.03	0.248	0.252
1533	-4151.62	4284.62	30.65	2.25	0.64	89.97	0.117	0.06	0.252	0.258
1533	-4151.93	4284.93	33.48	2.29	0.6	90.74	0.150	0.08	0.224	0.232
1533	-4152.23	4285.23	29.37	2.29	0.57	87.81	0.103	0.05	0.227	0.232
1533	-4152.54	4285.54	29.97	2.27	0.56	87.57	0.110	0.05	0.239	0.245
1533	-4152.84	4285.84	31.41	2.3	0.6	89.69	0.126	0.06	0.219	0.226
1533	-4153.15	4286.15	29.05	2.27	0.68	88.43	0.099	0.05	0.240	0.245
1533	-4153.45	4286.45	27.25	2.28	0.8	89.31	0.078	0.04	0.235	0.239
1533	-4153.76	4286.76	24.91	2.29	0.95	90.97	0.052	0.02	0.230	0.232
1533	-4154.06	4287.06	24.36	2.29	1.07	91.28	0.045	0.02	0.230	0.232
1533	-4154.37	4287.37	25.32	2.27	1	91.74	0.056	0.03	0.242	0.245
1533	-4154.67	4287.67	23.57	2.29	0.86	91.52	0.036	0.02	0.230	0.232
1533	-4154.98	4287.98	23.75	2.25	0.72	91.56	0.038	0.02	0.256	0.258
1533	-4155.28	4288.28	24.93	2.24	0.6	90.5	0.052	0.02	0.262	0.265
1533	-4155.59	4288.59	25.77	2.24	0.55	88.24	0.062	0.03	0.261	0.265
1533	-4155.89	4288.89	26.27	2.27	0.52	86.17	0.067	0.03	0.242	0.245
1533	-4156.19	4289.19	27.59	2.28	0.51	86.64	0.082	0.04	0.234	0.239
1533	-4156.5	4289.50	28.47	2.29	0.49	86.86	0.092	0.05	0.227	0.232
1533	-4156.8	4289.80	27.54	2.29	0.46	86.83	0.082	0.04	0.228	0.232
1533	-4157.11	4290.11	29.63	2.27	0.42	86.99	0.106	0.05	0.239	0.245
1533	-4157.41	4290.41	30.31	2.29	0.41	87.79	0.114	0.06	0.226	0.232
1533	-4157.72	4290.72	26.58	2.26	0.4	88.97	0.071	0.03	0.248	0.252
1533	-4158.02	4291.02	26.03	2.26	0.39	90.07	0.064	0.03	0.248	0.252
1533	-4158.33	4291.33	26.24	2.26	0.4	89.72	0.067	0.03	0.248	0.252
1533	-4158.63	4291.63	30.42	2.26	0.42	89.42	0.115	0.06	0.245	0.252
1533	-4158.94	4291.94	38.72	2.27	0.5	90.11	0.210	0.11	0.233	0.245
1533	-4159.24	4292.24	52.19	2.27	0.59	89.25	0.365	0.22	0.221	0.245
1533	-4159.55	4292.55	59.99	2.32	0.67	87.64	0.454	0.29	0.181	0.213
1533	-4159.85	4292.85	50.78	2.39	0.69	86.22	0.348	0.20	0.145	0.168
1533	-4160.16	4293.16	40.35	2.36	0.62	85.19	0.229	0.12	0.174	0.187
1533	-4160.46	4293.46	34.45	2.35	0.54	86.04	0.161	0.08	0.184	0.194
1533	-4160.77	4293.77	35.56	2.33	0.52	88.06	0.174	0.09	0.197	0.206
1533	-4161.07	4294.07	45.02	2.27	0.58	90.8	0.282	0.16	0.228	0.245
1533	-4161.68	4294.68	58.11	2.32	0.77	95.87	0.433	0.27	0.183	0.213
1533	-4161.99	4294.99	39.36	2.33	0.83	85.99	0.217	0.12	0.194	0.206
1533	-4162.29	4295.29	33.22	2.3	0.71	85.32	0.147	0.07	0.218	0.226
1533	-4162.6	4295.60	33.48	2.32	0.58	89.15	0.150	0.08	0.205	0.213
1533	-4162.9	4295.90	30.9	2.28	0.49	91.46	0.120	0.06	0.232	0.239
1533	-4163.21	4296.21	30.81	2.23	0.42	92.22	0.119	0.06	0.264	0.271
1533	-4163.51	4296.51	32.15	2.23	0.41	93.31	0.135	0.07	0.264	0.271
1533	-4163.81	4296.81	35.2	2.26	0.42	94.53	0.170	0.09	0.242	0.252
1533	-4164.12	4297.12	36.52	2.27	0.41	93.97	0.185	0.10	0.235	0.245
1533	-4164.42	4297.42	36.08	2.26	0.37	95.58	0.180	0.09	0.241	0.252
1533	-4164.73	4297.73	28.31	2.27	0.34	96.12	0.091	0.04	0.240	0.245
1533	-4165.03	4298.03	25.71	2.25	0.31	95.77	0.061	0.03	0.255	0.258
1533	-4165.34	4298.34	26.21	2.26	0.31	95.27	0.067	0.03	0.248	0.252
1533	-4165.64	4298.64	25.03	2.26	0.38	93.76	0.053	0.03	0.249	0.252
1533	-4165.95	4298.95	25.04	2.26	0.53	89.71	0.053	0.03	0.249	0.252
1533	-4166.25	4299.25	27.59	2.31	0.77	76.07	0.082	0.04	0.215	0.219
1533	-4166.56	4299.56	29.06	2.39	1.1	60.45	0.099	0.05	0.162	0.168
1533	-4166.86	4299.86	30.29	2.5	1.22	57.4	0.113	0.06	0.091	0.097
1533	-4167.17	4300.17	30.03	2.58	1.05	76.88	0.110	0.05	0.039	0.045
1533	-4167.47	4300.47	31.68	2.49	1.02	86.88	0.129	0.06	0.096	0.103
1533	-4167.78	4300.78	29.09	2.36	0.96	74.58	0.100	0.05	0.182	0.187
1533	-4168.08	4301.08	30.09	2.37	1.06	67.43	0.111	0.05	0.175	0.181
1533	-4168.39	4301.39	33.7	2.51	1.05	68.9	0.152	0.08	0.082	0.090
1533	-4168.69	4301.69	34.47	2.5	0.91	75.33	0.161	0.08	0.088	0.097
1533	-4169	4302.00	43.18	2.45	0.8	88.83	0.261	0.14	0.113	0.129

Well	TVDRSF	MD	GR	RHO	RD	DT	I_{GR} (4-7)	V_{sh} (4-5/6)	Porosity (eq 5-1)	Porosity (eq 4-4)
1533	-4169.3	4302.30	59.12	2.35	0.83	90.81	0.444	0.28	0.163	0.194
1533	-4171.13	4304.13	30.14	2.44	0.6	92.56	0.112	0.06	0.129	0.135
1533	-4171.43	4304.43	23.92	2.3	0.42	91.12	0.040	0.02	0.224	0.226
1533	-4171.74	4304.74	25.64	2.21	0.35	90.53	0.060	0.03	0.281	0.284
1533	-4172.04	4305.04	24.42	2.23	0.35	89.22	0.046	0.02	0.269	0.271
1533	-4172.35	4305.35	23.92	2.25	0.37	87.93	0.040	0.02	0.256	0.258
1533	-4172.65	4305.65	28.07	2.26	0.35	89.17	0.088	0.04	0.247	0.252
1533	-4172.96	4305.96	29.36	2.26	0.33	91.51	0.103	0.05	0.246	0.252
1533	-4173.26	4306.26	27.34	2.27	0.31	89.83	0.080	0.04	0.241	0.245
1533	-4173.57	4306.57	27.4	2.23	0.29	90.03	0.080	0.04	0.267	0.271
1533	-4173.87	4306.87	29.29	2.23	0.31	93.16	0.102	0.05	0.265	0.271
1533	-4174.18	4307.18	29.27	2.23	0.33	92.09	0.102	0.05	0.265	0.271
1533	-4174.48	4307.48	25.4	2.22	0.35	89.93	0.057	0.03	0.274	0.277
1533	-4174.79	4307.79	24.31	2.24	0.36	89.7	0.045	0.02	0.262	0.265
1533	-4175.09	4308.09	27.25	2.26	0.41	88.7	0.078	0.04	0.247	0.252
1533	-4175.4	4308.40	35.08	2.26	0.5	85.82	0.168	0.09	0.242	0.252
1533	-4175.7	4308.70	48.94	2.27	0.67	82.84	0.327	0.19	0.224	0.245
1533	-4176.01	4309.01	58.38	2.31	1	80.77	0.436	0.27	0.189	0.219
1533	-4177.84	4310.84	49.47	2.43	1.02	88.3	0.333	0.19	0.121	0.142
1533	-4178.14	4311.14	37.58	2.36	0.74	85.56	0.197	0.10	0.176	0.187
1533	-4178.45	4311.45	33.86	2.34	0.56	86.51	0.154	0.08	0.191	0.200
1533	-4178.75	4311.75	32.66	2.34	0.5	85.69	0.141	0.07	0.192	0.200
1533	-4179.05	4312.05	29.35	2.3	0.5	85.69	0.103	0.05	0.220	0.226
1533	-4179.36	4312.36	30.52	2.29	0.6	83.01	0.116	0.06	0.226	0.232
1533	-4179.66	4312.66	30.67	2.32	0.82	77.27	0.118	0.06	0.206	0.213
1533	-4179.97	4312.97	27.33	2.36	1.37	66.57	0.079	0.04	0.183	0.187
1533	-4180.27	4313.27	23.12	2.46	3.08	60.28	0.031	0.01	0.121	0.123
1533	-4180.58	4313.58	22.38	2.58	6.81	57.2	0.023	0.01	0.044	0.045
1533	-4180.88	4313.88	23.76	2.59	11.35	59.21	0.038	0.02	0.037	0.039
1533	-4181.19	4314.19	26.3	2.58	9.31	58.89	0.068	0.03	0.042	0.045
1533	-4181.49	4314.49	26.27	2.53	4.25	58.23	0.067	0.03	0.074	0.077
1533	-4181.8	4314.80	26.14	2.53	2.23	66.46	0.066	0.03	0.074	0.077
1533	-4182.1	4315.10	26	2.5	1.17	69.4	0.064	0.03	0.093	0.097
1533	-4182.41	4315.41	29.47	2.47	0.79	72.13	0.104	0.05	0.111	0.116
1533	-4182.71	4315.71	34.21	2.47	0.65	80.43	0.158	0.08	0.107	0.116
1533	-4183.02	4316.02	38.14	2.33	0.6	86.75	0.203	0.11	0.195	0.206
1533	-4183.32	4316.32	41.73	2.31	0.62	88.44	0.245	0.13	0.205	0.219
1533	-4183.63	4316.63	41.91	2.32	0.69	87.73	0.247	0.13	0.198	0.213
1533	-4183.93	4316.93	49.67	2.29	0.76	88.18	0.336	0.20	0.211	0.232
1533	-4184.24	4317.24	44.11	2.36	0.85	77.64	0.272	0.15	0.171	0.187
1533	-4184.54	4317.54	35.91	2.42	0.94	73.32	0.178	0.09	0.138	0.148
1533	-4184.85	4317.85	37.4	2.42	0.97	81.48	0.195	0.10	0.137	0.148
1533	-4185.15	4318.15	41.79	2.37	0.9	84.03	0.245	0.13	0.166	0.181
1533	-4185.46	4318.46	41.32	2.39	0.76	86.06	0.240	0.13	0.153	0.168
1533	-4185.76	4318.76	35.03	2.33	0.64	84.48	0.168	0.09	0.197	0.206
1533	-4186.07	4319.07	27.41	2.34	0.62	70.65	0.080	0.04	0.196	0.200
1533	-4186.37	4319.37	25.56	2.44	0.66	60.64	0.059	0.03	0.132	0.135
1533	-4186.67	4319.67	25.63	2.58	0.75	60.91	0.060	0.03	0.042	0.045
1533	-4186.98	4319.98	27.97	2.59	0.83	67.32	0.087	0.04	0.034	0.039
1533	-4187.28	4320.28	35.3	2.5	0.86	81.21	0.171	0.09	0.087	0.097
1533	-4187.59	4320.59	47.63	2.42	0.83	91.25	0.312	0.18	0.129	0.148
1533	-4187.89	4320.89	59.1	2.34	0.81	90.29	0.444	0.28	0.169	0.200
1533	-4188.5	4321.50	56.46	2.35	0.93	88.87	0.414	0.26	0.166	0.194
1533	-4188.81	4321.81	49.19	2.34	0.88	86.03	0.330	0.19	0.179	0.200
1533	-4189.11	4322.11	45.07	2.36	0.85	84.34	0.283	0.16	0.170	0.187
1533	-4189.42	4322.42	50.63	2.35	0.95	87.93	0.347	0.20	0.171	0.194
1533	-4190.79	4323.79	50.09	2.48	2.1	74.93	0.341	0.20	0.088	0.110
1533	-4191.09	4324.09	39.39	2.48	2.04	67.31	0.218	0.12	0.097	0.110
1533	-4191.4	4324.40	41.64	2.47	2.55	73.65	0.244	0.13	0.102	0.116
1533	-4191.7	4324.70	58.75	2.46	3.6	85.35	0.440	0.28	0.092	0.123
1533	-4196.12	4329.12	42.4	2.38	1.12	82.66	0.252	0.14	0.159	0.174
1533	-4196.43	4329.43	47	2.35	1.05	87.24	0.305	0.17	0.174	0.194
1533	-4196.73	4329.73	55.77	2.35	1.22	84.73	0.406	0.25	0.166	0.194

Well	TVDRSF	MD	GR	RHO	RD	DT	I_{GR} (4-7)	V_{sh} (4-5/6)	Porosity (eq 5-1)	Porosity (eq 4-4)
1533	-4197.04	4330.04	58.03	2.38	1.72	77.53	0.432	0.27	0.145	0.174
1533	-4199.17	4332.17	36.7	2.37	0.54	91.79	0.187	0.10	0.170	0.181
1533	-4199.48	4332.48	29.04	2.31	0.39	92.69	0.099	0.05	0.214	0.219
1533	-4199.78	4332.78	31.7	2.24	0.36	89.77	0.130	0.06	0.257	0.265
1533	-4200.09	4333.09	37.26	2.27	0.4	87.87	0.193	0.10	0.234	0.245
1533	-4200.39	4333.39	40.11	2.3	0.58	83.65	0.226	0.12	0.212	0.226
1533	-4200.7	4333.70	40.96	2.33	0.84	79.94	0.236	0.13	0.192	0.206
1533	-4201	4334.00	50.28	2.38	1.2	85.49	0.343	0.20	0.152	0.174
1533	-4202.22	4335.22	56.07	2.44	1.7	91.27	0.409	0.25	0.108	0.135
1533	-4202.52	4335.52	41.24	2.37	1.1	86.32	0.239	0.13	0.166	0.181
1533	-4202.83	4335.83	37.07	2.32	0.72	87.69	0.191	0.10	0.202	0.213
1533	-4203.13	4336.13	37.65	2.31	0.5	92.09	0.198	0.10	0.208	0.219
1533	-4203.44	4336.44	25.86	2.32	0.44	90.74	0.063	0.03	0.210	0.213
1533	-4203.74	4336.74	23.27	2.26	0.43	86.99	0.033	0.02	0.250	0.252
1533	-4204.05	4337.05	26.21	2.25	0.5	77.05	0.067	0.03	0.255	0.258
1533	-4204.35	4337.35	36.58	2.35	0.69	73.25	0.186	0.10	0.183	0.194
1533	-4204.66	4337.66	48	2.44	0.98	82.9	0.317	0.18	0.116	0.135
1533	-4205.42	4338.42	49.34	2.38	0.91	83.66	0.332	0.19	0.153	0.174
1533	-4205.72	4338.72	28.84	2.34	0.83	80.8	0.097	0.05	0.195	0.200
1533	-4206.03	4339.03	22.7	2.3	0.72	78.51	0.026	0.01	0.224	0.226
1533	-4206.33	4339.33	23.74	2.33	0.64	77.16	0.038	0.02	0.204	0.206
1533	-4206.64	4339.64	21.82	2.32	0.59	78	0.016	0.01	0.212	0.213
1533	-4206.94	4339.94	20.92	2.34	0.6	80.45	0.006	0.00	0.200	0.200
1533	-4207.25	4340.25	22.51	2.33	0.58	73.59	0.024	0.01	0.205	0.206
1533	-4207.55	4340.55	25.24	2.35	0.57	72.73	0.055	0.03	0.191	0.194
1533	-4207.86	4340.86	24.6	2.36	0.59	81.63	0.048	0.02	0.185	0.187
1533	-4208.16	4341.16	24.1	2.3	0.61	81.96	0.042	0.02	0.224	0.226
1533	-4208.47	4341.47	28.01	2.3	0.58	82.72	0.087	0.04	0.221	0.226
1533	-4208.77	4341.77	31.9	2.3	0.56	84.04	0.132	0.07	0.219	0.226
1533	-4209.08	4342.08	29.35	2.3	0.55	84.22	0.103	0.05	0.220	0.226
1533	-4209.38	4342.38	26.21	2.29	0.56	83.1	0.067	0.03	0.229	0.232
1533	-4209.69	4342.69	25.56	2.3	0.58	80.7	0.059	0.03	0.223	0.226
1533	-4209.99	4342.99	25.58	2.33	0.59	74.34	0.059	0.03	0.203	0.206
1533	-4210.3	4343.30	29.78	2.36	0.59	77.54	0.108	0.05	0.181	0.187
1533	-4210.6	4343.60	30.5	2.39	0.65	85.54	0.116	0.06	0.161	0.168
1533	-4210.91	4343.91	35.1	2.32	0.67	85.33	0.169	0.09	0.203	0.213
1533	-4211.21	4344.21	34.71	2.33	0.62	83.29	0.164	0.08	0.197	0.206
1533	-4211.52	4344.52	26.13	2.32	0.65	84.03	0.066	0.03	0.209	0.213
1533	-4211.82	4344.82	27.41	2.29	0.68	83.84	0.080	0.04	0.228	0.232
1533	-4212.13	4345.13	30.99	2.3	0.63	83.44	0.121	0.06	0.219	0.226
1533	-4212.43	4345.43	34.39	2.33	0.53	87.13	0.160	0.08	0.197	0.206
1533	-4212.74	4345.74	33.3	2.3	0.44	90.64	0.148	0.08	0.218	0.226
1533	-4213.04	4346.04	27.29	2.24	0.36	92.75	0.079	0.04	0.260	0.265
1533	-4213.34	4346.34	29.52	2.21	0.36	93.6	0.105	0.05	0.278	0.284
1533	-4213.65	4346.65	33.2	2.22	0.42	89.55	0.147	0.07	0.269	0.277
1533	-4213.95	4346.95	41.88	2.28	0.54	85.81	0.246	0.13	0.224	0.239
1533	-4214.26	4347.26	47.94	2.3	0.85	87.88	0.316	0.18	0.206	0.226
1533	-4214.56	4347.56	47.25	2.32	1.46	83.65	0.308	0.18	0.194	0.213
1533	-4214.87	4347.87	46.46	2.37	2.43	76.56	0.299	0.17	0.162	0.181
1533	-4215.17	4348.17	59.62	2.45	4.41	78.19	0.450	0.29	0.098	0.129
1533	-4220.51	4353.51	44.8	2.61	7.89	63.51	0.280	0.16	0.009	0.026
1533	-4220.81	4353.81	25.35	2.6	9.85	57.01	0.057	0.03	0.029	0.032
1533	-4221.12	4354.12	25.62	2.6	11.43	57.98	0.060	0.03	0.029	0.032
1533	-4221.42	4354.42	34.66	2.56	8.22	63.97	0.164	0.08	0.049	0.058
1533	-4221.73	4354.73	48.8	2.43	5.63	76.17	0.326	0.19	0.121	0.142
1533	-4222.03	4355.03	52.68	2.41	4.03	81.24	0.370	0.22	0.131	0.155
1533	-4222.34	4355.34	48.47	2.42	2.74	80.89	0.322	0.19	0.128	0.148
1533	-4222.64	4355.64	51.31	2.38	2.09	80.95	0.355	0.21	0.151	0.174
1533	-4222.95	4355.95	44.82	2.42	1.95	79.6	0.280	0.16	0.131	0.148
1533	-4224.47	4357.47	54.36	2.33	1.28	86.13	0.390	0.24	0.181	0.206
1533	-4224.77	4357.77	28.55	2.41	1.24	83.32	0.093	0.05	0.150	0.155
1533	-4225.08	4358.08	23.19	2.54	1.46	72.08	0.032	0.01	0.069	0.071
1533	-4225.38	4358.38	22.11	2.61	1.86	59.82	0.020	0.01	0.025	0.026

Well	TVDRSF	MD	GR	RHO	RD	DT	I_{GR} (4-7)	V_{sh} (4-5/6)	Porosity (eq 5-1)	Porosity (eq 4-4)
1533	-4225.69	4358.69	24.99	2.48	2.18	64.95	0.053	0.02	0.107	0.110
1533	-4225.99	4358.99	29.34	2.37	1.97	76.78	0.102	0.05	0.175	0.181
1533	-4226.3	4359.30	29.36	2.35	1.66	79.13	0.103	0.05	0.188	0.194
1533	-4226.6	4359.60	28.22	2.36	1.73	77.77	0.090	0.04	0.182	0.187
1533	-4226.91	4359.91	35.14	2.36	2	78.99	0.169	0.09	0.178	0.187
1533	-4227.21	4360.21	47.43	2.43	2.35	79.63	0.310	0.18	0.123	0.142
1533	-4227.52	4360.52	49.43	2.42	2.59	77.62	0.333	0.19	0.127	0.148
1533	-4230.57	4363.57	57.02	2.59	7.86	63.72	0.420	0.26	0.010	0.039
1533	-4233.92	4366.92	58.62	2.47	9.45	73.45	0.438	0.28	0.086	0.116
1533	-4235.75	4368.75	36.67	2.63	4.72	60.09	0.187	0.10	0.002	0.013
1533	-4236.05	4369.05	51.59	2.61	5.4	67.35	0.358	0.21	0.003	0.026
1533	-4322.16	4455.16	57.1	2.52	3.58	76.04	0.421	0.26	0.055	0.084
1533	-4330.39	4463.39	49.91	2.62	1.19	76.02	0.338	0.20	-0.002	0.019
1534	-3568.17	3700.17	58.06	2.46	3	114.75	0.453	0.29	0.091	0.123
1534	-3568.63	3700.63	59.69	2.48	2.95	113.19	0.493	0.32	0.074	0.110
1534	-3570.3	3702.30	58.91	2.44	3.09	112.19	0.474	0.31	0.102	0.135
1534	-3570.61	3702.61	54.34	2.46	2.94	109	0.361	0.21	0.099	0.123
1534	-3570.91	3702.91	50.88	2.48	2.85	110.38	0.276	0.15	0.093	0.110
1534	-3571.22	3703.22	58.13	2.49	2.7	109.56	0.455	0.29	0.071	0.103
1534	-3571.52	3703.52	53.97	2.48	2.65	104	0.352	0.21	0.087	0.110
1534	-3573.66	3705.66	57.06	2.52	2.72	100.38	0.428	0.27	0.055	0.084
1534	-3573.96	3705.96	57.5	2.52	2.96	105.38	0.439	0.28	0.054	0.084
1534	-3576.4	3708.40	57.19	2.46	3.33	106.19	0.431	0.27	0.093	0.123
1534	-3610.08	3742.08	56	2.58	1.66	94	0.402	0.25	0.018	0.045
1534	-3610.38	3742.38	58.63	2.57	1.61	91.38	0.467	0.30	0.019	0.052
1534	-3610.69	3742.69	55.44	2.6	1.64	90	0.388	0.24	0.006	0.032
1534	-3610.99	3742.99	52.66	2.63	1.83	89.56	0.320	0.18	-0.007	0.013
1534	-3611.3	3743.30	56.81	2.61	2	89.19	0.422	0.26	-0.003	0.026
1534	-3612.52	3744.52	48.75	2.57	2.33	84	0.224	0.12	0.038	0.052
1534	-3612.82	3744.82	53.84	2.57	2.38	88.19	0.349	0.21	0.029	0.052
1534	-3613.58	3745.58	53.19	2.53	2.84	86.75	0.333	0.19	0.056	0.077
1534	-3613.89	3745.89	39.66	2.54	2.83	69.75	0.000	0.00	0.071	0.071
1534	-3614.19	3746.19	58.22	2.55	2.98	74.38	0.457	0.29	0.033	0.065
1534	-3615.11	3747.11	54.41	2.51	1.76	91	0.363	0.22	0.067	0.090
1534	-3615.41	3747.41	57.75	2.57	1.77	94.56	0.445	0.28	0.021	0.052
1534	-3615.72	3747.72	53.44	2.6	1.83	91.38	0.339	0.20	0.011	0.032
1534	-3616.02	3748.02	54.5	2.6	2.08	87.56	0.365	0.22	0.008	0.032
1534	-3616.33	3748.33	58.59	2.58	2.1	86.75	0.466	0.30	0.012	0.045
1534	-3616.78	3748.78	57.22	2.57	2.14	85	0.432	0.27	0.022	0.052
1534	-3617.09	3749.09	50.63	2.58	2.04	81.56	0.270	0.15	0.029	0.045
1534	-3617.7	3749.70	53.31	2.62	1.59	78.19	0.336	0.20	-0.002	0.019
1534	-3618	3750.00	59.09	2.64	1.63	84.38	0.478	0.31	-0.028	0.006
1534	-3618.31	3750.31	55.09	2.64	1.49	82.75	0.380	0.23	-0.019	0.006
1534	-3618.61	3750.61	56.88	2.53	1.49	86.19	0.424	0.26	0.048	0.077
1534	-3619.07	3751.07	59.69	2.54	1.6	89.19	0.493	0.32	0.035	0.071
1534	-3621.97	3753.97	54.69	2.52	1.64	88.75	0.370	0.22	0.060	0.084
1534	-3622.27	3754.27	56.88	2.52	1.75	88.56	0.424	0.26	0.055	0.084
1534	-3623.03	3755.03	58.97	2.58	2.09	88	0.475	0.31	0.011	0.045
1534	-3623.95	3755.95	58.13	2.62	2.51	88.19	0.455	0.29	-0.012	0.019
1534	-3624.86	3756.86	47.53	2.61	2.89	73.19	0.194	0.10	0.015	0.026
1534	-3626.08	3758.08	59.94	2.62	1.82	86.56	0.499	0.33	-0.017	0.019
1534	-3626.39	3758.39	57.16	2.62	2.09	86.75	0.431	0.27	-0.010	0.019
1534	-3628.21	3760.21	47.72	2.62	3.67	78.19	0.198	0.10	0.008	0.019
1534	-3630.2	3762.20	59.47	2.58	1.91	93.75	0.488	0.32	0.010	0.045
1534	-3630.5	3762.50	54.97	2.58	2.05	89.56	0.377	0.23	0.020	0.045
1534	-3630.81	3762.81	51.53	2.6	2.06	85	0.292	0.16	0.014	0.032
1534	-3631.11	3763.11	54.84	2.62	2.23	83.56	0.374	0.22	-0.005	0.019
1534	-3631.41	3763.41	48.75	2.62	2.32	84.75	0.224	0.12	0.006	0.019
1534	-3631.72	3763.72	50.72	2.63	2.31	82.75	0.272	0.15	-0.004	0.013
1534	-3632.02	3764.02	58.06	2.61	2.19	87	0.453	0.29	-0.006	0.026
1534	-3632.33	3764.33	52.25	2.57	2	85.56	0.310	0.18	0.032	0.052
1534	-3632.63	3764.63	52.94	2.56	2.02	89	0.327	0.19	0.037	0.058
1534	-3633.55	3765.55	57.34	2.61	1.91	90.19	0.435	0.27	-0.004	0.026

Well	TVDRSF	MD	GR	RHO	RD	DT	I_{GR} (4-7)	V_{sh} (4-5/6)	Porosity (eq 5-1)	Porosity (eq 4-4)
1534	-3634.31	3766.31	55.19	2.61	1.93	85.75	0.382	0.23	0.001	0.026
1534	-3634.62	3766.62	58.38	2.56	1.97	84.56	0.461	0.30	0.026	0.058
1534	-3635.38	3767.38	58.03	2.53	1.97	90.75	0.452	0.29	0.046	0.077
1534	-3635.68	3767.68	57.34	2.51	2.15	87.75	0.435	0.27	0.060	0.090
1534	-3635.99	3767.99	52.5	2.47	2.29	83.38	0.316	0.18	0.096	0.116
1534	-3636.29	3768.29	56.81	2.53	2.22	83.75	0.422	0.26	0.049	0.077
1534	-3636.6	3768.60	59.81	2.58	2.24	91	0.496	0.33	0.009	0.045
1534	-3637.66	3769.66	52.91	2.61	2.49	83.19	0.326	0.19	0.005	0.026
1534	-3639.19	3771.19	56.34	2.59	1.66	85	0.411	0.25	0.011	0.039
1534	-3640.56	3772.56	56.72	2.64	2.61	80.38	0.420	0.26	-0.022	0.006
1534	-3640.86	3772.86	54.47	2.57	2.59	80.56	0.365	0.22	0.028	0.052
1534	-3641.32	3773.32	59.19	2.55	2.32	87.56	0.481	0.31	0.030	0.065
1534	-3648.48	3780.48	58.91	2.61	2.37	79.75	0.474	0.31	-0.008	0.026
1534	-3648.94	3780.94	58.34	2.59	2.34	89.56	0.460	0.29	0.006	0.039
1534	-3654.12	3786.12	54.53	2.63	3.4	89.19	0.366	0.22	-0.011	0.013
1535	-3680.07	3808.07	58.09	2.35	1.67	85.19	0.387	0.23	0.168	0.194
1535	-3680.53	3808.53	59.03	2.36	1.39	91.19	0.410	0.25	0.159	0.187
1535	-3680.83	3808.83	58.41	2.38	1.29	94.19	0.395	0.24	0.148	0.174
1535	-3700.64	3828.64	53.09	2.24	2.64	99.63	0.269	0.15	0.248	0.265
1535	-3700.95	3828.95	47.69	2.29	2.77	101.38	0.140	0.07	0.224	0.232
1535	-3701.25	3829.25	54.5	2.31	2.41	101.88	0.302	0.17	0.201	0.219
1535	-3701.56	3829.56	51.06	2.33	2.54	100.5	0.220	0.12	0.194	0.206
1535	-3701.86	3829.86	52.31	2.25	3.07	100.63	0.250	0.14	0.243	0.258
1535	-3702.17	3830.17	49.41	2.21	3.68	105	0.181	0.09	0.274	0.284
1535	-3702.47	3830.47	54.63	2.2	2.95	105.88	0.305	0.17	0.271	0.290
1535	-3702.78	3830.78	50.5	2.19	2.43	110.25	0.207	0.11	0.285	0.297
1535	-3703.08	3831.08	42.34	2.21	3.34	108.63	0.013	0.01	0.283	0.284
1535	-3703.39	3831.39	45.5	2.22	3.52	105	0.088	0.04	0.273	0.277
1535	-3703.69	3831.69	52.47	2.18	3.03	106.75	0.254	0.14	0.288	0.303
1535	-3704.3	3832.30	58.38	2.25	3.75	110.13	0.394	0.24	0.232	0.258
1535	-3704.6	3832.60	56.41	2.2	3.72	106.5	0.347	0.20	0.268	0.290
1535	-3755.51	3883.51	50.53	2.56	2.57	64.63	0.208	0.11	0.046	0.058
1535	-3767.24	3895.24	59.94	2.61	1.94	69.63	0.431	0.27	-0.004	0.026
1535	-3767.55	3895.55	46.69	2.62	2.28	61.38	0.117	0.06	0.013	0.019
1535	-3767.85	3895.85	46.13	2.61	2.04	60.63	0.103	0.05	0.020	0.026
1535	-3770.59	3898.59	58.19	2.6	0.43	78.13	0.390	0.24	0.006	0.032
1535	-3785.22	3913.22	50.09	2.63	2.52	74	0.197	0.10	0.002	0.013
1535	-3785.53	3913.53	59.81	2.62	2.63	76.13	0.428	0.27	-0.010	0.019
1535	-3787.05	3915.05	52.75	2.6	2.95	72.63	0.260	0.14	0.017	0.032
1535	-3787.36	3915.36	53.44	2.59	2.93	76.38	0.277	0.15	0.022	0.039
1535	-3807.47	3935.47	52.53	1.94	2.92	113	0.255	0.14	0.443	0.458
1535	-3807.78	3935.78	53.31	1.9	2.86	116.88	0.274	0.15	0.467	0.484
1537	-3946.7	4073.70	54.04	2.43	30.22	72.78	0.294	0.17	0.124	0.142
1537	-3947.62	4074.62	59.9	2.53	72.04	66.34	0.351	0.21	0.055	0.077
1537	-3947.92	4074.92	36.14	2.51	42.91	70.66	0.119	0.06	0.084	0.090
1537	-3948.23	4075.23	45.71	2.49	28.45	72.69	0.212	0.11	0.091	0.103
1537	-3963.31	4090.31	59.65	2.59	16.59	88.02	0.348	0.20	0.016	0.039
1537	-3991.66	4118.66	41.06	2.59	37.04	68.72	0.167	0.09	0.029	0.039
1537	-3991.96	4118.96	33.4	2.63	40.24	69.47	0.093	0.05	0.008	0.013
1537	-3992.27	4119.27	47.09	2.61	19.89	79.71	0.226	0.12	0.012	0.026
1537	-3993.95	4120.95	49.25	2.59	34.24	72.27	0.247	0.13	0.024	0.039
1537	-3994.25	4121.25	59.77	2.54	23.6	82.13	0.350	0.21	0.048	0.071
1537	-4001.72	4128.72	58.84	2.56	25.67	73.7	0.340	0.20	0.036	0.058
1537	-4005.98	4132.98	58.46	2.58	19.98	76.46	0.337	0.20	0.024	0.045
1537	-4007.2	4134.20	35.16	2.58	30.15	70.01	0.110	0.05	0.039	0.045
1537	-4007.51	4134.51	53.82	2.57	21.89	75.68	0.292	0.16	0.034	0.052
1537	-4017.26	4144.26	33.63	2.62	32.42	64.66	0.095	0.05	0.014	0.019
1537	-4017.57	4144.57	47.25	2.59	26.01	67.66	0.228	0.12	0.025	0.039
1537	-4017.87	4144.87	53.18	2.62	39.61	62.79	0.285	0.16	0.002	0.019
1537	-4018.79	4145.79	49.7	2.59	12.65	71.53	0.251	0.14	0.024	0.039
1537	-4019.7	4146.70	26.66	2.52	50.18	81.45	0.027	0.01	0.083	0.084
1537	-4020.01	4147.01	34.58	2.37	13.61	84.64	0.104	0.05	0.175	0.181
1537	-4023.21	4150.21	58.86	2.59	27.71	67.3	0.341	0.20	0.017	0.039

Well	TVDRSF	MD	GR	RHO	RD	DT	I_{GR} (4-7)	V_{sh} (4-5/6)	Porosity (eq 5-1)	Porosity (eq 4-4)
1537	-4023.51	4150.51	48.97	2.63	19.63	73.09	0.244	0.13	-0.002	0.013
1537	-4025.19	4152.19	42.15	2.62	20.3	72.09	0.178	0.09	0.009	0.019
1537	-4025.49	4152.49	59.64	2.55	14.05	79.17	0.348	0.20	0.042	0.065
1537	-4026.56	4153.56	44.78	2.63	14.46	73.67	0.203	0.11	0.001	0.013
1537	-4029.15	4156.15	44.46	2.61	40.57	64.35	0.200	0.11	0.014	0.026
1537	-4029.45	4156.45	30.8	2.63	16.74	65.79	0.067	0.03	0.009	0.013
1537	-4030.06	4157.06	58.88	2.6	18.41	65.19	0.341	0.20	0.010	0.032
1537	-4030.37	4157.37	48.8	2.63	33.55	66.57	0.243	0.13	-0.002	0.013
1537	-4033.11	4160.11	49.19	2.62	27.19	66.14	0.246	0.13	0.005	0.019
1537	-4033.42	4160.42	56.5	2.61	10.61	77.88	0.318	0.18	0.006	0.026
1537	-4038.6	4165.60	37.76	2.61	111.47	67.96	0.135	0.07	0.018	0.026
1537	-4038.9	4165.90	47	2.6	47.29	77.14	0.225	0.12	0.019	0.032
1537	-4083.56	4210.56	59.82	2.53	7.2	72.65	0.350	0.21	0.055	0.077
1537	-4087.67	4214.67	44.89	2.29	18.99	77.76	0.205	0.11	0.220	0.232
1537	-4087.98	4214.98	50.12	2.3	8.04	79.82	0.255	0.14	0.210	0.226
1537	-4091.48	4218.48	40.83	2.42	21.51	80.37	0.165	0.08	0.139	0.148
1537	-4091.79	4218.79	42.08	2.5	17.25	77.51	0.177	0.09	0.087	0.097
1537	-4092.85	4219.85	56.92	2.27	23.63	62.08	0.322	0.19	0.225	0.245
1537	-4093.16	4220.16	42.59	2.49	42.05	59.56	0.182	0.09	0.093	0.103
1537	-4094.38	4221.38	31.74	2.61	56.69	56.63	0.076	0.04	0.022	0.026
1537	-4094.68	4221.68	34.97	2.6	41.09	56.35	0.108	0.05	0.026	0.032
1537	-4094.99	4221.99	35.82	2.58	24.48	62.08	0.116	0.06	0.039	0.045
1537	-4095.29	4222.29	39.57	2.53	16.53	83.82	0.153	0.08	0.069	0.077
1537	-4095.9	4222.90	53.86	2.21	15.02	93.73	0.292	0.16	0.266	0.284
1537	-4096.21	4223.21	45.52	2.22	12.09	97.74	0.211	0.11	0.265	0.277
1537	-4096.51	4223.51	54.17	2.18	8.26	102.94	0.295	0.17	0.285	0.303
1537	-4096.82	4223.82	52.24	2.12	9.82	106.21	0.276	0.15	0.325	0.342
1537	-4097.12	4224.12	42.97	2.11	11.51	105	0.186	0.10	0.338	0.348
1537	-4097.42	4224.42	43.99	2.16	13.92	97.33	0.196	0.10	0.305	0.316
1537	-4098.64	4225.64	51.83	2.18	13.48	100.27	0.272	0.15	0.287	0.303
1537	-4098.95	4225.95	43.24	2.12	20.72	101.14	0.188	0.10	0.331	0.342
1537	-4099.25	4226.25	42.45	2.14	25.81	100.99	0.181	0.09	0.319	0.329
1537	-4099.56	4226.56	43.74	2.16	20.79	99.76	0.193	0.10	0.305	0.316
1537	-4099.86	4226.86	42.79	2.15	17.6	99.94	0.184	0.10	0.312	0.323
1537	-4100.17	4227.17	41.73	2.17	14.72	98.67	0.174	0.09	0.300	0.310
1537	-4100.47	4227.47	39.83	2.2	14.31	94.48	0.155	0.08	0.282	0.290
1537	-4100.78	4227.78	52.4	2.25	11.1	90.68	0.278	0.15	0.241	0.258
1537	-4109.92	4236.92	46.58	2.61	31.53	65.43	0.221	0.12	0.013	0.026
1537	-4140.1	4267.10	53.82	2.6	6.33	69.77	0.292	0.16	0.014	0.032
1537	-4140.86	4267.86	41.94	2.49	6.5	66.41	0.176	0.09	0.093	0.103
1537	-4141.16	4268.16	47.04	2.53	8.82	63.29	0.225	0.12	0.064	0.077
1537	-4141.47	4268.47	45.69	2.59	8.56	64.29	0.212	0.11	0.026	0.039
1537	-4141.77	4268.77	55.96	2.57	6.13	71.86	0.312	0.18	0.032	0.052
1537	-4145.13	4272.13	40.06	2.54	9.09	80.48	0.157	0.08	0.062	0.071
1537	-4148.94	4275.94	44.12	2.48	4.66	73.48	0.197	0.10	0.098	0.110
1537	-4149.24	4276.24	40.41	2.49	4.62	73.1	0.161	0.08	0.094	0.103
1537	-4150.76	4277.76	51.97	2.58	9.97	66.05	0.274	0.15	0.028	0.045
1537	-4151.07	4278.07	56.61	2.53	5.93	75.27	0.319	0.18	0.057	0.077
1537	-4157.47	4284.47	50.49	2.32	1.35	89.71	0.259	0.14	0.197	0.213
1537	-4157.78	4284.78	43.26	2.28	1.09	90.35	0.189	0.10	0.228	0.239
1537	-4158.54	4285.54	46.95	2.36	5.99	61.37	0.225	0.12	0.174	0.187
1537	-4158.84	4285.84	32.5	2.58	13.42	60.27	0.084	0.04	0.041	0.045
1537	-4159.45	4286.45	29.52	2.62	27.58	57.83	0.055	0.03	0.017	0.019
1537	-4159.76	4286.76	41.23	2.6	15.93	64.45	0.169	0.09	0.023	0.032
1537	-4162.65	4289.65	50.43	2.29	1.5	84.71	0.259	0.14	0.217	0.232
1537	-4162.96	4289.96	45.14	2.3	1.54	80.32	0.207	0.11	0.214	0.226
1537	-4163.26	4290.26	39.83	2.37	1.66	81.67	0.155	0.08	0.172	0.181
1537	-4163.57	4290.57	46.27	2.32	1.8	85.51	0.218	0.12	0.200	0.213
1537	-4164.48	4291.48	45.1	2.53	6.69	61.46	0.207	0.11	0.065	0.077
1537	-4164.79	4291.79	27.62	2.61	9.3	58.79	0.036	0.02	0.024	0.026
1537	-4165.09	4292.09	27.11	2.62	8.92	62.44	0.031	0.01	0.018	0.019
1537	-4165.4	4292.40	42	2.5	4.3	70.99	0.176	0.09	0.087	0.097
1537	-4166.77	4293.77	56.74	2.38	2.39	79.45	0.320	0.18	0.154	0.174

Well	TVDRSF	MD	GR	RHO	RD	DT	I_{GR} (4-7)	V_{sh} (4-5/6)	Porosity (eq 5-1)	Porosity (eq 4-4)
1537	-4167.07	4294.07	31.04	2.45	2.94	66.57	0.069	0.03	0.125	0.129
1537	-4167.38	4294.38	25.11	2.55	3.57	65.01	0.012	0.01	0.064	0.065
1537	-4167.68	4294.68	25.91	2.5	2.84	69.95	0.019	0.01	0.096	0.097
1537	-4167.99	4294.99	33.78	2.42	1.66	77.71	0.096	0.05	0.143	0.148
1537	-4168.29	4295.29	38.3	2.33	1.75	84.11	0.140	0.07	0.199	0.206
1537	-4168.6	4295.60	46.73	2.32	2.41	82.7	0.222	0.12	0.200	0.213
1537	-4170.73	4297.73	50.95	2.37	4.58	75.78	0.264	0.15	0.165	0.181
1537	-4171.03	4298.03	36.64	2.46	7.55	64.71	0.124	0.06	0.116	0.123
1537	-4171.34	4298.34	27.01	2.6	10	56.96	0.030	0.01	0.031	0.032
1537	-4173.78	4300.78	28.4	2.55	12.03	64.44	0.044	0.02	0.062	0.065
1537	-4174.08	4301.08	34.32	2.55	10.74	70.5	0.101	0.05	0.059	0.065
1537	-4192.07	4319.07	42.99	2.64	21.71	62.69	0.186	0.10	-0.004	0.006
1537	-4193.89	4320.89	59.91	2.46	1.93	83.9	0.351	0.21	0.100	0.123
1537	-4194.81	4321.81	53.06	2.36	3.37	66.79	0.284	0.16	0.170	0.187
1537	-4195.11	4322.11	43.72	2.51	7.97	57.25	0.193	0.10	0.079	0.090
1537	-4195.72	4322.72	27.33	2.63	9.53	69.55	0.033	0.02	0.011	0.013
1537	-4196.03	4323.03	30.27	2.55	2.88	81.58	0.062	0.03	0.061	0.065
1537	-4196.33	4323.33	57.6	2.32	1.56	94.51	0.328	0.19	0.192	0.213
1537	-4198.01	4325.01	51.96	2.38	5.38	75.17	0.273	0.15	0.158	0.174
1537	-4198.31	4325.31	59.86	2.38	4.27	81.13	0.350	0.21	0.152	0.174
1537	-4202.12	4329.12	52.78	2.27	1.02	89.28	0.281	0.16	0.228	0.245
1537	-4202.43	4329.43	31.24	2.27	0.83	86.6	0.071	0.03	0.241	0.245
1537	-4202.73	4329.73	28.49	2.3	0.94	79.65	0.045	0.02	0.223	0.226
1537	-4203.04	4330.04	28.15	2.36	1.3	80.07	0.041	0.02	0.185	0.187
1537	-4203.34	4330.34	50.9	2.45	1.42	87.16	0.263	0.15	0.113	0.129
1537	-4204.56	4331.56	39.85	2.29	0.86	89.02	0.155	0.08	0.224	0.232
1537	-4204.87	4331.87	40.94	2.28	0.74	89.23	0.166	0.09	0.229	0.239
1537	-4205.17	4332.17	46.76	2.27	0.64	89.82	0.223	0.12	0.232	0.245
1537	-4205.48	4332.48	42.69	2.25	0.55	90.9	0.183	0.10	0.248	0.258
1537	-4205.78	4332.78	35.07	2.21	0.56	94.43	0.109	0.05	0.278	0.284
1537	-4206.09	4333.09	32.33	2.21	0.57	93.07	0.082	0.04	0.280	0.284
1537	-4206.39	4333.39	35.14	2.23	0.79	92.6	0.109	0.05	0.265	0.271
1537	-4206.7	4333.70	35.78	2.25	0.83	89.74	0.116	0.06	0.252	0.258
1537	-4207	4334.00	35.77	2.23	0.76	89.39	0.116	0.06	0.265	0.271
1537	-4207.31	4334.31	35.24	2.3	0.98	82.77	0.110	0.05	0.220	0.226
1537	-4207.61	4334.61	34.24	2.3	0.88	80.18	0.101	0.05	0.220	0.226
1537	-4207.91	4334.91	37.85	2.26	0.69	80.96	0.136	0.07	0.244	0.252
1537	-4208.22	4335.22	36.7	2.26	0.69	86.52	0.125	0.06	0.245	0.252
1537	-4208.52	4335.52	49.15	2.27	0.73	90.46	0.246	0.13	0.230	0.245
1537	-4209.13	4336.13	44.55	2.28	0.54	91.56	0.201	0.11	0.227	0.239
1537	-4209.44	4336.44	34.02	2.2	0.49	91.21	0.099	0.05	0.285	0.290
1537	-4209.74	4336.74	34.6	2.21	0.47	89.42	0.104	0.05	0.278	0.284
1537	-4210.05	4337.05	33	2.22	0.48	87.88	0.089	0.04	0.273	0.277
1537	-4210.35	4337.35	31.5	2.24	0.77	79.56	0.074	0.04	0.261	0.265
1537	-4210.66	4337.66	29.93	2.47	2.36	68.19	0.059	0.03	0.113	0.116
1537	-4210.96	4337.96	28.21	2.64	6.83	56.64	0.042	0.02	0.004	0.006
1537	-4212.18	4339.18	29.44	2.57	5.32	69.85	0.054	0.03	0.049	0.052
1537	-4212.49	4339.49	30.94	2.36	1.35	85.86	0.069	0.03	0.183	0.187
1537	-4212.79	4339.79	35.67	2.26	0.8	90.94	0.115	0.06	0.245	0.252
1537	-4213.1	4340.10	34.45	2.22	0.65	90.62	0.103	0.05	0.272	0.277
1537	-4213.4	4340.40	34.95	2.23	0.57	88.3	0.108	0.05	0.265	0.271
1537	-4213.71	4340.71	33.8	2.27	0.62	86.28	0.096	0.05	0.240	0.245
1537	-4214.01	4341.01	44.81	2.29	0.92	86.1	0.204	0.11	0.220	0.232
1537	-4215.99	4342.99	42.53	2.27	0.64	89.14	0.181	0.09	0.235	0.245
1537	-4216.3	4343.30	35.22	2.25	0.54	89.69	0.110	0.05	0.252	0.258
1537	-4216.6	4343.60	31.31	2.25	0.51	89.08	0.072	0.03	0.254	0.258
1537	-4216.91	4343.91	39.39	2.27	0.49	86.25	0.151	0.08	0.237	0.245
1537	-4217.21	4344.21	39.55	2.29	0.49	83.52	0.152	0.08	0.224	0.232
1537	-4217.52	4344.52	31.43	2.37	0.62	69.11	0.073	0.04	0.177	0.181
1537	-4217.82	4344.82	23.75	2.6	0.82	59.85	-0.002	0.00	0.032	0.032
1537	-4218.13	4345.13	25.21	2.64	0.89	56.2	0.013	0.01	0.006	0.006
1537	-4221.78	4348.78	26.1	2.62	2.15	61.61	0.021	0.01	0.018	0.019

Well	TVDRSF	MD	GR	RHO	RD	DT	I_{GR} (4-7)	V_{sh} (4-5/6)	Porosity (eq 5-1)	Porosity (eq 4-4)
1537	-4222.09	4349.09	27.6	2.48	1.72	66.46	0.036	0.02	0.108	0.110
1537	-4222.39	4349.39	27.95	2.41	2.02	68.15	0.039	0.02	0.153	0.155
1537	-4222.7	4349.70	25.87	2.54	1.91	70.13	0.019	0.01	0.070	0.071
1537	-4223	4350.00	28.11	2.48	1.16	75.15	0.041	0.02	0.108	0.110
1537	-4223.31	4350.31	30.64	2.36	0.85	82.94	0.066	0.03	0.184	0.187
1537	-4223.61	4350.61	35.88	2.3	0.69	85.38	0.117	0.06	0.219	0.226
1537	-4223.92	4350.92	43.5	2.32	0.61	84.82	0.191	0.10	0.202	0.213
1537	-4224.22	4351.22	34.02	2.29	0.63	79.19	0.099	0.05	0.227	0.232
1537	-4224.53	4351.53	32.32	2.36	0.85	77.62	0.082	0.04	0.183	0.187
1537	-4224.83	4351.83	41.99	2.39	0.86	80.43	0.176	0.09	0.158	0.168
1537	-4225.14	4352.14	41.46	2.32	0.85	77.77	0.171	0.09	0.203	0.213
1537	-4225.44	4352.44	45.76	2.33	0.85	81.27	0.213	0.11	0.194	0.206
1537	-4225.75	4352.75	56.48	2.35	0.85	82.82	0.317	0.18	0.174	0.194
1537	-4226.05	4353.05	41.36	2.29	0.85	82.32	0.170	0.09	0.223	0.232
1537	-4226.36	4353.36	35.76	2.27	0.93	85.47	0.116	0.06	0.239	0.245
1537	-4226.66	4353.66	37.01	2.27	1.04	87.15	0.128	0.06	0.238	0.245
1537	-4226.96	4353.96	34.25	2.23	1.15	79.74	0.101	0.05	0.266	0.271
1537	-4227.27	4354.27	28.34	2.32	1.74	75.98	0.043	0.02	0.211	0.213
1537	-4228.79	4355.79	33.57	2.53	2.28	69.11	0.094	0.05	0.072	0.077
1537	-4229.1	4356.10	48.5	2.41	1.8	74.78	0.240	0.13	0.141	0.155
1537	-4229.4	4356.40	44.02	2.4	1.37	76.3	0.196	0.10	0.150	0.161
1537	-4229.71	4356.71	33.52	2.36	0.97	79.26	0.094	0.05	0.182	0.187
1537	-4230.01	4357.01	34.5	2.33	0.86	79.64	0.103	0.05	0.201	0.206
1537	-4230.32	4357.32	33.7	2.36	0.79	80.86	0.095	0.05	0.182	0.187
1537	-4230.62	4357.62	30.06	2.31	0.71	83.48	0.060	0.03	0.216	0.219
1537	-4230.93	4357.93	38.02	2.3	0.65	83.82	0.138	0.07	0.218	0.226
1537	-4231.23	4358.23	29.81	2.3	0.69	83.43	0.058	0.03	0.223	0.226
1537	-4231.54	4358.54	28.59	2.28	0.68	84.07	0.046	0.02	0.236	0.239
1537	-4231.84	4358.84	26.46	2.29	0.62	84.62	0.025	0.01	0.231	0.232
1537	-4232.15	4359.15	24.64	2.3	0.59	80.67	0.007	0.00	0.225	0.226
1537	-4232.45	4359.45	25.79	2.32	0.63	73.81	0.018	0.01	0.212	0.213
1537	-4232.76	4359.76	25.33	2.38	0.84	64.02	0.014	0.01	0.173	0.174
1537	-4233.06	4360.06	25.19	2.55	1.6	58.05	0.012	0.01	0.064	0.065
1537	-4233.98	4360.98	25.33	2.63	2.78	59.2	0.014	0.01	0.012	0.013
1537	-4234.28	4361.28	28.54	2.53	1.54	63.94	0.045	0.02	0.075	0.077
1537	-4234.58	4361.58	40.39	2.39	1.07	73.74	0.161	0.08	0.159	0.168
1537	-4234.89	4361.89	34.97	2.38	1.02	78.02	0.108	0.05	0.168	0.174
1537	-4235.19	4362.19	40.23	2.37	0.86	80.34	0.159	0.08	0.172	0.181
1537	-4235.5	4362.50	45.01	2.33	0.67	85.28	0.206	0.11	0.195	0.206
1537	-4235.8	4362.80	42.52	2.3	0.55	84.69	0.181	0.09	0.215	0.226
1537	-4236.11	4363.11	36.2	2.29	0.55	78.45	0.120	0.06	0.226	0.232
1537	-4236.41	4363.41	28.33	2.35	0.6	74.71	0.043	0.02	0.191	0.194
1537	-4236.72	4363.72	27.44	2.4	0.64	70.23	0.034	0.02	0.160	0.161
1537	-4237.02	4364.02	28.2	2.45	0.75	64.14	0.042	0.02	0.127	0.129
1537	-4237.33	4364.33	27.29	2.58	0.9	58.18	0.033	0.02	0.043	0.045
1537	-4241.29	4368.29	26.86	2.61	1.43	60.85	0.029	0.01	0.024	0.026
1537	-4241.6	4368.60	29.81	2.53	0.94	72.2	0.058	0.03	0.074	0.077
1537	-4241.9	4368.90	32.59	2.34	0.72	78.71	0.085	0.04	0.195	0.200
1537	-4242.2	4369.20	32.09	2.31	0.66	81.78	0.080	0.04	0.215	0.219
1537	-4242.51	4369.51	32.45	2.33	0.59	83.62	0.083	0.04	0.202	0.206
1537	-4242.81	4369.81	32.5	2.31	0.53	85.4	0.084	0.04	0.215	0.219
1537	-4243.12	4370.12	31.7	2.27	0.49	85.7	0.076	0.04	0.241	0.245
1537	-4243.42	4370.42	30.17	2.25	0.47	84.85	0.061	0.03	0.255	0.258
1537	-4243.73	4370.73	28.41	2.25	0.51	76.68	0.044	0.02	0.256	0.258
1537	-4244.03	4371.03	29.97	2.27	0.74	75.73	0.059	0.03	0.242	0.245
1537	-4244.34	4371.34	29.69	2.31	0.71	78.98	0.056	0.03	0.216	0.219
1537	-4244.64	4371.64	27.08	2.25	0.52	82.85	0.031	0.01	0.256	0.258
1537	-4244.95	4371.95	27.88	2.26	0.57	85.29	0.039	0.02	0.250	0.252
1537	-4245.25	4372.25	37.52	2.27	0.78	87.08	0.133	0.07	0.238	0.245
1537	-4246.93	4373.93	36.02	2.37	1.82	76.05	0.118	0.06	0.174	0.181
1537	-4247.23	4374.23	45.12	2.38	1.44	81.94	0.207	0.11	0.162	0.174
1537	-4248	4375.00	41.22	2.24	0.59	88.82	0.169	0.09	0.255	0.265
1537	-4248.3	4375.30	36.82	2.25	0.53	88.2	0.126	0.06	0.251	0.258

Well	TVDRSF	MD	GR	RHO	RD	DT	I_{GR} (4-7)	V_{sh} (4-5/6)	Porosity (eq 5-1)	Porosity (eq 4-4)
1537	-4248.61	4375.61	39.25	2.27	0.54	88.72	0.150	0.08	0.237	0.245
1537	-4248.91	4375.91	32.14	2.23	0.53	88.77	0.080	0.04	0.267	0.271
1537	-4249.22	4376.22	31.98	2.25	0.54	87.4	0.079	0.04	0.254	0.258
1537	-4249.52	4376.52	32.22	2.27	0.56	85.55	0.081	0.04	0.241	0.245
1537	-4249.82	4376.82	38.23	2.32	0.68	83.38	0.140	0.07	0.205	0.213
1537	-4250.13	4377.13	49.15	2.36	0.86	83.31	0.246	0.13	0.172	0.187
1537	-4250.43	4377.43	46.46	2.33	0.88	80	0.220	0.12	0.194	0.206
1537	-4250.74	4377.74	37.32	2.34	1.22	68.94	0.131	0.07	0.193	0.200
1537	-4251.04	4378.04	27.49	2.49	2.28	59.59	0.035	0.02	0.101	0.103
1537	-4251.35	4378.35	28	2.61	4.05	57.5	0.040	0.02	0.024	0.026
1537	-4252.57	4379.57	28.86	2.64	9.24	60.35	0.048	0.02	0.004	0.006
1537	-4252.87	4379.87	30.69	2.6	3.08	67.77	0.066	0.03	0.029	0.032
1537	-4253.18	4380.18	31.61	2.4	1.19	79.54	0.075	0.04	0.157	0.161
1537	-4253.48	4380.48	40.93	2.31	0.84	85.6	0.166	0.09	0.210	0.219
1537	-4253.79	4380.79	52.14	2.33	0.76	86.33	0.275	0.15	0.190	0.206
1537	-4254.09	4381.09	42.93	2.28	0.64	88.23	0.185	0.10	0.228	0.239
1537	-4254.4	4381.40	38.17	2.25	0.61	88.92	0.139	0.07	0.250	0.258
1537	-4254.7	4381.70	42.39	2.25	0.6	89.26	0.180	0.09	0.248	0.258
1537	-4255.01	4382.01	46.67	2.3	0.58	90.51	0.222	0.12	0.213	0.226
1537	-4255.31	4382.31	37.96	2.23	0.51	91.23	0.137	0.07	0.263	0.271
1537	-4255.62	4382.62	37.96	2.2	0.46	91.16	0.137	0.07	0.283	0.290
1537	-4255.92	4382.92	40.96	2.26	0.46	88.31	0.166	0.09	0.242	0.252
1537	-4256.23	4383.23	38.23	2.26	0.51	87.35	0.140	0.07	0.244	0.252
1537	-4256.53	4383.53	38.44	2.24	0.53	88.45	0.142	0.07	0.257	0.265
1537	-4256.84	4383.84	39.9	2.25	0.57	89.09	0.156	0.08	0.249	0.258
1537	-4257.14	4384.14	38.42	2.27	0.56	89.49	0.141	0.07	0.237	0.245
1537	-4257.44	4384.44	42.06	2.28	0.58	88.34	0.177	0.09	0.229	0.239
1537	-4257.75	4384.75	39.69	2.26	0.58	88.97	0.154	0.08	0.243	0.252
1537	-4258.05	4385.05	35.33	2.27	0.64	88.29	0.111	0.06	0.239	0.245
1537	-4258.36	4385.36	33.51	2.29	0.66	87.17	0.094	0.05	0.227	0.232
1537	-4258.66	4385.66	48.47	2.32	0.6	88.84	0.239	0.13	0.199	0.213
1537	-4258.97	4385.97	40.45	2.26	0.54	88.1	0.161	0.08	0.243	0.252
1537	-4259.27	4386.27	32.32	2.23	0.58	85.01	0.082	0.04	0.267	0.271
1537	-4259.58	4386.58	35.85	2.34	1.08	73.23	0.116	0.06	0.194	0.200
1537	-4259.88	4386.88	35.99	2.53	2	66.22	0.118	0.06	0.071	0.077
1537	-4260.19	4387.19	35.3	2.5	2.42	67.41	0.111	0.05	0.091	0.097
1537	-4260.49	4387.49	32.37	2.36	2.2	72.64	0.082	0.04	0.183	0.187
1537	-4260.8	4387.80	33.65	2.34	2.19	74.8	0.095	0.05	0.195	0.200
1537	-4261.1	4388.10	36.7	2.42	2.94	67.3	0.125	0.06	0.142	0.148
1537	-4261.41	4388.41	30.64	2.63	6	59.05	0.066	0.03	0.009	0.013
1537	-4262.63	4389.63	42.85	2.63	5.11	66.07	0.185	0.10	0.002	0.013
1537	-4263.39	4390.39	59.78	2.34	1.32	84.3	0.350	0.21	0.177	0.200
1537	-4263.69	4390.69	54.29	2.35	1.19	81.34	0.296	0.17	0.175	0.194
1537	-4264	4391.00	43.2	2.33	1.33	81.23	0.188	0.10	0.196	0.206
1537	-4264.3	4391.30	36.37	2.31	1.36	80.66	0.121	0.06	0.213	0.219
1537	-4264.61	4391.61	48.23	2.34	1.63	81.5	0.237	0.13	0.186	0.200
1537	-4265.52	4392.52	53	2.47	5.24	70.75	0.284	0.16	0.099	0.116
1537	-4265.83	4392.83	42.51	2.45	5.97	68.26	0.181	0.09	0.119	0.129
1537	-4266.13	4393.13	43.41	2.53	7.38	65.34	0.190	0.10	0.067	0.077
1537	-4266.44	4393.44	38.13	2.6	4.79	68.52	0.139	0.07	0.025	0.032
1537	-4266.74	4393.74	36.55	2.45	2.21	72.79	0.123	0.06	0.122	0.129
1537	-4267.05	4394.05	28.29	2.32	1.52	82.03	0.043	0.02	0.211	0.213
1537	-4267.35	4394.35	27.14	2.26	1.1	79.32	0.031	0.01	0.250	0.252
1537	-4267.66	4394.66	26.13	2.31	1.12	76.39	0.022	0.01	0.218	0.219
1537	-4267.96	4394.96	23.91	2.52	1.21	75.24	0.000	0.00	0.084	0.084
1537	-4268.27	4395.27	27.92	2.57	0.9	75.22	0.039	0.02	0.050	0.052
1537	-4268.57	4395.57	31.3	2.39	0.78	69.32	0.072	0.03	0.164	0.168
1537	-4268.87	4395.87	29.13	2.26	1.02	65.19	0.051	0.02	0.249	0.252
1537	-4269.18	4396.18	25.11	2.36	1.48	71.94	0.012	0.01	0.187	0.187
1537	-4269.48	4396.48	25.06	2.46	1.26	77.44	0.011	0.01	0.122	0.123
1537	-4269.79	4396.79	43.15	2.29	0.95	85.19	0.188	0.10	0.222	0.232
1537	-4270.25	4397.25	53.13	2.3	1.06	86.15	0.285	0.16	0.208	0.226
1537	-4270.55	4397.55	39.64	2.26	1.22	86.46	0.153	0.08	0.243	0.252

Well	TVDRSF	MD	GR	RHO	RD	DT	I_{GR} (4-7)	V_{sh} (4-5/6)	Porosity (eq 5-1)	Porosity (eq 4-4)
1537	-4276.49	4403.49	32.02	2.41	2.35	77.59	0.079	0.04	0.151	0.155
1537	-4276.8	4403.80	26.11	2.34	2.02	79.42	0.021	0.01	0.199	0.200
1537	-4280.76	4407.76	53.44	2.4	8.37	70.59	0.288	0.16	0.144	0.161
1537	-4281.07	4408.07	32.38	2.39	7	73.8	0.083	0.04	0.163	0.168
1615	-1894.13	2024.13	56.49	2.32	0.74	90.79	0.251	0.08	0.205	0.213
1615	-1894.38	2024.38	55.89	2.25	0.67	91.7	0.229	0.07	0.251	0.258
1615	-1904	2034.00	59.44	2.26	0.61	86.16	0.361	0.13	0.238	0.252
1615	-1917.5	2047.50	58.14	2.22	0.37	100.64	0.313	0.10	0.266	0.277
1615	-1918	2048.00	58.59	2.24	0.36	101.19	0.329	0.11	0.252	0.265
1615	-1918.25	2048.25	53.6	2.19	0.35	101.24	0.145	0.04	0.293	0.297
1615	-1918.75	2048.75	59.5	2.16	0.34	101.39	0.363	0.13	0.302	0.316
1615	-1919	2049.00	56.78	2.21	0.34	101.29	0.262	0.08	0.275	0.284
1615	-1919.25	2049.25	53.25	2.21	0.34	101.22	0.132	0.03	0.280	0.284
1615	-1919.5	2049.50	52.54	2.2	0.34	101.25	0.105	0.03	0.287	0.290
1615	-1919.75	2049.75	52.54	2.2	0.33	101.36	0.105	0.03	0.287	0.290
1615	-1920	2050.00	54.5	2.21	0.33	101.4	0.178	0.05	0.279	0.284
1615	-1920.25	2050.25	59.83	2.21	0.33	101.42	0.375	0.13	0.269	0.284
1615	-1920.63	2050.63	59.47	2.19	0.33	101.45	0.362	0.13	0.283	0.297
1615	-1920.88	2050.88	57.24	2.2	0.33	101.48	0.279	0.09	0.281	0.290
1615	-1921.13	2051.13	56.03	2.2	0.33	101.56	0.234	0.07	0.283	0.290
1615	-1921.38	2051.38	52.24	2.19	0.33	101.63	0.094	0.02	0.294	0.297
1615	-1921.63	2051.63	53.16	2.19	0.33	101.67	0.128	0.03	0.293	0.297
1615	-1921.88	2051.88	55.28	2.18	0.32	101.67	0.207	0.06	0.297	0.303
1615	-1922.13	2052.13	56.46	2.18	0.32	101.67	0.250	0.07	0.295	0.303
1615	-1922.38	2052.38	57.04	2.17	0.32	101.66	0.272	0.08	0.301	0.310
1615	-1922.63	2052.63	57.51	2.21	0.32	101.6	0.289	0.09	0.274	0.284
1615	-1922.88	2052.88	57.97	2.2	0.32	101.59	0.306	0.10	0.279	0.290
1615	-1923.25	2053.25	59.16	2.19	0.33	101.57	0.350	0.12	0.284	0.297
1615	-1923.88	2053.88	58.5	2.19	0.33	101.45	0.326	0.11	0.285	0.297
1615	-1924.5	2054.50	58.15	2.18	0.34	101.44	0.313	0.10	0.292	0.303
1615	-1924.75	2054.75	54.83	2.19	0.34	101.52	0.190	0.05	0.291	0.297
1615	-1925	2055.00	55.74	2.17	0.34	101.54	0.224	0.06	0.303	0.310
1615	-1925.25	2055.25	58.06	2.19	0.34	101.44	0.310	0.10	0.286	0.297
1615	-1925.5	2055.50	56.52	2.2	0.35	100.55	0.253	0.08	0.282	0.290
1615	-1925.88	2055.88	58.2	2.22	0.35	99.17	0.315	0.10	0.266	0.277
1615	-1926.5	2056.50	59.23	2.2	0.36	99.64	0.353	0.12	0.277	0.290
1615	-1926.88	2056.88	58.94	2.19	0.36	101.13	0.342	0.12	0.284	0.297
1615	-1927.25	2057.25	54.52	2.19	0.37	100.92	0.179	0.05	0.291	0.297
1615	-1928	2058.00	58.92	2.16	0.38	101.04	0.341	0.12	0.303	0.316
1615	-1933.13	2063.13	59.04	2.21	0.33	103.5	0.346	0.12	0.271	0.284
1615	-1933.38	2063.38	53.19	2.14	0.33	104.65	0.129	0.03	0.325	0.329
1615	-1933.63	2063.63	56.11	2.17	0.33	106.73	0.237	0.07	0.302	0.310
1615	-1933.88	2063.88	54.34	2.16	0.33	107.67	0.172	0.05	0.311	0.316
1615	-1934.13	2064.13	55.06	2.18	0.33	108.14	0.199	0.06	0.297	0.303
1615	-1934.38	2064.38	54.16	2.18	0.35	106.68	0.165	0.04	0.298	0.303
1615	-1934.63	2064.63	57.48	2.31	0.37	102.39	0.288	0.09	0.209	0.219
1615	-1937	2067.00	59.45	2.21	0.45	107.37	0.361	0.13	0.270	0.284
1615	-1937.25	2067.25	51.44	2.19	0.4	107.71	0.065	0.01	0.295	0.297
1615	-1937.5	2067.50	50.84	2.22	0.37	108.07	0.043	0.01	0.276	0.277
1615	-1937.75	2067.75	58.48	2.15	0.35	108.37	0.325	0.11	0.311	0.323
1615	-1939.38	2069.38	56.85	2.17	0.29	100.06	0.265	0.08	0.301	0.310
1615	-1939.63	2069.63	53.89	2.19	0.29	102.62	0.155	0.04	0.292	0.297
1615	-1939.88	2069.88	53.48	2.18	0.29	105.83	0.140	0.04	0.299	0.303
1615	-1940.13	2070.13	54.78	2.19	0.29	106.35	0.188	0.05	0.285	0.297
1615	-1940.38	2070.38	56.31	2.2	0.29	106.18	0.245	0.07	0.274	0.290
1615	-1940.63	2070.63	56.05	2.2	0.29	105.93	0.235	0.07	0.275	0.290
1615	-1940.88	2070.88	54.25	2.23	0.3	105.83	0.169	0.04	0.261	0.271
1615	-1941.13	2071.13	54.76	2.23	0.31	105.52	0.188	0.05	0.259	0.271
1615	-1941.38	2071.38	57.42	2.24	0.32	102.98	0.286	0.09	0.244	0.265
1615	-1941.63	2071.63	56.98	2.24	0.34	98.14	0.270	0.08	0.246	0.265
1615	-1941.88	2071.88	59.5	2.24	0.36	91.35	0.363	0.13	0.236	0.265
1615	-1942.75	2072.75	57.34	2.52	0.49	74.24	0.283	0.09	0.064	0.084
1615	-1946	2076.00	52.93	2.18	0.42	95.3	0.120	0.03	0.296	0.303

Well	TVDRSF	MD	GR	RHO	RD	DT	I_{GR} (4-7)	V_{sh} (4-5/6)	Porosity (eq 5-1)	Porosity (eq 4-4)
1615	-1946.25	2076.25	58.19	2.18	0.39	103.88	0.314	0.10	0.280	0.303
1615	-1946.5	2076.50	55.68	2.19	0.36	105.86	0.222	0.06	0.282	0.297
1615	-1946.75	2076.75	58.65	2.19	0.34	106.17	0.331	0.11	0.272	0.297
1615	-1947	2077.00	56.32	2.18	0.33	104.64	0.245	0.07	0.287	0.303
1615	-1947.25	2077.25	57.96	2.2	0.32	103.78	0.306	0.10	0.268	0.290
1615	-1947.5	2077.50	55.89	2.23	0.32	102.22	0.229	0.07	0.256	0.271
1615	-1947.75	2077.75	57.86	2.28	0.32	101	0.302	0.10	0.217	0.239
1615	-1948	2078.00	57.86	2.36	0.33	100.4	0.302	0.10	0.165	0.187
1615	-1948.25	2078.25	58.13	2.31	0.34	99.36	0.312	0.10	0.196	0.219
1615	-1948.5	2078.50	57.06	2.31	0.35	98.48	0.273	0.08	0.200	0.219
1615	-1949.88	2079.88	59.7	2.56	0.48	64.76	0.370	0.13	0.028	0.058
1615	-1963.88	2093.88	51.22	2.24	0.36	100.78	0.057	0.01	0.262	0.265
1615	-1964.13	2094.13	53.82	2.24	0.35	101.21	0.153	0.04	0.256	0.265
1615	-1964.38	2094.38	51.31	2.22	0.34	101.83	0.060	0.01	0.274	0.277
1615	-1964.63	2094.63	51.54	2.22	0.33	102.17	0.068	0.02	0.274	0.277
1615	-1964.88	2094.88	53.08	2.23	0.32	102.72	0.125	0.03	0.264	0.271
1615	-1965.13	2095.13	53.41	2.22	0.31	102.79	0.138	0.04	0.269	0.277
1615	-1965.38	2095.38	52.76	2.23	0.31	102.74	0.114	0.03	0.265	0.271
1615	-1965.63	2095.63	51.69	2.24	0.31	102.79	0.074	0.02	0.261	0.265
1615	-1965.88	2095.88	54.33	2.24	0.31	102.81	0.172	0.05	0.254	0.265
1615	-1966.13	2096.13	53.68	2.27	0.31	102.75	0.148	0.04	0.237	0.245
1615	-1966.38	2096.38	52.76	2.24	0.31	102.75	0.114	0.03	0.258	0.265
1615	-1966.63	2096.63	55.16	2.24	0.31	102.79	0.202	0.06	0.252	0.265
1615	-1966.88	2096.88	54.38	2.23	0.32	102.86	0.173	0.05	0.260	0.271
1615	-1967.13	2097.13	55.45	2.23	0.32	103.52	0.213	0.06	0.257	0.271
1615	-1967.38	2097.38	55.29	2.24	0.33	103.97	0.207	0.06	0.251	0.265
1615	-1967.63	2097.63	58.2	2.25	0.34	102.61	0.315	0.10	0.235	0.258
1615	-1967.88	2097.88	55.41	2.26	0.35	96.45	0.212	0.06	0.238	0.252
1615	-1968.13	2098.13	58.8	2.26	0.36	92.89	0.337	0.11	0.226	0.252
1615	-1968.38	2098.38	59.91	2.32	0.37	87.91	0.378	0.14	0.182	0.213
1615	-1973.5	2103.50	58.95	2.17	0.48	98.41	0.342	0.12	0.283	0.310
1615	-1978.88	2108.88	59.56	2.16	0.38	102.41	0.365	0.13	0.287	0.316
1615	-1979.13	2109.13	56.93	2.21	0.37	102.42	0.268	0.08	0.265	0.284
1615	-1979.38	2109.38	49.79	2.16	0.35	102.83	0.004	0.00	0.316	0.316
1615	-1979.63	2109.63	50.48	2.18	0.35	103.59	0.029	0.01	0.302	0.303
1615	-1979.88	2109.88	55.69	2.19	0.34	103.85	0.222	0.06	0.282	0.297
1615	-1980.13	2110.13	58.99	2.16	0.34	103.79	0.344	0.12	0.290	0.316
1615	-1981.25	2111.25	55.59	2.19	0.32	102.7	0.218	0.06	0.283	0.297
1615	-1981.5	2111.50	58.26	2.19	0.32	103.28	0.317	0.10	0.273	0.297
1615	-1981.75	2111.75	54.53	2.19	0.31	103.65	0.179	0.05	0.286	0.297
1615	-1982	2112.00	53.29	2.19	0.31	103.57	0.133	0.03	0.289	0.297
1615	-1982.25	2112.25	53.28	2.2	0.31	102.99	0.133	0.03	0.283	0.290
1615	-1982.5	2112.50	57.14	2.21	0.31	102.34	0.276	0.09	0.265	0.284
1615	-1982.75	2112.75	54.76	2.21	0.31	102.12	0.188	0.05	0.272	0.284
1615	-1983	2113.00	58.29	2.22	0.32	101.99	0.318	0.10	0.254	0.277
1615	-1983.25	2113.25	58.38	2.22	0.33	102.2	0.321	0.11	0.253	0.277
1615	-1983.5	2113.50	58.99	2.23	0.34	102.46	0.344	0.12	0.244	0.271
1615	-1984.5	2114.50	55.55	2.29	0.41	90.65	0.217	0.06	0.218	0.232
1615	-1984.75	2114.75	54.68	2.25	0.43	89.6	0.185	0.05	0.247	0.258
1615	-1987	2117.00	54.53	2.17	0.36	101.31	0.179	0.05	0.299	0.310
1615	-1987.25	2117.25	55.79	2.18	0.34	104.45	0.226	0.07	0.289	0.303
1615	-1987.5	2117.50	56.02	2.19	0.32	105.17	0.234	0.07	0.281	0.297
1615	-1987.75	2117.75	54.8	2.19	0.31	106.09	0.189	0.05	0.285	0.297
1615	-1988	2118.00	57.36	2.18	0.29	106.28	0.284	0.09	0.283	0.303
1615	-1988.25	2118.25	56.48	2.18	0.29	106.06	0.251	0.08	0.286	0.303
1615	-1988.5	2118.50	55.09	2.18	0.28	105.21	0.200	0.06	0.291	0.303
1615	-1988.75	2118.75	59.23	2.22	0.28	103.83	0.353	0.12	0.250	0.277
1615	-1989.13	2119.13	57.75	2.2	0.29	102.54	0.298	0.10	0.269	0.290
1615	-1989.38	2119.38	58.28	2.21	0.3	102.2	0.318	0.10	0.260	0.284
1615	-1989.63	2119.63	59.41	2.21	0.31	102.41	0.359	0.13	0.255	0.284
1615	-1989.88	2119.88	54.47	2.21	0.32	103.13	0.177	0.05	0.273	0.284
1615	-1990.13	2120.13	56.67	2.23	0.34	103.66	0.258	0.08	0.253	0.271
1615	-1990.63	2120.63	59.25	2.21	0.39	100.81	0.354	0.12	0.256	0.284

Well	TVDRSF	MD	GR	RHO	RD	DT	I_{GR} (4-7)	V_{sh} (4-5/6)	Porosity (eq 5-1)	Porosity (eq 4-4)
1615	-1990.88	2120.88	59.9	2.23	0.42	96.96	0.378	0.14	0.240	0.271
1615	-1993.25	2123.25	58.98	2.16	0.35	101.72	0.344	0.12	0.290	0.316
1615	-1993.5	2123.50	57.89	2.19	0.33	103.1	0.303	0.10	0.275	0.297
1615	-1993.75	2123.75	55.92	2.16	0.31	104.13	0.230	0.07	0.301	0.316
1615	-1994	2124.00	54.55	2.2	0.31	105.13	0.180	0.05	0.279	0.290
1615	-1994.25	2124.25	49.69	2.19	0.3	105.96	0.000	0.00	0.297	0.297
1615	-1994.5	2124.50	55.57	2.19	0.29	106.15	0.217	0.06	0.283	0.297
1615	-1994.75	2124.75	54.83	2.18	0.29	106.5	0.190	0.05	0.291	0.303
1615	-1995	2125.00	53.31	2.18	0.28	106.74	0.134	0.03	0.296	0.303
1615	-1995.25	2125.25	56.37	2.2	0.29	106.78	0.247	0.07	0.274	0.290
1615	-1995.5	2125.50	52.25	2.21	0.29	106.4	0.095	0.02	0.279	0.284
1615	-1995.75	2125.75	58.68	2.19	0.29	105.73	0.332	0.11	0.272	0.297
1615	-1996	2126.00	57.04	2.18	0.3	105.1	0.272	0.08	0.284	0.303
1615	-1996.25	2126.25	57.59	2.23	0.3	104.64	0.292	0.09	0.250	0.271
1615	-1996.5	2126.50	57.14	2.18	0.31	104.62	0.276	0.09	0.284	0.303
1615	-1996.75	2126.75	53.77	2.21	0.32	104.72	0.151	0.04	0.275	0.284
1615	-1997	2127.00	57.22	2.2	0.34	103.56	0.278	0.09	0.271	0.290
1615	-1997.25	2127.25	59.42	2.21	0.36	101.65	0.360	0.13	0.255	0.284
1615	-1997.5	2127.50	57.74	2.22	0.38	95.11	0.298	0.10	0.256	0.277
1615	-1997.75	2127.75	57.35	2.31	0.41	87.7	0.283	0.09	0.199	0.219
1615	-1998	2128.00	52.03	2.39	0.45	84.89	0.087	0.02	0.163	0.168
1615	-2001.88	2131.88	57.95	2.18	0.38	103.49	0.305	0.10	0.281	0.303
1615	-2002.13	2132.13	55.96	2.17	0.37	104.75	0.232	0.07	0.294	0.310
1615	-2002.38	2132.38	57.85	2.18	0.36	105.58	0.302	0.10	0.281	0.303
1615	-2002.63	2132.63	59.05	2.18	0.36	104.57	0.346	0.12	0.276	0.303
1615	-2007	2137.00	59.89	2.17	0.33	99.07	0.377	0.14	0.279	0.310
1615	-2007.38	2137.38	57.28	2.16	0.33	95.23	0.281	0.09	0.296	0.316
1615	-2007.63	2137.63	56.84	2.17	0.33	93.74	0.264	0.08	0.291	0.310
1615	-2007.88	2137.88	55.45	2.19	0.34	92.78	0.213	0.06	0.283	0.297
1615	-2008.13	2138.13	56.01	2.23	0.34	92.75	0.234	0.07	0.256	0.271
1615	-2008.38	2138.38	54.88	2.25	0.35	93.27	0.192	0.05	0.246	0.258
1615	-2008.75	2138.75	59.93	2.29	0.37	95.45	0.379	0.14	0.201	0.232
1615	-2010.75	2140.75	57.59	2.17	0.4	102.77	0.292	0.09	0.289	0.310
1615	-2011	2141.00	55.11	2.2	0.39	104	0.200	0.06	0.278	0.290
1615	-2011.38	2141.38	57.68	2.21	0.38	103.94	0.295	0.09	0.263	0.284
1615	-2011.63	2141.63	57.8	2.2	0.37	103.47	0.300	0.10	0.269	0.290
1615	-2011.88	2141.88	58.5	2.18	0.37	102.48	0.326	0.11	0.279	0.303
2491	-4190.24	4333.24	58.55	2.47	6.76	99.99	0.340	0.20	0.085	0.116
2491	-4190.54	4333.54	59.57	2.46	6.35	98.98	0.351	0.21	0.091	0.123
2491	-4197.25	4340.25	56.56	2.39	7.11	102.43	0.320	0.18	0.139	0.168
2491	-4197.55	4340.55	54	2.39	8.23	101.8	0.293	0.17	0.142	0.168
2491	-4197.86	4340.86	58.62	2.38	9.7	102.3	0.341	0.20	0.143	0.174
2491	-4198.16	4341.16	59.03	2.36	10.62	99.36	0.345	0.20	0.156	0.187
2491	-4200.14	4343.14	59.79	2.4	7.07	103.78	0.353	0.21	0.129	0.161
2491	-4200.45	4343.45	59.57	2.39	7.14	103.65	0.351	0.21	0.136	0.168
2491	-4202.13	4345.13	57.43	2.39	7.08	102.55	0.329	0.19	0.138	0.168
2491	-4202.43	4345.43	53.91	2.41	6.74	100.39	0.292	0.16	0.129	0.155
2491	-4202.74	4345.74	52.79	2.47	5.91	97	0.281	0.16	0.092	0.116
2491	-4203.04	4346.04	56.43	2.54	5.96	96.83	0.318	0.18	0.043	0.071
2491	-4203.34	4346.34	55.48	2.57	6.05	94.68	0.308	0.18	0.024	0.052
2491	-4203.65	4346.65	58.68	2.56	6.34	92.07	0.342	0.20	0.027	0.058
2491	-4205.17	4348.17	59.94	2.36	7.86	103.54	0.355	0.21	0.155	0.187
2491	-4209.44	4352.44	59.22	2.37	10.8	104.68	0.347	0.20	0.149	0.181
2491	-4261.71	4404.71	49.37	2.38	8.85	99.9	0.245	0.13	0.154	0.174
2491	-4262.02	4405.02	39.72	2.38	12.66	87.5	0.145	0.07	0.163	0.174
2491	-4262.32	4405.32	38.51	2.44	17.25	70.23	0.133	0.07	0.125	0.135
2491	-4262.63	4405.63	51.7	2.44	14.76	69.29	0.269	0.15	0.112	0.135
2491	-4271.01	4414.01	44.92	2.4	10.27	95.92	0.199	0.10	0.145	0.161
2491	-4271.32	4414.32	30.58	2.48	13.56	77.5	0.051	0.02	0.106	0.110
2491	-4271.62	4414.62	32.87	2.54	15.84	68.21	0.074	0.04	0.065	0.071
2491	-4271.92	4414.92	43.45	2.56	14.59	68.98	0.184	0.10	0.043	0.058
2491	-4272.23	4415.23	59.41	2.51	11.62	87.42	0.349	0.21	0.059	0.090
2491	-4293.87	4436.87	58.07	2.38	13.8	97.81	0.335	0.20	0.144	0.174

Well	TVDRSF	MD	GR	RHO	RD	DT	I_{GR} (4-7)	V_{sh} (4-5/6)	Porosity (eq 5-1)	Porosity (eq 4-4)
2491	-4341.27	4484.27	56.67	2.57	11.25	74.57	0.321	0.18	0.023	0.052
2491	-4348.28	4491.28	52.79	2.46	15.74	82.55	0.281	0.16	0.098	0.123
2491	-4348.58	4491.58	36.84	2.5	19.45	71.37	0.115	0.06	0.088	0.097
2491	-4348.89	4491.89	35.68	2.49	17.83	75.1	0.103	0.05	0.095	0.103
2491	-4349.19	4492.19	56.22	2.41	15.81	90.36	0.316	0.18	0.127	0.155
2491	-4374.19	4517.19	47.24	2.6	12.26	66.24	0.223	0.12	0.014	0.032
2491	-4386.53	4529.53	53.53	2.41	11.07	84.28	0.288	0.16	0.130	0.155
2491	-4386.83	4529.83	34.68	2.52	15.94	69.11	0.093	0.05	0.077	0.084
2491	-4387.14	4530.14	26.13	2.58	26.16	60.62	0.004	0.00	0.045	0.045
2491	-4387.44	4530.44	28.88	2.49	29.75	56.87	0.033	0.02	0.101	0.103
2491	-4387.75	4530.75	41.84	2.4	18.83	59.62	0.167	0.09	0.148	0.161
2491	-4404.21	4547.21	53.56	2.35	11.94	93.8	0.289	0.16	0.168	0.194
2491	-4404.51	4547.51	40.88	2.37	16.03	84.02	0.157	0.08	0.168	0.181
2491	-4404.82	4547.82	31.61	2.44	17.93	71.15	0.061	0.03	0.131	0.135
2491	-4405.12	4548.12	37.28	2.5	16.57	67.2	0.120	0.06	0.088	0.097
2491	-4405.43	4548.43	54.69	2.48	13.31	74.81	0.300	0.17	0.083	0.110
2491	-4406.49	4549.49	48.42	2.43	10.89	80.14	0.235	0.13	0.122	0.142
2491	-4406.8	4549.80	30.75	2.49	14.6	63.55	0.052	0.02	0.099	0.103
2491	-4407.1	4550.10	32.88	2.57	15.56	60.96	0.074	0.04	0.046	0.052
2491	-4407.41	4550.41	49.61	2.58	11.88	75.06	0.248	0.14	0.024	0.045
2491	-4417.16	4560.16	53.81	2.45	8.74	67.6	0.291	0.16	0.104	0.129
2491	-4447.95	4590.95	50.18	2.49	14.21	74.06	0.254	0.14	0.082	0.103
2491	-4448.25	4591.25	35.99	2.48	15.08	74.47	0.107	0.05	0.102	0.110
2491	-4448.56	4591.56	35.21	2.47	14.25	75.92	0.098	0.05	0.109	0.116
2491	-4448.86	4591.86	47.38	2.47	11.59	77.24	0.225	0.12	0.097	0.116
2491	-4477.82	4620.82	53.47	2.4	20.41	75.73	0.288	0.16	0.136	0.161
2491	-4478.12	4621.12	43.78	2.44	19.53	75.26	0.187	0.10	0.120	0.135
2491	-4478.43	4621.43	48.29	2.45	16.81	74.96	0.234	0.13	0.109	0.129
2491	-4624.58	4767.58	57.14	2.59	20.76	62.83	0.326	0.19	0.010	0.039
2491	-4656.73	4799.73	55.56	2.51	21.88	70.31	0.309	0.18	0.063	0.090
2491	-4657.04	4800.04	50.94	2.5	21.49	69.86	0.261	0.14	0.074	0.097
2491	-4657.34	4800.34	50.49	2.5	20.83	69.78	0.257	0.14	0.075	0.097
2491	-4657.65	4800.65	48.43	2.49	21.55	69.6	0.235	0.13	0.084	0.103
2491	-4657.95	4800.95	46.07	2.49	21.96	69.52	0.211	0.11	0.086	0.103
2491	-4658.26	4801.26	52.3	2.48	19.1	69.31	0.276	0.15	0.086	0.110
2491	-4670.15	4813.15	57.44	2.46	8.91	80.06	0.329	0.19	0.093	0.123
2491	-4670.45	4813.45	48.89	2.41	8.83	78.92	0.240	0.13	0.135	0.155
2491	-4670.76	4813.76	40.29	2.41	8.81	78.64	0.151	0.08	0.143	0.155
2491	-4671.06	4814.06	34.64	2.38	8.73	78.74	0.093	0.05	0.167	0.174
2491	-4671.37	4814.37	33.38	2.34	8.2	76.75	0.080	0.04	0.194	0.200
2491	-4671.67	4814.67	32.85	2.37	6.97	75.08	0.074	0.04	0.175	0.181
2491	-4671.97	4814.97	32.66	2.44	6.29	75.52	0.072	0.03	0.130	0.135
2491	-4672.28	4815.28	31.83	2.42	6.23	76.36	0.063	0.03	0.144	0.148
2491	-4672.58	4815.58	32.54	2.41	6.61	76.42	0.071	0.03	0.150	0.155
2491	-4672.89	4815.89	34.72	2.41	7.19	76.17	0.093	0.05	0.148	0.155
2491	-4673.19	4816.19	36.71	2.4	7.77	76.23	0.114	0.06	0.153	0.161
2491	-4673.5	4816.50	40.51	2.41	7.73	77.44	0.153	0.08	0.143	0.155
2491	-4673.8	4816.80	55.55	2.43	6.44	76.48	0.309	0.18	0.115	0.142
2491	-4676.7	4819.70	45.11	2.46	7.81	72.79	0.201	0.11	0.106	0.123
2491	-4677	4820.00	33.37	2.43	7.78	70.71	0.079	0.04	0.136	0.142
2491	-4677.31	4820.31	28.08	2.44	8.75	64.89	0.025	0.01	0.134	0.135
2491	-4677.61	4820.61	27.58	2.45	10.25	61.01	0.019	0.01	0.128	0.129
2491	-4677.92	4820.92	30.25	2.49	10.83	64.42	0.047	0.02	0.100	0.103
2491	-4678.22	4821.22	38.03	2.53	9.93	70.6	0.128	0.06	0.068	0.077
2491	-4678.53	4821.53	45.31	2.5	8.38	72.81	0.203	0.11	0.080	0.097
2491	-4678.83	4821.83	51.78	2.46	8.14	74.77	0.270	0.15	0.099	0.123
2491	-4680.51	4823.51	55.58	2.47	7.57	74.57	0.309	0.18	0.089	0.116
2491	-4682.8	4825.80	55.16	2.5	6.64	77.36	0.305	0.17	0.070	0.097
2491	-4683.1	4826.10	47.14	2.45	6.32	76.17	0.222	0.12	0.111	0.129
2491	-4683.4	4826.40	57.18	2.43	6.56	77.42	0.326	0.19	0.113	0.142
2491	-4684.62	4827.62	46.28	2.47	9.24	75.27	0.213	0.11	0.099	0.116
2491	-4684.93	4827.93	34.93	2.47	9.81	72.34	0.096	0.05	0.109	0.116
2491	-4685.23	4828.23	27.79	2.49	9.91	66.15	0.022	0.01	0.102	0.103

Well	TVDRSF	MD	GR	RHO	RD	DT	I_{GR} (4-7)	V_{sh} (4-5/6)	Porosity (eq 5-1)	Porosity (eq 4-4)
2491	-4685.54	4828.54	27.65	2.54	9.74	64.73	0.020	0.01	0.070	0.071
2491	-4685.84	4828.84	33.71	2.53	8.96	72.13	0.083	0.04	0.071	0.077
2491	-4686.15	4829.15	43.8	2.47	8.45	76.06	0.187	0.10	0.101	0.116
2491	-4690.42	4833.42	58.49	2.45	7.13	77.04	0.340	0.20	0.098	0.129
2491	-4690.72	4833.72	51.44	2.47	7.03	75.73	0.267	0.15	0.093	0.116
2491	-4691.02	4834.02	45.72	2.49	7.38	71.56	0.207	0.11	0.086	0.103
2491	-4691.33	4834.33	50.27	2.52	8.17	69.12	0.254	0.14	0.062	0.084
2491	-4693.77	4836.77	47	2.46	6.13	77.83	0.221	0.12	0.104	0.123
2491	-4694.07	4837.07	51.71	2.43	6.1	78.47	0.269	0.15	0.119	0.142
2491	-4696.97	4839.97	37.93	2.52	18.52	62.21	0.127	0.06	0.074	0.084
2491	-4697.27	4840.27	26.45	2.45	28.82	58.41	0.008	0.00	0.128	0.129
2491	-4697.58	4840.58	26.29	2.44	40.6	57.32	0.006	0.00	0.135	0.135
2491	-4697.88	4840.88	29.96	2.45	30.09	58.14	0.044	0.02	0.126	0.129
2491	-4698.19	4841.19	36.79	2.44	19.84	63.25	0.115	0.06	0.127	0.135
2491	-4698.49	4841.49	49.14	2.45	14.57	69.74	0.243	0.13	0.109	0.129
2491	-4723.03	4866.03	44.1	2.49	15.18	68.64	0.191	0.10	0.088	0.103
2491	-4723.33	4866.33	48.48	2.48	17.72	70.19	0.236	0.13	0.090	0.110
2491	-4742.99	4885.99	54.92	2.44	11.06	75.87	0.303	0.17	0.109	0.135
24121	-4022.42	4160.42	55.45	2.55	5.59	75.39	0.459	0.29	0.032	0.065
24121	-4022.72	4160.72	52.1	2.6	6.09	78.76	0.425	0.26	0.003	0.032
24121	-4024.86	4162.86	54.3	2.61	14.55	74.75	0.447	0.28	-0.005	0.026
24121	-4025.16	4163.16	41.58	2.59	15.91	68.41	0.318	0.18	0.019	0.039
24121	-4025.46	4163.46	27.23	2.57	19.08	63.8	0.173	0.09	0.042	0.052
24121	-4025.77	4163.77	24.39	2.55	21.85	66.04	0.144	0.07	0.056	0.065
24121	-4026.07	4164.07	23.36	2.56	21.88	67.29	0.134	0.07	0.051	0.058
24121	-4026.38	4164.38	26.68	2.54	19.44	69.31	0.168	0.09	0.062	0.071
24121	-4026.68	4164.68	30.02	2.54	16.98	72.01	0.201	0.11	0.059	0.071
24121	-4026.99	4164.99	31.15	2.53	15.68	72.56	0.213	0.11	0.065	0.077
24121	-4027.29	4165.29	34.86	2.53	15.24	71.98	0.250	0.14	0.062	0.077
24121	-4027.6	4165.60	37.84	2.54	16.18	71.82	0.281	0.16	0.054	0.071
24121	-4027.9	4165.90	39.84	2.55	18.26	69.41	0.301	0.17	0.046	0.065
24121	-4028.21	4166.21	34.63	2.55	18.88	67.2	0.248	0.14	0.050	0.065
24121	-4028.51	4166.51	36.09	2.54	18.64	68.26	0.263	0.15	0.055	0.071
24121	-4028.82	4166.82	39.92	2.51	16.89	71.11	0.302	0.17	0.072	0.090
24121	-4029.12	4167.12	43.42	2.51	15.05	72.58	0.337	0.20	0.069	0.090
24121	-4029.43	4167.43	50.42	2.52	14.75	73.15	0.408	0.25	0.056	0.084
24121	-4029.73	4167.73	51.62	2.51	15.25	72.49	0.420	0.26	0.062	0.090
24121	-4030.04	4168.04	34.48	2.5	15.96	72.39	0.247	0.13	0.082	0.097
24121	-4030.34	4168.34	28.3	2.5	16.46	72.36	0.184	0.10	0.086	0.097
24121	-4030.65	4168.65	28.42	2.5	15.6	72.34	0.185	0.10	0.086	0.097
24121	-4030.95	4168.95	27.5	2.5	16.1	72.44	0.176	0.09	0.087	0.097
24121	-4031.26	4169.26	26.13	2.53	18.21	73.5	0.162	0.08	0.068	0.077
24121	-4031.56	4169.56	20.51	2.57	21.51	73.03	0.105	0.05	0.046	0.052
24121	-4031.87	4169.87	16.16	2.58	29.02	68.81	0.061	0.03	0.042	0.045
24121	-4032.17	4170.17	15.01	2.56	37.68	64.53	0.049	0.02	0.055	0.058
24121	-4032.48	4170.48	15.6	2.55	42.43	64.59	0.055	0.03	0.062	0.065
24121	-4032.78	4170.78	16.11	2.56	38.85	64.62	0.061	0.03	0.055	0.058
24121	-4033.08	4171.08	12.86	2.55	35.1	64.64	0.028	0.01	0.063	0.065
24121	-4033.39	4171.39	12.73	2.55	29.53	64.67	0.026	0.01	0.063	0.065
24121	-4033.69	4171.69	11.76	2.55	27.29	64.69	0.017	0.01	0.064	0.065
24121	-4034	4172.00	13.05	2.55	27.63	64.72	0.030	0.01	0.063	0.065
24121	-4034.3	4172.30	16.49	2.52	25.87	65.04	0.064	0.03	0.080	0.084
24121	-4034.61	4172.61	18.87	2.51	25.03	66.55	0.089	0.04	0.086	0.090
24121	-4034.91	4172.91	22.17	2.51	24.75	68.05	0.122	0.06	0.084	0.090
24121	-4035.22	4173.22	26.38	2.51	22.36	69.98	0.165	0.08	0.081	0.090
24121	-4035.52	4173.52	28.97	2.52	21.01	69.34	0.191	0.10	0.073	0.084
24121	-4035.83	4173.83	29.67	2.54	20.31	69.68	0.198	0.10	0.060	0.071
24121	-4036.13	4174.13	27.27	2.56	20.21	69.26	0.174	0.09	0.048	0.058
24121	-4036.44	4174.44	24.3	2.56	21.67	68.98	0.144	0.07	0.050	0.058
24121	-4036.74	4174.74	16.75	2.54	23.26	65.99	0.067	0.03	0.067	0.071
24121	-4037.05	4175.05	14.54	2.54	27.48	64.63	0.045	0.02	0.069	0.071
24121	-4037.35	4175.35	16.04	2.54	30.09	65.22	0.060	0.03	0.068	0.071
24121	-4037.66	4175.66	17.48	2.55	32.1	66.88	0.074	0.04	0.061	0.065

Well	TVDRSF	MD	GR	RHO	RD	DT	I_{GR} (4-7)	V_{sh} (4-5/6)	Porosity (eq 5-1)	Porosity (eq 4-4)
24121	-4037.96	4175.96	18.11	2.56	34.02	68	0.081	0.04	0.054	0.058
24121	-4038.27	4176.27	18.43	2.55	35.36	69.22	0.084	0.04	0.060	0.065
24121	-4038.57	4176.57	16.97	2.55	36.04	66.72	0.069	0.03	0.061	0.065
24121	-4038.88	4176.88	17.31	2.55	35.82	65.32	0.073	0.04	0.061	0.065
24121	-4039.18	4177.18	16.82	2.55	33.45	66.57	0.068	0.03	0.061	0.065
24121	-4039.49	4177.49	17.44	2.55	29.2	67.27	0.074	0.04	0.061	0.065
24121	-4039.79	4177.79	17.99	2.54	21.35	66.22	0.080	0.04	0.067	0.071
24121	-4040.1	4178.10	21.69	2.53	15.43	68.53	0.117	0.06	0.071	0.077
24121	-4040.4	4178.40	19.34	2.52	11.63	66.25	0.093	0.05	0.079	0.084
24121	-4040.7	4178.70	13.09	2.52	8.75	62.43	0.030	0.01	0.082	0.084
24121	-4041.01	4179.01	13.77	2.52	5.96	62.41	0.037	0.02	0.082	0.084
24121	-4041.31	4179.31	16.01	2.53	4.89	62.7	0.060	0.03	0.074	0.077
24121	-4041.62	4179.62	15.78	2.54	5.31	62.16	0.057	0.03	0.068	0.071
24121	-4041.92	4179.92	16.13	2.56	6.73	61.94	0.061	0.03	0.055	0.058
24121	-4042.23	4180.23	18.64	2.55	9.75	63.04	0.086	0.04	0.060	0.065
24121	-4042.53	4180.53	22.06	2.56	15.15	64.58	0.121	0.06	0.051	0.058
24121	-4042.84	4180.84	26.36	2.55	19.45	67.14	0.164	0.08	0.055	0.065
24121	-4043.14	4181.14	24.35	2.54	18.56	67.7	0.144	0.07	0.063	0.071
24121	-4043.45	4181.45	19.49	2.54	16.76	63.95	0.095	0.05	0.066	0.071
24121	-4043.75	4181.75	17.23	2.53	16.15	62.1	0.072	0.03	0.074	0.077
24121	-4044.06	4182.06	16.05	2.54	16.03	62.75	0.060	0.03	0.068	0.071
24121	-4044.36	4182.36	15.29	2.55	16.66	62.01	0.052	0.02	0.062	0.065
24121	-4044.67	4182.67	16.76	2.57	18.82	61.49	0.067	0.03	0.048	0.052
24121	-4044.97	4182.97	19.06	2.58	22.51	61.06	0.090	0.04	0.040	0.045
24121	-4045.28	4183.28	18.16	2.58	25.79	60.85	0.081	0.04	0.041	0.045
24121	-4045.58	4183.58	18.14	2.58	28.97	61.29	0.081	0.04	0.041	0.045
24121	-4045.89	4183.89	20.25	2.58	33.64	62.09	0.103	0.05	0.040	0.045
24121	-4046.19	4184.19	19.96	2.57	37.76	62.44	0.100	0.05	0.046	0.052
24121	-4046.5	4184.50	22.15	2.58	44.4	64.37	0.122	0.06	0.039	0.045
24121	-4046.8	4184.80	22.87	2.58	49.35	65.47	0.129	0.06	0.038	0.045
24121	-4047.11	4185.11	26.72	2.59	51.51	65.4	0.168	0.09	0.029	0.039
24121	-4047.41	4185.41	29.56	2.58	53.54	65.61	0.197	0.10	0.034	0.045
24121	-4047.72	4185.72	31.68	2.59	52	65.78	0.218	0.12	0.026	0.039
24121	-4048.02	4186.02	33.13	2.57	51.86	65.59	0.233	0.13	0.038	0.052
24121	-4048.32	4186.32	30.56	2.56	53.17	65.89	0.207	0.11	0.046	0.058
24121	-4048.63	4186.63	29.41	2.55	55.49	67.09	0.195	0.10	0.053	0.065
24121	-4048.93	4186.93	30.87	2.56	57.87	67.41	0.210	0.11	0.046	0.058
24121	-4049.24	4187.24	33.78	2.57	60.8	68.32	0.239	0.13	0.037	0.052
24121	-4049.54	4187.54	33.71	2.56	58.66	68.2	0.239	0.13	0.044	0.058
24121	-4049.85	4187.85	34.83	2.55	52.58	67.97	0.250	0.14	0.050	0.065
24121	-4050.15	4188.15	38	2.55	46.27	68.05	0.282	0.16	0.047	0.065
24121	-4050.46	4188.46	40.25	2.55	40.48	68.02	0.305	0.17	0.045	0.065
24121	-4050.76	4188.76	39.53	2.55	37.94	68.99	0.298	0.17	0.046	0.065
24121	-4051.07	4189.07	39.09	2.55	36.12	70.52	0.293	0.17	0.046	0.065
24121	-4051.37	4189.37	40.16	2.55	35.22	68.72	0.304	0.17	0.046	0.065
24121	-4051.68	4189.68	41.68	2.56	35.6	68	0.319	0.18	0.038	0.058
24121	-4051.98	4189.98	40.88	2.56	35.44	67.67	0.311	0.18	0.039	0.058
24121	-4052.29	4190.29	38.37	2.56	35.86	67.61	0.286	0.16	0.040	0.058
24121	-4052.59	4190.59	36.81	2.56	34.6	66.72	0.270	0.15	0.042	0.058
24121	-4052.9	4190.90	35.52	2.55	37.29	67.54	0.257	0.14	0.049	0.065
24121	-4053.2	4191.20	34.52	2.55	41.35	66.68	0.247	0.13	0.050	0.065
24121	-4053.51	4191.51	26.73	2.57	46.29	66.23	0.168	0.09	0.042	0.052
24121	-4053.81	4191.81	23.57	2.57	59.69	66.61	0.136	0.07	0.044	0.052
24121	-4054.12	4192.12	21.41	2.59	69.25	66.03	0.114	0.06	0.032	0.039
24121	-4054.42	4192.42	23.19	2.57	72.94	65.56	0.132	0.07	0.044	0.052
24121	-4054.73	4192.73	23.24	2.57	70.91	65.63	0.133	0.07	0.044	0.052
24121	-4055.03	4193.03	23.19	2.57	68.94	64.6	0.132	0.07	0.044	0.052
24121	-4055.34	4193.34	23.39	2.55	73.8	63.42	0.134	0.07	0.057	0.065
24121	-4055.64	4193.64	23.84	2.56	64.73	63.94	0.139	0.07	0.050	0.058
24121	-4055.94	4193.94	26.05	2.56	58.54	65.02	0.161	0.08	0.049	0.058
24121	-4056.25	4194.25	24.49	2.56	53.27	65.08	0.145	0.07	0.050	0.058
24121	-4056.55	4194.55	25.71	2.54	52.59	66.04	0.158	0.08	0.062	0.071
24121	-4056.86	4194.86	25.74	2.54	52.24	66.13	0.158	0.08	0.062	0.071

Well	TVDRSF	MD	GR	RHO	RD	DT	I_{GR} (4-7)	V_{sh} (4-5/6)	Porosity (eq 5-1)	Porosity (eq 4-4)
24121	-4057.16	4195.16	24.57	2.55	51.64	66.5	0.146	0.07	0.056	0.065
24121	-4057.47	4195.47	27.31	2.54	49.75	66.97	0.174	0.09	0.061	0.071
24121	-4057.77	4195.77	29.86	2.54	47.65	67.43	0.200	0.11	0.059	0.071
24121	-4058.08	4196.08	34.55	2.55	44.47	67.22	0.247	0.13	0.050	0.065
24121	-4058.38	4196.38	39.48	2.56	37.5	67.58	0.297	0.17	0.040	0.058
24121	-4058.69	4196.69	42.99	2.56	31.54	69.2	0.333	0.19	0.037	0.058
24121	-4058.99	4196.99	41.4	2.58	26.16	70.37	0.317	0.18	0.025	0.045
24121	-4059.3	4197.30	42.64	2.58	22.45	71.34	0.329	0.19	0.024	0.045
24121	-4059.6	4197.60	43.15	2.57	19.9	70.87	0.334	0.19	0.030	0.052
24121	-4059.91	4197.91	39.61	2.56	17.55	70.34	0.298	0.17	0.040	0.058
24121	-4060.21	4198.21	37.39	2.57	16.26	70.39	0.276	0.15	0.035	0.052
24121	-4060.52	4198.52	38.25	2.56	15.17	70.96	0.285	0.16	0.041	0.058
24121	-4060.82	4198.82	39.51	2.57	14.37	71.33	0.297	0.17	0.033	0.052
24121	-4061.13	4199.13	39.5	2.58	14.03	70.71	0.297	0.17	0.027	0.045
24121	-4061.43	4199.43	40.34	2.58	14.13	70.18	0.306	0.17	0.026	0.045
24121	-4061.74	4199.74	36.8	2.57	14.41	70.45	0.270	0.15	0.035	0.052
24121	-4062.04	4200.04	33.7	2.58	14.74	71.1	0.239	0.13	0.031	0.045
24121	-4062.35	4200.35	34.15	2.59	15.26	71.99	0.243	0.13	0.024	0.039
24121	-4062.65	4200.65	36.98	2.58	16.93	71.77	0.272	0.15	0.029	0.045
24121	-4062.96	4200.96	36.34	2.57	19.33	69.47	0.265	0.15	0.036	0.052
24121	-4063.26	4201.26	37.97	2.56	22.52	69.5	0.282	0.16	0.041	0.058
24121	-4063.56	4201.56	36.76	2.56	27.23	69.37	0.270	0.15	0.042	0.058
24121	-4063.87	4201.87	36.5	2.57	31.77	68.98	0.267	0.15	0.035	0.052
24121	-4064.17	4202.17	35.83	2.58	32.9	69.51	0.260	0.14	0.029	0.045
24121	-4064.48	4202.48	31.46	2.57	31.11	67.24	0.216	0.12	0.039	0.052
24121	-4064.78	4202.78	29.04	2.59	26.76	67.07	0.191	0.10	0.028	0.039
24121	-4065.09	4203.09	27.37	2.59	23.09	67.54	0.175	0.09	0.029	0.039
24121	-4065.39	4203.39	28.71	2.58	20.32	69.22	0.188	0.10	0.034	0.045
24121	-4065.7	4203.70	29.18	2.57	21.19	69.79	0.193	0.10	0.041	0.052
24121	-4066	4204.00	23.51	2.58	22.29	67.27	0.136	0.07	0.038	0.045
24121	-4066.31	4204.31	14.25	2.59	27.77	64.15	0.042	0.02	0.037	0.039
24121	-4066.61	4204.61	11.11	2.59	39.03	62.68	0.010	0.00	0.038	0.039
24121	-4066.92	4204.92	12.24	2.58	50.77	62.5	0.021	0.01	0.044	0.045
24121	-4067.22	4205.22	13.12	2.56	58.14	60.27	0.030	0.01	0.057	0.058
24121	-4067.53	4205.53	12.16	2.55	61.1	58.82	0.021	0.01	0.063	0.065
24121	-4067.83	4205.83	12.48	2.57	66.54	58.66	0.024	0.01	0.050	0.052
24121	-4068.14	4206.14	12.29	2.59	72.76	59.01	0.022	0.01	0.038	0.039
24121	-4068.44	4206.44	11.49	2.6	86.63	58.6	0.014	0.01	0.032	0.032
24121	-4068.75	4206.75	11.94	2.6	103.68	59.62	0.018	0.01	0.031	0.032
24121	-4069.05	4207.05	12.39	2.6	128.85	59.6	0.023	0.01	0.031	0.032
24121	-4069.36	4207.36	12.12	2.6	156.47	58.86	0.020	0.01	0.031	0.032
24121	-4069.66	4207.66	13.24	2.62	127.48	60	0.032	0.01	0.018	0.019
24121	-4069.97	4207.97	12.5	2.6	137.17	58.67	0.024	0.01	0.031	0.032
24121	-4070.27	4208.27	13.01	2.6	112.25	58.89	0.029	0.01	0.031	0.032
24121	-4070.58	4208.58	13.03	2.6	103.06	60.3	0.029	0.01	0.031	0.032
24121	-4070.88	4208.88	12.69	2.58	87.92	61.41	0.026	0.01	0.044	0.045
24121	-4071.18	4209.18	13.55	2.58	66.04	62.64	0.035	0.02	0.043	0.045
24121	-4071.49	4209.49	12.47	2.59	61.67	61.88	0.024	0.01	0.037	0.039
24121	-4071.79	4209.79	12.17	2.58	52	60.81	0.021	0.01	0.044	0.045
24121	-4072.1	4210.10	12.72	2.57	45.57	60.24	0.026	0.01	0.050	0.052
24121	-4072.4	4210.40	12.93	2.57	42.91	61.02	0.028	0.01	0.050	0.052
24121	-4072.71	4210.71	12.89	2.57	48.86	61.6	0.028	0.01	0.050	0.052
24121	-4073.01	4211.01	12.13	2.57	50.28	63.88	0.020	0.01	0.051	0.052
24121	-4073.32	4211.32	12.81	2.59	48.54	65.02	0.027	0.01	0.037	0.039
24121	-4073.62	4211.62	14.47	2.58	45.13	65.19	0.044	0.02	0.043	0.045
24121	-4073.93	4211.93	13.83	2.57	45.57	65.36	0.038	0.02	0.050	0.052
24121	-4074.23	4212.23	13.98	2.57	50.1	65.53	0.039	0.02	0.050	0.052
24121	-4074.54	4212.54	14.5	2.57	45.53	65.7	0.044	0.02	0.049	0.052
24121	-4074.84	4212.84	15.35	2.56	41.29	65.87	0.053	0.03	0.055	0.058
24121	-4075.15	4213.15	16.38	2.56	44.03	66.04	0.063	0.03	0.055	0.058
24121	-4075.45	4213.45	15.92	2.57	43.64	66.21	0.059	0.03	0.049	0.052
24121	-4075.76	4213.76	15.15	2.58	41.25	66.34	0.051	0.02	0.043	0.045
24121	-4076.06	4214.06	13.93	2.58	42.13	66.42	0.039	0.02	0.043	0.045

Well	TVDRSF	MD	GR	RHO	RD	DT	I_{GR} (4-7)	V_{sh} (4-5/6)	Porosity (eq 5-1)	Porosity (eq 4-4)
24121	-4076.37	4214.37	11.99	2.57	43.21	66.5	0.019	0.01	0.051	0.052
24121	-4076.67	4214.67	12.2	2.57	42.39	66.57	0.021	0.01	0.051	0.052
24121	-4076.98	4214.98	13.67	2.58	36.54	66.65	0.036	0.02	0.043	0.045
24121	-4077.28	4215.28	15.3	2.58	28.81	66.72	0.052	0.02	0.042	0.045
24121	-4077.59	4215.59	21.38	2.58	24.66	67.41	0.114	0.06	0.039	0.045
24121	-4077.89	4215.89	31.41	2.59	17.96	71.1	0.215	0.11	0.026	0.039
24121	-4078.2	4216.20	43.64	2.6	10.34	71.2	0.339	0.20	0.011	0.032
24121	-4078.5	4216.50	57.83	2.64	6.24	74.21	0.483	0.31	-0.028	0.006
24121	-4097.7	4235.70	39.23	2.59	6.84	80.79	0.295	0.17	0.020	0.039
24121	-4098.01	4236.01	19.22	2.6	10.21	67.43	0.092	0.04	0.027	0.032
24121	-4098.31	4236.31	20.42	2.59	11.56	66.54	0.104	0.05	0.033	0.039
24121	-4098.62	4236.62	30.25	2.59	9.76	74.27	0.204	0.11	0.027	0.039
24121	-4098.92	4236.92	42.74	2.6	9.35	95.77	0.330	0.19	0.011	0.032
24121	-4099.23	4237.23	51.8	2.6	8.91	83.83	0.422	0.26	0.003	0.032
24121	-4099.53	4237.53	45.48	2.6	9.47	87.49	0.358	0.21	0.009	0.032
24121	-4099.84	4237.84	38.42	2.59	12.59	83.52	0.286	0.16	0.021	0.039
24121	-4100.14	4238.14	41.17	2.59	15.69	70.29	0.314	0.18	0.019	0.039
24121	-4100.45	4238.45	37.92	2.6	17.08	68.71	0.281	0.16	0.015	0.032
24121	-4100.75	4238.75	28.71	2.6	17.17	66.39	0.188	0.10	0.021	0.032
24121	-4101.06	4239.06	25.84	2.63	17.75	63.86	0.159	0.08	0.004	0.013
24121	-4102.27	4240.27	21.68	2.63	10.57	67.45	0.117	0.06	0.007	0.013
24121	-4102.58	4240.58	26.69	2.59	9.34	69.55	0.168	0.09	0.029	0.039
24121	-4102.88	4240.88	33.6	2.58	8.46	73.54	0.238	0.13	0.031	0.045
24121	-4103.19	4241.19	39.03	2.57	8.15	75.89	0.293	0.17	0.034	0.052
24121	-4103.49	4241.49	45.2	2.63	8.52	76.77	0.355	0.21	-0.010	0.013
24121	-4103.8	4241.80	51.69	2.64	9.17	77.28	0.421	0.26	-0.022	0.006
24121	-4104.1	4242.10	57.41	2.62	9.94	74.86	0.479	0.31	-0.015	0.019
24121	-4104.41	4242.41	50.66	2.63	10.95	73.95	0.410	0.25	-0.015	0.013
24121	-4104.71	4242.71	47.5	2.63	12.03	75.89	0.378	0.23	-0.012	0.013
24121	-4105.02	4243.02	47.92	2.61	12.54	75.58	0.383	0.23	0.000	0.026
24121	-4105.32	4243.32	48.46	2.59	13.12	73.79	0.388	0.24	0.013	0.039
24121	-4105.63	4243.63	51.11	2.6	13.79	74.9	0.415	0.26	0.004	0.032
24121	-4105.93	4243.93	51.85	2.61	13.45	75.04	0.422	0.26	-0.003	0.026
24121	-4106.24	4244.24	53.11	2.6	13.25	73.78	0.435	0.27	0.002	0.032
24121	-4106.54	4244.54	48.19	2.61	13.78	74.01	0.385	0.23	0.000	0.026
24121	-4107.46	4245.46	31.09	2.61	14.64	73.93	0.212	0.11	0.013	0.026
24121	-4107.76	4245.76	35.02	2.54	15.7	74.76	0.252	0.14	0.056	0.071
24121	-4108.07	4246.07	39.94	2.53	17.96	73.8	0.302	0.17	0.059	0.077
24121	-4108.37	4246.37	41.19	2.53	19.84	72.6	0.314	0.18	0.058	0.077
24121	-4108.68	4246.68	39.77	2.56	18.53	70	0.300	0.17	0.039	0.058
24121	-4108.98	4246.98	37.91	2.6	14.72	66.89	0.281	0.16	0.015	0.032
24121	-4109.28	4247.28	45.39	2.63	14.79	71.63	0.357	0.21	-0.010	0.013
24121	-4109.59	4247.59	51.66	2.58	15.25	76.04	0.420	0.26	0.017	0.045
24121	-4109.89	4247.89	38.89	2.55	13.61	69.58	0.291	0.16	0.047	0.065
24121	-4110.2	4248.20	38.55	2.55	18.86	67.99	0.288	0.16	0.047	0.065
24121	-4110.5	4248.50	37.01	2.56	26.85	68.64	0.272	0.15	0.041	0.058
24121	-4110.81	4248.81	33.78	2.56	27.48	69.21	0.239	0.13	0.044	0.058
24121	-4111.11	4249.11	28.55	2.55	28.78	69.31	0.187	0.10	0.054	0.065
24121	-4111.42	4249.42	24.14	2.56	29.62	69.11	0.142	0.07	0.050	0.058
24121	-4111.72	4249.72	25.38	2.55	26.17	69.07	0.154	0.08	0.056	0.065
24121	-4112.03	4250.03	31.24	2.53	22.69	70.48	0.214	0.11	0.065	0.077
24121	-4112.33	4250.33	34.46	2.54	22.05	69.88	0.246	0.13	0.056	0.071
24121	-4112.64	4250.64	33.07	2.54	24.17	69.65	0.232	0.13	0.057	0.071
24121	-4112.94	4250.94	27.66	2.56	24.78	67.82	0.178	0.09	0.048	0.058
24121	-4113.25	4251.25	27.56	2.59	25.79	64.42	0.177	0.09	0.029	0.039
24121	-4113.55	4251.55	33.4	2.6	28.88	64.6	0.236	0.13	0.018	0.032
24121	-4115.08	4253.08	26.64	2.6	38.94	63.93	0.167	0.09	0.023	0.032
24121	-4115.38	4253.38	29	2.61	38.47	64.99	0.191	0.10	0.015	0.026
24121	-4115.69	4253.69	30.05	2.61	38.45	65.26	0.202	0.11	0.014	0.026
24121	-4115.99	4253.99	29.74	2.61	39.59	64.71	0.199	0.10	0.014	0.026
24121	-4116.3	4254.30	29.92	2.61	39.69	63.12	0.200	0.11	0.014	0.026
24121	-4116.6	4254.60	29	2.64	32.45	61.76	0.191	0.10	-0.005	0.006
24121	-4117.82	4255.82	20.98	2.6	22.16	61.73	0.110	0.05	0.026	0.032

Well	TVDRSF	MD	GR	RHO	RD	DT	I_{GR} (4-7)	V_{sh} (4-5/6)	Porosity (eq 5-1)	Porosity (eq 4-4)
24121	-4118.12	4256.12	24.97	2.59	31.89	60.48	0.150	0.08	0.030	0.039
24121	-4118.43	4256.43	22.46	2.6	61.47	60.48	0.125	0.06	0.025	0.032
24121	-4118.73	4256.73	19.75	2.59	95.77	60.34	0.097	0.05	0.033	0.039
24121	-4119.04	4257.04	21.11	2.59	123.22	59.82	0.111	0.06	0.033	0.039
24121	-4119.34	4257.34	22.78	2.6	126.25	60.31	0.128	0.06	0.025	0.032
24121	-4119.65	4257.65	22	2.61	123.95	60.22	0.120	0.06	0.019	0.026
24121	-4119.95	4257.95	24	2.61	129.3	60.05	0.140	0.07	0.018	0.026
24121	-4120.26	4258.26	23.77	2.61	129.78	59.75	0.138	0.07	0.018	0.026
24121	-4120.56	4258.56	22.83	2.62	129.94	59.43	0.129	0.06	0.012	0.019
24121	-4120.87	4258.87	24.31	2.62	118.04	60.95	0.144	0.07	0.011	0.019
24121	-4121.17	4259.17	25.62	2.63	106.48	61.14	0.157	0.08	0.004	0.013
24121	-4126.96	4264.96	36.43	2.57	31.16	60.04	0.266	0.15	0.035	0.052
24121	-4127.27	4265.27	38.77	2.54	28.17	67.12	0.290	0.16	0.053	0.071
24121	-4127.57	4265.57	39.25	2.54	25.69	71.91	0.295	0.17	0.053	0.071
24121	-4127.88	4265.88	36.04	2.56	22.22	69.73	0.262	0.14	0.042	0.058
24121	-4128.18	4266.18	34.54	2.57	23.68	68.2	0.247	0.13	0.037	0.052
24121	-4128.49	4266.49	33.74	2.6	22.64	68.06	0.239	0.13	0.018	0.032
24121	-4129.4	4267.40	31.6	2.58	23.62	64.36	0.217	0.12	0.032	0.045
24121	-4129.71	4267.71	36.09	2.55	22.29	66.5	0.263	0.15	0.049	0.065
24121	-4130.01	4268.01	34.56	2.56	21.76	68.02	0.247	0.13	0.043	0.058
24121	-4130.32	4268.32	35.7	2.59	20.62	69.46	0.259	0.14	0.023	0.039
24121	-4130.62	4268.62	35.44	2.61	19.57	67.97	0.256	0.14	0.010	0.026
24121	-4130.93	4268.93	35.46	2.61	17.93	67.45	0.256	0.14	0.010	0.026
24121	-4131.84	4269.84	42.74	2.61	16.14	68.44	0.330	0.19	0.005	0.026
24121	-4132.14	4270.14	43.85	2.63	17.01	68.15	0.341	0.20	-0.009	0.013
24121	-4132.45	4270.45	39.68	2.62	17.63	67.55	0.299	0.17	0.001	0.019
24121	-4132.75	4270.75	35.69	2.64	15.79	66.95	0.259	0.14	-0.009	0.006
24121	-4133.36	4271.36	33.15	2.61	15.12	67.35	0.233	0.13	0.012	0.026
24121	-4133.67	4271.67	37.31	2.57	15.32	67.75	0.275	0.15	0.035	0.052
24121	-4133.97	4271.97	37.95	2.57	15.2	67.55	0.282	0.16	0.034	0.052
24121	-4134.28	4272.28	36.25	2.58	13.86	66.23	0.264	0.15	0.029	0.045
24121	-4134.58	4272.58	37.34	2.58	13.49	66.22	0.275	0.15	0.028	0.045
24121	-4134.89	4272.89	34.05	2.55	13.64	69.18	0.242	0.13	0.050	0.065
24121	-4135.19	4273.19	38.61	2.56	12.46	69.55	0.288	0.16	0.040	0.058
24121	-4135.5	4273.50	40.35	2.59	11.37	68.15	0.306	0.17	0.020	0.039
24121	-4135.8	4273.80	37.95	2.58	11.83	68.87	0.282	0.16	0.028	0.045
24121	-4136.11	4274.11	39.87	2.55	11.91	70.21	0.301	0.17	0.046	0.065
24121	-4136.41	4274.41	44.09	2.54	12.64	69.89	0.344	0.20	0.049	0.071
24121	-4136.72	4274.72	41.89	2.56	16.43	69.09	0.322	0.19	0.038	0.058
24121	-4137.02	4275.02	35.83	2.58	20.29	67.9	0.260	0.14	0.029	0.045
24121	-4137.33	4275.33	29.85	2.57	20.7	65.73	0.200	0.11	0.040	0.052
24121	-4137.63	4275.63	22.55	2.57	19.95	64.35	0.126	0.06	0.045	0.052
24121	-4137.94	4275.94	20.14	2.58	21.79	65.74	0.101	0.05	0.040	0.045
24121	-4138.24	4276.24	18.6	2.59	24.02	65.72	0.086	0.04	0.034	0.039
24121	-4138.55	4276.55	16.47	2.6	36.47	63.13	0.064	0.03	0.029	0.032
24121	-4138.85	4276.85	13	2.59	56.73	60.54	0.029	0.01	0.037	0.039
24121	-4139.16	4277.16	13.84	2.58	85.84	59.92	0.038	0.02	0.043	0.045
24121	-4139.46	4277.46	13.34	2.57	86.03	60.6	0.033	0.02	0.050	0.052
24121	-4139.76	4277.76	14.09	2.57	80.18	61	0.040	0.02	0.050	0.052
24121	-4140.07	4278.07	14.2	2.57	79.71	60.79	0.041	0.02	0.049	0.052
24121	-4140.37	4278.37	14.4	2.58	84.87	61.11	0.043	0.02	0.043	0.045
24121	-4140.68	4278.68	11.9	2.58	94.87	61.11	0.018	0.01	0.044	0.045
24121	-4140.98	4278.98	10.31	2.59	106.18	60.6	0.002	0.00	0.039	0.039
24121	-4141.29	4279.29	10.16	2.6	108.28	60.21	0.000	0.00	0.032	0.032
24121	-4141.59	4279.59	12.36	2.59	119.63	60.71	0.023	0.01	0.038	0.039
24121	-4141.9	4279.90	14.88	2.58	110.2	61.19	0.048	0.02	0.043	0.045
24121	-4142.2	4280.20	13.21	2.58	85	61.13	0.031	0.01	0.044	0.045
24121	-4142.51	4280.51	13.19	2.57	86.78	61.1	0.031	0.01	0.050	0.052
24121	-4142.81	4280.81	13.59	2.57	76.52	61.75	0.035	0.02	0.050	0.052
24121	-4143.12	4281.12	14.61	2.58	69.88	61.97	0.045	0.02	0.043	0.045
24121	-4143.42	4281.42	14.41	2.61	76.46	61.95	0.043	0.02	0.024	0.026
24121	-4143.73	4281.73	13.48	2.59	76.33	61.41	0.034	0.02	0.037	0.039
24121	-4144.03	4282.03	14.01	2.58	98.81	61.28	0.039	0.02	0.043	0.045

Well	TVDRSF	MD	GR	RHO	RD	DT	I_{GR} (4-7)	V_{sh} (4-5/6)	Porosity (eq 5-1)	Porosity (eq 4-4)
24121	-4144.34	4282.34	14.56	2.58	98.31	60.81	0.045	0.02	0.043	0.045
24121	-4144.64	4282.64	12.87	2.57	85.58	60.8	0.028	0.01	0.050	0.052
24121	-4144.95	4282.95	11.65	2.58	86.72	61.16	0.015	0.01	0.044	0.045
24121	-4145.25	4283.25	11.77	2.61	85.02	61.62	0.017	0.01	0.025	0.026
24121	-4145.56	4283.56	11.77	2.61	85.13	62.61	0.017	0.01	0.025	0.026
24121	-4145.86	4283.86	11.57	2.63	70.79	62.02	0.015	0.01	0.012	0.013
24121	-4146.17	4284.17	12.5	2.63	66.1	62.93	0.024	0.01	0.012	0.013
24121	-4146.47	4284.47	11.81	2.63	63.73	62.02	0.017	0.01	0.012	0.013
24121	-4146.78	4284.78	11.76	2.57	56.93	61.22	0.017	0.01	0.051	0.052
24121	-4147.08	4285.08	11.56	2.54	56.11	61.19	0.015	0.01	0.070	0.071
24121	-4147.38	4285.38	12.15	2.54	53.41	59.75	0.021	0.01	0.070	0.071
24121	-4147.69	4285.69	11.55	2.6	47.45	60.88	0.014	0.01	0.032	0.032
24121	-4147.99	4285.99	14	2.57	46.13	62.72	0.039	0.02	0.050	0.052
24121	-4148.3	4286.30	14.27	2.56	47.13	61.83	0.042	0.02	0.056	0.058
24121	-4148.6	4286.60	14.82	2.57	52.05	62.37	0.048	0.02	0.049	0.052
24121	-4148.91	4286.91	15.12	2.62	66.52	62.13	0.051	0.02	0.017	0.019
24121	-4149.21	4287.21	14.61	2.62	73.66	61.78	0.045	0.02	0.017	0.019
24121	-4149.52	4287.52	11.86	2.62	78.1	61.49	0.018	0.01	0.018	0.019
24121	-4149.82	4287.82	11.14	2.62	87.3	62.03	0.010	0.00	0.019	0.019
24121	-4150.13	4288.13	12.66	2.62	99.37	61.09	0.026	0.01	0.018	0.019
24121	-4150.43	4288.43	12.61	2.62	101.52	60.11	0.025	0.01	0.018	0.019
24121	-4150.74	4288.74	13.32	2.62	101.34	60.04	0.032	0.02	0.018	0.019
24121	-4151.04	4289.04	11.96	2.62	101.94	60.14	0.019	0.01	0.018	0.019
24121	-4151.35	4289.35	12.19	2.63	88.95	60	0.021	0.01	0.012	0.013
24121	-4151.65	4289.65	13.08	2.62	82.73	59.75	0.030	0.01	0.018	0.019
24121	-4151.96	4289.96	13.7	2.61	78.21	60.23	0.036	0.02	0.024	0.026
24121	-4153.18	4291.18	13.71	2.43	58.3	60.05	0.036	0.02	0.140	0.142
24121	-4153.48	4291.48	14.29	2.46	51.53	59.76	0.042	0.02	0.120	0.123
24121	-4153.79	4291.79	14.31	2.43	55.19	61.29	0.042	0.02	0.140	0.142
24121	-4154.09	4292.09	15.32	2.39	59.2	61.61	0.053	0.02	0.165	0.168
24121	-4154.4	4292.40	14.08	2.39	54.5	61.59	0.040	0.02	0.166	0.168
24121	-4154.7	4292.70	16.87	2.41	54.81	61.73	0.068	0.03	0.151	0.155
24121	-4155	4293.00	20.9	2.4	37.06	63.26	0.109	0.05	0.155	0.161
24121	-4155.31	4293.31	31.6	2.39	20.56	63.65	0.217	0.12	0.155	0.168
24121	-4155.61	4293.61	52.52	2.43	10.98	66.13	0.429	0.27	0.113	0.142
24121	-4174.36	4312.36	56.2	2.59	4.24	84.26	0.466	0.30	0.006	0.039
24121	-4174.66	4312.66	30.94	2.56	5.22	73.71	0.211	0.11	0.046	0.058
24121	-4174.97	4312.97	17.82	2.55	6.09	70.49	0.078	0.04	0.060	0.065
24121	-4175.27	4313.27	16.14	2.53	6.11	67.09	0.061	0.03	0.074	0.077
24121	-4175.58	4313.58	16.09	2.53	5.88	67.13	0.060	0.03	0.074	0.077
24121	-4175.88	4313.88	15.99	2.54	5.71	67.76	0.059	0.03	0.068	0.071
24121	-4176.19	4314.19	16.2	2.54	5.62	67.35	0.062	0.03	0.068	0.071
24121	-4176.49	4314.49	20.04	2.53	5.56	66.96	0.100	0.05	0.072	0.077
24121	-4176.8	4314.80	24.38	2.53	5.32	69.36	0.144	0.07	0.069	0.077
24121	-4177.1	4315.10	28.46	2.53	5.03	70.99	0.186	0.10	0.067	0.077
24121	-4177.41	4315.41	29.94	2.52	4.85	72.18	0.201	0.11	0.072	0.084
24121	-4177.71	4315.71	29.97	2.51	4.67	72.89	0.201	0.11	0.079	0.090
24121	-4178.02	4316.02	30.15	2.51	4.65	72.31	0.203	0.11	0.079	0.090
24121	-4178.32	4316.32	29.99	2.53	4.92	73.1	0.201	0.11	0.066	0.077
24121	-4178.63	4316.63	33.93	2.53	5.13	74.41	0.241	0.13	0.063	0.077
24121	-4178.93	4316.93	36.36	2.53	5.52	74.62	0.266	0.15	0.061	0.077
24121	-4179.24	4317.24	32.75	2.53	5.84	74.63	0.229	0.12	0.064	0.077
24121	-4179.54	4317.54	33.21	2.53	5.88	74.3	0.234	0.13	0.064	0.077
24121	-4179.85	4317.85	31.76	2.53	5.79	73.9	0.219	0.12	0.065	0.077
24121	-4180.15	4318.15	33.77	2.52	5.67	72.84	0.239	0.13	0.070	0.084
24121	-4180.46	4318.46	34.05	2.53	5.8	73.57	0.242	0.13	0.063	0.077
24121	-4180.76	4318.76	29.07	2.56	6.21	74.5	0.192	0.10	0.047	0.058
24121	-4181.07	4319.07	25.25	2.56	6.77	72.51	0.153	0.08	0.050	0.058
24121	-4181.37	4319.37	27.47	2.58	7.07	71.5	0.176	0.09	0.035	0.045
24121	-4181.67	4319.67	32.56	2.59	6.61	72.89	0.227	0.12	0.025	0.039
24121	-4181.98	4319.98	40.68	2.62	5.96	73.69	0.309	0.18	0.000	0.019
24121	-4182.28	4320.28	56.03	2.62	5.2	75.28	0.465	0.30	-0.013	0.019
24121	-4184.42	4322.42	49.11	2.62	5.01	76.76	0.395	0.24	-0.007	0.019

Well	TVDRSF	MD	GR	RHO	RD	DT	I_{GR} (4-7)	V_{sh} (4-5/6)	Porosity (eq 5-1)	Porosity (eq 4-4)
24121	-4185.64	4323.64	29.35	2.6	7.15	63.47	0.195	0.10	0.021	0.032
24121	-4185.94	4323.94	26.6	2.53	6.51	66.49	0.167	0.09	0.068	0.077
24121	-4186.25	4324.25	18.7	2.51	5.88	67.09	0.087	0.04	0.086	0.090
24121	-4186.55	4324.55	18.2	2.52	5.37	68.08	0.082	0.04	0.080	0.084
24121	-4186.86	4324.86	19.49	2.53	5.28	70.07	0.095	0.05	0.072	0.077
24121	-4187.16	4325.16	18.78	2.54	5.45	70.21	0.088	0.04	0.066	0.071
24121	-4187.47	4325.47	20.1	2.54	5.64	71.09	0.101	0.05	0.066	0.071
24121	-4187.77	4325.77	21.38	2.53	5.87	70.56	0.114	0.06	0.071	0.077
24121	-4188.08	4326.08	19.28	2.54	5.9	70.08	0.093	0.05	0.066	0.071
24121	-4188.38	4326.38	24.13	2.54	5.94	72.28	0.142	0.07	0.063	0.071
24121	-4188.69	4326.69	25.11	2.54	5.9	73.05	0.152	0.08	0.062	0.071
24121	-4188.99	4326.99	24.87	2.55	5.93	72.05	0.149	0.08	0.056	0.065
24121	-4189.29	4327.29	23.84	2.57	5.9	72.44	0.139	0.07	0.044	0.052
24121	-4189.6	4327.60	23.59	2.56	5.94	73.44	0.136	0.07	0.051	0.058
24121	-4189.9	4327.90	23.2	2.59	5.96	72.52	0.132	0.07	0.031	0.039
24121	-4190.21	4328.21	21.39	2.62	6.13	71.95	0.114	0.06	0.013	0.019
24121	-4190.51	4328.51	21.81	2.63	6.32	72.09	0.118	0.06	0.006	0.013
24121	-4190.82	4328.82	20.52	2.62	6.46	72.89	0.105	0.05	0.014	0.019
24121	-4191.12	4329.12	19.53	2.59	6.72	72.91	0.095	0.05	0.034	0.039
24121	-4191.43	4329.43	21.67	2.57	7.11	72.74	0.117	0.06	0.045	0.052
24121	-4191.73	4329.73	24.35	2.55	7.92	72.94	0.144	0.07	0.057	0.065
24121	-4192.04	4330.04	26.13	2.56	9.11	76.08	0.162	0.08	0.049	0.058
24121	-4192.34	4330.34	25.8	2.56	10.22	75.28	0.159	0.08	0.049	0.058
24121	-4192.65	4330.65	23.94	2.53	11.07	72.9	0.140	0.07	0.070	0.077
24121	-4192.95	4330.95	26.84	2.52	10.83	76.05	0.169	0.09	0.074	0.084
24121	-4193.26	4331.26	31.66	2.54	9.97	77.51	0.218	0.12	0.058	0.071
24121	-4193.56	4331.56	37.51	2.6	9.26	75.46	0.277	0.15	0.015	0.032
24121	-4207.13	4345.13	48.4	2.64	15.14	64.68	0.387	0.23	-0.019	0.006
24121	-4207.43	4345.43	57.23	2.63	12.42	69.94	0.477	0.31	-0.021	0.013
24122	-4160.31	4309.31	57.41	2.49	14.34	103.12	0.495	0.33	0.067	0.103
24122	-4160.62	4309.62	28.36	2.57	22.42	81.77	0.148	0.08	0.043	0.052
24122	-4160.92	4309.92	20.09	2.62	40.25	80.19	0.049	0.02	0.017	0.019
24122	-4161.23	4310.23	24.17	2.56	59.31	92.85	0.098	0.05	0.053	0.058
24122	-4177.08	4326.08	57.16	2.48	14.93	152.08	0.492	0.32	0.074	0.110
24122	-4177.38	4326.38	54.94	2.34	10.85	151.43	0.466	0.30	0.167	0.200
24122	-4213.65	4362.65	48.47	2.5	16.02	136.24	0.388	0.24	0.071	0.097
24122	-4219.29	4368.29	53.56	2.5	11.68	136.8	0.449	0.29	0.065	0.097
24122	-4219.6	4368.60	56.5	2.51	12.37	135.42	0.484	0.32	0.056	0.090
24122	-4222.64	4371.64	41.66	2.54	14.05	127.42	0.307	0.18	0.052	0.071
24122	-4228.89	4377.89	51.81	2.47	10.24	128.14	0.428	0.27	0.087	0.116
24122	-4231.79	4380.79	54.88	2.47	12.7	132.91	0.465	0.30	0.083	0.116
24122	-4236.82	4385.82	49.31	2.51	14.71	124.1	0.398	0.24	0.064	0.090
24122	-4237.12	4386.12	37	2.61	16.98	120.35	0.251	0.14	0.011	0.026
24122	-4238.34	4387.34	54.44	2.46	11.33	130.65	0.460	0.29	0.090	0.123
24122	-4248.86	4397.86	52.03	2.54	11.72	125.27	0.431	0.27	0.041	0.071
24122	-4249.77	4398.77	52.69	2.52	13.26	109.11	0.439	0.28	0.054	0.084
24122	-4250.08	4399.08	39.88	2.53	10.54	108.27	0.286	0.16	0.060	0.077
24122	-4252.51	4401.51	53.34	2.47	13.16	87.18	0.447	0.28	0.085	0.116
24122	-4253.28	4402.28	51.56	2.54	22.19	78.38	0.425	0.27	0.042	0.071
24122	-4253.58	4402.58	23.25	2.62	17.5	76.19	0.087	0.04	0.015	0.019
24122	-4253.89	4402.89	37.78	2.61	12.92	82.45	0.261	0.14	0.010	0.026
24122	-4256.63	4405.63	35.94	2.51	10.29	113.02	0.239	0.13	0.076	0.090
24122	-4256.93	4405.93	57.28	2.52	9.13	117.4	0.494	0.32	0.048	0.084
24122	-4258.46	4407.46	43.22	2.55	10.71	107.76	0.326	0.19	0.044	0.065
24122	-4258.76	4407.76	43.25	2.5	12.77	107.98	0.326	0.19	0.076	0.097
24122	-4267.3	4416.30	46.47	2.46	13.93	115.33	0.364	0.22	0.099	0.123
24122	-4267.6	4416.60	26.22	2.46	16.06	109.42	0.122	0.06	0.116	0.123
24122	-4267.91	4416.91	40.84	2.45	15.81	109.06	0.297	0.17	0.111	0.129
24122	-4271.87	4420.87	58.88	2.53	10.27	139.44	0.513	0.34	0.040	0.077
24122	-4272.17	4421.17	48.47	2.49	9.91	138.17	0.388	0.24	0.077	0.103
24122	-4274.92	4423.92	29.77	2.62	15.23	72.18	0.165	0.08	0.010	0.019
24122	-4275.22	4424.22	23.69	2.63	24.2	70.89	0.092	0.04	0.008	0.013
24122	-4275.83	4424.83	50.53	2.5	22.23	90.51	0.413	0.26	0.069	0.097

Well	TVDRSF	MD	GR	RHO	RD	DT	I_{GR} (4-7)	V_{sh} (4-5/6)	Porosity (eq 5-1)	Porosity (eq 4-4)
24122	-4289.39	4438.39	34.25	2.52	17.89	93.63	0.218	0.12	0.071	0.084
24122	-4289.7	4438.70	25.8	2.59	23.38	80.4	0.117	0.06	0.032	0.039
24122	-4290	4439.00	26.8	2.61	17.92	86.46	0.129	0.06	0.019	0.026
24122	-4309.97	4458.97	51.28	2.51	24.48	97.09	0.422	0.26	0.062	0.090
24122	-4310.27	4459.27	25.67	2.64	32.16	80.25	0.116	0.06	0.000	0.006
24122	-4310.58	4459.58	33.25	2.56	34.53	81.06	0.206	0.11	0.046	0.058
24122	-4310.88	4459.88	50.47	2.49	18.8	93.83	0.412	0.25	0.075	0.103
24122	-4315.91	4464.91	46.06	2.52	7.83	106.81	0.360	0.21	0.060	0.084
24122	-4316.22	4465.22	50.84	2.52	8.76	104.22	0.417	0.26	0.056	0.084
24122	-4324.6	4473.60	42.13	2.59	13.36	123.57	0.313	0.18	0.019	0.039
24122	-4344.41	4493.41	53.56	2.43	17.27	103.88	0.449	0.29	0.111	0.142
24122	-4344.72	4493.72	25.69	2.48	25.59	86.56	0.116	0.06	0.103	0.110
24122	-4345.02	4494.02	34.84	2.48	20.58	87.73	0.225	0.12	0.096	0.110
24122	-4432.04	4581.04	53.97	2.55	19.36	87.05	0.454	0.29	0.033	0.065
24122	-4432.35	4581.35	34.72	2.64	19.61	83.03	0.224	0.12	-0.007	0.006
24122	-4447.89	4596.89	47.59	2.56	15.55	102.98	0.378	0.23	0.033	0.058
24122	-4448.2	4597.20	47.94	2.6	22.91	94.78	0.382	0.23	0.007	0.032
24122	-4448.5	4597.50	46.47	2.56	27.34	91.72	0.364	0.22	0.034	0.058
24122	-4448.8	4597.80	41.75	2.47	24.83	95.42	0.308	0.18	0.097	0.116
24122	-4449.11	4598.11	43.13	2.54	18.63	104	0.325	0.19	0.050	0.071
24122	-4496.05	4645.05	48.63	2.48	10.68	109.85	0.390	0.24	0.084	0.110
24122	-4496.35	4645.35	49.16	2.52	10.01	109.13	0.397	0.24	0.057	0.084
24122	-4502.3	4651.30	51.81	2.51	9.13	102.55	0.428	0.27	0.061	0.090
24122	-4502.6	4651.60	50.88	2.54	10.26	98.07	0.417	0.26	0.043	0.071
24122	-4503.36	4652.36	51.5	2.55	12.09	93.44	0.425	0.26	0.036	0.065
24122	-4503.67	4652.67	45.59	2.56	12.24	95.6	0.354	0.21	0.035	0.058
24122	-4503.97	4652.97	54.06	2.54	11.95	101.67	0.455	0.29	0.039	0.071
24122	-4504.28	4653.28	53.59	2.53	9.98	109.17	0.450	0.29	0.046	0.077
24122	-4508.09	4657.09	56.63	2.58	6.89	115.05	0.486	0.32	0.010	0.045
24122	-4515.86	4664.86	47	2.54	11.55	107.24	0.371	0.22	0.047	0.071
24122	-4516.17	4665.17	48.34	2.59	6.54	109.29	0.387	0.23	0.013	0.039
24122	-4519.37	4668.37	52.63	2.54	3.61	115.07	0.438	0.28	0.041	0.071
24122	-4519.67	4668.67	32.84	2.55	3.99	112.04	0.201	0.11	0.053	0.065
24122	-4521.8	4670.80	56.53	2.54	5.98	114.78	0.485	0.32	0.036	0.071
24122	-4522.11	4671.11	54.81	2.53	6.75	112.35	0.464	0.30	0.045	0.077
24122	-4523.48	4672.48	53.41	2.56	12.55	98.74	0.447	0.28	0.027	0.058
24122	-4523.79	4672.79	49.91	2.54	13.1	95.44	0.406	0.25	0.044	0.071
24122	-4524.09	4673.09	56.38	2.54	14.41	95.4	0.483	0.31	0.036	0.071
24122	-4524.4	4673.40	50.69	2.51	12.56	100.44	0.415	0.26	0.062	0.090
24122	-4524.7	4673.70	43.22	2.55	7.21	106.63	0.326	0.19	0.044	0.065
24122	-4525	4674.00	47	2.57	5.04	113.49	0.371	0.22	0.027	0.052
24122	-4532.02	4681.02	53.47	2.54	5.9	116.67	0.448	0.28	0.040	0.071
24122	-4532.32	4681.32	59.03	2.59	5.9	115.55	0.515	0.34	0.001	0.039
24122	-4536.28	4685.28	53.13	2.57	8.4	100.81	0.444	0.28	0.021	0.052
24122	-4536.59	4685.59	55.63	2.56	8.2	102.42	0.474	0.31	0.024	0.058
24122	-4536.89	4685.89	55.44	2.53	5.74	105.9	0.472	0.30	0.044	0.077
24122	-4544.05	4693.05	58.53	2.55	10.05	97.8	0.509	0.34	0.027	0.065
24122	-4544.36	4693.36	56.25	2.58	8.61	96.07	0.481	0.31	0.011	0.045
24122	-4544.66	4693.66	55.03	2.51	6.8	97.86	0.467	0.30	0.057	0.090
24122	-4550.3	4699.30	43.16	2.61	6.27	81.19	0.325	0.19	0.005	0.026
24122	-4550.61	4699.61	32.38	2.64	8.91	80.96	0.196	0.10	-0.005	0.006
24122	-4554.88	4703.88	53.63	2.52	10.23	89.74	0.450	0.29	0.053	0.084
24122	-4555.18	4704.18	37.84	2.57	12.31	85.86	0.261	0.14	0.036	0.052
24122	-4555.48	4704.48	36.31	2.5	13.53	83.75	0.243	0.13	0.082	0.097
24122	-4555.79	4704.79	53.31	2.47	13.13	85.83	0.446	0.28	0.085	0.116
24122	-4556.4	4705.40	47.25	2.6	11.41	91.07	0.374	0.22	0.008	0.032
24122	-4557.77	4706.77	57.53	2.51	9.08	93.17	0.497	0.33	0.054	0.090
24122	-4558.08	4707.08	40.66	2.52	9.5	90.47	0.295	0.17	0.066	0.084
24122	-4558.38	4707.38	54.28	2.52	9.49	92.37	0.458	0.29	0.052	0.084
24122	-4561.58	4710.58	54.59	2.51	10.5	93.5	0.462	0.30	0.058	0.090
24122	-4561.89	4710.89	49.69	2.47	7.93	93.44	0.403	0.25	0.089	0.116
24122	-4564.17	4713.17	54.03	2.63	8.94	91.9	0.455	0.29	-0.019	0.013
24122	-4564.48	4713.48	51.09	2.61	8.1	91.69	0.420	0.26	-0.003	0.026

Well	TVDRSF	MD	GR	RHO	RD	DT	I_{GR} (4-7)	V_{sh} (4-5/6)	Porosity (eq 5-1)	Porosity (eq 4-4)
24122	-4565.54	4714.54	56.09	2.54	5.75	88.78	0.480	0.31	0.037	0.071
24122	-4565.85	4714.85	48	2.48	6.61	82.5	0.383	0.23	0.084	0.110
24122	-4566.15	4715.15	34.34	2.51	7.49	79.97	0.219	0.12	0.077	0.090
24122	-4566.46	4715.46	31.83	2.57	7.64	80.18	0.189	0.10	0.041	0.052
24122	-4566.76	4715.76	29.05	2.57	8.34	85.37	0.156	0.08	0.043	0.052
24122	-4567.07	4716.07	29.5	2.47	8.59	92.38	0.161	0.08	0.107	0.116
24122	-4567.37	4716.37	52.13	2.48	8.52	98.92	0.432	0.27	0.080	0.110
24122	-4568.29	4717.29	46.25	2.48	8.25	112.48	0.362	0.21	0.086	0.110
24122	-4569.81	4718.81	50.91	2.52	8.37	109.42	0.418	0.26	0.055	0.084
24122	-4570.12	4719.12	36	2.46	8.78	104.84	0.239	0.13	0.108	0.123
24122	-4570.42	4719.42	29.55	2.46	8.27	100.49	0.162	0.08	0.113	0.123
24122	-4570.72	4719.72	23.13	2.6	7.51	99.26	0.085	0.04	0.028	0.032
24122	-4571.03	4720.03	32.06	2.52	7.19	101.56	0.192	0.10	0.073	0.084
24122	-4571.33	4720.33	40.38	2.43	6.58	103.01	0.292	0.16	0.124	0.142
24122	-4571.64	4720.64	59.97	2.5	6.05	104.99	0.526	0.35	0.058	0.097
24122	-4572.4	4721.40	44.41	2.56	7.96	107.59	0.340	0.20	0.036	0.058
24122	-4572.71	4721.71	40.47	2.63	6.5	107.21	0.293	0.17	-0.005	0.013
24122	-4573.93	4722.93	55	2.56	5.04	111.35	0.467	0.30	0.025	0.058
24122	-4574.23	4723.23	51	2.56	5.96	114.54	0.419	0.26	0.030	0.058
24122	-4576.06	4725.06	54.28	2.64	6.17	108.01	0.458	0.29	-0.026	0.006
24122	-4584.29	4733.29	51.16	2.57	4.42	113.75	0.421	0.26	0.023	0.052
24122	-4585.51	4734.51	52.16	2.55	5.28	110.34	0.433	0.27	0.035	0.065
24122	-4585.81	4734.81	54.09	2.61	5.05	112.03	0.456	0.29	-0.006	0.026
24122	-4588.1	4737.10	49.22	2.53	6.35	115.43	0.397	0.24	0.051	0.077
24122	-4589.32	4738.32	56.66	2.54	4.77	115.71	0.486	0.32	0.036	0.071
24122	-4590.08	4739.08	35.5	2.48	6.72	110.6	0.233	0.13	0.096	0.110
24122	-4590.38	4739.38	25.13	2.46	6.63	105.21	0.109	0.05	0.117	0.123
24122	-4590.69	4739.69	24.72	2.46	6.04	101.61	0.104	0.05	0.117	0.123
24122	-4590.99	4739.99	31.16	2.49	5.59	101.24	0.181	0.09	0.093	0.103
24122	-4591.3	4740.30	49.88	2.54	5.26	102.45	0.405	0.25	0.044	0.071
24122	-4591.91	4740.91	59.53	2.52	5.33	93.42	0.521	0.35	0.046	0.084
24122	-4592.21	4741.21	57.16	2.54	6.19	91.89	0.492	0.32	0.036	0.071
24122	-4592.98	4741.98	44.16	2.53	7.52	79.72	0.337	0.20	0.056	0.077
24122	-4593.28	4742.28	53.09	2.55	10.8	76.16	0.444	0.28	0.034	0.065
24122	-4593.58	4742.58	42	2.64	12.59	75.74	0.311	0.18	-0.013	0.006
24122	-4594.5	4743.50	38.84	2.56	9.51	91.83	0.273	0.15	0.041	0.058
24122	-4594.8	4743.80	32.59	2.46	7.5	96.4	0.198	0.10	0.111	0.123
24122	-4595.11	4744.11	32.63	2.43	6.83	102.91	0.199	0.10	0.130	0.142
24122	-4595.41	4744.41	39.44	2.43	6.26	109.84	0.280	0.16	0.125	0.142
24122	-4595.72	4744.72	43.44	2.49	5.54	109.8	0.328	0.19	0.082	0.103
24122	-4596.02	4745.02	43.34	2.5	5.62	108.39	0.327	0.19	0.076	0.097
24122	-4596.33	4745.33	56.31	2.56	5.87	107.98	0.482	0.31	0.024	0.058
24122	-4596.63	4745.63	37.06	2.6	5.92	106.18	0.252	0.14	0.017	0.032
24122	-4596.94	4745.94	33.09	2.49	6.55	103.18	0.204	0.11	0.091	0.103
24122	-4597.24	4746.24	41.47	2.47	7.12	101.58	0.305	0.17	0.097	0.116
24122	-4597.55	4746.55	34.16	2.48	7.28	100.5	0.217	0.12	0.097	0.110
24122	-4597.85	4746.85	26.19	2.47	6.84	98.96	0.122	0.06	0.109	0.116
24122	-4598.16	4747.16	35.53	2.45	6.46	98.02	0.234	0.13	0.115	0.129
24122	-4598.46	4747.46	39.31	2.46	6.23	95.7	0.279	0.16	0.106	0.123
24122	-4598.77	4747.77	40.47	2.48	6.29	92.78	0.293	0.17	0.092	0.110
24122	-4599.07	4748.07	37.5	2.53	6.97	91.35	0.257	0.14	0.062	0.077
24122	-4599.38	4748.38	29.63	2.61	7.73	91.19	0.163	0.08	0.017	0.026
24122	-4599.68	4748.68	29.06	2.57	7.43	92.05	0.156	0.08	0.043	0.052
24122	-4599.99	4748.99	50.75	2.51	5.85	96	0.416	0.26	0.062	0.090
24122	-4602.88	4751.88	57.56	2.57	5.84	102.12	0.497	0.33	0.016	0.052
24122	-4603.49	4752.49	41.22	2.5	7.22	93.79	0.302	0.17	0.078	0.097
24122	-4603.8	4752.80	24.97	2.59	6.6	89.01	0.107	0.05	0.033	0.039
24122	-4604.1	4753.10	30.47	2.56	5.8	86.72	0.173	0.09	0.048	0.058
24122	-4604.71	4753.71	55.06	2.57	5.25	90.37	0.467	0.30	0.019	0.052
24122	-4605.01	4754.01	54.84	2.53	5.01	89.5	0.465	0.30	0.045	0.077
24122	-4605.32	4754.32	57.97	2.51	5.25	90.85	0.502	0.33	0.054	0.090
24122	-4605.62	4754.62	47.31	2.48	5.73	91.92	0.375	0.22	0.085	0.110
24122	-4605.93	4754.93	45.31	2.55	5.26	92.21	0.351	0.21	0.042	0.065

Well	TVDRSF	MD	GR	RHO	RD	DT	I_{GR} (4-7)	V_{sh} (4-5/6)	Porosity (eq 5-1)	Porosity (eq 4-4)
24122	-4606.23	4755.23	50.63	2.52	4.9	95.5	0.414	0.26	0.056	0.084
24122	-4613.09	4762.09	57.38	2.6	14.73	74.5	0.495	0.33	-0.003	0.032
24122	-4614.01	4763.01	45.22	2.6	13.68	80.78	0.350	0.21	0.010	0.032
24122	-4614.31	4763.31	48.5	2.54	9.3	88.82	0.389	0.24	0.045	0.071
24122	-4619.95	4768.95	47.13	2.57	6.9	85.07	0.372	0.22	0.027	0.052
24122	-4620.25	4769.25	31.09	2.62	9.49	81.27	0.181	0.09	0.009	0.019
24122	-4621.32	4770.32	51.09	2.57	11.18	96.47	0.420	0.26	0.023	0.052
24122	-4621.63	4770.63	48.94	2.64	9.49	95.18	0.394	0.24	-0.020	0.006
24122	-4628.18	4777.18	59.69	2.64	5.25	102.63	0.523	0.35	-0.032	0.006
24122	-4654.24	4803.24	52.69	2.64	8.34	86.71	0.439	0.28	-0.024	0.006
24122	-4654.54	4803.54	52.56	2.63	8.03	85.56	0.437	0.28	-0.017	0.013
24122	-4669.02	4818.02	51.13	2.53	16.28	94.13	0.420	0.26	0.049	0.077
24122	-4669.33	4818.33	51.63	2.6	15.84	94.96	0.426	0.27	0.003	0.032
24122	-4684.72	4833.72	59.16	2.63	5.63	96.35	0.516	0.35	-0.025	0.013
24122	-4703.77	4852.77	56.13	2.62	5.87	96.66	0.480	0.31	-0.015	0.019
24122	-4711.54	4860.54	55.16	2.61	4.2	95.97	0.468	0.30	-0.007	0.026
24122	-4711.85	4860.85	56.41	2.58	4.21	97.44	0.483	0.31	0.011	0.045
24122	-4717.03	4866.03	57.91	2.63	8.23	82.65	0.501	0.33	-0.023	0.013
24122	-4737.45	4886.45	59.47	2.61	6.04	99.45	0.520	0.35	-0.012	0.026
24122	-4772.81	4921.81	59.53	2.64	8.94	74.54	0.521	0.35	-0.032	0.006
24122	-4787.89	4936.89	54.44	2.64	14.15	66.71	0.460	0.29	-0.026	0.006
24122	-4794.3	4943.30	54.63	2.62	6.97	93.7	0.462	0.30	-0.013	0.019
24122	-4801.31	4950.31	54.91	2.61	8.84	83.21	0.465	0.30	-0.007	0.026
24122	-4801.61	4950.61	50.31	2.58	9.66	85.24	0.410	0.25	0.017	0.045
24122	-4805.42	4954.42	59.31	2.63	6.91	95.66	0.518	0.35	-0.025	0.013
24122	-4806.34	4955.34	49.47	2.55	12.23	85.66	0.400	0.24	0.038	0.065
24122	-4806.64	4955.64	26.75	2.55	11.98	82.72	0.129	0.06	0.057	0.065
24122	-4806.94	4955.94	17.08	2.51	10.79	79.9	0.013	0.01	0.090	0.090
24122	-4807.25	4956.25	21.16	2.5	9.95	80.18	0.062	0.03	0.094	0.097
24122	-4807.55	4956.55	19.06	2.52	9.63	82.76	0.037	0.02	0.082	0.084
24122	-4807.86	4956.86	18.56	2.49	9.97	85.55	0.031	0.01	0.102	0.103
24122	-4808.16	4957.16	19.61	2.5	10.52	87.6	0.043	0.02	0.095	0.097
24122	-4808.47	4957.47	38.22	2.48	10.25	88.6	0.266	0.15	0.094	0.110
24122	-4808.77	4957.77	42.22	2.55	10.06	87.77	0.314	0.18	0.045	0.065
24122	-4809.08	4958.08	25.14	2.57	9.45	85.76	0.109	0.05	0.046	0.052
24122	-4809.38	4958.38	17.45	2.52	9.09	84.25	0.017	0.01	0.083	0.084
24122	-4809.69	4958.69	19.52	2.54	8.9	83.74	0.042	0.02	0.069	0.071
24122	-4809.99	4958.99	23.7	2.52	8.66	83.6	0.092	0.04	0.079	0.084
24122	-4810.3	4959.30	23.17	2.51	8.33	84.26	0.086	0.04	0.086	0.090
24122	-4810.6	4959.60	21.7	2.48	8.43	85.17	0.068	0.03	0.106	0.110
24122	-4810.91	4959.91	25.81	2.49	8.52	86.12	0.117	0.06	0.097	0.103
24122	-4811.21	4960.21	41.88	2.5	8.84	86.68	0.310	0.18	0.077	0.097
24122	-4811.52	4960.52	29.95	2.56	9.02	86.05	0.167	0.09	0.049	0.058
24122	-4811.82	4960.82	21.17	2.54	9.3	83.78	0.062	0.03	0.068	0.071
24122	-4812.13	4961.13	22.19	2.49	9.54	81.27	0.074	0.04	0.099	0.103
24122	-4812.43	4961.43	19.03	2.5	8.99	79.86	0.036	0.02	0.095	0.097
24122	-4812.74	4961.74	19.03	2.53	8.39	78.81	0.036	0.02	0.076	0.077
24122	-4813.04	4962.04	21.66	2.53	7.96	77.91	0.068	0.03	0.074	0.077
24122	-4813.35	4962.35	16	2.53	7.46	77.94	0.000	0.00	0.077	0.077
24122	-4813.65	4962.65	18.11	2.52	6.99	79.32	0.025	0.01	0.083	0.084
24122	-4813.96	4962.96	26.91	2.51	6.73	80.55	0.131	0.07	0.083	0.090
24122	-4814.26	4963.26	37.09	2.48	6.63	78.55	0.252	0.14	0.095	0.110
24122	-4814.56	4963.56	22.75	2.48	6.6	73.43	0.081	0.04	0.105	0.110
24122	-4814.87	4963.87	21.19	2.49	6.86	69.49	0.062	0.03	0.100	0.103
24122	-4815.17	4964.17	19.09	2.47	8.06	67.86	0.037	0.02	0.114	0.116
24122	-4815.48	4964.48	21.63	2.51	10.73	64.04	0.067	0.03	0.087	0.090
24122	-4818.22	4967.22	29.36	2.64	7.12	82.8	0.160	0.08	-0.003	0.006
24122	-4818.53	4967.53	34.06	2.54	6.36	83.59	0.216	0.12	0.058	0.071
24122	-4818.83	4967.83	24.67	2.54	6.1	84.13	0.104	0.05	0.065	0.071
24122	-4819.14	4968.14	28.28	2.5	5.82	85.62	0.147	0.07	0.089	0.097
24122	-4819.44	4968.44	53.34	2.5	5.71	88.2	0.447	0.28	0.066	0.097
24122	-4820.66	4969.66	39.81	2.52	5.7	87.38	0.285	0.16	0.066	0.084
24122	-4820.97	4969.97	20.17	2.5	5.55	79.7	0.050	0.02	0.094	0.097

Well	TVDRSF	MD	GR	RHO	RD	DT	I_{GR} (4-7)	V_{sh} (4-5/6)	Porosity (eq 5-1)	Porosity (eq 4-4)
24122	-4821.27	4970.27	20.14	2.51	5.24	74.23	0.050	0.02	0.088	0.090
24122	-4821.58	4970.58	25.83	2.53	5.61	73.42	0.118	0.06	0.071	0.077
24122	-4821.88	4970.88	23.19	2.52	6.66	71.48	0.086	0.04	0.079	0.084
24122	-4822.18	4971.18	16.45	2.6	8.16	67.33	0.005	0.00	0.032	0.032
24122	-4823.1	4972.10	22.69	2.5	6.82	87.06	0.080	0.04	0.093	0.097
24122	-4823.4	4972.40	38.81	2.56	6.4	87.97	0.273	0.15	0.041	0.058
24122	-4823.71	4972.71	59.53	2.61	8.1	87.54	0.521	0.35	-0.012	0.026
24122	-4824.62	4973.62	43.44	2.58	10.12	89.76	0.328	0.19	0.024	0.045
24122	-4824.93	4973.93	37.19	2.57	9.09	89.66	0.253	0.14	0.036	0.052
24122	-4825.23	4974.23	54.56	2.56	8.2	90.88	0.461	0.30	0.026	0.058
24122	-4825.54	4974.54	43.69	2.54	7.09	91.8	0.331	0.19	0.050	0.071
24122	-4825.84	4974.84	31.89	2.52	6.35	91.24	0.190	0.10	0.073	0.084
24122	-4826.15	4975.15	28.75	2.52	5.96	89.85	0.153	0.08	0.075	0.084
24122	-4826.45	4975.45	27.33	2.48	5.02	88.05	0.136	0.07	0.102	0.110
24122	-4826.76	4975.76	30.48	2.52	4.48	86.47	0.173	0.09	0.074	0.084
24122	-4827.06	4976.06	35.19	2.53	4.23	86.1	0.230	0.12	0.064	0.077
24122	-4827.37	4976.37	31.56	2.53	4.23	86.12	0.186	0.10	0.067	0.077
24122	-4827.67	4976.67	29.47	2.55	4.54	86.97	0.161	0.08	0.055	0.065
24122	-4827.98	4976.98	51.5	2.59	5.48	88.21	0.425	0.26	0.010	0.039
24122	-4838.95	4987.95	57.44	2.57	10.4	92.17	0.496	0.33	0.016	0.052
24122	-4839.25	4988.25	57.69	2.55	12.67	83.35	0.499	0.33	0.028	0.065
24122	-4839.56	4988.56	41.38	2.53	13.89	77.41	0.304	0.17	0.058	0.077
24122	-4839.86	4988.86	33.56	2.53	14.84	76.25	0.210	0.11	0.065	0.077
24122	-4840.17	4989.17	40.28	2.55	14.21	75.92	0.290	0.16	0.047	0.065
24122	-4840.47	4989.47	37.59	2.54	12.92	77.83	0.258	0.14	0.055	0.071
24122	-4840.78	4989.78	31.59	2.52	12.34	82.42	0.186	0.10	0.073	0.084
24122	-4841.08	4990.08	24.22	2.56	11.31	85.19	0.098	0.05	0.053	0.058
24122	-4841.39	4990.39	31.81	2.56	10	86.26	0.189	0.10	0.047	0.058
24122	-4841.69	4990.69	45.66	2.56	8.82	89.5	0.355	0.21	0.035	0.058
24122	-4842	4991.00	43.72	2.59	8.42	92.55	0.332	0.19	0.018	0.039
24122	-4843.06	4992.06	58.28	2.59	12.71	79.05	0.506	0.34	0.002	0.039
24122	-4843.37	4992.37	51.25	2.6	14.57	77.9	0.422	0.26	0.004	0.032
24122	-4843.67	4992.67	38.22	2.63	18.7	76.82	0.266	0.15	-0.003	0.013
24122	-4843.98	4992.98	38.19	2.6	18.67	77.86	0.265	0.15	0.016	0.032
24122	-4844.89	4993.89	44.75	2.59	14.4	88.26	0.344	0.20	0.017	0.039
24122	-4845.2	4994.20	31.98	2.59	13.13	85.54	0.191	0.10	0.028	0.039
24122	-4845.96	4994.96	58.5	2.61	10.05	91.28	0.508	0.34	-0.011	0.026
24122	-4846.26	4995.26	38.16	2.64	8.79	95.89	0.265	0.15	-0.010	0.006
24122	-4858.3	5007.30	57.72	2.57	7.21	96.74	0.499	0.33	0.016	0.052
24122	-4860.13	5009.13	40.75	2.64	11.27	73.36	0.296	0.17	-0.012	0.006
24122	-4860.44	5009.44	51.16	2.6	14.22	77.37	0.421	0.26	0.004	0.032
24122	-4860.74	5009.74	51.56	2.58	14.55	79.28	0.425	0.27	0.016	0.045
24122	-4861.5	5010.50	57.69	2.61	11.95	86.89	0.499	0.33	-0.010	0.026
24122	-4861.81	5010.81	45.41	2.61	11.98	90.62	0.352	0.21	0.003	0.026
24122	-4862.11	5011.11	34.03	2.56	9.28	93.62	0.216	0.12	0.045	0.058
24122	-4862.42	5011.42	31.45	2.58	8.68	92.98	0.185	0.10	0.035	0.045
24122	-4894.73	5043.73	41.03	2.63	19.25	80.37	0.299	0.17	-0.006	0.013
24122	-4896.1	5045.10	52.5	2.53	12.79	88.1	0.437	0.27	0.047	0.077
24122	-4896.4	5045.40	48.19	2.52	14.38	90.86	0.385	0.23	0.058	0.084
24122	-4896.71	5045.71	52.97	2.55	23.73	86.36	0.442	0.28	0.034	0.065
24122	-4897.78	5046.78	58.72	2.56	28.14	68.86	0.511	0.34	0.021	0.058
24122	-4900.37	5049.37	45.34	2.59	30.55	85.73	0.351	0.21	0.016	0.039
24122	-4900.67	5049.67	42.59	2.52	32.13	80.41	0.318	0.18	0.064	0.084
24122	-4900.98	5049.98	50.72	2.57	26.25	80.47	0.415	0.26	0.023	0.052
24122	-4901.28	5050.28	59.88	2.6	22.66	82.83	0.525	0.35	-0.006	0.032
24122	-4902.8	5051.80	56.25	2.63	21.11	89.34	0.481	0.31	-0.021	0.013
24122	-4904.18	5053.18	56.5	2.55	26.16	76.4	0.484	0.32	0.030	0.065
24122	-4904.48	5053.48	58.16	2.55	22.45	81.05	0.504	0.33	0.028	0.065
24122	-4910.58	5059.58	44.16	2.64	26.61	88.05	0.337	0.20	-0.015	0.006
24122	-4910.88	5059.88	56.81	2.58	22.75	90.77	0.488	0.32	0.010	0.045
24122	-4911.19	5060.19	57.53	2.58	18.05	97.07	0.497	0.33	0.009	0.045
24122	-4911.49	5060.49	56.44	2.6	11.73	98.23	0.484	0.32	-0.002	0.032
24122	-4913.78	5062.78	58.25	2.6	9.23	127.23	0.505	0.33	-0.004	0.032

Well	TVDRSF	MD	GR	RHO	RD	DT	I_{GR} (4-7)	V_{sh} (4-5/6)	Porosity (eq 5-1)	Porosity (eq 4-4)
24122	-4915.45	5064.45	58.28	2.61	4.69	123.92	0.506	0.34	-0.011	0.026
24122	-4915.76	5064.76	56.69	2.61	4.19	125.44	0.487	0.32	-0.009	0.026
24122	-4918.2	5067.20	55.03	2.59	14.27	103.04	0.467	0.30	0.006	0.039
24122	-4918.5	5067.50	43.28	2.55	19.27	96.25	0.326	0.19	0.044	0.065
24122	-4918.81	5067.81	36.22	2.52	20.88	91.23	0.242	0.13	0.069	0.084
24122	-4919.11	5068.11	33.78	2.55	24.55	88.42	0.213	0.11	0.052	0.065
24122	-4919.42	5068.42	30.17	2.52	22.09	82.89	0.169	0.09	0.074	0.084
24122	-4919.72	5068.72	37.97	2.49	16.63	72.69	0.263	0.15	0.087	0.103
24122	-4920.03	5069.03	54	2.58	12.69	66.08	0.455	0.29	0.013	0.045
24122	-4920.64	5069.64	48.78	2.59	13.03	62.85	0.392	0.24	0.013	0.039
24122	-4920.94	5069.94	40.72	2.58	12.69	64.35	0.296	0.17	0.027	0.045
24122	-4921.24	5070.24	38	2.64	13.61	72.41	0.263	0.15	-0.009	0.006
24122	-4923.23	5072.23	56.22	2.53	7.01	126.31	0.481	0.31	0.043	0.077
24122	-4923.53	5072.53	58.16	2.57	7.43	126.86	0.504	0.33	0.015	0.052
24122	-4925.51	5074.51	52.94	2.55	6.23	123.7	0.442	0.28	0.034	0.065
24122	-4929.93	5078.93	57.69	2.53	15.86	77.78	0.499	0.33	0.041	0.077
24122	-4930.85	5079.85	45.94	2.55	10.63	85.32	0.358	0.21	0.041	0.065
24122	-4931.15	5080.15	56.09	2.63	8.43	98.9	0.480	0.31	-0.021	0.013
24122	-4935.57	5084.57	57.16	2.54	5.09	128.57	0.492	0.32	0.036	0.071
24122	-4935.88	5084.88	48.78	2.56	5.09	127	0.392	0.24	0.032	0.058
24122	-4936.94	5085.94	54.97	2.61	4.9	122.64	0.466	0.30	-0.007	0.026
24122	-4937.25	5086.25	52.81	2.6	4.85	124.41	0.440	0.28	0.002	0.032
24122	-4938.01	5087.01	43.97	2.55	5.24	121.6	0.335	0.19	0.043	0.065
24122	-4938.31	5087.31	44.28	2.53	5.02	121.85	0.338	0.20	0.056	0.077
24122	-4938.62	5087.62	58.44	2.5	4.73	115.98	0.508	0.34	0.060	0.097
24122	-4939.08	5088.08	57.38	2.56	4.32	105.96	0.495	0.33	0.022	0.058
24122	-4939.38	5088.38	52.94	2.52	5	99.47	0.442	0.28	0.053	0.084
24122	-4939.69	5088.69	51.22	2.54	5.98	93.9	0.421	0.26	0.042	0.071
24122	-4939.99	5088.99	44.47	2.56	7.8	87.44	0.341	0.20	0.036	0.058
24122	-4940.29	5089.29	46.75	2.58	11.63	73.31	0.368	0.22	0.021	0.045
24122	-4940.6	5089.60	43.44	2.63	17.7	68.81	0.328	0.19	-0.008	0.013
24122	-4940.9	5089.90	42.81	2.61	19.97	74.4	0.321	0.18	0.006	0.026
24122	-4941.21	5090.21	54.56	2.6	24.59	74.55	0.461	0.30	0.000	0.032
24122	-4941.67	5090.67	56.16	2.54	25.89	81.99	0.480	0.31	0.037	0.071
24122	-4948.07	5097.07	57.41	2.54	2.95	144.96	0.495	0.33	0.035	0.071
24122	-4948.52	5097.52	57.88	2.57	3.68	145.54	0.501	0.33	0.015	0.052
24122	-4949.13	5098.13	56.19	2.55	2.98	145.96	0.481	0.31	0.030	0.065
24122	-4949.44	5098.44	53.16	2.55	2.55	146.72	0.444	0.28	0.034	0.065
24122	-4949.74	5098.74	54.16	2.53	2.48	146.93	0.456	0.29	0.045	0.077
24122	-4950.81	5099.81	59.16	2.52	2.07	146.77	0.516	0.35	0.046	0.084
24122	-4952.18	5101.18	58.72	2.54	2.2	146.68	0.511	0.34	0.034	0.071
24122	-4953.25	5102.25	57.38	2.53	2.55	147.16	0.495	0.33	0.042	0.077
24122	-4953.55	5102.55	56.75	2.53	2.32	146.44	0.487	0.32	0.042	0.077
24122	-4953.86	5102.86	59.16	2.53	2.36	146.33	0.516	0.35	0.040	0.077
24122	-4954.16	5103.16	55.59	2.55	2.49	146.56	0.474	0.31	0.031	0.065
24122	-4954.47	5103.47	58.88	2.53	2.6	146.87	0.513	0.34	0.040	0.077
24122	-4954.93	5103.93	56.5	2.55	2.62	146.84	0.484	0.32	0.030	0.065
24122	-4955.84	5104.84	59.28	2.52	2.64	146.57	0.518	0.35	0.046	0.084
24122	-4956.14	5105.14	58.09	2.52	2.63	146.62	0.503	0.33	0.047	0.084
24122	-4956.45	5105.45	54.41	2.55	2.62	146.51	0.459	0.29	0.032	0.065
24122	-4957.06	5106.06	52.81	2.56	2.63	146.38	0.440	0.28	0.028	0.058
24122	-4957.52	5106.52	57.28	2.53	2.62	146.38	0.494	0.32	0.042	0.077
24122	-4957.82	5106.82	55.91	2.54	2.62	146.38	0.477	0.31	0.037	0.071
24122	-4958.13	5107.13	57.5	2.55	2.63	146.38	0.496	0.33	0.029	0.065
24122	-4958.43	5107.43	57.03	2.52	2.62	146.38	0.491	0.32	0.049	0.084
24122	-4958.74	5107.74	57.38	2.53	2.62	146.38	0.495	0.33	0.042	0.077
24122	-4959.04	5108.04	57.38	2.52	2.62	146.38	0.495	0.33	0.048	0.084
24122	-4959.34	5108.34	57.38	2.53	2.62	146.38	0.495	0.33	0.042	0.077
24122	-4959.65	5108.65	57.38	2.55	2.62	146.38	0.495	0.33	0.029	0.065
24122	-4959.95	5108.95	57.38	2.53	2.62	146.38	0.495	0.33	0.042	0.077
24122	-4960.26	5109.26	57.38	2.55	2.62	146.38	0.495	0.33	0.029	0.065
24122	-4960.56	5109.56	57.38	2.55	2.62	146.38	0.495	0.33	0.029	0.065
24122	-4960.87	5109.87	57.38	2.55	2.63	146.38	0.495	0.33	0.029	0.065

Well	TVDRSF	MD	GR	RHO	RD	DT	I_{GR} (4-7)	V_{sh} (4-5/6)	Porosity (eq 5-1)	Porosity (eq 4-4)
2572	-3966.07	4091.07	34.5	2.61	12.66	63.84	0.295	0.17	0.008	0.026
2572	-3966.38	4091.38	30.7	2.53	17.66	63.09	0.242	0.13	0.063	0.077
2572	-3966.68	4091.68	33.65	2.52	17.4	65	0.283	0.16	0.066	0.084
2572	-3966.99	4091.99	45.36	2.57	12.73	74.66	0.446	0.28	0.021	0.052
2572	-3994.57	4119.57	47.46	2.63	6.56	77.38	0.475	0.31	-0.021	0.013
2572	-3994.88	4119.88	46.62	2.63	6.37	71.29	0.464	0.30	-0.020	0.013
2572	-3995.18	4120.18	44.53	2.62	6.37	64.48	0.435	0.27	-0.011	0.019
2572	-3995.49	4120.49	43.29	2.62	6.61	58.98	0.417	0.26	-0.009	0.019
2572	-3997.01	4122.01	53.8	2.63	7.16	67.31	0.564	0.39	-0.030	0.013
2572	-3997.32	4122.32	48.3	2.63	7.16	68.42	0.487	0.32	-0.022	0.013
2572	-3997.62	4122.62	44.26	2.63	7.16	65.58	0.431	0.27	-0.017	0.013
2572	-3997.93	4122.93	45.11	2.64	7.26	65.38	0.443	0.28	-0.024	0.006
2572	-3998.23	4123.23	48	2.64	7.81	66.08	0.483	0.31	-0.028	0.006
2572	-3998.54	4123.54	42.38	2.61	9.38	64.5	0.405	0.25	-0.001	0.026
2572	-4002.5	4127.50	43.86	2.63	17.82	59.59	0.425	0.27	-0.016	0.013
2572	-4004.02	4129.02	45.05	2.64	10.98	66.73	0.442	0.28	-0.024	0.006
2572	-4014.23	4139.23	59.15	2.23	7.74	83.23	0.638	0.47	0.220	0.271
2572	-4014.54	4139.54	56.84	2.24	7.92	86.87	0.606	0.43	0.217	0.265
2572	-4015.3	4140.30	58.57	2.48	7.04	84.65	0.630	0.46	0.059	0.110
2572	-4015.6	4140.60	57.9	2.64	6.61	72.7	0.621	0.45	-0.043	0.006
2572	-4016.52	4141.52	56.52	2.57	6.51	74.89	0.601	0.43	0.004	0.052
2572	-4016.82	4141.82	57.24	2.53	6.21	75.06	0.611	0.44	0.029	0.077
2572	-4017.13	4142.13	59.49	2.5	5.87	77.64	0.643	0.47	0.045	0.097
2572	-4017.43	4142.43	53.44	2.58	5.54	75.8	0.559	0.39	0.003	0.045
2572	-4022.46	4147.46	39.17	2.57	12.4	79.14	0.360	0.21	0.028	0.052
2572	-4022.77	4147.77	35.17	2.47	14.02	84.07	0.304	0.17	0.097	0.116
2572	-4023.07	4148.07	24.25	2.43	15.99	87.58	0.153	0.08	0.133	0.142
2572	-4023.38	4148.38	19.43	2.39	17.27	88.19	0.086	0.04	0.163	0.168
2572	-4023.68	4148.68	20.16	2.36	17.33	87.02	0.096	0.05	0.182	0.187
2572	-4023.99	4148.99	24.51	2.4	17.01	86.53	0.156	0.08	0.153	0.161
2572	-4024.29	4149.29	25.66	2.44	17.89	82.42	0.172	0.09	0.126	0.135
2572	-4024.6	4149.60	23.88	2.47	17.2	77.58	0.147	0.07	0.108	0.116
2572	-4024.9	4149.90	24.12	2.52	15.18	76.22	0.151	0.08	0.075	0.084
2572	-4025.21	4150.21	32.29	2.5	13.76	77.71	0.264	0.15	0.081	0.097
2572	-4025.51	4150.51	44.57	2.54	13.23	75.46	0.435	0.27	0.041	0.071
2572	-4028.86	4153.86	56.23	2.56	10.81	77.3	0.597	0.43	0.011	0.058
2572	-4029.17	4154.17	47.23	2.64	14.43	67.86	0.472	0.31	-0.027	0.006
2572	-4029.47	4154.47	31.77	2.59	19.52	63.75	0.257	0.14	0.023	0.039
2572	-4029.78	4154.78	30.53	2.52	26.29	74.06	0.240	0.13	0.070	0.084
2572	-4030.08	4155.08	37.05	2.52	32.19	70.97	0.331	0.19	0.063	0.084
2572	-4030.39	4155.39	30.78	2.56	34.56	60.87	0.243	0.13	0.044	0.058
2572	-4031.61	4156.61	28.55	2.55	21.67	68.89	0.212	0.11	0.052	0.065
2572	-4031.91	4156.91	37.8	2.55	16.61	69.89	0.341	0.20	0.043	0.065
2572	-4032.22	4157.22	43.45	2.63	13.78	68.74	0.420	0.26	-0.016	0.013
2572	-4032.52	4157.52	45.07	2.64	11.7	66.74	0.442	0.28	-0.024	0.006
2572	-4034.2	4159.20	57.47	2.64	6.94	66.57	0.615	0.44	-0.042	0.006
2572	-4034.5	4159.50	59.68	2.62	6.02	67.96	0.645	0.48	-0.033	0.019
2572	-4040.45	4165.45	56.31	2.57	7.84	74.04	0.598	0.43	0.005	0.052
2572	-4040.75	4165.75	42.46	2.59	8.12	65.02	0.406	0.25	0.011	0.039
2572	-4043.19	4168.19	23.81	2.55	11.91	76.63	0.146	0.07	0.056	0.065
2572	-4043.49	4168.49	28.4	2.46	13.1	78.1	0.210	0.11	0.110	0.123
2572	-4043.8	4168.80	43.98	2.51	11.88	79.31	0.427	0.27	0.061	0.090
2572	-4044.1	4169.10	57.87	2.49	10.14	80.29	0.620	0.45	0.054	0.103
2572	-4044.41	4169.41	57.53	2.46	9.23	80.99	0.615	0.44	0.074	0.123
2572	-4044.71	4169.71	47.71	2.48	9.07	80.73	0.479	0.31	0.076	0.110
2572	-4045.02	4170.02	43.77	2.52	9.42	80.14	0.424	0.26	0.055	0.084
2572	-4045.32	4170.32	44.73	2.6	10.13	79.5	0.437	0.28	0.002	0.032
2572	-4045.63	4170.63	55.66	2.62	10.88	79.46	0.589	0.42	-0.026	0.019
2572	-4046.39	4171.39	55.86	2.64	15.04	80.2	0.592	0.42	-0.040	0.006
2572	-4046.69	4171.69	56.57	2.62	20.78	82.4	0.602	0.43	-0.028	0.019
2572	-4047	4172.00	54.31	2.59	26.47	79.7	0.571	0.40	-0.005	0.039
2572	-4047.3	4172.30	44.25	2.54	26.94	74.08	0.431	0.27	0.041	0.071
2572	-4047.61	4172.61	40.23	2.51	29.04	73.22	0.375	0.22	0.066	0.090

Well	TVDRSF	MD	GR	RHO	RD	DT	I_{GR} (4-7)	V_{sh} (4-5/6)	Porosity (eq 5-1)	Porosity (eq 4-4)
2572	-4047.91	4172.91	34.82	2.5	29.74	74.47	0.300	0.17	0.078	0.097
2572	-4048.22	4173.22	35.3	2.47	22.56	77.36	0.306	0.17	0.097	0.116
2572	-4048.52	4173.52	53.77	2.45	16.63	81.97	0.563	0.39	0.086	0.129
2572	-4049.59	4174.59	55.01	2.63	12.2	75.33	0.580	0.41	-0.032	0.013
2572	-4049.89	4174.89	53.98	2.61	10.26	76.24	0.566	0.39	-0.017	0.026
2572	-4051.88	4176.88	56.83	2.58	9.57	77.06	0.606	0.43	-0.002	0.045
2572	-4052.18	4177.18	58.51	2.57	10.82	74.72	0.629	0.46	0.001	0.052
2572	-4052.49	4177.49	51.08	2.57	11.94	72.76	0.526	0.35	0.013	0.052
2572	-4052.79	4177.79	48.52	2.59	13.03	73.4	0.490	0.32	0.004	0.039
2572	-4053.1	4178.10	56.06	2.61	14.21	74.43	0.595	0.42	-0.021	0.026
2572	-4053.4	4178.40	58.6	2.61	14.28	74.35	0.630	0.46	-0.025	0.026
2572	-4053.7	4178.70	56.65	2.57	14.6	74.19	0.603	0.43	0.004	0.052
2572	-4054.01	4179.01	59.2	2.56	15.7	76.46	0.639	0.47	0.007	0.058
2572	-4054.31	4179.31	51.84	2.58	16.87	82.47	0.536	0.36	0.005	0.045
2572	-4054.62	4179.62	59.52	2.45	18.31	87.25	0.643	0.47	0.077	0.129
2572	-4055.53	4180.53	50.56	2.48	16.98	69.65	0.518	0.35	0.072	0.110
2572	-4055.84	4180.84	47.66	2.61	12.66	72.34	0.478	0.31	-0.008	0.026
2572	-4056.14	4181.14	55.62	2.58	10.11	76.54	0.589	0.42	-0.001	0.045
2572	-4056.75	4181.75	55.97	2.45	9.48	81.83	0.594	0.42	0.083	0.129
2572	-4057.06	4182.06	40.66	2.39	10.15	79.94	0.381	0.23	0.143	0.168
2572	-4057.36	4182.36	43.86	2.39	12.63	81.36	0.425	0.27	0.139	0.168
2572	-4057.67	4182.67	52.71	2.42	14.36	78.81	0.548	0.38	0.107	0.148
2572	-4057.97	4182.97	57.53	2.42	13.01	75.73	0.615	0.44	0.100	0.148
2572	-4058.28	4183.28	59.81	2.43	11.62	77.63	0.647	0.48	0.089	0.142
2572	-4060.41	4185.41	54.11	2.02	7.65	81.83	0.568	0.40	0.363	0.406
2572	-4060.72	4185.72	55	1.97	8.81	84.19	0.580	0.41	0.394	0.439
2572	-4061.02	4186.02	53.95	2.42	9.18	84.17	0.566	0.39	0.105	0.148
2572	-4061.32	4186.32	42.72	2.54	8.99	81.58	0.409	0.25	0.043	0.071
2572	-4061.63	4186.63	29.26	2.5	8.51	79.96	0.222	0.12	0.084	0.097
2572	-4061.93	4186.93	39.21	2.44	7.89	77.4	0.361	0.21	0.112	0.135
2572	-4064.22	4189.22	54.14	2.62	9.65	65.87	0.568	0.40	-0.024	0.019
2572	-4070.16	4195.16	51.53	2.6	9.46	77.32	0.532	0.36	-0.007	0.032
2572	-4070.47	4195.47	26.44	2.56	10.54	76.02	0.183	0.10	0.048	0.058
2572	-4070.77	4195.77	27.3	2.49	9.38	77.68	0.195	0.10	0.092	0.103
2572	-4071.08	4196.08	54.63	2.52	7.28	85.15	0.575	0.40	0.040	0.084
2572	-4072.91	4197.91	55.68	2.63	6.83	75.42	0.590	0.42	-0.033	0.013
2572	-4073.21	4198.21	51.69	2.56	7.8	77.22	0.534	0.36	0.018	0.058
2572	-4073.52	4198.52	44.54	2.59	8.3	77.71	0.435	0.27	0.009	0.039
2572	-4073.82	4198.82	44.96	2.56	7.86	79.97	0.441	0.28	0.028	0.058
2572	-4074.13	4199.13	44.98	2.5	7.27	82.88	0.441	0.28	0.066	0.097
2572	-4074.43	4199.43	43.76	2.45	6.57	83.77	0.424	0.26	0.100	0.129
2572	-4074.74	4199.74	44.67	2.46	5.97	86.61	0.437	0.27	0.092	0.123
2572	-4075.04	4200.04	45	2.43	5.47	92	0.441	0.28	0.111	0.142
2572	-4075.35	4200.35	48.59	2.38	5.28	89.74	0.491	0.32	0.139	0.174
2572	-4075.65	4200.65	46.25	2.41	5.48	86.13	0.459	0.29	0.123	0.155
2572	-4075.96	4200.96	41.45	2.45	5.68	82.34	0.392	0.24	0.103	0.129
2572	-4076.26	4201.26	40.43	2.46	5.75	78.23	0.378	0.23	0.098	0.123
2572	-4076.56	4201.56	40.77	2.53	5.7	78.48	0.382	0.23	0.052	0.077
2572	-4076.87	4201.87	48.15	2.53	5.37	80.87	0.485	0.32	0.043	0.077
2572	-4079.61	4204.61	38.28	2.58	15.1	75.31	0.348	0.20	0.023	0.045
2572	-4079.92	4204.92	38.44	2.47	17.15	76.93	0.350	0.21	0.094	0.116
2572	-4080.22	4205.22	36.86	2.44	18.29	76.59	0.328	0.19	0.115	0.135
2572	-4080.53	4205.53	38.97	2.45	18.94	76.65	0.357	0.21	0.106	0.129
2572	-4080.83	4205.83	38.8	2.45	19.36	76.63	0.355	0.21	0.106	0.129
2572	-4081.14	4206.14	38.98	2.46	19.46	76.02	0.357	0.21	0.099	0.123
2572	-4081.44	4206.44	40.9	2.46	19.75	74.96	0.384	0.23	0.097	0.123
2572	-4081.75	4206.75	40.43	2.47	21.04	72.13	0.378	0.23	0.091	0.116
2572	-4082.05	4207.05	41.89	2.51	24.67	64.4	0.398	0.24	0.064	0.090
2572	-4082.36	4207.36	37.87	2.62	29.37	58.6	0.342	0.20	-0.003	0.019
2572	-4086.01	4211.01	39.7	2.63	20.83	70.59	0.367	0.22	-0.011	0.013
2572	-4086.32	4211.32	40.66	2.56	17.31	72.54	0.381	0.23	0.033	0.058
2572	-4086.62	4211.62	37.17	2.52	14.98	73.29	0.332	0.19	0.063	0.084
2572	-4086.93	4211.93	38.07	2.49	14.64	72.95	0.345	0.20	0.081	0.103

Well	TVDRSF	MD	GR	RHO	RD	DT	I_{GR} (4-7)	V_{sh} (4-5/6)	Porosity (eq 5-1)	Porosity (eq 4-4)
2572	-4087.23	4212.23	48.03	2.53	15.19	72.8	0.483	0.31	0.043	0.077
2572	-4087.54	4212.54	50.51	2.59	15.63	71.66	0.518	0.35	0.001	0.039
2572	-4087.84	4212.84	46.23	2.6	16.51	69.97	0.458	0.29	0.000	0.032
2572	-4088.15	4213.15	44.41	2.59	16.41	68.89	0.433	0.27	0.009	0.039
2572	-4088.45	4213.45	44.1	2.59	14.71	70.41	0.429	0.27	0.009	0.039
2572	-4088.76	4213.76	48.92	2.6	12.64	75.72	0.496	0.33	-0.004	0.032
2572	-4089.06	4214.06	57.55	2.57	10.86	76.52	0.616	0.44	0.003	0.052
2572	-4089.37	4214.37	50.27	2.56	9.09	73.56	0.514	0.34	0.020	0.058
2572	-4089.67	4214.67	27.83	2.58	7.94	75.36	0.202	0.11	0.033	0.045
2572	-4089.98	4214.98	21.95	2.48	7.6	75.36	0.121	0.06	0.103	0.110
2572	-4090.28	4215.28	16.21	2.45	7.64	73.08	0.041	0.02	0.127	0.129
2572	-4090.59	4215.59	27.45	2.46	7.59	76.57	0.197	0.10	0.111	0.123
2572	-4092.57	4217.57	56.25	2.57	9.24	63.32	0.598	0.43	0.005	0.052
2572	-4103.69	4228.69	52	2.58	7.29	78.24	0.539	0.37	0.005	0.045
2572	-4106.28	4231.28	50.13	2.62	13.17	66.75	0.513	0.34	-0.018	0.019
2572	-4123.5	4248.50	40.21	2.61	7.94	74.24	0.375	0.22	0.001	0.026
2572	-4123.81	4248.81	27.48	2.55	7.79	72.62	0.197	0.10	0.053	0.065
2572	-4124.11	4249.11	25.39	2.54	8.08	71.17	0.168	0.09	0.061	0.071
2572	-4124.42	4249.42	25.72	2.54	8.61	70.15	0.173	0.09	0.061	0.071
2572	-4124.72	4249.72	22.21	2.55	8.27	69.58	0.124	0.06	0.058	0.065
2572	-4125.03	4250.03	21.67	2.56	7.19	69.34	0.117	0.06	0.052	0.058
2572	-4125.33	4250.33	31.58	2.57	6.69	71.85	0.255	0.14	0.036	0.052
2572	-4125.64	4250.64	39.58	2.59	7.06	72.4	0.366	0.22	0.015	0.039
2572	-4125.94	4250.94	29.41	2.59	8.36	69.13	0.224	0.12	0.026	0.039
2572	-4126.25	4251.25	19.79	2.56	13.15	62.25	0.091	0.04	0.053	0.058
2572	-4128.99	4253.99	27.61	2.57	11.71	74.65	0.199	0.11	0.040	0.052
2572	-4129.3	4254.30	21.51	2.47	12.68	74.58	0.114	0.06	0.110	0.116
2572	-4129.6	4254.60	17.82	2.49	13.47	74.96	0.063	0.03	0.100	0.103
2572	-4129.9	4254.90	16.86	2.47	14.6	73.04	0.050	0.02	0.114	0.116
2572	-4130.21	4255.21	20.21	2.44	14.96	72.11	0.096	0.05	0.130	0.135
2572	-4130.51	4255.51	18.79	2.46	14.48	71.42	0.077	0.04	0.119	0.123
2572	-4130.82	4255.82	17.51	2.45	14.36	71.86	0.059	0.03	0.126	0.129
2572	-4131.12	4256.12	18.97	2.41	14.71	72.12	0.079	0.04	0.151	0.155
2572	-4131.43	4256.43	19.91	2.43	15.18	71.83	0.092	0.04	0.137	0.142
2572	-4131.73	4256.73	15.96	2.46	15.77	69.25	0.037	0.02	0.121	0.123
2572	-4132.04	4257.04	14.47	2.47	16.4	64.71	0.017	0.01	0.115	0.116
2572	-4132.34	4257.34	15.33	2.51	16.62	65.15	0.029	0.01	0.089	0.090
2572	-4132.65	4257.65	15.32	2.54	16.21	67.83	0.028	0.01	0.070	0.071
2572	-4132.95	4257.95	16.21	2.51	14.45	69.75	0.041	0.02	0.088	0.090
2572	-4133.26	4258.26	15.29	2.51	11.53	72.56	0.028	0.01	0.089	0.090
2572	-4133.56	4258.56	28.69	2.49	8.52	83.1	0.214	0.11	0.091	0.103
2572	-4133.87	4258.87	56.96	2.5	6.55	95.1	0.608	0.44	0.049	0.097
2572	-4134.93	4259.93	31.32	2.62	7.32	75.94	0.251	0.14	0.004	0.019
2572	-4135.24	4260.24	28.64	2.57	8.17	70.49	0.214	0.11	0.039	0.052
2572	-4135.54	4260.54	28.46	2.51	8.59	68.21	0.211	0.11	0.078	0.090
2572	-4135.85	4260.85	28.46	2.54	8.47	72.16	0.211	0.11	0.059	0.071
2572	-4137.68	4262.68	20.01	2.63	9.54	76.95	0.094	0.05	0.008	0.013
2572	-4137.98	4262.98	20.81	2.48	11.86	70.68	0.105	0.05	0.104	0.110
2572	-4138.29	4263.29	16.42	2.44	15.08	62.86	0.044	0.02	0.133	0.135
2572	-4138.59	4263.59	12.3	2.58	17.74	58.24	-0.014	-0.01	0.046	0.045
2572	-4139.51	4264.51	17.67	2.61	9.68	74.47	0.061	0.03	0.023	0.026
2572	-4139.81	4264.81	21.05	2.54	7.1	77.89	0.108	0.05	0.065	0.071
2572	-4140.12	4265.12	22.52	2.52	6.15	78.05	0.129	0.06	0.077	0.084
2572	-4140.42	4265.42	23.03	2.48	5.82	78.43	0.136	0.07	0.102	0.110
2572	-4140.73	4265.73	21.49	2.46	5.66	77.58	0.114	0.06	0.116	0.123
2572	-4141.03	4266.03	18.43	2.46	5.52	77.82	0.072	0.03	0.119	0.123
2572	-4141.33	4266.33	20.61	2.44	5.65	77.57	0.102	0.05	0.130	0.135
2572	-4141.64	4266.64	23.43	2.44	5.74	73.47	0.141	0.07	0.128	0.135
2572	-4141.94	4266.94	22.74	2.5	5.36	68.16	0.132	0.07	0.090	0.097
2572	-4142.25	4267.25	26.08	2.6	5.29	72.47	0.178	0.09	0.022	0.032
2572	-4142.55	4267.55	34.18	2.55	5.4	72.35	0.291	0.16	0.047	0.065
2572	-4142.86	4267.86	39.6	2.57	5.45	67.51	0.366	0.22	0.028	0.052

Well	TVDRSF	MD	GR	RHO	RD	DT	I_{GR} (4-7)	V_{sh} (4-5/6)	Porosity (eq 5-1)	Porosity (eq 4-4)
2572	-4143.77	4268.77	26.59	2.55	4.41	79.02	0.185	0.10	0.054	0.065
2572	-4144.08	4269.08	30.73	2.45	3.87	84.12	0.243	0.13	0.115	0.129
2572	-4144.38	4269.38	30.9	2.37	3.79	83.46	0.245	0.13	0.166	0.181
2572	-4144.69	4269.69	26.03	2.38	4.25	76.45	0.177	0.09	0.164	0.174
2572	-4144.99	4269.99	20.35	2.45	5.31	66.29	0.098	0.05	0.124	0.129
2572	-4145.3	4270.30	18.67	2.58	6.49	62	0.075	0.04	0.041	0.045
2572	-4145.6	4270.60	17.38	2.6	7.25	66.4	0.057	0.03	0.029	0.032
2572	-4145.91	4270.91	13.59	2.55	7.41	68.78	0.004	0.00	0.064	0.065
2572	-4146.21	4271.21	14.5	2.54	7	69.28	0.017	0.01	0.070	0.071
2572	-4146.52	4271.52	16.95	2.51	6.54	76.07	0.051	0.02	0.088	0.090
2572	-4146.82	4271.82	17.47	2.43	6.49	82.34	0.058	0.03	0.139	0.142
2572	-4147.13	4272.13	20.29	2.42	6.76	75.46	0.097	0.05	0.143	0.148
2572	-4147.43	4272.43	19.66	2.56	6.58	66.11	0.089	0.04	0.053	0.058
2572	-4148.04	4273.04	22.88	2.63	5.07	76.03	0.134	0.07	0.006	0.013
2572	-4148.35	4273.35	27.12	2.46	4.09	83.84	0.192	0.10	0.112	0.123
2572	-4148.65	4273.65	28.63	2.38	3.22	86.3	0.213	0.11	0.162	0.174
2572	-4148.95	4273.95	34.61	2.39	2.65	84.73	0.297	0.17	0.149	0.168
2572	-4149.26	4274.26	42.41	2.43	2.36	85.64	0.405	0.25	0.115	0.142
2572	-4149.56	4274.56	58.73	2.56	2.24	83.48	0.632	0.46	0.007	0.058
2572	-4153.53	4278.53	20.83	2.63	3.35	87.7	0.105	0.05	0.007	0.013
2572	-4153.83	4278.83	24.81	2.51	2.99	87.24	0.160	0.08	0.081	0.090
2572	-4154.14	4279.14	25.62	2.44	2.93	87.77	0.172	0.09	0.126	0.135
2572	-4154.44	4279.44	27.39	2.42	2.94	88.09	0.196	0.10	0.137	0.148
2572	-4154.75	4279.75	30.38	2.41	2.94	88.31	0.238	0.13	0.141	0.155
2572	-4155.05	4280.05	32.75	2.4	2.86	87.27	0.271	0.15	0.145	0.161
2572	-4155.36	4280.36	31.9	2.41	2.82	85.3	0.259	0.14	0.139	0.155
2572	-4155.66	4280.66	31.02	2.43	2.79	84.29	0.247	0.13	0.127	0.142
2572	-4155.97	4280.97	32.12	2.46	2.82	83.5	0.262	0.14	0.107	0.123
2572	-4156.27	4281.27	35.91	2.45	2.91	81.16	0.315	0.18	0.109	0.129
2572	-4156.57	4281.57	36.02	2.49	2.97	80.59	0.316	0.18	0.083	0.103
2572	-4156.88	4281.88	35.21	2.51	2.98	83.26	0.305	0.17	0.071	0.090
2572	-4157.18	4282.18	36.78	2.51	3.05	84.19	0.327	0.19	0.070	0.090
2572	-4157.49	4282.49	43.88	2.5	3.3	81.42	0.426	0.27	0.068	0.097
2572	-4157.79	4282.79	53.04	2.52	3.73	79.51	0.553	0.38	0.042	0.084
2572	-4158.1	4283.10	51.96	2.57	4.04	78.38	0.538	0.37	0.012	0.052
2572	-4158.4	4283.40	52.82	2.6	3.99	78.68	0.550	0.38	-0.009	0.032
2572	-4158.71	4283.71	58.56	2.64	3.96	80.52	0.630	0.46	-0.044	0.006
2572	-4159.62	4284.62	13.94	2.47	3.88	83.74	0.009	0.00	0.116	0.116
2572	-4159.93	4284.93	14.65	2.4	4.06	85.79	0.019	0.01	0.160	0.161
2572	-4160.23	4285.23	14.67	2.39	3.99	85.87	0.019	0.01	0.167	0.168
2572	-4160.54	4285.54	14.22	2.38	3.71	84.62	0.013	0.01	0.174	0.174
2572	-4160.84	4285.84	16.91	2.37	3.37	84.07	0.050	0.02	0.178	0.181
2572	-4161.15	4286.15	21.57	2.39	3.06	83.32	0.115	0.06	0.161	0.168
2572	-4161.45	4286.45	23.41	2.39	2.74	83.27	0.141	0.07	0.160	0.168
2572	-4161.76	4286.76	20.07	2.4	2.46	84.58	0.094	0.05	0.156	0.161
2572	-4162.06	4287.06	19.17	2.43	2.33	85.2	0.082	0.04	0.138	0.142
2572	-4162.37	4287.37	19.59	2.43	2.32	84.81	0.088	0.04	0.137	0.142
2572	-4162.67	4287.67	19.19	2.42	2.41	84.42	0.082	0.04	0.144	0.148
2572	-4162.98	4287.98	17.88	2.44	2.56	82.92	0.064	0.03	0.132	0.135
2572	-4163.28	4288.28	16.52	2.44	2.72	80.4	0.045	0.02	0.133	0.135
2572	-4163.59	4288.59	19.3	2.43	2.86	78.78	0.084	0.04	0.137	0.142
2572	-4163.89	4288.89	20.84	2.44	2.93	76.9	0.105	0.05	0.130	0.135
2572	-4164.19	4289.19	20.5	2.44	2.9	74.26	0.100	0.05	0.130	0.135
2572	-4164.5	4289.50	22.04	2.48	2.92	74.32	0.122	0.06	0.103	0.110
2572	-4164.8	4289.80	27.42	2.48	2.95	74.53	0.197	0.10	0.098	0.110
2572	-4165.11	4290.11	31.19	2.48	2.98	74.19	0.249	0.14	0.095	0.110
2572	-4165.41	4290.41	39.14	2.59	3.08	76.5	0.360	0.21	0.015	0.039
2572	-4166.02	4291.02	36.8	2.6	3.27	81.81	0.327	0.19	0.011	0.032
2572	-4166.33	4291.33	22.26	2.45	3.4	78.99	0.125	0.06	0.122	0.129
2572	-4166.63	4291.63	19.04	2.37	3.61	76.78	0.080	0.04	0.176	0.181
2572	-4166.94	4291.94	19.64	2.39	4.03	78.94	0.088	0.04	0.163	0.168
2572	-4167.24	4292.24	20.19	2.36	4.59	76.85	0.096	0.05	0.182	0.187
2572	-4167.55	4292.55	27.03	2.35	4.95	75.83	0.191	0.10	0.183	0.194

Well	TVDRSF	MD	GR	RHO	RD	DT	I_{GR} (4-7)	V_{sh} (4-5/6)	Porosity (eq 5-1)	Porosity (eq 4-4)
2572	-4167.85	4292.85	44	2.44	4.99	83.24	0.427	0.27	0.106	0.135
2572	-4168.16	4293.16	59.37	2.56	4.76	84.71	0.641	0.47	0.006	0.058
2572	-4170.44	4295.44	45.64	2.57	3.37	74.9	0.450	0.29	0.020	0.052
2572	-4170.75	4295.75	39.53	2.62	3.76	65.98	0.365	0.22	-0.004	0.019
2572	-4171.36	4296.36	22.99	2.58	4.35	73.91	0.135	0.07	0.038	0.045
2572	-4171.66	4296.66	41.2	2.53	4.33	78.72	0.388	0.24	0.052	0.077
2572	-4211.74	4336.74	59.85	2.59	3.2	93.29	0.648	0.48	-0.014	0.039
2572	-4212.05	4337.05	59.8	2.59	3.23	93.91	0.647	0.48	-0.014	0.039
2572	-4215.86	4340.86	46.55	2.54	3.1	93.23	0.463	0.30	0.038	0.071
2572	-4216.16	4341.16	47.35	2.52	3.06	92.8	0.474	0.31	0.050	0.084
2572	-4216.47	4341.47	59.41	2.54	3.06	92.93	0.642	0.47	0.019	0.071
2572	-4216.77	4341.77	50.69	2.6	3.41	87.97	0.520	0.35	-0.006	0.032
2572	-4217.08	4342.08	52.12	2.62	3.68	96.63	0.540	0.37	-0.021	0.019
2572	-4228.96	4353.96	55.73	2.49	2.58	95.1	0.590	0.42	0.057	0.103
2572	-4229.27	4354.27	53.4	2.48	2.65	99.5	0.558	0.39	0.067	0.110
2572	-4229.57	4354.57	54.85	2.48	2.72	97.46	0.578	0.41	0.065	0.110
2572	-4229.88	4354.88	55.22	2.47	2.73	94.57	0.583	0.41	0.071	0.116
2572	-4230.49	4355.49	59.83	2.49	2.51	91.87	0.647	0.48	0.051	0.103
2572	-4230.79	4355.79	57.89	2.52	2.51	92.96	0.620	0.45	0.035	0.084
2572	-4232.32	4357.32	49.6	2.56	3.29	82.63	0.505	0.33	0.021	0.058
2572	-4253.2	4378.20	59.41	2.57	2.47	96.26	0.642	0.47	0.000	0.052
2572	-4253.5	4378.50	55.91	2.51	2.43	97.37	0.593	0.42	0.044	0.090
2572	-4253.81	4378.81	58.44	2.56	2.42	95.73	0.628	0.46	0.008	0.058
2572	-4254.11	4379.11	58.83	2.57	2.5	95.32	0.634	0.46	0.001	0.052
2572	-4264.02	4389.02	58.88	2.52	3.9	95.59	0.634	0.46	0.033	0.084
1613	-2574.13	2707.13	46.21	2.39	7.12	72.5	0.238	0.07	0.156	0.168
1613	-2579.63	2712.63	58.7	2.4	4.48	79.48	0.512	0.23	0.122	0.161
1613	-2579.88	2712.88	58.34	2.38	4.63	81.9	0.504	0.22	0.136	0.174
1613	-2582.63	2715.63	55.68	2.29	6.35	86.89	0.446	0.18	0.201	0.232
1613	-2582.88	2715.88	44.92	2.3	6.75	81.45	0.210	0.06	0.215	0.226
1613	-2583.13	2716.13	47.46	2.31	6.19	80.16	0.266	0.08	0.205	0.219
1613	-2583.38	2716.38	47.46	2.32	5.31	86.82	0.266	0.08	0.199	0.213
1613	-2583.63	2716.63	44.6	2.34	4.68	94.34	0.203	0.06	0.190	0.200
1613	-2583.88	2716.88	42.86	2.39	4.22	93.64	0.165	0.04	0.160	0.168
1613	-2584.13	2717.13	48.68	2.45	3.81	86.32	0.292	0.09	0.113	0.129
1613	-2584.38	2717.38	54.98	2.46	3.47	80.1	0.430	0.17	0.093	0.123
1613	-2584.63	2717.63	56.77	2.41	3.22	81.75	0.470	0.19	0.121	0.155
1613	-2584.88	2717.88	57.09	2.34	2.97	90.12	0.477	0.20	0.165	0.200
1613	-2585.13	2718.13	54.75	2.31	2.7	97.47	0.425	0.16	0.191	0.219
1613	-2585.38	2718.38	46.57	2.32	2.57	99.47	0.246	0.07	0.200	0.213
1613	-2585.63	2718.63	42.4	2.34	2.65	96.71	0.155	0.04	0.193	0.200
1613	-2585.88	2718.88	44.91	2.35	2.75	91.74	0.210	0.06	0.183	0.194
1613	-2586.13	2719.13	48.1	2.36	2.73	89.23	0.280	0.09	0.172	0.187
1613	-2586.38	2719.38	50.34	2.36	2.63	90.85	0.329	0.11	0.168	0.187
1613	-2586.63	2719.63	49.93	2.37	2.47	94.06	0.320	0.11	0.162	0.181
1613	-2586.88	2719.88	49.81	2.4	2.25	94.24	0.317	0.10	0.143	0.161
1613	-2587.13	2720.13	49.59	2.44	2.11	91.43	0.312	0.10	0.118	0.135
1613	-2587.38	2720.38	44.68	2.49	2.11	89.11	0.205	0.06	0.093	0.103
1613	-2587.63	2720.63	41.4	2.51	2.2	88.08	0.133	0.03	0.084	0.090
1613	-2587.88	2720.88	41.56	2.53	2.32	87.29	0.137	0.03	0.071	0.077
1613	-2588.13	2721.13	41.2	2.54	2.44	85.35	0.129	0.03	0.065	0.071
1613	-2588.38	2721.38	44.8	2.55	2.54	84.08	0.208	0.06	0.054	0.065
1613	-2588.63	2721.63	46.61	2.53	2.58	85.2	0.247	0.07	0.065	0.077
1613	-2588.88	2721.88	44.95	2.49	2.59	87	0.211	0.06	0.093	0.103
1613	-2589.13	2722.13	45.91	2.47	2.56	89.07	0.232	0.07	0.104	0.116
1613	-2589.38	2722.38	46.5	2.48	2.5	90.73	0.245	0.07	0.097	0.110
1613	-2589.63	2722.63	48.81	2.5	2.42	90.66	0.295	0.09	0.080	0.097
1613	-2589.88	2722.88	50.38	2.49	2.37	90.2	0.330	0.11	0.084	0.103
1613	-2590.13	2723.13	45.41	2.47	2.33	90.09	0.221	0.06	0.105	0.116
1613	-2590.38	2723.38	38.9	2.46	2.27	89.66	0.078	0.02	0.119	0.123
1613	-2590.63	2723.63	35.32	2.47	2.22	89.77	0.000	0.00	0.116	0.116
1613	-2590.88	2723.88	37.31	2.47	2.22	90.13	0.044	0.01	0.114	0.116
1613	-2591.13	2724.13	46.82	2.46	2.26	89.3	0.252	0.08	0.109	0.123

Well	TVDRSF	MD	GR	RHO	RD	DT	I_{GR} (4-7)	V_{sh} (4-5/6)	Porosity (eq 5-1)	Porosity (eq 4-4)
1613	-2591.38	2724.38	57.21	2.46	2.31	88.25	0.479	0.20	0.088	0.123
1613	-2591.63	2724.63	59.23	2.47	2.35	88	0.523	0.23	0.075	0.116
1613	-2591.88	2724.88	54.43	2.48	2.38	87.73	0.418	0.16	0.082	0.110
1613	-2592.13	2725.13	54.74	2.47	2.41	87.74	0.425	0.16	0.088	0.116
1613	-2594.13	2727.13	52.84	2.48	2.24	99.72	0.384	0.14	0.085	0.110
1613	-2594.38	2727.38	48.91	2.5	2.13	101.41	0.298	0.10	0.080	0.097
1613	-2594.63	2727.63	47.79	2.49	2.1	105.67	0.273	0.08	0.089	0.103
1613	-2594.88	2727.88	44.05	2.46	2.11	114.4	0.191	0.05	0.113	0.123
1613	-2595.13	2728.13	41.86	2.42	2.08	120.05	0.143	0.04	0.142	0.148
1613	-2595.38	2728.38	41.42	2.37	2.07	116.03	0.134	0.03	0.175	0.181
1613	-2595.63	2728.63	44.77	2.34	2.15	108.44	0.207	0.06	0.190	0.200
1613	-2595.88	2728.88	51.18	2.38	2.26	104.67	0.347	0.12	0.153	0.174
1613	-2596.13	2729.13	52.18	2.44	2.29	106.88	0.369	0.13	0.113	0.135
1613	-2596.38	2729.38	54.71	2.45	2.28	107.76	0.424	0.16	0.101	0.129
25108	-1768.43	3107.03	57.56	2.43	4.2	100	0.425	0.16	0.115	0.142
25108	-1781.45	3128.36	52.93	2.36	4.54	100	0.343	0.12	0.168	0.187
25108	-1781.63	3128.67	53.5	2.37	4.73	100	0.353	0.12	0.161	0.181
25108	-1796.13	3152.44	54.71	2.29	2.38	100	0.375	0.13	0.211	0.232
25108	-1796.32	3152.75	50.31	2.27	2.19	100	0.297	0.09	0.230	0.245
25108	-1796.51	3153.05	48.87	2.26	1.78	100	0.271	0.08	0.238	0.252
25108	-1796.69	3153.36	51.84	2.27	1.49	100	0.324	0.11	0.228	0.245
25108	-1805.24	3167.38	57.06	2.31	2.12	100	0.416	0.16	0.194	0.219
25108	-1805.43	3167.68	47.67	2.33	1.31	100	0.250	0.07	0.194	0.206
25108	-1805.62	3167.99	44.84	2.35	1.35	100	0.199	0.06	0.185	0.194
25108	-1805.8	3168.29	43.31	2.39	1.92	100	0.172	0.05	0.160	0.168
25108	-1805.99	3168.60	44.06	2.33	1.98	100	0.186	0.05	0.198	0.206
25108	-1806.17	3168.90	47.22	2.24	0.56	100	0.242	0.07	0.253	0.265
25108	-1852.84	3245.41	57.6	2.18	2.24	100	0.426	0.16	0.277	0.303
25108	-1853.03	3245.71	53.82	2.14	1.08	100	0.359	0.13	0.309	0.329
25108	-1853.21	3246.02	53.64	2.15	0.53	100	0.356	0.12	0.303	0.323
25108	-1853.4	3246.32	53.63	2.15	0.4	100	0.356	0.12	0.303	0.323
25108	-1853.59	3246.63	53.75	2.15	0.28	100	0.358	0.12	0.302	0.323
25108	-1853.77	3246.93	55.21	2.15	0.42	100	0.384	0.14	0.300	0.323
25108	-1853.96	3247.24	56.68	2.16	0.9	100	0.410	0.15	0.291	0.316
25108	-1854.14	3247.54	57.59	2.16	3.88	100	0.426	0.16	0.290	0.316
25108	-1854.33	3247.85	57.96	2.15	2.51	100	0.432	0.17	0.295	0.323
25108	-1854.51	3248.15	58.45	2.14	1.65	100	0.441	0.17	0.301	0.329
25108	-1854.7	3248.46	57.58	2.13	1.07	100	0.426	0.16	0.309	0.335
25108	-1854.89	3248.76	56.09	2.13	0.75	100	0.399	0.15	0.312	0.335
25108	-1855.07	3249.06	53.17	2.11	0.43	100	0.347	0.12	0.329	0.348
25108	-1855.26	3249.37	50.45	2.11	0.3	100	0.299	0.10	0.333	0.348
25108	-1855.44	3249.67	49.76	2.12	0.29	100	0.287	0.09	0.327	0.342
25108	-1855.63	3249.98	49.82	2.13	0.3	100	0.288	0.09	0.321	0.335
25108	-1855.82	3250.28	49.99	2.14	0.3	100	0.291	0.09	0.314	0.329
25108	-1856	3250.59	50.15	2.14	0.3	100	0.294	0.09	0.314	0.329
25108	-1856.19	3250.89	50.34	2.15	0.3	100	0.297	0.09	0.307	0.323
25108	-1856.37	3251.20	50.53	2.15	0.3	100	0.300	0.10	0.307	0.323
25108	-1856.56	3251.50	50.65	2.16	0.31	100	0.303	0.10	0.300	0.316
25108	-1856.75	3251.81	50	2.17	0.31	100	0.291	0.09	0.295	0.310
25108	-1856.93	3252.11	49.18	2.17	0.31	100	0.276	0.09	0.296	0.310
25108	-1857.12	3252.42	48.47	2.17	0.31	100	0.264	0.08	0.297	0.310
25108	-1857.3	3252.72	48.31	2.16	0.31	100	0.261	0.08	0.303	0.316
25108	-1857.49	3253.03	47.91	2.16	0.3	100	0.254	0.08	0.304	0.316
25108	-1857.68	3253.33	47.61	2.16	0.3	100	0.249	0.07	0.304	0.316
25108	-1857.86	3253.64	47.81	2.15	0.3	100	0.252	0.08	0.310	0.323
25108	-1858.05	3253.94	48.62	2.15	0.3	100	0.267	0.08	0.309	0.323
25108	-1858.23	3254.25	49.04	2.15	0.3	100	0.274	0.08	0.309	0.323
25108	-1858.42	3254.55	49.05	2.15	0.29	100	0.274	0.08	0.309	0.323
25108	-1858.61	3254.86	48.73	2.15	0.29	100	0.268	0.08	0.309	0.323
25108	-1858.79	3255.16	48.58	2.15	0.3	100	0.266	0.08	0.309	0.323
25108	-1858.98	3255.47	48.92	2.15	0.3	100	0.272	0.08	0.309	0.323
25108	-1859.16	3255.77	49.66	2.15	0.3	100	0.285	0.09	0.308	0.323
25108	-1859.35	3256.08	50.03	2.15	0.31	100	0.292	0.09	0.308	0.323

Well	TVDRSF	MD	GR	RHO	RD	DT	I_{GR} (4-7)	V_{sh} (4-5/6)	Porosity (eq 5-1)	Porosity (eq 4-4)
25108	-1859.54	3256.38	50.29	2.15	0.3	100	0.296	0.09	0.307	0.323
25108	-1859.72	3256.68	50.02	2.15	0.31	100	0.291	0.09	0.308	0.323
25108	-1859.91	3256.99	50.13	2.16	0.31	100	0.293	0.09	0.301	0.316
25108	-1860.09	3257.29	50.12	2.16	0.3	100	0.293	0.09	0.301	0.316
25108	-1860.28	3257.60	49.88	2.16	0.3	100	0.289	0.09	0.301	0.316
25108	-1860.46	3257.90	49.3	2.16	0.31	100	0.279	0.09	0.302	0.316
25108	-1860.65	3258.21	49.77	2.17	0.31	100	0.287	0.09	0.295	0.310
25108	-1860.84	3258.51	50.29	2.17	0.31	100	0.296	0.09	0.294	0.310
25108	-1861.02	3258.82	50.63	2.17	0.32	100	0.302	0.10	0.294	0.310
25108	-1861.21	3259.12	49.81	2.18	0.32	100	0.288	0.09	0.289	0.303
25108	-1861.39	3259.43	47.88	2.19	0.32	100	0.253	0.08	0.285	0.297
25108	-1861.58	3259.73	46.16	2.2	0.31	100	0.223	0.06	0.280	0.290
25108	-1861.77	3260.04	45.44	2.21	1	100	0.210	0.06	0.274	0.284
25108	-1861.95	3260.34	44.1	2.26	3.58	100	0.186	0.05	0.243	0.252
25108	-1862.14	3260.65	42.17	2.37	3.37	100	0.152	0.04	0.174	0.181
25108	-1862.32	3260.95	41.78	2.49	3.89	100	0.145	0.04	0.097	0.103
25108	-1862.51	3261.26	43.77	2.47	5.89	100	0.180	0.05	0.108	0.116
25108	-1862.7	3261.56	46.52	2.37	2.58	100	0.229	0.07	0.170	0.181
25108	-1862.88	3261.87	48.21	2.22	0.68	100	0.259	0.08	0.265	0.277
25108	-1863.07	3262.17	48.71	2.18	0.45	100	0.268	0.08	0.290	0.303
25108	-1863.25	3262.48	48.2	2.18	0.34	100	0.259	0.08	0.291	0.303
25108	-1863.44	3262.78	46.56	2.22	0.81	100	0.230	0.07	0.267	0.277
25108	-1863.63	3263.09	46.38	2.34	4.03	100	0.227	0.07	0.189	0.200
25108	-1863.81	3263.39	52.56	2.49	3.3	100	0.337	0.11	0.085	0.103
25108	-1880.54	3290.82	58.13	2.37	0.58	100	0.436	0.17	0.153	0.181
25108	-1880.73	3291.13	51.01	2.4	1.44	100	0.309	0.10	0.145	0.161
25108	-1880.92	3291.43	47.39	2.46	1.23	100	0.245	0.07	0.111	0.123
25108	-1881.1	3291.74	46.29	2.43	0.86	100	0.225	0.06	0.131	0.142
25108	-1881.29	3292.04	48.16	2.31	0.52	100	0.258	0.08	0.207	0.219
25108	-1881.47	3292.35	52.39	2.2	1.53	100	0.334	0.11	0.272	0.290
25108	-1881.66	3292.65	56.26	2.16	1.73	100	0.402	0.15	0.292	0.316
25108	-1888.17	3303.32	59	2.39	6.71	100	0.451	0.18	0.139	0.168
25108	-1888.35	3303.62	49.55	2.43	0.88	100	0.283	0.09	0.128	0.142
25108	-1888.54	3303.93	44.53	2.42	0.92	100	0.194	0.05	0.140	0.148
25108	-1888.73	3304.23	44.02	2.36	0.47	100	0.185	0.05	0.179	0.187
25108	-1888.91	3304.54	43.22	2.28	0.83	100	0.171	0.05	0.231	0.239
25108	-1889.1	3304.84	42.24	2.21	0.93	100	0.153	0.04	0.277	0.284
25108	-1889.28	3305.15	41.78	2.15	0.49	100	0.145	0.04	0.317	0.323
25108	-1889.47	3305.45	41.55	2.13	0.28	100	0.141	0.04	0.330	0.335
25108	-1889.66	3305.76	41.14	2.11	0.34	100	0.134	0.03	0.343	0.348
25108	-1889.84	3306.06	40.65	2.1	0.36	100	0.125	0.03	0.350	0.355
25108	-1890.03	3306.37	40.81	2.1	0.35	100	0.128	0.03	0.350	0.355
25108	-1890.21	3306.67	40.98	2.12	0.42	100	0.131	0.03	0.337	0.342
25108	-1890.4	3306.98	40.84	2.15	0.71	100	0.128	0.03	0.317	0.323
25108	-1890.58	3307.28	40.98	2.19	0.74	100	0.131	0.03	0.291	0.297
25108	-1890.77	3307.59	41.12	2.23	2.21	100	0.133	0.03	0.266	0.271
25108	-1890.96	3307.89	41.21	2.26	2.18	100	0.135	0.03	0.246	0.252
25108	-1891.14	3308.20	41.17	2.26	1.13	100	0.134	0.03	0.246	0.252
25108	-1891.33	3308.50	41.28	2.25	2.59	100	0.136	0.03	0.252	0.258
25108	-1891.51	3308.81	41.14	2.23	1.38	100	0.134	0.03	0.265	0.271
25108	-1891.7	3309.11	40.77	2.21	0.67	100	0.127	0.03	0.279	0.284
25108	-1891.89	3309.42	40.47	2.19	0.43	100	0.122	0.03	0.292	0.297
25108	-1892.07	3309.72	39.93	2.2	0.5	100	0.112	0.03	0.286	0.290
25108	-1892.26	3310.02	39.67	2.22	0.5	100	0.107	0.03	0.273	0.277
25108	-1892.44	3310.33	39.53	2.23	0.34	100	0.105	0.03	0.267	0.271
25108	-1892.63	3310.63	39.65	2.2	0.33	100	0.107	0.03	0.286	0.290
25108	-1892.82	3310.94	39.47	2.18	0.35	100	0.104	0.03	0.299	0.303
25108	-1893	3311.24	39.46	2.17	0.34	100	0.104	0.03	0.306	0.310
25108	-1893.19	3311.55	39.54	2.17	0.34	100	0.105	0.03	0.306	0.310
25108	-1893.37	3311.85	38.9	2.19	0.34	100	0.094	0.02	0.293	0.297
25108	-1893.56	3312.16	37.46	2.24	0.41	100	0.068	0.02	0.262	0.265
25108	-1893.75	3312.46	35.83	2.32	0.68	100	0.039	0.01	0.211	0.213
25108	-1893.93	3312.77	35.2	2.4	1	100	0.028	0.01	0.160	0.161

Well	TVDRSF	MD	GR	RHO	RD	DT	I_{GR} (4-7)	V_{sh} (4-5/6)	Porosity (eq 5-1)	Porosity (eq 4-4)
25108	-1894.12	3313.07	35.2	2.44	1.88	100	0.028	0.01	0.134	0.135
25108	-1894.3	3313.38	36.1	2.44	3.47	100	0.044	0.01	0.134	0.135
25108	-1894.49	3313.68	37.24	2.43	3.07	100	0.064	0.01	0.140	0.142
25108	-1894.68	3313.99	37.51	2.4	0.91	100	0.069	0.02	0.159	0.161
25108	-1894.86	3314.29	37.93	2.32	0.62	100	0.077	0.02	0.210	0.213
25108	-1895.05	3314.60	38.09	2.26	0.44	100	0.079	0.02	0.249	0.252
25108	-1895.23	3314.90	37.59	2.23	0.41	100	0.071	0.02	0.268	0.271
25108	-1895.42	3315.21	37.43	2.22	0.43	100	0.068	0.02	0.275	0.277
25108	-1895.61	3315.51	37.21	2.21	0.35	100	0.064	0.01	0.281	0.284
25108	-1895.79	3315.82	37.03	2.21	0.83	100	0.061	0.01	0.282	0.284
25108	-1895.98	3316.12	35.99	2.2	3.43	100	0.042	0.01	0.289	0.290
25108	-1896.16	3316.43	35.54	2.19	3.42	100	0.034	0.01	0.296	0.297
25108	-1896.35	3316.73	35.3	2.2	2.55	100	0.030	0.01	0.289	0.290
25108	-1896.53	3317.04	35.02	2.25	0.74	100	0.025	0.01	0.257	0.258
25108	-1896.72	3317.34	34.63	2.31	0.47	100	0.018	0.00	0.219	0.219
25108	-1896.91	3317.64	34.02	2.39	1.32	100	0.007	0.00	0.167	0.168
25108	-1897.09	3317.95	33.63	2.46	2.48	100	0.000	0.00	0.123	0.123
25108	-1897.28	3318.25	34.27	2.51	2.49	100	0.012	0.00	0.090	0.090
25108	-1897.46	3318.56	35.27	2.52	2.27	100	0.029	0.01	0.083	0.084
25108	-1897.65	3318.86	34.61	2.51	1.81	100	0.018	0.00	0.090	0.090
25108	-1897.84	3319.17	33.62	2.49	1.33	100	0.000	0.00	0.103	0.103
25108	-1898.02	3319.47	34.69	2.47	0.87	100	0.019	0.00	0.115	0.116
25108	-1898.21	3319.78	36.03	2.42	0.69	100	0.043	0.01	0.147	0.148
25108	-1898.39	3320.08	36.99	2.34	0.67	100	0.060	0.01	0.198	0.200
25108	-1898.58	3320.39	35.77	2.27	0.62	100	0.038	0.01	0.244	0.245
25108	-1898.77	3320.69	35.42	2.24	0.64	100	0.032	0.01	0.263	0.265
25108	-1898.95	3321.00	35.61	2.25	0.57	100	0.035	0.01	0.257	0.258
25108	-1899.14	3321.30	36.01	2.25	0.48	100	0.042	0.01	0.257	0.258
25108	-1899.32	3321.61	35.39	2.25	0.44	100	0.031	0.01	0.257	0.258
25108	-1899.51	3321.91	35.62	2.24	0.44	100	0.036	0.01	0.263	0.265
25108	-1899.7	3322.22	36.09	2.23	0.42	100	0.044	0.01	0.269	0.271
25108	-1899.88	3322.52	36.57	2.23	0.4	100	0.052	0.01	0.269	0.271
25108	-1900.07	3322.83	36.47	2.22	0.39	100	0.051	0.01	0.276	0.277
25108	-1900.25	3323.13	36.56	2.21	0.35	100	0.052	0.01	0.282	0.284
25108	-1900.44	3323.44	36.58	2.21	0.35	100	0.053	0.01	0.282	0.284
25108	-1900.62	3323.74	36.7	2.21	0.36	100	0.055	0.01	0.282	0.284
25108	-1900.81	3324.05	36.61	2.22	0.35	100	0.053	0.01	0.275	0.277
25108	-1901	3324.35	36.68	2.23	0.36	100	0.054	0.01	0.269	0.271
25108	-1901.18	3324.66	37.6	2.23	0.36	100	0.071	0.02	0.268	0.271
25108	-1901.37	3324.96	38.51	2.23	0.34	100	0.087	0.02	0.268	0.271
25108	-1901.55	3325.26	37.87	2.24	0.32	100	0.076	0.02	0.262	0.265
25108	-1901.74	3325.57	36.52	2.24	0.35	100	0.052	0.01	0.263	0.265
25108	-1901.93	3325.87	35.9	2.23	0.55	100	0.041	0.01	0.270	0.271
25108	-1902.11	3326.18	35.87	2.22	0.61	100	0.040	0.01	0.276	0.277
25108	-1902.3	3326.48	35.83	2.22	0.48	100	0.039	0.01	0.276	0.277
25108	-1902.48	3326.79	36.23	2.23	0.46	100	0.046	0.01	0.269	0.271
25108	-1902.67	3327.09	36.81	2.23	0.58	100	0.057	0.01	0.269	0.271
25108	-1902.86	3327.40	37.48	2.23	0.62	100	0.069	0.02	0.268	0.271
25108	-1903.04	3327.70	37.56	2.22	0.72	100	0.070	0.02	0.275	0.277
25108	-1903.23	3328.01	37.33	2.22	0.63	100	0.066	0.02	0.275	0.277
25108	-1903.41	3328.31	37.28	2.22	0.52	100	0.065	0.02	0.275	0.277
25108	-1903.6	3328.62	37.45	2.23	1.02	100	0.068	0.02	0.268	0.271
25108	-1903.79	3328.92	37.98	2.24	2.16	100	0.077	0.02	0.262	0.265
25108	-1903.97	3329.23	38.57	2.28	2	100	0.088	0.02	0.235	0.239
25108	-1904.16	3329.53	38.97	2.36	2.56	100	0.095	0.02	0.183	0.187
25108	-1904.34	3329.84	41.66	2.43	2.25	100	0.143	0.04	0.136	0.142
25108	-1904.53	3330.14	50.28	2.47	2.42	100	0.296	0.09	0.101	0.116
25108	-1908.62	3336.85	57.66	2.4	0.91	100	0.427	0.17	0.135	0.161
25108	-1908.81	3337.15	51.99	2.39	0.49	100	0.326	0.11	0.150	0.168
25108	-1908.99	3337.46	51.17	2.35	0.41	100	0.312	0.10	0.177	0.194
25108	-1909.18	3337.76	51.4	2.33	0.45	100	0.316	0.10	0.190	0.206
25108	-1909.36	3338.07	51.27	2.29	1.03	100	0.314	0.10	0.216	0.232
25108	-1909.55	3338.37	50.54	2.19	1.94	100	0.301	0.10	0.281	0.297

Well	TVDRSF	MD	GR	RHO	RD	DT	I_{GR} (4-7)	V_{sh} (4-5/6)	Porosity (eq 5-1)	Porosity (eq 4-4)
25108	-1909.74	3338.68	50.67	2.18	1.96	100	0.303	0.10	0.287	0.303
25108	-1909.92	3338.98	50.98	2.23	2.22	100	0.308	0.10	0.255	0.271
25108	-1910.11	3339.29	51.44	2.31	2.73	100	0.317	0.10	0.203	0.219
25108	-1910.29	3339.59	53.36	2.38	2.92	100	0.351	0.12	0.155	0.174
25108	-1922.38	3359.40	54.87	2.41	1.1	100	0.378	0.14	0.133	0.155
25108	-1922.56	3359.71	47.55	2.43	0.91	100	0.248	0.07	0.130	0.142
25108	-1922.75	3360.01	45.01	2.44	0.71	100	0.202	0.06	0.126	0.135
25108	-1922.94	3360.32	42.03	2.44	0.85	100	0.149	0.04	0.129	0.135
25108	-1923.12	3360.62	40.37	2.42	1.38	100	0.120	0.03	0.144	0.148
25108	-1923.31	3360.93	40.55	2.41	1.65	100	0.123	0.03	0.150	0.155
25108	-1923.49	3361.23	41.65	2.41	0.66	100	0.143	0.04	0.149	0.155
25108	-1923.68	3361.54	42.76	2.35	0.41	100	0.162	0.04	0.187	0.194
25108	-1923.87	3361.84	43.87	2.22	0.39	100	0.182	0.05	0.269	0.277
25108	-1924.05	3362.15	44.89	2.15	0.33	100	0.200	0.06	0.314	0.323
25108	-1924.24	3362.45	45.06	2.12	0.27	100	0.203	0.06	0.333	0.342
25108	-1924.42	3362.76	44.28	2.12	0.27	100	0.189	0.05	0.334	0.342
25108	-1924.61	3363.06	43.65	2.13	0.27	100	0.178	0.05	0.328	0.335
25108	-1924.8	3363.36	43.66	2.13	0.28	100	0.178	0.05	0.328	0.335
25108	-1924.98	3363.67	44.17	2.14	0.28	100	0.187	0.05	0.321	0.329
25108	-1925.17	3363.97	44.23	2.15	0.29	100	0.189	0.05	0.314	0.323
25108	-1925.35	3364.28	43.39	2.16	0.28	100	0.174	0.05	0.309	0.316
25108	-1925.54	3364.58	42.98	2.16	0.28	100	0.166	0.04	0.309	0.316
25108	-1925.72	3364.89	43.41	2.16	0.3	100	0.174	0.05	0.309	0.316
25108	-1925.91	3365.19	43.84	2.17	0.31	100	0.182	0.05	0.302	0.310
25108	-1926.1	3365.50	43.92	2.17	0.31	100	0.183	0.05	0.302	0.310
25108	-1926.28	3365.80	44.05	2.18	0.32	100	0.185	0.05	0.295	0.303
25108	-1926.47	3366.11	43.97	2.18	0.33	100	0.184	0.05	0.295	0.303
25108	-1926.65	3366.41	42.88	2.19	0.34	100	0.165	0.04	0.290	0.297
25108	-1926.84	3366.72	41.61	2.21	0.36	100	0.142	0.04	0.278	0.284
25108	-1927.03	3367.02	40.69	2.23	0.37	100	0.126	0.03	0.266	0.271
25108	-1927.21	3367.33	41.18	2.25	0.41	100	0.134	0.03	0.253	0.258
25108	-1927.4	3367.63	41.18	2.26	0.42	100	0.134	0.03	0.246	0.252
25108	-1927.58	3367.94	40.48	2.27	0.43	100	0.122	0.03	0.240	0.245
25108	-1927.77	3368.24	39.43	2.28	0.47	100	0.103	0.03	0.235	0.239
25108	-1927.96	3368.55	38.4	2.29	0.49	100	0.085	0.02	0.229	0.232
25108	-1928.14	3368.85	37.89	2.29	0.5	100	0.076	0.02	0.229	0.232
25108	-1928.33	3369.16	38.55	2.29	0.49	100	0.088	0.02	0.229	0.232
25108	-1928.51	3369.46	39.28	2.29	0.5	100	0.101	0.02	0.228	0.232
25108	-1928.7	3369.77	38.7	2.29	0.6	100	0.090	0.02	0.229	0.232
25108	-1928.89	3370.07	38.17	2.29	0.91	100	0.081	0.02	0.229	0.232
25108	-1929.07	3370.38	38.16	2.29	0.73	100	0.081	0.02	0.229	0.232
25108	-1929.26	3370.68	38.47	2.3	0.73	100	0.086	0.02	0.222	0.226
25108	-1929.44	3370.98	38.56	2.3	0.89	100	0.088	0.02	0.222	0.226
25108	-1929.63	3371.29	39.16	2.3	0.69	100	0.098	0.02	0.222	0.226
25108	-1929.82	3371.59	39.37	2.3	0.61	100	0.102	0.02	0.222	0.226
25108	-1930	3371.90	38.93	2.31	0.67	100	0.094	0.02	0.216	0.219
25108	-1930.19	3372.20	38.2	2.35	0.87	100	0.081	0.02	0.190	0.194
25108	-1930.37	3372.51	37.36	2.38	0.92	100	0.066	0.02	0.172	0.174
25108	-1930.56	3372.81	37.24	2.37	0.86	100	0.064	0.01	0.178	0.181
25108	-1930.75	3373.12	37.03	2.33	0.91	100	0.061	0.01	0.204	0.206
25108	-1930.93	3373.42	36.77	2.31	0.99	100	0.056	0.01	0.217	0.219
25108	-1931.12	3373.73	36.29	2.3	0.88	100	0.047	0.01	0.224	0.226
25108	-1931.3	3374.03	35.9	2.31	0.73	100	0.041	0.01	0.218	0.219
25108	-1931.49	3374.34	35.63	2.32	1.11	100	0.036	0.01	0.212	0.213
25108	-1931.67	3374.64	35.63	2.3	0.82	100	0.036	0.01	0.225	0.226
25108	-1931.86	3374.95	35.54	2.3	0.48	100	0.034	0.01	0.225	0.226
25108	-1932.05	3375.25	36.09	2.3	0.36	100	0.044	0.01	0.224	0.226
25108	-1932.23	3375.56	36.95	2.3	0.34	100	0.059	0.01	0.224	0.226
25108	-1932.42	3375.86	37.86	2.3	0.33	100	0.075	0.02	0.223	0.226
25108	-1932.6	3376.17	38.23	2.28	0.38	100	0.082	0.02	0.236	0.239
25108	-1932.79	3376.47	38.25	2.26	0.41	100	0.082	0.02	0.248	0.252
25108	-1932.98	3376.78	38.25	2.24	0.41	100	0.082	0.02	0.261	0.265
25108	-1933.16	3377.08	38.79	2.24	0.41	100	0.092	0.02	0.261	0.265

Well	TVDRSF	MD	GR	RHO	RD	DT	I_{GR} (4-7)	V_{sh} (4-5/6)	Porosity (eq 5-1)	Porosity (eq 4-4)
25108	-1933.35	3377.39	39.27	2.24	0.41	100	0.100	0.02	0.261	0.265
25108	-1933.53	3377.69	39.19	2.25	0.42	100	0.099	0.02	0.254	0.258
25108	-1933.72	3378.00	38.57	2.25	0.42	100	0.088	0.02	0.255	0.258
25108	-1933.91	3378.30	38.9	2.24	0.39	100	0.094	0.02	0.261	0.265
25108	-1934.09	3378.60	39.59	2.23	0.37	100	0.106	0.03	0.267	0.271
25108	-1934.28	3378.91	39.65	2.23	0.37	100	0.107	0.03	0.267	0.271
25108	-1934.46	3379.21	39.53	2.22	0.36	100	0.105	0.03	0.273	0.277
25108	-1934.65	3379.52	39.55	2.22	0.36	100	0.105	0.03	0.273	0.277
25108	-1934.84	3379.82	39.49	2.22	0.36	100	0.104	0.03	0.273	0.277
25108	-1935.02	3380.13	38.44	2.22	0.36	100	0.086	0.02	0.274	0.277
25108	-1935.21	3380.43	37.29	2.21	0.36	100	0.065	0.02	0.281	0.284
25108	-1935.39	3380.74	37.05	2.21	0.37	100	0.061	0.01	0.282	0.284
25108	-1935.58	3381.04	37.6	2.21	0.36	100	0.071	0.02	0.281	0.284
25108	-1935.77	3381.35	38.06	2.22	0.35	100	0.079	0.02	0.274	0.277
25108	-1935.95	3381.65	38.28	2.22	0.35	100	0.083	0.02	0.274	0.277
25108	-1936.14	3381.96	38.15	2.22	0.35	100	0.080	0.02	0.274	0.277
25108	-1936.32	3382.26	38.08	2.22	0.34	100	0.079	0.02	0.274	0.277
25108	-1936.51	3382.57	38	2.22	0.34	100	0.078	0.02	0.274	0.277
25108	-1936.7	3382.87	37.88	2.22	0.34	100	0.076	0.02	0.275	0.277
25108	-1936.88	3383.18	37.67	2.22	0.35	100	0.072	0.02	0.275	0.277
25108	-1937.07	3383.48	37.48	2.21	0.34	100	0.069	0.02	0.281	0.284
25108	-1937.25	3383.79	37.03	2.22	0.33	100	0.061	0.01	0.275	0.277
25108	-1937.44	3384.09	37	2.22	0.34	100	0.060	0.01	0.275	0.277
25108	-1937.62	3384.40	37.42	2.22	0.33	100	0.068	0.02	0.275	0.277
25108	-1937.81	3384.70	38.5	2.22	0.34	100	0.087	0.02	0.274	0.277
25108	-1938	3385.01	38.55	2.21	0.34	100	0.088	0.02	0.280	0.284
25108	-1938.18	3385.31	38.12	2.22	0.34	100	0.080	0.02	0.274	0.277
25108	-1938.37	3385.62	37.08	2.22	0.34	100	0.061	0.01	0.275	0.277
25108	-1938.55	3385.92	37	2.22	0.34	100	0.060	0.01	0.275	0.277
25108	-1938.74	3386.22	37.96	2.23	0.34	100	0.077	0.02	0.268	0.271
25108	-1938.93	3386.53	39.15	2.23	0.39	100	0.098	0.02	0.267	0.271
25108	-1939.11	3386.83	39.74	2.23	0.41	100	0.109	0.03	0.267	0.271
25108	-1939.3	3387.14	39.2	2.25	0.43	100	0.099	0.02	0.254	0.258
25108	-1939.48	3387.44	38.79	2.27	0.53	100	0.092	0.02	0.242	0.245
25108	-1939.67	3387.75	38.47	2.28	0.91	100	0.086	0.02	0.235	0.239
25108	-1939.86	3388.05	37.91	2.29	1.34	100	0.076	0.02	0.229	0.232
25108	-1940.04	3388.36	36.42	2.31	1.9	100	0.050	0.01	0.218	0.219
25108	-1940.23	3388.66	35.3	2.35	2.38	100	0.030	0.01	0.192	0.194
25108	-1940.41	3388.97	35.13	2.41	2.06	100	0.027	0.01	0.154	0.155
25108	-1940.6	3389.27	35.92	2.48	2.23	100	0.041	0.01	0.108	0.110
25108	-1940.79	3389.58	39.22	2.56	2.6	100	0.100	0.02	0.054	0.058
25108	-1940.97	3389.88	48.28	2.59	3.14	100	0.260	0.08	0.026	0.039
2589	-2233.28	2383.28	56.05	2.39	1.26	114.08	0.485	0.21	0.127	0.168
2589	-2235.11	2385.11	58.27	2.36	1.21	120.45	0.533	0.24	0.139	0.187
2589	-2242.42	2392.42	59.07	2.31	1.22	120.99	0.551	0.26	0.168	0.219
2589	-2243.95	2393.95	57.58	2.28	1.08	122.36	0.518	0.23	0.193	0.239
2589	-2244.25	2394.25	57.57	2.28	1.23	120.94	0.518	0.23	0.193	0.239
2589	-2244.56	2394.56	59.73	2.29	1.16	120.05	0.565	0.27	0.178	0.232
2589	-2274.73	2424.73	54.27	2.48	0.87	109.35	0.447	0.18	0.074	0.110
2589	-2275.04	2425.04	57.95	2.49	0.97	109.44	0.526	0.24	0.056	0.103

APPENDIX D: SEDIMENTOLOGICAL CORE LOGS

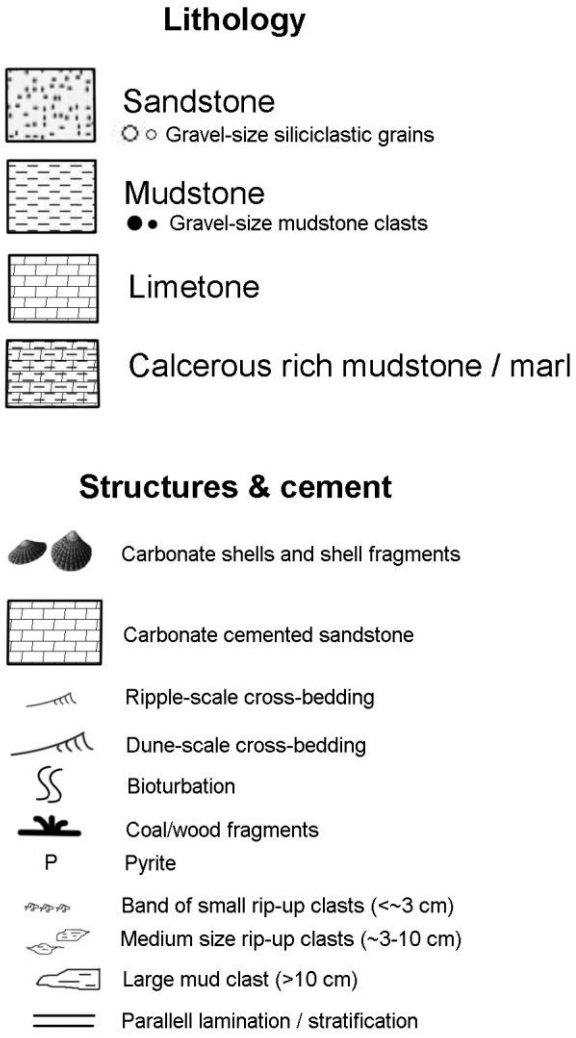

CORE SEDIMENTOLOGICAL LOG

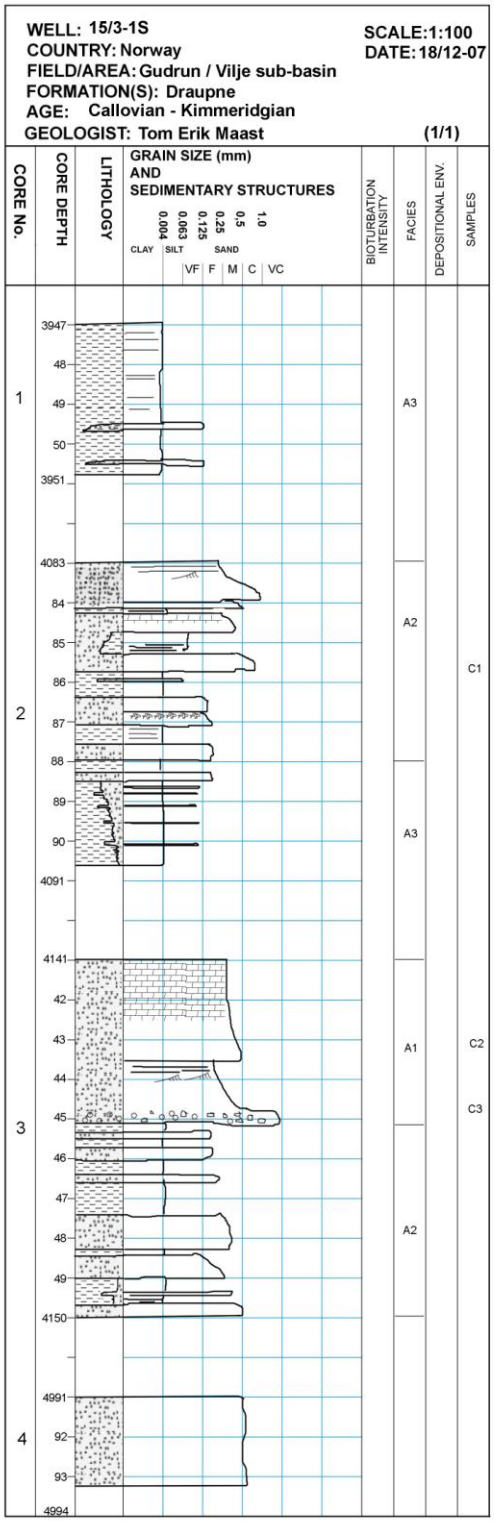

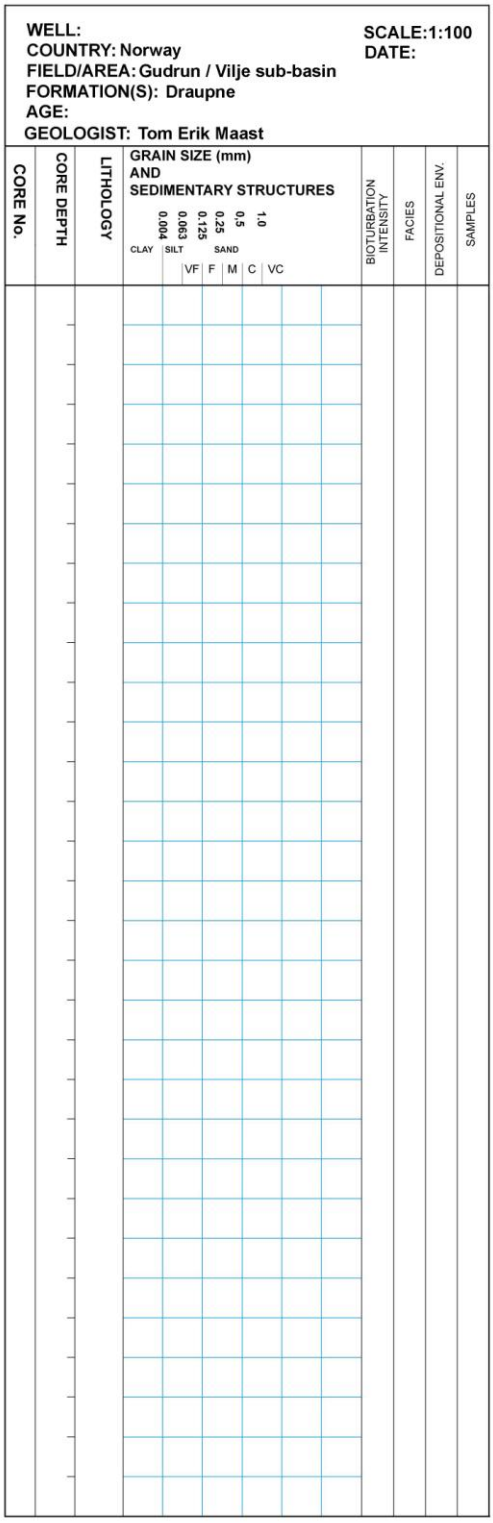

CORE SEDIMENTOLOGICAL LOG

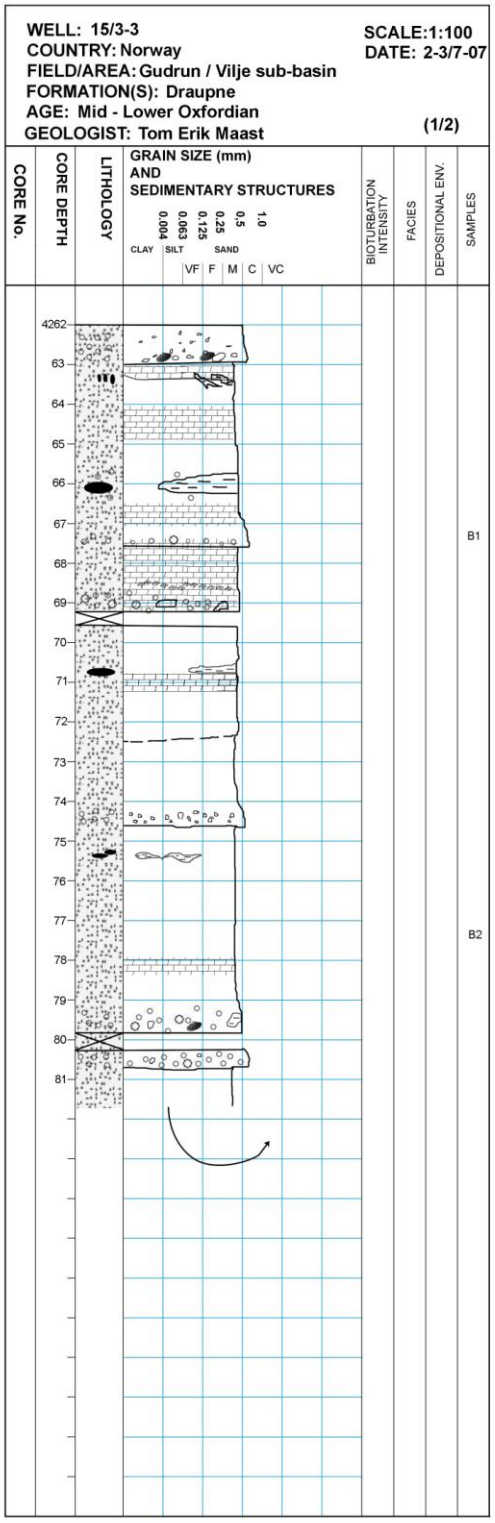

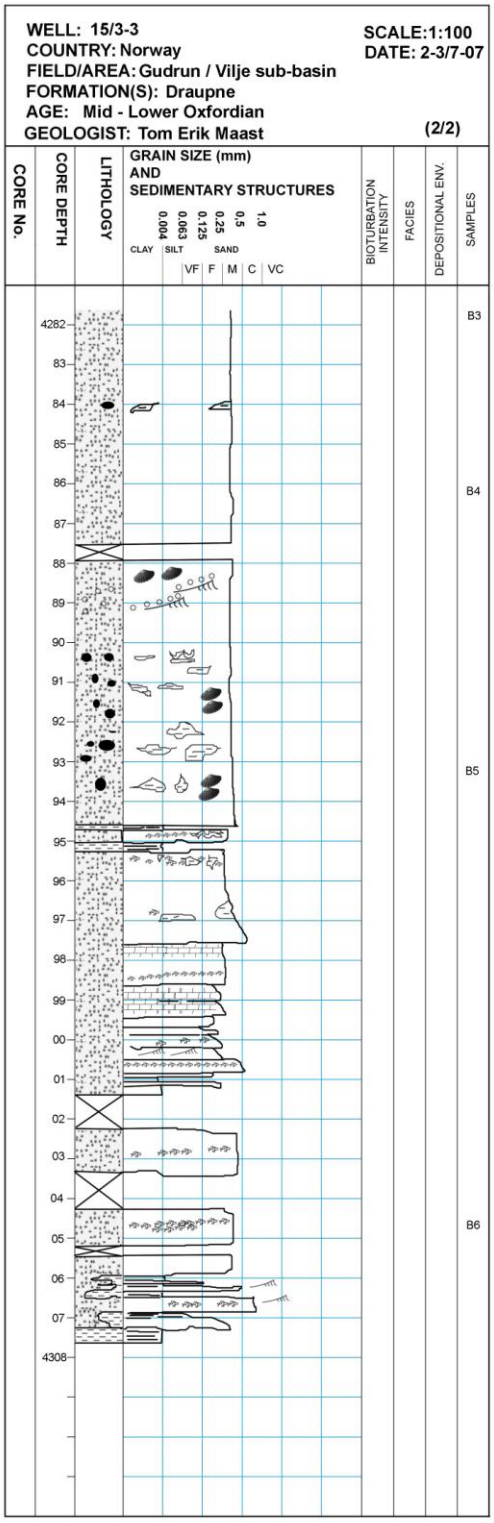

CORE SEDIMENTOLOGICAL LOG

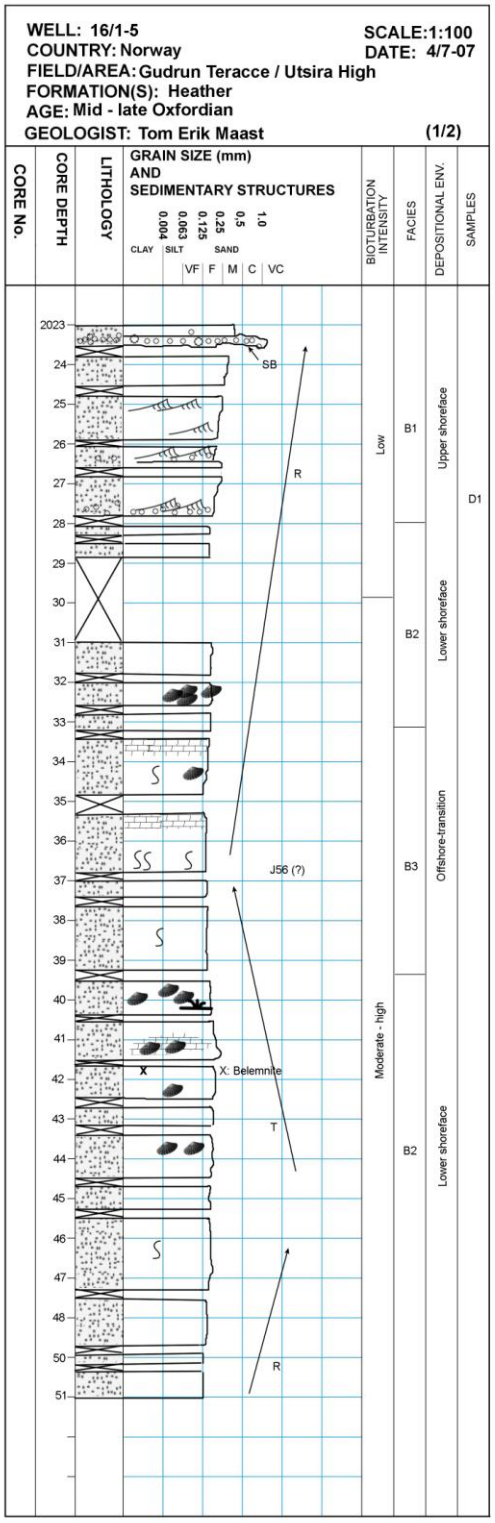

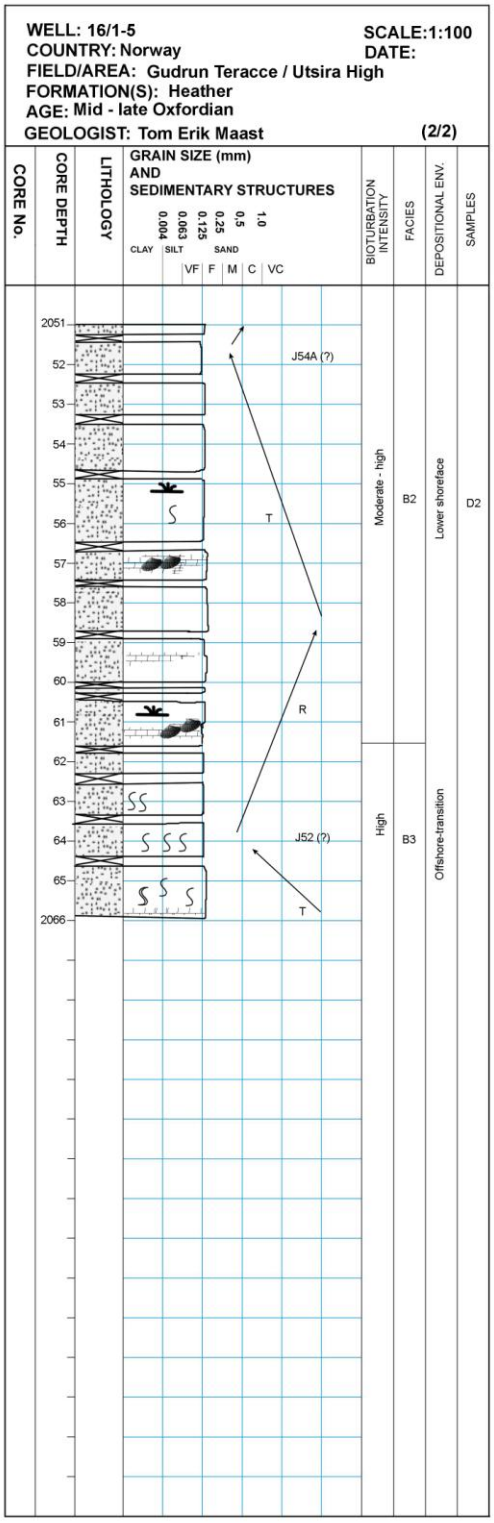

CORE SEDIMENTOLOGICAL LOG

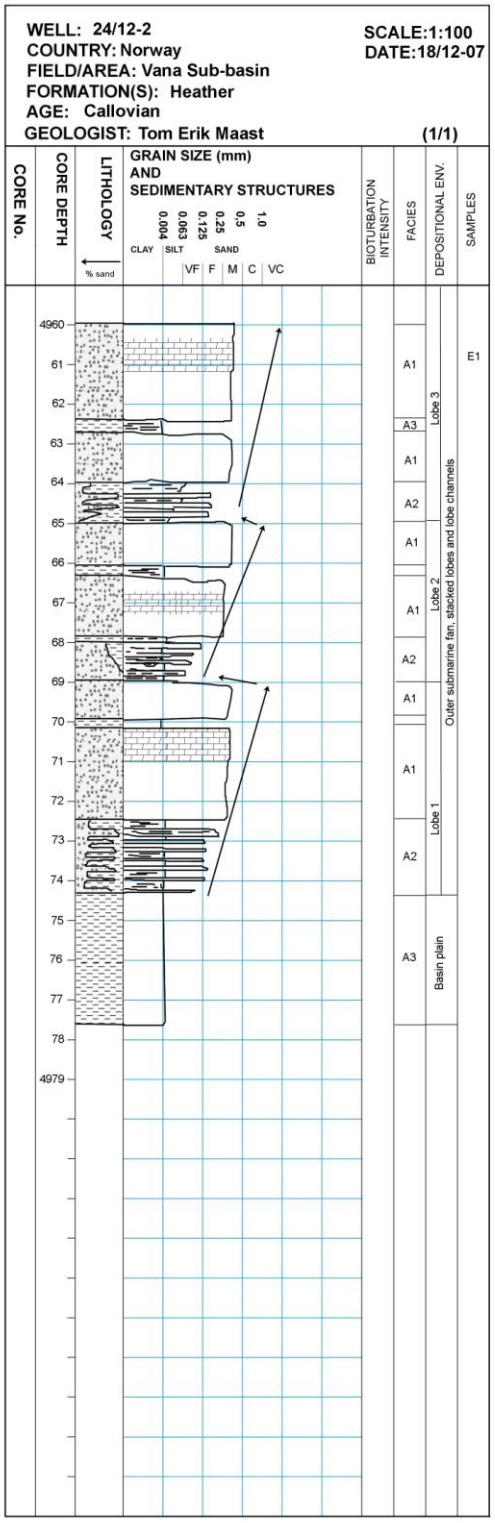

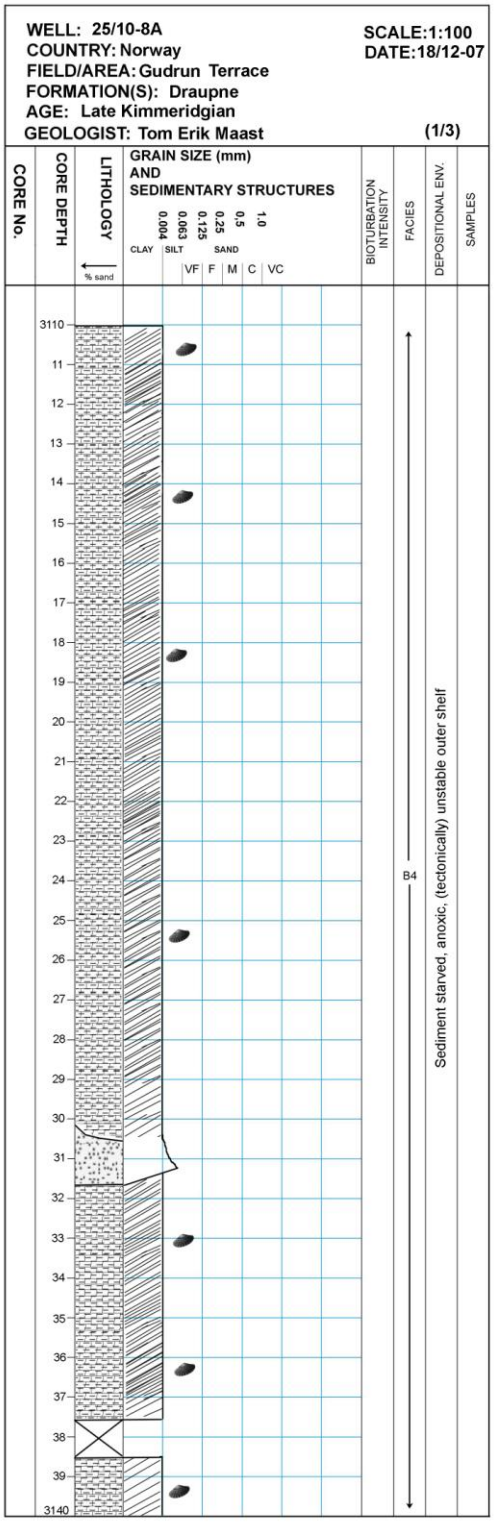

CORE SEDIMENTOLOGICAL LOG

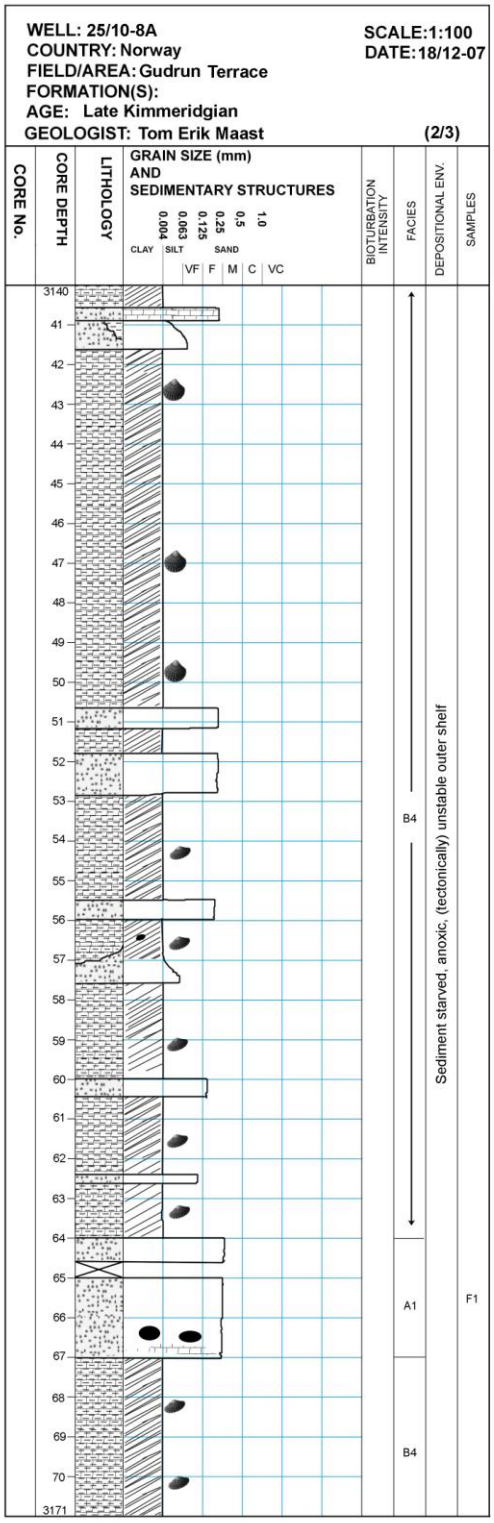

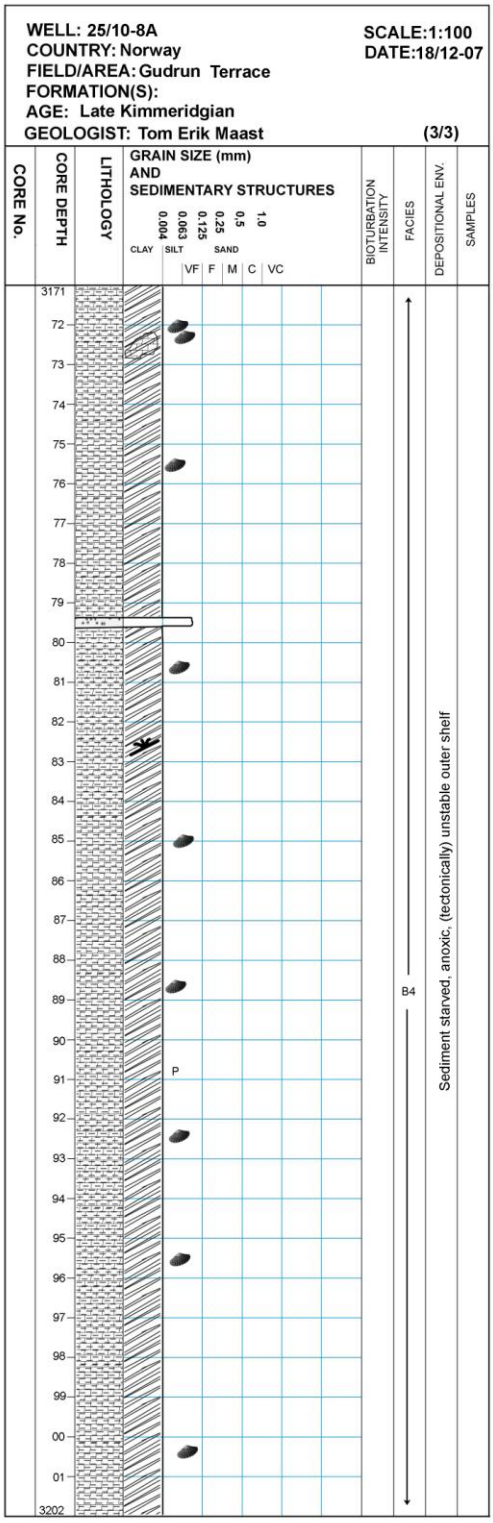

APPENDIX E: BIOSTRATIGRAPHY

WELL: 25/10-8A

CONSULTANT: Stratlab, 1997

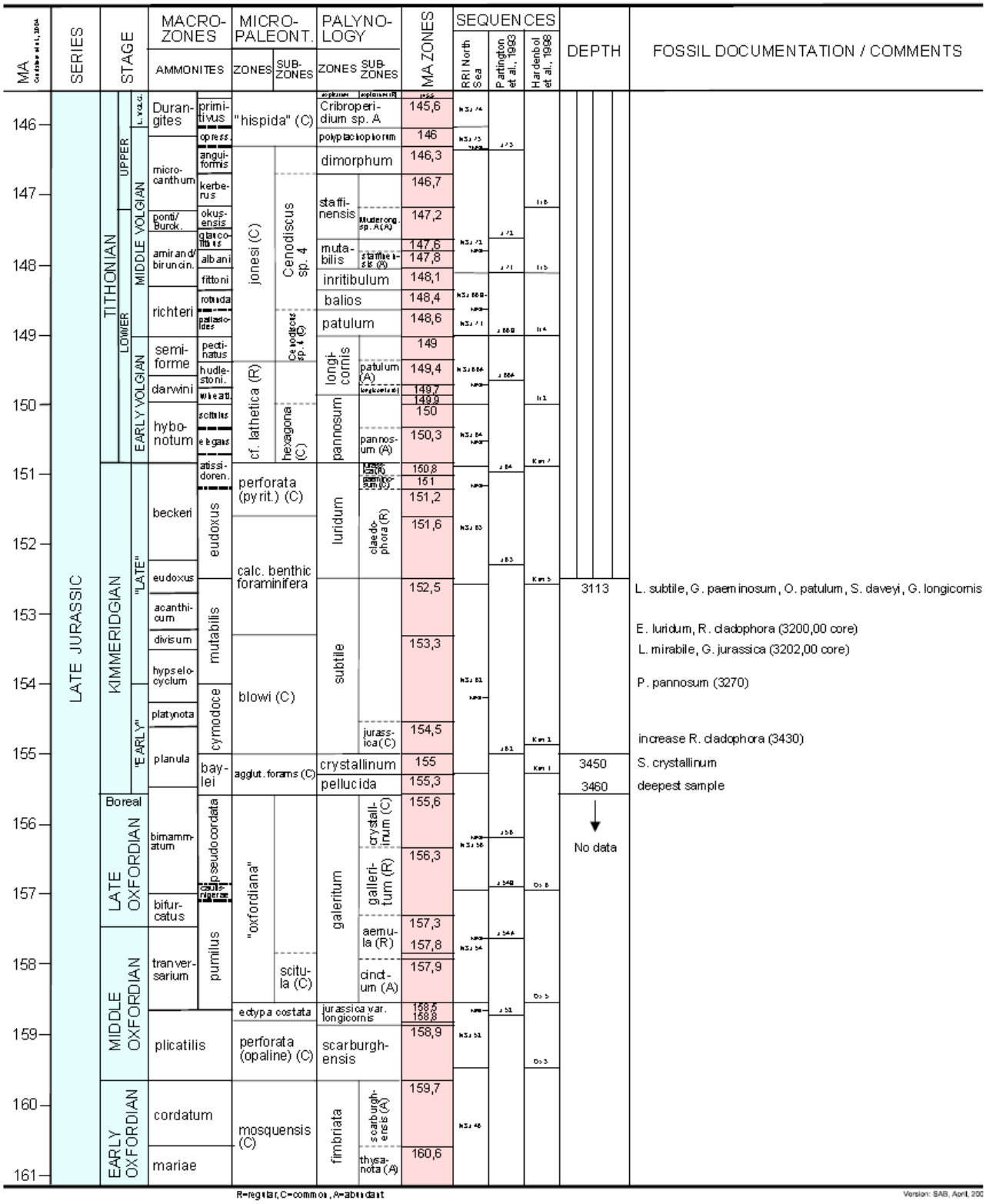

WELL: 16/1-5

CONSULTANT: RRI, 1999

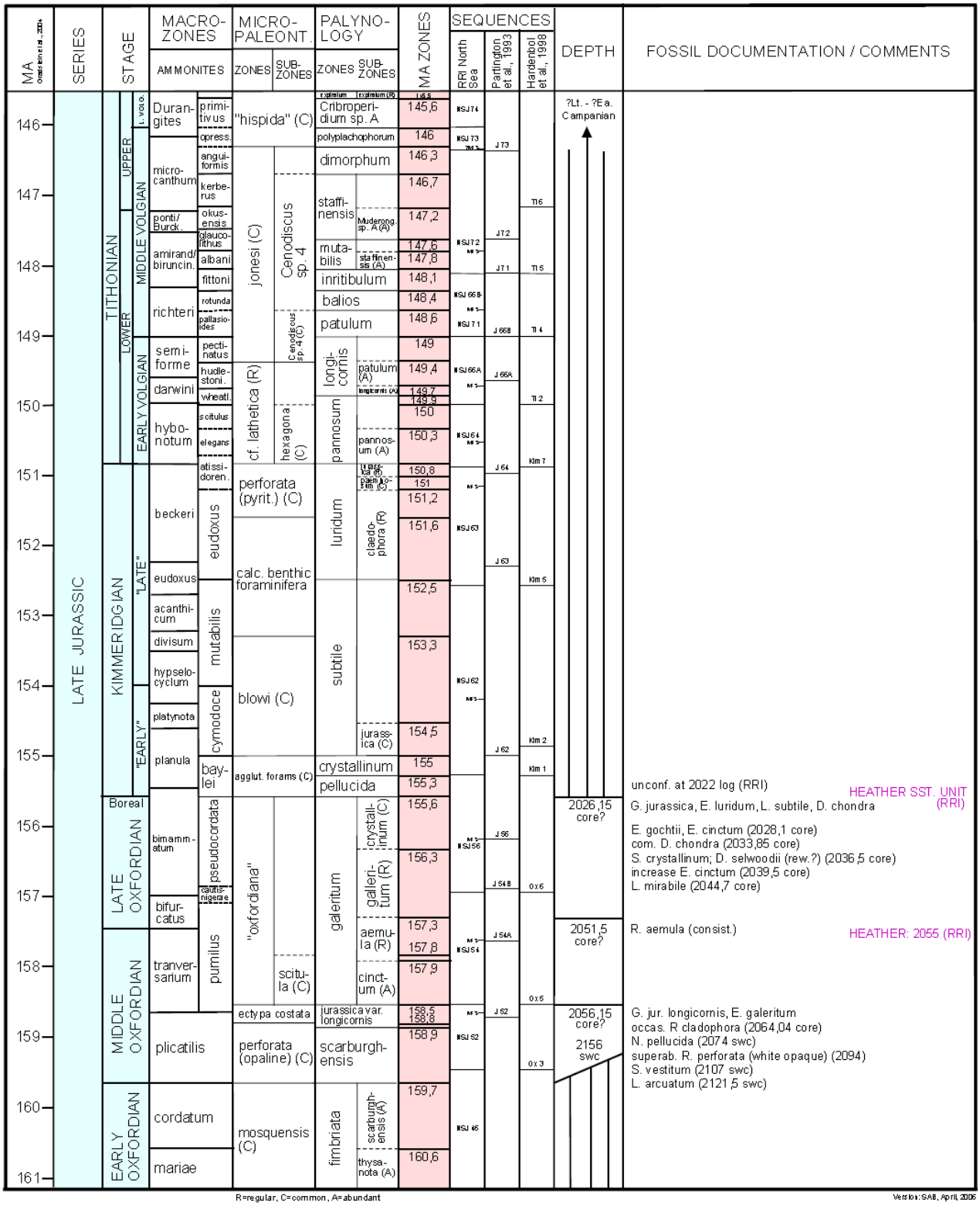

APPENDIX F: IHF PRESSURE DATA

UWI	WELL	MD	TVD	TVDSS	TVDRSF	Frm P(MPa)	FRAC P(MPa)	SOURCE
203283	'15/2-1'	655	655	630	-530		11.136	LOT
203283	'15/2-1'	2737	2737	2712	-2612		42.726	LOT
203283	'15/2-1'	3770	3770	3745	-3645		75.43	LOT
201212	'15/3-1S'		4089	4064	-3964	77.703		FIT
201212	'15/3-1S'		4168.5	4143.5	-4043.5	78.055		FIT
201212	'15/3-1S'		4217	4192	-4092	78.751		FIT
201212	'15/3-1S'		4243.5	4218.5	-4118.5	78.965		FIT
201212	'15/3-1S'		4443.3	4418.3	-4318.3	81.985		FIT
201212	'15/3-1S'		4479.5	4454.5	-4354.5	82.144		FIT
201681	'15/3-2R'	774	774	749	-649		11.473	FIT
201681	'15/3-2R'	2862	2862	2837	-2737		52.101	LOT
201681	'15/3-2R'	4401	4401	4376	-4276	75.145		RWLT
202194	'15/3-3'	2845	2845	2821	-2721		50.427	FIT
202194	'15/3-3'	4117	4117	4093	-3993	77.896		RWLT
202194	'15/3-3'	4181	4181	4157	-4057	78.841		RWLT
202194	'15/3-3'	4233	4233	4209	-4109	78.51		RWLT
202194	'15/3-3'	4235.5	4235.5	4211.5	-4111.5	78.531		RWLT
202194	'15/3-3'	4242	4242	4218	-4118	78.593		RWLT
202194	'15/3-3'	4261.5	4261.5	4237.5	-4137.5	78.841		RWLT
202194	'15/3-3'	4261.6	4261.6	4237.6	-4137.6	79.324		RWLT
202194	'15/3-3'	4262	4262	4238	-4138	79.365		RWLT
202194	'15/3-3'	4262	4262	4238	-4138	78.848		RWLT
202194	'15/3-3'	4264	4264	4240	-4140	78.834		RWLT
202194	'15/3-3'	4267.2	4267.2	4243.2	-4143.2	78.862		RWLT
202194	'15/3-3'	4278.5	4278.5	4254.5	-4154.5	78.958		RWLT
202194	'15/3-3'	4291	4291	4267	-4167	79.089		RWLT
202194	'15/3-3'	4305	4305	4281	-4181	79.234		RWLT
202194	'15/3-3'	4342	4342	4318	-4218	79.606		RWLT
202194	'15/3-3'	4524.5	4524.5	4500.5	-4400.5	78.289		RWLT
202194	'15/3-3'	4588.6	4588.6	4564.6	-4464.6	77.689		RWLT
202194	'15/3-3'	4611	4611	4587	-4487	77.758		RWLT
202194	'15/3-3'	4620	4620	4596	-4496	77.772		RWLT
202194	'15/3-3'	4626.5	4626.5	4602.5	-4502.5	77.813		FIT
202194	'15/3-3'	4630	4630	4606	-4506	77.807		RWLT
202194	'15/3-3'	4683.5	4683.5	4659.5	-4559.5	78.02		RWLT
202194	'15/3-3'	4685.5	4685.5	4661.5	-4561.5	78.055		RWLT
202194	'15/3-3'	4769.5	4769.5	4745.5	-4645.5	82.33		RWLT
202194	'15/3-3'	4809	4809	4785	-4685	83.006		RWLT
202194	'15/3-3'	4828.3	4828.3	4804.3	-4704.3	81.896		RWLT
202194	'15/3-3'	4851.2	4851.2	4827.2	-4727.2	83.571		RWLT
202194	'15/3-3'	4870	4870	4846	-4746	85.688		RWLT
202194	'15/3-3'	4912	4912	4888	-4788	83.144		RWLT
202194	'15/3-3'	4972.6	4972.6	4948.6	-4848.6	84.957		RWLT
202194	'15/3-3'	4981.5	4981.5	4957.5	-4857.5	85.061		RWLT
202194	'15/3-3'	4988.7	4988.7	4964.7	-4864.7	84.668		RWLT
202194	'15/3-3'	4989.5	4989.5	4965.5	-4865.5	84.33		FIT
202194	'15/3-3'	4989.8	4989.8	4965.8	-4865.8	84.426		RWLT
202194	'15/3-3'	4990	4990	4966	-4866	85.385		RWLT
202194	'15/3-3'	4990	4990	4966	-4866	84.84		RWLT
203191	'15/3-4'	3797	3797	3772	-3672	57.037		FIT
203191	'15/3-4'	3798	3798	3773	-3673	57.051		FIT
203191	'15/3-4'	3801	3801	3776	-3676	57.051		FIT
203191	'15/3-4'	3802	3802	3777	-3677	57.065		FIT
203191	'15/3-4'	3804	3804	3779	-3679	57.079		FIT

UWI	WELL	MD	TVD	TVDSS	TVDRSF	Frm P(MPa)	FRAC P(MPa)	SOURCE
203191	'15/3-4'	3814	3814	3789	-3689	57.141		FIT
203191	'15/3-4'	3822	3822	3797	-3697	56.817		FIT
203191	'15/3-4'	3822.5	3822.5	3797.5	-3697.5	56.575		FIT
203191	'15/3-4'	3823	3823	3798	-3698	56.83		FIT
203191	'15/3-4'	3850	3850	3825	-3725	53.569		FIT
203191	'15/3-4'	3852.5	3852.5	3827.5	-3727.5	52.852		FIT
203191	'15/3-4'	3854	3854	3829	-3729	53.617		FIT
203191	'15/3-4'	3872	3872	3847	-3747	52.99		FIT
203191	'15/3-4'	3873.5	3873.5	3848.5	-3748.5	53.19		FIT
203191	'15/3-4'	3915	3915	3890	-3790	52.976		FIT
203191	'15/3-4'	3928	3928	3903	-3803	52.341		FIT
203191	'15/3-4'	3930	3930	3905	-3805	52.348		FIT
204268	'15/3-5'	3969	3969	3944	-3844	63.064		RWLT
204268	'15/3-5'	3969.9	3969.9	3944.9	-3844.9	63.119		RWLT
204268	'15/3-5'	3984	3984	3959	-3859	63.188		RWLT
204268	'15/3-5'	3984	3984	3959	-3859	63.174		RWLT
204268	'15/3-5'	4022.2	4022.2	3997.2	-3897.2	54.389		RWLT
200704	'15/3-6'	1001	1001	978	-878		20.027	LOT
200704	'15/3-6'	1246	1245.8	1222.81	-1122.81	12.427		MDT
200704	'15/3-6'	1673	1672.7	1649.65	-1549.65	16.756		MDT
200704	'15/3-6'	1824	1823.4	1800.4	-1700.4	18.275		MDT
200704	'15/3-6'	1984	1982.9	1959.91	-1859.91	19.892		MDT
200704	'15/3-6'	2159	2157	2134.04	-2034.04	21.657		MDT
200704	'15/3-6'	2162	2160.1	2137.07	-2037.07	21.676		MDT
200704	'15/3-6'	2165	2163.1	2140.06	-2040.06	21.717		MDT
200704	'15/3-6'	2174	2172.1	2149.05	-2049.05	21.809		MDT
200704	'15/3-6'	2195	2192.9	2169.93	-2069.93	22.02		MDT
200704	'15/3-6'	2298	2295.7	2272.7	-2172.7	23.071		MDT
200704	'15/3-6'	2324	2321.6	2298.6	-2198.6	23.332		MDT
200704	'15/3-6'	2430	2427.4	2404.37	-2304.37	24.395		MDT
200704	'15/3-6'	2560	2556.7	2533.7	-2433.7	25.716		MDT
201603	'16/1-2'	2729	2729	2704	-2604		31.547	LC
203663	'16/1-3'	506	506	481	-381		7.783	FIT
203663	'16/1-3'	1263	1263	1238	-1138		21.131	FIT
203663	'16/1-3'	1850	1850	1825	-1725	18.836		RWLT
203663	'16/1-3'	2145.5	2145.5	2120.5	-2020.5	22.808		RWLT
203663	'16/1-3'	2280	2280	2255	-2155	25.683		RWLT
203663	'16/1-3'	2435	2435	2410	-2310	24.773		RWLT
203663	'16/1-3'	2440	2440	2415	-2315	24.801		RWLT
203663	'16/1-3'	2635	2635	2610	-2510	26.828		RWLT
203663	'16/1-3'	2638	2638	2613	-2513		32.657	LC
203663	'16/1-3'	2703	2703	2678	-2578	27.497		RWLT
203663	'16/1-3'	2727	2727	2702	-2602		48.179	FIT
203663	'16/1-3'	2741.5	2741.5	2716.5	-2616.5	28.317		RWLT
203663	'16/1-3'	2742	2742	2717	-2617	28.255		RWLT
203663	'16/1-3'	2742.5	2742.5	2717.5	-2617.5	28.414		RWLT
203663	'16/1-3'	2743	2743	2718	-2618	28.276		RWLT
203663	'16/1-3'	2768.5	2768.5	2743.5	-2643.5	28.586		RWLT
203663	'16/1-3'	2772.5	2772.5	2747.5	-2647.5	28.559		RWLT
203663	'16/1-3'	2782	2782	2757	-2657	28.71		RWLT
203663	'16/1-3'	2787	2787	2762	-2662	28.786		RWLT
203663	'16/1-3'	2797	2797	2772	-2672	29.145		RWLT
203663	'16/1-3'	2798	2798	2773	-2673	29.159		RWLT
203663	'16/1-3'	2802	2802	2777	-2677	29.145		RWLT
203663	'16/1-3'	2803	2803	2778	-2678	29.145		RWLT
203663	'16/1-3'	3194	3194	3169	-3069	33.324		RWLT
203663	'16/1-3'	3219	3219	3194	-3094	34.454		RWLT
201002	'16/1-5'	1410	1409.8	1384.75	-1284.75		25.093	FIT
201002	'16/1-5'	1993	1992.1	1967.07	-1867.07		29.368	FIT
201002	'16/1-5'	2024.5	2023.7	1998.7	-1898.7	20.324		FMT
201002	'16/1-5'	2024.5	2023.7	1998.7	-1898.7	20.354		FMT
201002	'16/1-5'	2031.2	2030.4	2005.4	-1905.4	20.394		FMT

UWI	WELL	MD	TVD	TVDSS	TVDRSF	Frm P(MPa)	FRAC P(MPa)	SOURCE
201002	'16/1-5'	2042	2041.4	2016.4	-1916.4	20.504		FMT
201002	'16/1-5'	2055	2054.1	2029.1	-1929.1	20.634		FMT
201002	'16/1-5'	2068	2067	2042	-1942	20.764		FMT
201002	'16/1-5'	2090	2088.9	2063.9	-1963.9	20.984		FMT
201002	'16/1-5'	2123	2121.8	2096.8	-1996.8	21.314		FMT
201002	'16/1-5'	2183.5	2182	2157	-2057	22.064		FMT
201002	'16/1-5'	2184.5	2183	2158	-2058	22.224		FMT
201002	'16/1-5'	2202.5	2200.9	2175.9	-2075.9	22.244		FMT
201810	'24/12-1R'	755	755	730	-630		9.6	LOT
201810	'24/12-1R'	2855	2855	2830	-2730		49.112	LOT
201810	'24/12-1R'	3966	3966	3941	-3841		85.439	LOT
201810	'24/12-1R'	4323	4323	4298	-4198		86.513	LC
203087	'24/12-2'	992	992	960	-860		14.675	FIT
203087	'24/12-2'	2873	2873	2841	-2741		50.472	FIT
203087	'24/12-2'	3965	3965	3933	-3833		82.822	FIT
203087	'24/12-2'	4956.7	4956.7	4924.66	-4824.66	93.756		RFT
203087	'24/12-2'	4971.6	4971.6	4939.6	-4839.6	94.183		RFT
200559	'25/10-8A'	1067	1067	1042.5	-942.5		16.509	LOT
200559	'25/10-8A'	2077.5	2077.5	2053	-1953	20.742		RFT
200559	'25/10-8A'	2081	2081	2056.5	-1956.5	20.762		RFT
200559	'25/10-8A'	2086	2086	2061.5	-1961.5	20.822		RFT
200559	'25/10-8A'	2117.5	2117.5	2093	-1993	21.132		RFT
200559	'25/10-8A'	2120.8	2120.8	2096.3	-1996.3	21.172		RFT
200559	'25/10-8A'	2252	2252	2227.5	-2127.5	23.272		RFT
200559	'25/10-8A'	2373	2373	2348.5	-2248.5	24.132		RFT
200559	'25/10-8A'	2373.5	2373.5	2349	-2249	24.132		RFT
200559	'25/10-8A'	2374.5	2374.5	2350	-2250	24.152		RFT
200559	'25/10-8A'	2378.5	2378.5	2354	-2254	24.172		RFT
200559	'25/10-8A'	2380	2380	2355.5	-2255.5	24.172		RFT
200559	'25/10-8A'	2380.8	2380.8	2356.3	-2256.3	24.162		RFT
200559	'25/10-8A'	2392	2391.4	2366.9	-2266.9	24.165		DST
200559	'25/10-8A'	2392	2391.4	2366.9	-2266.9	24.165		DST
200559	'25/10-8A'	2392.5	2392.5	2368	-2268	24.222		RFT
200559	'25/10-8A'	2394	2394	2369.5	-2269.5	24.232		RFT
200559	'25/10-8A'	2395	2395	2370.5	-2270.5	24.232		RFT
200559	'25/10-8A'	2397	2397	2372.5	-2272.5	24.242		RFT
200559	'25/10-8A'	2404.5	2404.5	2380	-2280	24.292		RFT
200559	'25/10-8A'	2404.6	2404.6	2380.1	-2280.1	24.292		RFT
200559	'25/10-8A'	2411	2411	2386.5	-2286.5	24.342		RFT
200559	'25/10-8A'	2436.4	2436.4	2411.9	-2311.9	24.592		RFT
200559	'25/10-8A'	2512	2512	2487.5	-2387.5	25.442		RFT
200559	'25/10-8A'	2515	2515	2490.5	-2390.5	25.432		RFT
200559	'25/10-8A'	2520	2520	2495.5	-2395.5	25.482		RFT
200559	'25/10-8A'	2526.5	2526.5	2502	-2402	25.552		RFT
200559	'25/10-8A'	2528.6	2528.6	2504.1	-2404.1	25.582		RFT
200333	'25/7-2'	3906	3906	3881	-3781		82.311	LOT
200333	'25/7-2'	4255	4248.7	4223.7	-4123.7	67.567		RWLT
200333	'25/7-2'	4285	4278.5	4253.5	-4153.5	70.547		RWLT
200550	'25/8-9'	1097	1096.8	1071.8	-971.8		17.075	LOT
200550	'25/8-9'	2097.8	2094	2069.01	-1969.01	20.01		RFT
200550	'25/8-9'	2103	2099.2	2074.2	-1974.2	20.065		RFT
200550	'25/8-9'	2103.2	2099.4	2074.4	-1974.4	20.079		RFT
200550	'25/8-9'	2111	2107.2	2082.19	-1982.19	20.07		RFT
200550	'25/8-9'	2113.5	2109.7	2084.68	-1984.68	20.098		RFT
200550	'25/8-9'	2118	2114.2	2089.17	-1989.17	20.184		RFT
200550	'25/8-9'	2151	2147.1	2122.12	-2022.12	20.454		RFT
200550	'25/8-9'	2180	2176.1	2151.07	-2051.07	20.743		RFT
200550	'25/8-9'	2182	2178.1	2153.07	-2053.07	20.763		RFT
200550	'25/8-9'	2184	2180.1	2155.07	-2055.07	20.782		RFT
200550	'25/8-9'	2186	2182.1	2157.06	-2057.06	20.802		RFT
200550	'25/8-9'	2188	2184.1	2159.06	-2059.06	20.821		RFT
200550	'25/8-9'	2230	2225.9	2200.93	-2100.93	21.233		RFT

UWI	WELL	MD	TVD	TVDSS	TVDRSF	Frm P(MPa)	FRAC P(MPa)	SOURCE
200550	'25/8-9'	2232	2227.9	2202.91	-2102.91	21.254		RFT
200550	'25/8-9'	2234	2229.9	2204.88	-2104.88	21.275		RFT
200550	'25/8-9'	2236	2231.9	2206.86	-2106.86	21.291		RFT
200550	'25/8-9'	2270	2265.4	2240.43	-2140.43	21.628		RFT
200550	'25/8-9'	2296	2266.1	2241.11	-2141.11	21.888		RFT
200550	'25/8-9'	2302	2272	2247.03	-2147.03	21.944		RFT
200550	'25/8-9'	2280	2275.3	2250.31	-2150.31	21.727		RFT
200550	'25/8-9'	2290	2285.2	2260.18	-2160.18	21.826		RFT
200550	'25/8-9'	2434	2402.3	2377.28	-2277.28	23.999		RFT
200550	'25/8-9'	2444	2412.2	2387.16	-2287.16	24.089		RFT
200550	'25/8-9'	2447	2415.1	2390.13	-2290.13	24.122		RFT
200550	'25/8-9'	2452	2420.1	2395.07	-2295.07	24.175		RFT
200550	'25/8-9'	2462	2430	2404.95	-2304.95	24.277		RFT
200550	'25/8-9'	2474	2441.8	2416.81	-2316.81	24.383		RFT
200550	'25/8-9'	2476	2443.8	2418.79	-2318.79	24.403		RFT
200618	'25/8-9A'	2495	2103.2	2078.2	-1978.2	20.223		RFT
200618	'25/8-9A'	2508	2113.2	2088.2	-1988.2	21.003		RFT
200618	'25/8-9A'	2509	2113.4	2088.4	-1988.4	20.3		RFT
200618	'25/8-9A'	2512	2115.6	2090.6	-1990.6	20.109		RFT
200618	'25/8-9A'	2512	2115.6	2090.61	-1990.61	20.141		RFT
200618	'25/8-9A'	2531	2127.2	2102.22	-2002.22	20.185		RFT
200618	'25/8-9A'	2549	2138.4	2113.35	-2013.35	20.291		RFT
200618	'25/8-9A'	2552	2140.2	2115.2	-2015.2	20.311		RFT
200618	'25/8-9A'	2557	2143	2117.98	-2017.98	20.339		RFT
200618	'25/8-9A'	2585	2160.3	2135.32	-2035.32	20.511		RFT
200618	'25/8-9A'	2585	2160.4	2135.38	-2035.38	20.513		RFT
200618	'25/8-9A'	2593	2165.6	2140.58	-2040.58	20.554		RFT
200618	'25/8-9A'	2595	2166.8	2141.82	-2041.82	20.58		RFT
200618	'25/8-9A'	2595	2166.8	2141.82	-2041.82	20.562		RFT
200618	'25/8-9A'	2599	2169.3	2144.29	-2044.29	20.593		RFT